MOROCCO

SPRING BREAK TRIP 2026#

UNIVERSITY OF PITTSBURGH AT JOHNSTOWN - GEOLOGY CLUB

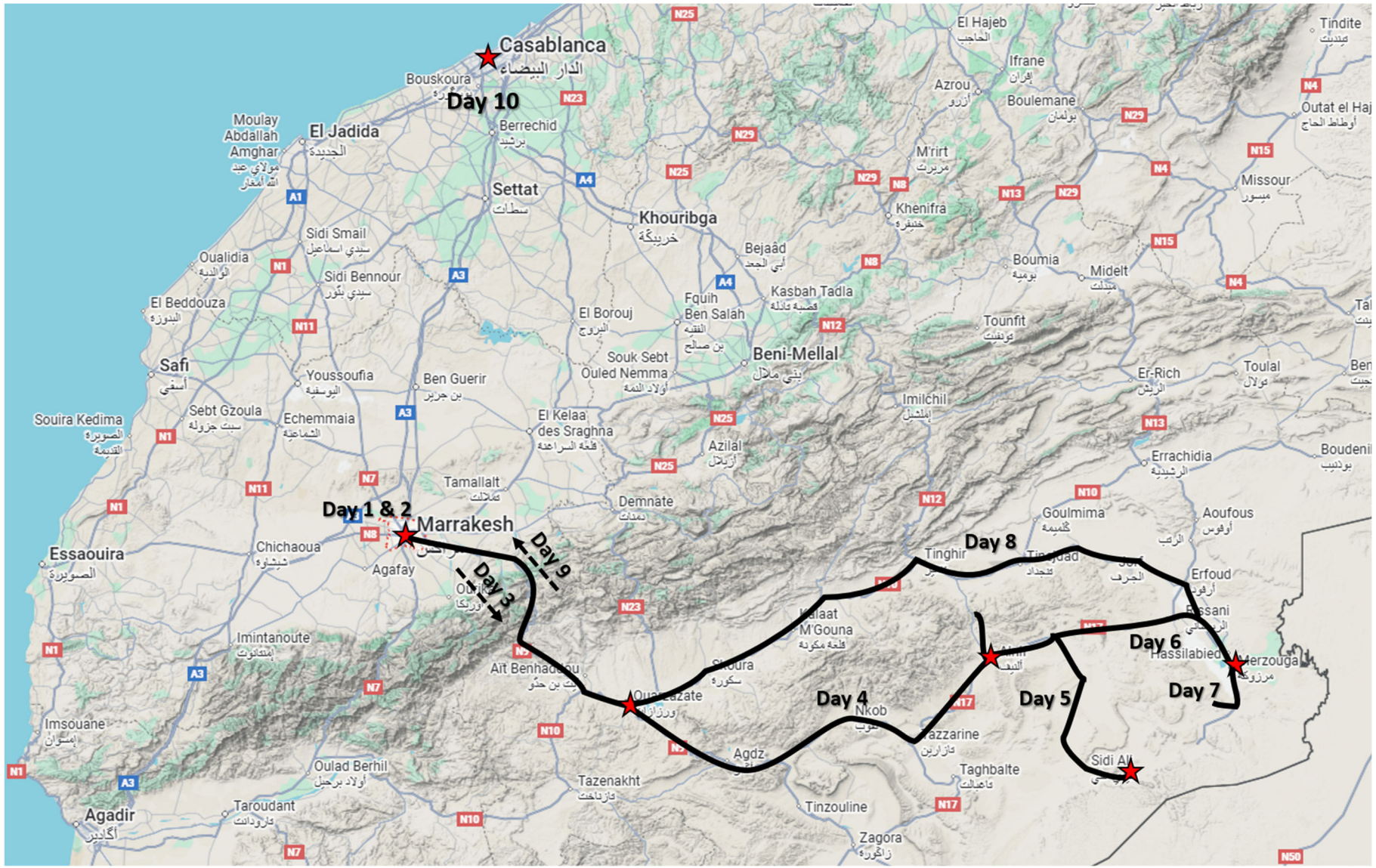
Casablanca
الدار البيضاء
Day 10
Bouskoura
Berrechid
Moulay Abdallah
El Jadida
Amghar
Settat
Khouribga
Sidi Smail
Oualidia
Sidi Bennour
El Beddouza
Safi
Youssoufia
Ben Guerir
Souira Kedima
Sebt Gzoula
Echemmaia
El Kelaa des Sraghna
Azilal
Tamallalt
Demnate
Day 1 & 2
Marrakesh
Day 9
Day 3
Essaouira
Chichaoua
Agafay
Imintanoute
Ait Benhaddou
Ouarzazate
Day 4
Imsouane
Oulad Berhil
Agadir
Taroudant
Tazenakht
Agdz
Nkob
Tinzouline
Zagora
Taghbalte
Tazzarine
Sidi Ali
Day 5
Day 6
Day 7
Day 8
Tinghir
Goulmima
Erfoud
Rissani
Hassilabied
Merzouga
Aoufous
Errachidia
Imilchil
Beni-Mellal
Souk Sebt Ouled Nemma
El Borouj
Fquih Ben Salah
Kasbah Tadla
Bejaâd
Khenifra
M'rirt
Azrou
Ifrane
El Hajeb
Boulemane
Boumia
Midelt
Tounfit
Er-Rich
Toulal
Outat el Haj
Missour
Tindite

The following was compiled by Ryan Kerrigan, Associate Professor pf Geology at University of Pittsburgh a Johnstown, Johnstown, PA in the winter of 2025-2026 as supporting material for the Pitt-Johnstown Geology Club Spring Break Trip to Morocco on March 6th to March 15th, 2026.

Much of the details come from Wikipedia. If you use this field guide, please consider donating to Wikipedia.

TABLE OF CONTENTS

THINGS YOU SHOULD BRING

Please limit yourself to one checked bag and one carry-on (day-pack)

Most Important:
• Passport & credit card

Personal Items:
• Sunscreen
• Lip balm with sunscreen
• Sunglasses
• Tissues
• Toiletries
• Van/Plane Entertainment (books, cards, small board games, etc.)
• Travel Towel
• Outlet converter (Type C or E)

Clothes:
• *It should be warm… but it might be chilly in the mountains*
• Hiking boots or good cross trainers
• Lightweight hiking pants
• Swimming Suit
• Hats (both for sun protection and warmth)

Equipment:
• Water Bottle
• Field Notebook
• Pencils/Pens
• Rock Hammer (must be packed in checked luggage)
• Hand lens

Money:
• You cannot get Moroccan Dirhams from your bank. It is a closed currency, meaning it is not traded as a currency globally.
• We will have to exchange money at the airport or at ATMs in Morocco.
• Your credit/bank cards should work fine, but it is always a good idea to tell those companies you are going overseas so they don't shut you down to thinking it might be fraudulent.

Other:
• **WhatsApp** – I would like everyone to download WhatsApp. This is a phone/text service that is free and will allow us to stay in contact via Wifi. This way we will not need to add expensive international calling/data plans to our phone.

TRIP RULES

1. Don't do anything that would put yourself or others else in danger.
2. Buddy System – do not wander off by yourself, ALWAYS have another group member with you AT ALL TIMES!!!
3. Do not invite strangers back to our hotels
4. Please practice moderation – do not overdo it. Please.

You are representing the University of Pittsburgh at Johnstown. Do not embarrass the university. Do not do anything that would jeopardize future trips of the Geology Club!

After the trip:

After the trip, I would like you to upload your pictures to shared cloud folder. I use these pictures in lectures and advertising for future trips.

You will attend the Geosciences Banquet on Friday April 24th, where the attendees of the Geology Club Spring Break trip will present pictures from the trip.

Important Phone Numbers

Pitt-Johnstown Geology Prof Ryan Kerrigan: +1 612 229 6810
Morocco Explorer Guide Youssef: +00212662-895-735

FLIGHTS

Flights

Booking Reference: XAHAS7

Departing Flights

Flight #1: <u>*Departure:*</u> Royal Air Maroc, AT219, Friday, March 6, 2026, 8:45PM, Washington DC (Dulles – IAD) to Casablanca (CMN)
<u>*Arrival:*</u> Casablanca on Saturday, March 7, 2026 at 8:50AM

Flight #2: <u>*Departure:*</u> Royal Air Maroc, AT411, Saturday, March 7, 2026, 10:55AM, Casablanca (CMN) to Marrakech (RAK)
<u>*Arrival:*</u> Marrakech on Saturday, March 7, 2026, 11:45AM

Return Flight

Flight #1: <u>*Departure:*</u> Royal Air Maroc, AT412, Saturday, March 14, 2026, 5:50PM, Marrakech (RAK) to Casablanca (CMN)
<u>*Arrival:*</u> Casablanca on Saturday, March 14, 2026 at 6:50PM

Long layover (~22hrs) for sight-seeing in Casablanca

Flight #2: <u>*Departure:*</u> Royal Air Maroc, AT218, Sunday, March 15, 2026, 3:25PM, Casablanca (CMN) to Washington DC (Dulles – IAD)
<u>*Arrival:*</u> Washington DC on Sunday, March 15, 2026, 7:45PM

MOROCCAN BASICS

Emergency Number: 19 (Police) and 15 (Ambulance)
USA embassy: 05-37-63-72-00 or +212-537-63-72-00

- *Currency:* Moroccan Dirhams (MAD)
- *Exchange Rate:* 1 USD = ~9.21 MAD or… 100 MAD = ~$11 USD
- *Time zone:* +1 Greenwich Mean Time (GMT) (add 5 hours to EST (our time))
- *Credit Cards:* While cards will be accepted in many locations, we will definitely encounter "cash only" establishments. Please bring cash with you. You probably will not need a lot of Moroccan Dirham (most meals are covered) but the shops and markets will only take Dirhams.
- *ATMs:* Available in most towns
- *Electrical outlets:* Morocco uses European style outlets (Type C and E). These have two round prongs. You will need these to charge your devices. If you forget, they have stores.
- *Tipping:* Tipping in Morocco is expected but not as high as the US. Restaurants – about 10% tip is usually appropriate, but you can tip more if the service was exceptional. Upscale restaurants may automatically include a tip on the bill.
- *Etiquette:* Learn a couple of Arabic phrases before going on the trip. You are in their country, at least make an attempt to conform to their culture, it is only courteous. Hello, Goodbye, Please, Thank you at a minimum.
- *Temperature:* March weather and climate: it's going to be warm. Daily highs average around mid-70's°F and lows around 50°F. Up in the mountains it will be cooler.
- *Precipitation:* We will be there at the tail-end of rainy season, but it is generally dry where we will be.
- *Daylight:* ~12 hours of daylight (~06:45–18:45)

Fun Facts About Morocco

- The official name of Morocco is the Kingdom of Morocco.
- The King of Morocco is Mohammed VI. He accepted the throne on the 23rd of July 1999.
- Morocco borders Algeria to the east, the Mediterranean Sea to the north, the Atlantic Ocean to the west, and Mauritania and Mali to the south.
- The south of the country is blanketed by the Sahara Desert, the hottest desert on the planet.
- 11.5% of Morocco is forested.
- The High Atlas Mountains are the highest mountains in North Africa and run from Morocco to Tunisia. The highest peak is called Toubkal and is 4,167 m (13,671 ft) high.
- Morocco is approximately the same size as the US state of California.
- The largest city in Morocco is Casablanca, but the capital city is Rabat.
- Marrakesh is the cultural capital of the country. It's known for its markets (called souks), and colorful traditional Moroccan houses (called riads).
- Morocco's population is approximately 37.6 million people.
- 99% of Moroccans are Muslims, and the other 1% are Jewish or Christians.

Basic Travel Arabic

Greetings and Polite Expressions

Salam alaykum (سلام عليكم) – Hello (common greeting).
Sbah l-khir (صباح الخير) – Good morning.
Msaa l-khir (مساء الخير) – Good evening.
La, shukran (لا، شكرا) – No, thank you.
Naam, barakallahu fik (نعم، بارك الله فيك) – Yes, may God bless you.
Afak (عفاك) – Please.
Shukran (شكرا) – Thank you.
Tfaddal (تفضل) – You're welcome.

Getting Around

Fin toilet? (فين طواليط؟) – Where is the bathroom?
Kayn taxi? (كاين تاكسي؟) – Is there a taxi?
Mechi (مشي) – Go (useful when giving directions).
Asif/ Smahli (سمحلي/أسف) – Excuse me or pardon.
Kifach nmchi lsaha? (كيفاش نمشي للساحة؟) – How do I get to the square?

Shopping and Bargaining

Bshwiya bshwiya (بشوية بشوية) – Little by little (when haggling).
Bchhal hada? (بشحال هاذا؟) – How much is this?
Ghali/rahh ghali (غالي/راح غالي) – Expensive/It's too expensive.
Khelliha b… (خليها ب…) – Give it to me for…
Maakayn mushkil (ماكاين مشكل) – No problem.
Bchhal tkhali hali? (بشحال تخليها لي؟) – How much can you do it for?

Eating and Dining

Bismillah (بسم الله) – In the name of God (said before meals).
Shwiya bshwiya (شوية بشوية) – A little bit (when serving food).
Hnaya (هنايا) – Here you go (when offering something).
Lma (لما) – Water.
Atay (اتاي) – Tea (a staple of Moroccan hospitality).
Rzala (غزالة) – Delicious.

Making Friends

Shno smiytk? (شنو اسميتك؟) – What's your name?
Ismi… (اسمي…) – My name is…
Ana min… (أنا من…) – I'm from…
Sbar Alaya (صبر عليا) – Wait for me.

Emergency Phrases

Musa'ida! (مساعدة!) – Help!
Mcha li baztam (مشالي البزطام) – I lost my wallet.
Ana bghit doctor (انا بغيت دكتور) – I need a doctor.

BRIEF ITINERARY

Day 1: Friday, March 6th, 2026 – Fly to Morocco

Find your way to Washington Dulles International Airport!

Overnight flight to Morocco

Flight #1: *Departure:* Royal Air Maroc, AT219, Friday, March 6, 2026, 8:45PM, Washington DC (Dulles – IAD) to Casablanca (CMN)

Arrival: Casablanca on Saturday, March 7, 2026 at 8:50AM

Day 2: Saturday, March 7th, 2026 – Arrive in Marrakech

8:50 AM: Arrive in Casablanca. Clear immigration.

10:55 AM: Depart Casablanca for Marrakech

Flight #2: *Departure:* Royal Air Maroc, AT411, Saturday, March 7, 2026, 10:55AM, Casablanca (CMN) to Marrakech (RAK)

Arrival: Marrakech on Saturday, March 7, 2026, 11:45AM

12:00 PM: Arrive in Marrakech

1:00 PM: Arrive at the Hotel

Kennedy Hospitality Resort – Marrakech

Av. du Président Kennedy, Marrakech 40000, Morocco

https://www.kennedyhospitalityresort.com/

Rest of the day: Free afternoon and evening to explore Marrakech.

Day 3: Sunday, March 8th, 2026 – Marrakech – Sidi Rahal – High Atlas – Ait ben Haddou – Ouarzazate

STOP 3.1 – Sidi Rahal Agate Mine
STOP 3.2 – Fault near Zerkten
Lunch Stop
STOP 3.3 – Col du Tichka
STOP 3.4 – Telouet Salt Mine
STOP 3.5 – Ounila Valley
STOP 3.6 – Ait-Ben-Haddou
STOP 3.7 – Ouarzazate

Hotel Information:

Les Jardins de Ouarzazate
13 N9, Tarmigt 45000, Morocco
http://www.lesjardinsdeouarzazate.com/

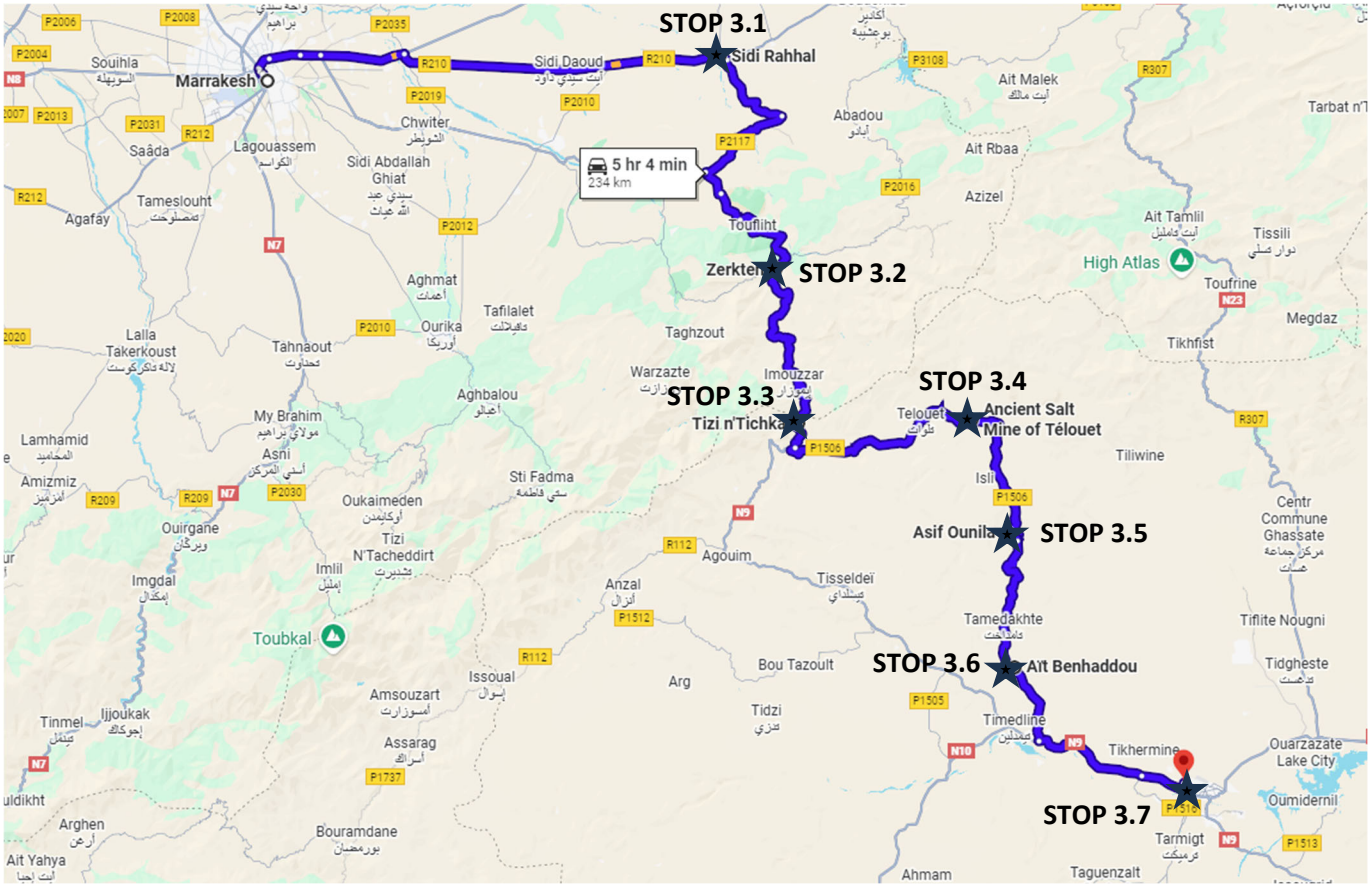

Day 4: Monday, March 9th, 2026 – Ouarzazate – Anit-Atlas Stromatolites – Draa Valley – Alnif Fossils

STOP 4.1 – Ediacaran Stromatolites
STOP 4.2 – Tizi-n-Tinififft Pass
STOP 4.3 – Agdz and The Draa Valley
STOP 4.4 – Orthoceras Quarry near Tazzarine
STOP 4.5 – Trilobite Preparation Workshop near Alnif

Hotel Information:

Auberge Kasbah Meteorites
Ksar Tighirna à 13 km d'Alnif BP138, Alnif 52452, Morocco
http://www.kasbah-meteorites.com/

Day 5: Tuesday, March 10th, 2026 – Around Alnif – Trilobites of the Maider Basin – Mharch Desert Oasis

STOP 5.1 – Cambrian Trilobite Fossils
STOP 5.2 – Ordovician Trilobite Fossils
STOP 5.3 – Devonian Trilobite Fossils
STOP 5.4 – Desert Oasis in Mharch

Hotel Information:

Auberge Camping Oasis El Mharech
QC6P+4J6, Sidi Ali, Morocco
https://www.tripadvisor.com/Hotel_Review-g304019-d1733903-Reviews-Auberge_Camping_Oasis_El_Mharech-Rissani_Meknes_Tafilalet_Region.html

Day 6: Wednesday, March 11th, 2026 – Maider Basin to Erg Chebbi Dunes (So many fossils, you are going to throw up…)

STOP 6.1 – Guelb el Mharch
STOP 6.2 – Aferdou el Mrakib
STOP 6.3 – Jebel el Krabis
STOP 6.4 – Fezzou for lunch
STOP 6.5 – Butte 760
STOP 6.6 – Jebel Amelane
STOP 6.7 – Eifelian-Givetian GSSP Golden Spike
STOP 6.8 – Merzouga

Hotel Information:

Mohayut Camp
4XMP+4MG, village hassi labiad, Merzouga 52202, Morocco

Day 7: Thursday, March 12th, 2026 – Kem Kem Dinosaur Beds & Filon 12 Mine

STOP 7.1 – Fulgerites!
STOP 7.2 – Kem Kem Dinosaur Mine
STOP 7.3 – Tadaout-Tizi n'Rsas anticline
STOP 7.4 – Silurian Orthoceras and Permian dikes
STOP 7.5 – Filon 12 Hematite Mine
STOP 7.6 – Late Devonian Anticline
Possible Stop – Camel Ride into the Erg Chebbi Dunes ***SAME HOTEL AS LAST NIGHT***

Day 8: Friday, March 13th, 2026 – Merzouga – Todra Gorge – Ouarzazate

STOP 8.1 – Hamar Laghdad (Kes Kes) Overlook
STOP 8.2 – Erfoud Orthoceras Quarry
STOP 8.3 – Erfoud Fossil Factory
STOP 8.4 – Todra Gorge Overlook
STOP 8.5 – Ouarzazate

Hotel Information:

Les Jardins de Ouarzazate
13 N9, Tarmigt 45000, Morocco
http://www.lesjardinsdeouarzazate.com/

Day 9: Saturday, March 14th, 2026 – Ouarzazate – High Atlas – Marrakech – Casablanca

STOP 9.1 – Mostly Driving back to Marrakech

STOP 9.2 – Marrakech

STOP 9.3 – Casablanca

Hotel Information:

Silver Suites Hotel & Spa Casablanca
9 Rue Kaddour El Alami, Casablanca 20250, Morocco
https://silversuiteshotel.com/

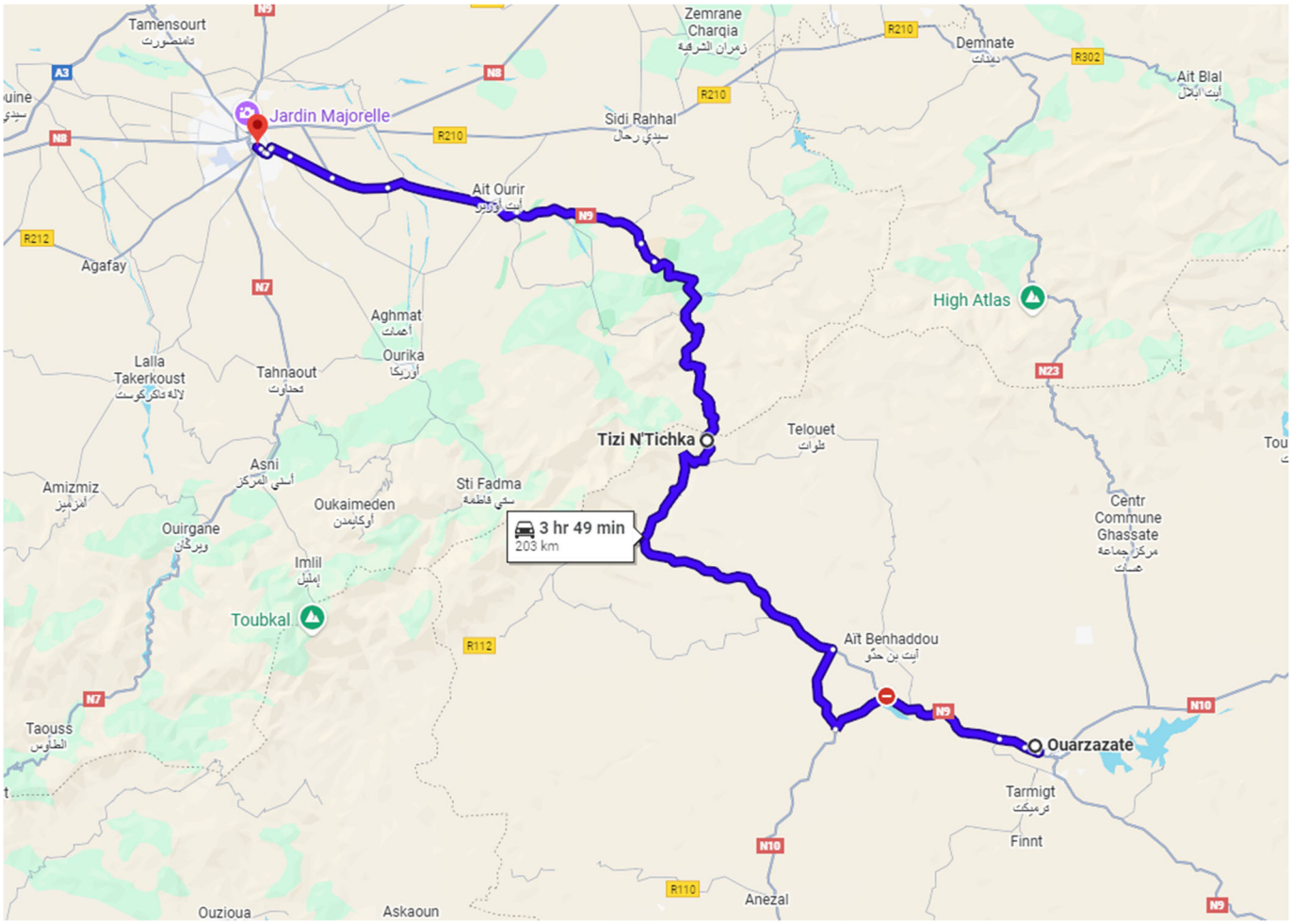

Return Flight

Flight #1: *Departure:* Royal Air Maroc, AT412, Saturday, March 14, 2026, 5:50PM, Marrakech (RAK) to Casablanca (CMN)
Arrival: Casablanca on Saturday, March 14, 2026 at 6:50PM
Long layover (~22hrs) for sight-seeing in Casablanca

Day 10: Sunday, March 15th, 2026 – Casablanca and flight home

Flight #2: *Departure:* Royal Air Maroc, AT218, Sunday, March 15, 2026, 3:25PM, Casablanca (CMN) to Washington DC (Dulles – IAD)
Arrival: Washington DC on Sunday, March 15, 2026, 7:45PM

Make sure you have made arrangements for a ride home from Dulles International Airport

VERY BRIEF HISTORY OF MOROCCO

Morocco, with a history stretching from ancient Berber roots through Roman and Arab influence, emerged as an independent kingdom in 789 under the Idrisid dynasty. It was later ruled by powerful Berber dynasties (Almoravids, Almohads) before becoming a French/Spanish protectorate in 1912, finally regaining independence in 1956 and establishing a constitutional monarchy under the Alaouite dynasty.

Key Historical Eras:

- **Ancient Period:** Originally inhabited by Berbers (Amazigh), the coast was settled by Phoenicians, Carthaginians, and Romans.
- **Islamic Conquest & Early Dynasties (7th–11th Century):** Arab forces arrived in the late 7th century, bringing Islam. The Idrisid dynasty (789) established the first independent Moroccan state, building cities like Fez.
- **Berber Empires (11th–16th Century):** The Almoravid and Almohad dynasties united the region, controlling North Africa and parts of Spain, with Marrakech as a key hub.
- **The Alaouite Dynasty (1631–Present):** The current ruling dynasty came to power in the 17th century, maintaining independence for centuries, even becoming the first nation to recognize the United States in 1777.
- **Colonial Rule & Independence (1912–1956):** Morocco was divided into French and Spanish protectorates in 1912. Resistance led to independence in 1956.
- **Modern Era (1956–Present):** Under Hassan II and currently King Mohammed VI (since 1999), Morocco has functioned as a constitutional monarchy, navigating issues like the Western Sahara dispute.

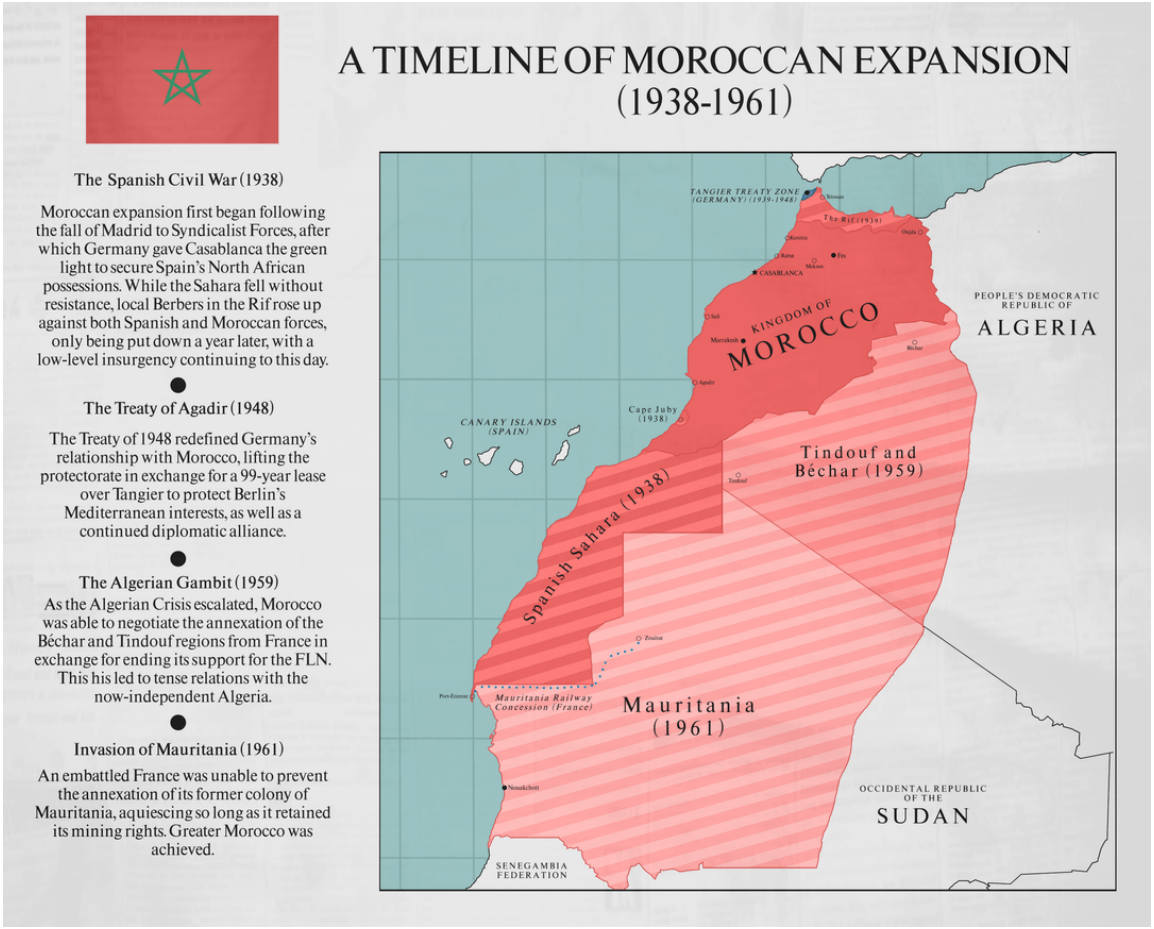

MOROCCAN FOODS

I found this Moroccan food guide that was pretty good…
https://www.celebritycruises.com/blog/moroccan-food

Moroccan food is a rich blend of flavors and traditions, including Arabic, Andalusian, and Mediterranean influences. At its heart is a blend of spices, called ras el hanout, dominated by cumin, coriander, turmeric, cinnamon, and saffron.

Ras el hanout means "head of the shop", meaning the best on offer in the bazaar. Every cook has their own mix, often handed down through generations, with some said to involve up to 100 ingredients.

The art is in balancing the flavors, without overwhelming any ingredient. That's a philosophy that extends to the communal meals that are a symbol of Morocco's hospitality and warm social tolerance.

Tajine

Morocco is known for tagine, the quintessential dish named after the conical earthenware pot in which it is cooked. The conical lid of a tajine/tagine allows steam from cooking to condense and fall back into the food.

This self-basting process produces really tender meat and vegetables, the flavors of which are infused together with the typical Moroccan spice mix. Common combinations include lamb with prunes or chicken with lemon and olives.

A distinctive feature of tajines is the contrast of preserved fruit, such as lemon or prunes, with the meat and vegetables. The tajine is brought to the table, where the dish is eaten with bread to soak up the flavourful sauce.

Couscous

If you're looking for Morocco's national food, couscous might well be it. Its base is hand-rolled grains of semolina, steamed over a rich broth and kept fluffy by constant stirring.

The light, airy couscous is then served with toppings of cooked vegetables and tender meats such as lamb or chicken. The broth is put out separately to add according to personal taste.

It's traditional to have couscous as a family meal after visiting the mosque on Friday afternoons, eating it by hand or with a spoon.

Pastilla/Bastilla

Once made with pigeon but now usually chicken, pastilla—or bastilla—is a savory-sweet filled pastry treat. The meat, combined with almond, egg, and spices, is cooked in warka, a phyllo-like layered wrapping.

The finished pastry is dusted with powdered sugar and cinnamon. Biting through the crisp, sweet shell, you hit the tender, spicy meat in a sensational mix of tastes and textures.

The dish has its roots in Andalusian cuisine, brought by Moors fleeing Spain in the 15th century. Taking great skill to do well, modern variations include seafood or vegetarian fillings.

Harissa

Harissa is a red, chili-hot paste, one Algeria claims as its own, but Morocco has its own, milder regional versions. It's made from a mix of roasted red peppers, chili pepper, herbs, and various spices, such as cumin and coriander.

These are all mixed with olive oil to create a distinctive, red paste that is a common seasoning for many dishes. It has a complex balance of heat, earthiness, and fragrance that can become addictive.

Every region of Morocco has its own variations, including ones that add ingredients such as preserved lemon. A preference for less heat and more depth reflects the subtleties of Moroccan cuisine.

Harira

Harira is a traditional Moroccan soup, a staple for breaking the Ramadan fast but enjoyed year-round. It's a hearty mix of lentils, chickpeas, and often lamb, with broken spaghetti, onion, celery, and a tomato base.

The soup is thickened with flour and egg, giving it a distinct mouth feel. Its flavor is enhanced by spices such as turmeric, cinnamon, ginger, and pepper.

The addition of fresh cilantro, and parsley—and a dash of lemon—is also key to harira's appeal. It's served with dates and chebakia, honey-coated sesame cookies, or hard-boiled eggs.

Khobz

A warm loaf of khobz bread is an essential at every Moroccan meal. Flat and round, it has a distinctive crusty top traditionally patterned with a fork.

Khobz has to be soft enough to tear into chunks, yet firm enough to use in scooping up food, especially juices. It's a real skill to get it right from a simple recipe of flour, yeast, salt, and water.

Semolina is added to help give some of that necessary texture. Anise or cumin seeds may also be added, among several regional variations.

Msemmen

Another traditional flatbread, msemmen differs from Khobz in having a multi-folded dough, like puff pastry. The Moroccan equivalent of a pancake, it's as light and delicious as it sounds.

The basic dough is similar to khobz but is folded into layers with butter or oil between each. Rolled thin, it's cooked on a hot griddle until crispy on the outside.

Among the popular street foods in Morocco, many vendors will make it fresh in an appetizing display of skill. It's eaten for breakfast or as a snack with mint tea and comes with a choice of fillings or toppings from ground beef to honey.

Rfissa

This traditional dish combines shredded msemmen—layered flatbread—or day-old bread with a rich lentil and chicken stew. It's seasoned with a blend of spices that includes ginger, pepper, turmeric, and fenugreek.

Time-intensive to prepare, rfissa is a special occasion food in Morocco. It is often given to new mothers, as the fenugreek is believed to give strength and boost milk production.

The slow-cooked chicken and lentil broth, soaked up by the layered bread, gives a satisfying mix of textures. The fenugreek helps thicken the dish while adding its distinctive bitter-sweet flavor.

Bissara

Bessara is a hearty soup with a base of dried fava beans or split peas, simmered to a smooth, thick consistency. It's flavored with garlic, olive oil, cumin, and paprika.

Like any soup, long, slow cooking is essential for the best flavor. The dish is particularly popular in northern Morocco and during the winter months.

Comfort food at its best, bissara is often eaten at breakfast with fresh bread. You'll find street vendors selling it in the morning hours.

Loubia

Stewed white beans might sound very bland, but the addition of Moroccan spices lifts it to another level. Comfort food at its most basic, loubia is eaten with bread at any time of the day.

The beans are soaked overnight, then slowly cooked with fresh tomatoes, ginger, paprika, and cumin. Garlic and fresh herbs—and even a dash of chili—add even more depth of flavor.

While loubia is a vegetarian dish, it might also have some meat or meat stock added. It's eaten with a spoon, or by using crusty khobz bread as a scoop.

Zaalouk

Zaalouk is a staple of Moroccan cuisine, based on roasted or grilled eggplant. Cooked until soft and smoky, the eggplant is mashed with cooked tomato.

Flavored with garlic, cumin, and paprika, the dish is then cooked slowly with olive oil while it thickens. Zaalouk can be served hot or cold, usually as part of a mezze platter.

Typically eaten as a dip with fresh bread, this vegetable dish is both healthy and delicious. The mix of smoky eggplant, rich tomato, and spices creates a rich, complex taste.

Mechoui

A meal for celebrations and festivals, mechoui is a whole roasted lamb. It's eaten communally, with the tender meat being torn off using portions of flatbread.

The lamb is marinated in a mix of cumin, paprika, black pepper, and other spices, often with saffron as well. It's then cooked for hours on a spit or in an oven until the meat falls off the bone.

Ideally, the skin is still crisp but not burnt, so careful cooking is needed. Typical seasoning is salt and cumin, available to diners to add to individual taste.

Tangia

Another dish named after the urn-shaped pot it is cooked in, tangia is simpler than tajine. Often called a "bachelor's meal", it's usually just meat, normally lamb, and preserved lemon.

Traditionally, the pot was prepared in the morning and left at the local hammam. It was then cooked in the fire that heated the bathhouse water.

This slow cooking method blends the rich spice seasoning with the juices of the tenderized meat and contrasting fruit. The resulting dish—comfort food at its finest—is eaten straight from the pot with fresh bread.

Sardines Mchermel

The key to this popular Moroccan dish is a marinade of chermoula. This is a mix of cilantro, parsley, garlic, cumin, paprika, and preserved lemon in a base of olive oil.

Fresh sardines are stuffed with chermoula and covered in more before being baked in a tajine. The tajine will also hold a mix of vegetables, such as peppers, carrots, and olives.

The dish can be served hot or cold, as a main course or as part of a mezze spread. Of course, some fresh khobz is essential to make sure you can soak up all the rich juices.

Makouda

These deep-fried potato balls are a popular street food in Morocco and throughout North Africa. Mashed potato is mixed with flour and herbs, then rolled into balls, patties, or croquettes, and fried until golden.

The result can be eaten as a snack, starter, or as a meal when served in bread. The makouda will be put into a baguette or wrapped in khobz and topped with various fillings.

Harissa is a popular filling, with its spiciness nicely complementing the carb-heavy sandwich. Other toppings range from tuna and olives to simple lettuce and tomato.

Merguez

This famous Moroccan sausage is made with lamb, or beef—but usually both—seasoned with harissa, paprika, cumin, fennel, or other spices. Grilled, it is best eaten with fresh khobz bread but you'll find it served many other ways.

The sausage has a distinct red color from the spicy harissa and paprika. Its heat lends itself to its popular pairing with eggs or bread.

While often part of a mixed grill, you will also see merguez in tajines, couscous, and stews. Served either whole or sliced, it is also crumbled into other dishes as a tasty seasoning.

Mint Tea

Mint tea is as much a symbol of Moroccan hospitality as it is a refreshing drink on a hot day. It's traditionally made with fresh mint leaves and Chinese gunpowder green tea.

The hot tea is also usually made with sugar, although you can ask for it without in a restaurant. Be warned, it will taste very bitter without at least a touch of sugar.

Making the tea is a fascinating ritual, using a special pot called a "berrad". It's poured from a height to create a foam, with three glasses per person being the traditional protocol.

Chebakia

Chebakia is a flower-shaped cookie made from a dough with anise and sesame seeds, cinnamon, and saffron. This sweet pastry is another food traditionally associated with Ramadan, along with harira soup.

Folded into the shape of a rose, it is deep-fried until golden. Each is then soaked in honey and sprinkled with sesame seeds.

The result combines crispness, sweetness from the honey and flavor from the spices. After all that, the sesame seeds add yet another hit of deliciousness.

Kaab El Ghazal

"Gazelle Horns" are croissant-shaped cookies now popular throughout the Arab world but originating in Morocco. A cinnamon-rich almond paste filling is wrapped in very thin, orange blossom-flavored pastry and topped with crushed almonds.

The curved shape, with a serrated edge, gives these delicious cookies their name. Often eaten with mint tea, they are commonly served during festivities.

For weddings, it is traditional for the bride's family to prepare kaab el ghazal to show off their cooking skills. With recipes handed down through generations, they have a special place in Moroccan food culture.

RAMADAN

We will be in Morocco (a majority Muslim country) during Ramadan. This year Ramadan falls between February 18th, 2026 to March 19th, 2026. It is important that we are respectful while we are visiting their country. Learning a little about Ramadan is a good start.
The following is taken from Wikipedia….

Introduction

Ramadan is the ninth month of the Islamic calendar. It is observed by Muslims worldwide as a month of fasting (sawm), communal prayer (salah), reflection, and community. It is also the month in which the Quran is believed to have been revealed to the Islamic prophet Muhammad. The annual observance of Ramadan is regarded as one of the five pillars of Islam and lasts twenty-nine to thirty days, from one sighting of the crescent moon to the next.

Fasting from dawn to sunset is obligatory (fard) for all adult Muslims who are not acutely or chronically ill, travelling, elderly, breastfeeding, pregnant, or menstruating. The predawn meal is referred to as suhur, and the nightly feast that breaks the fast is called iftar. Although rulings (fatawa) have been issued declaring that Muslims who live in regions with a midnight sun or polar night should follow the timetable of Mecca, it is common practice to follow the timetable of the closest country in which night can be distinguished from day.

The spiritual rewards (thawab) of fasting are believed to be multiplied during Ramadan. Accordingly, during the hours of fasting, Muslims refrain not only from food and drink, but also from all behavior deemed to be sinful in Islam, devoting themselves instead to prayer and study of the Quran.

Etymology

The word Ramadan derives from the Arabic root R-M-Ḍ (ر-م-ض) 'scorching heat', which is the Classical Arabic verb ramiḍa (رَمِضَ) meaning 'become intensely hot – become burning; become scorching; be blazing; be glowing'.

Ramadan is thought of as one of the names of God in Islam by some, and as such it is reported in many hadiths that it is prohibited to say only "Ramadan" in reference to the calendar month and that it is necessary to say "month of Ramadan", as reported in Sunni, Shia, and Zaydi sources. However, the report has been graded by others as Mawḍūʿ (fabricated) and inauthentic.

In the Persian language, the Arabic letter ض (Ḍād) is pronounced as /z/. The Muslim communities in some countries with historical Persian influence, such as Afghanistan, Azerbaijan, Iran, India, Pakistan and Turkey, use the word Ramazan or Ramzan. The word Romzan is used in Bangladesh.[38]

History

> *Ramadan is the month on which the Quran was revealed as a guide for humanity with clear proofs of guidance and the standard ˹to distinguish between right and wrong˺. So whoever is present this month, let them fast. But whoever is ill or on a journey, then ˹let them fast˺ an equal number of days ˹after Ramaḍân˺. Allah intends ease for you, not hardship, so that you may complete the prescribed period and proclaim the greatness of Allah for guiding you, and perhaps you will be grateful.*—
> Surah Al-Baqara 2:185

Muslims hold that all scriptures were revealed during Ramadan, the scrolls of Abraham, Torah, Psalms, Gospel, and Quran having been handed down during that month. Muhammad is said to have received his first quranic revelation on Laylat al-Qadr, one of five odd-numbered nights that fall during the last ten days of Ramadan.

Although Muslims were first commanded to fast in the second year of Hijra (624 CE), they believe that the practice of fasting is not in fact an innovation of monotheism but rather has always been necessary for believers to attain fear of God (taqwa).[Quran 2:183] They point to the fact that the pre-Islamic pagans of Mecca fasted on the tenth day of Muharram to expiate sin and avoid drought. Philip Jenkins argues that the observance of Ramadan fasting grew out of "the strict Lenten discipline of the Syrian Churches", a postulation corroborated by other scholars, including theologian Paul-Gordon Chandler, but disputed by some Muslim academics. The Quran itself emphasizes that the fast it prescribes had already been prescribed to earlier biblical communities (2:183), even though an explicit intertext for this pre-Islamic practice does not exist.

Important dates

The Islamic calendar is a lunar one, where each month begins when the first crescent of a new moon is sighted. The Islamic year consists of 12 lunar cycles, and consequently it is 10 to 11 days shorter than the solar year, and as it contains no intercalation,[c] Ramadan migrates throughout the seasons. The Islamic day starts after sunset. The estimated start and end dates for Ramadan, based on the Umm al-Qura calendar of Saudi Arabia. *This year Ramadan falls between February 18th, 2026 to March 19th, 2026.*

Many Muslims insist on the local physical sighting of the moon to mark the beginning of Ramadan, but others use the calculated time of the new moon or the Saudi Arabian declaration to determine the start of the month. Since the new moon is not in the same state at the same time globally, the beginning and ending dates of Ramadan depend on what lunar sightings are received in each respective location. As a result, Ramadan dates vary in different countries, but usually only by a day. This is due to the cycles of the moon; the moon may not meet the criteria to qualify as a waxing crescent, which delineates the change in months, at the time of sundown in one location while later meeting it in another location. Astronomical projections that approximate the start of Ramadan are available.

In Shia Islam, one of the special dates of this month is the day of the assassination of Ali, the fourth Rashidun caliph and the first Shia Imam. Ali was struck during morning prayer on the 19th day of Ramadan, 40 AH, and he died on the 21st day of the month. They engage in mourning and prayer on these nights, especially in Iran.

Beginning

Because the hilāl, or crescent moon, typically occurs approximately one day after the new moon, Muslims can usually estimate the beginning of Ramadan; however, many Muslims prefer to confirm the opening of Ramadan by direct visual observation of the crescent.

Laylat al-Qadr

The Laylat al-Qadr (Arabic: ليلة القدر) or "Night of Power" is the night that Muslims believe the Quran was first sent down to the world, and Muhammad received his first quranic revelation from it. The night is considered to be the holiest night of the year. It is generally believed to have occurred on an odd-numbered night during the last ten days of Ramadan; the Dawoodi Bohra believe that Laylat al-Qadr was the twenty-third night of Ramadan.

Eid

The holiday of Eid al-Fitr (Arabic: عيد الفطر), which marks the end of Ramadan and the beginning of Shawwal, the next lunar month, is declared after a crescent new moon has been sighted or after completion of thirty days of fasting if no sighting of the moon is possible. Eid celebrates the return to a more natural disposition (fitra) of eating, drinking, and marital intimacy.

GEOLOGIC OVERVIEWS

An Outline of the Geology of Morocco

The following publication is as follows:

Michard, A., Frizon de Lamotte, D., Saddiqi, O., and Chalouan, A. (2008) An Outline of the Geology of Morocco. In Michard, A. et al, (Eds.) Continental Evolution: The Geology of Morocco. Lecture Notes in Earth Sciences 116, Springer-Verlag, Pgs. 1-31.

Chapter 1
An Outline of the Geology of Morocco

A. Michard, D. Frizon de Lamotte, O. Saddiqi and A. Chalouan

Morocco is one of the most fascinating lands in the world for studying geology. It is a friendly country, provided with a good network of roads. Most of Morocco being situated within the Mediterranean to Sub-Saharan climatic zones, with a mean annual precipitation ranging from 300 to 600 mm, it offers wide landscapes, with subsurface rocks exposed in splendid outcrops. Last but not least, Morocco is located at a triple junction (Fig. 1.1) between a continent (Africa), an ocean (the Atlantic) and an active plate collision zone (the Alpine belt system). This results in a rugged topography with a wide range of outcropping terranes spanning from Archean to Cenozoic in age, as well as diverse tectonic systems from sedimentary basins to metamorphic fold belts. Minerals and fossils from Morocco are curated in museums the world over. Finally, it is worth emphasizing that natural resources extracted from the Moroccan subsoil are important for the national economy (phosphate, Ag, Pb, Zn, barite, fluorspar, etc.). At the moment, there is also active offshore exploration for oil and gas.

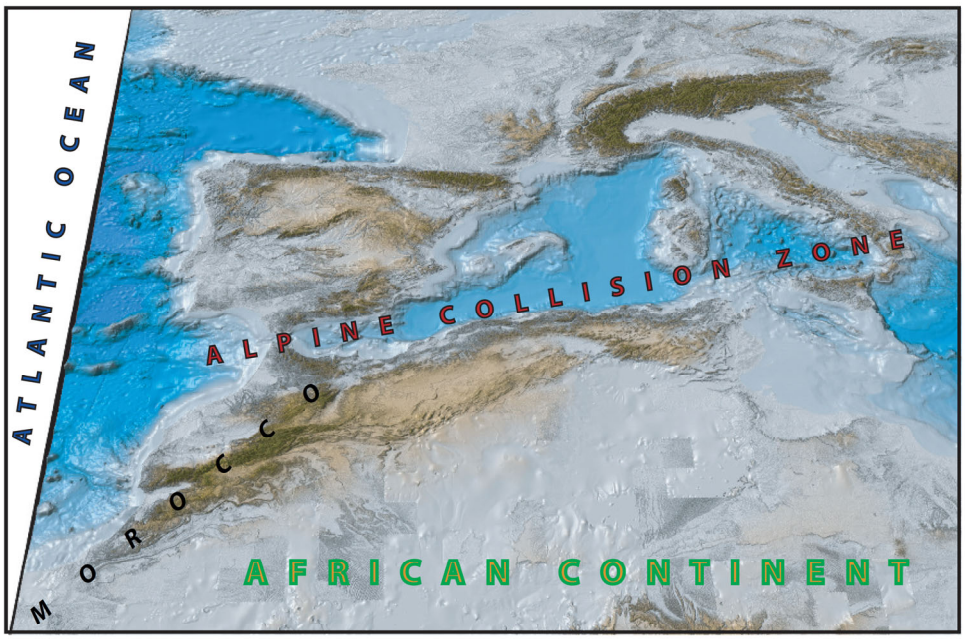

Fig. 1.1 Location of Morocco at the triple junction of the African continent, Atlantic Ocean and Alpine subduction-collision zone. Numerical modelling of elevation and bathymetry data, oblique view of the West Mediterranean area, by courtesy of N. Chamot-Rooke (E.N.S., Paris)

1.1 Topography and Major Geological Domains

At first sight, the topography of Morocco is comparable with that of the central and eastern Maghreb, i.e. Algeria and Tunisia (Fig. 1.2). To the north, the Rif Range extends along the Mediterranean coast (Alboran Sea), maintaining the continuity

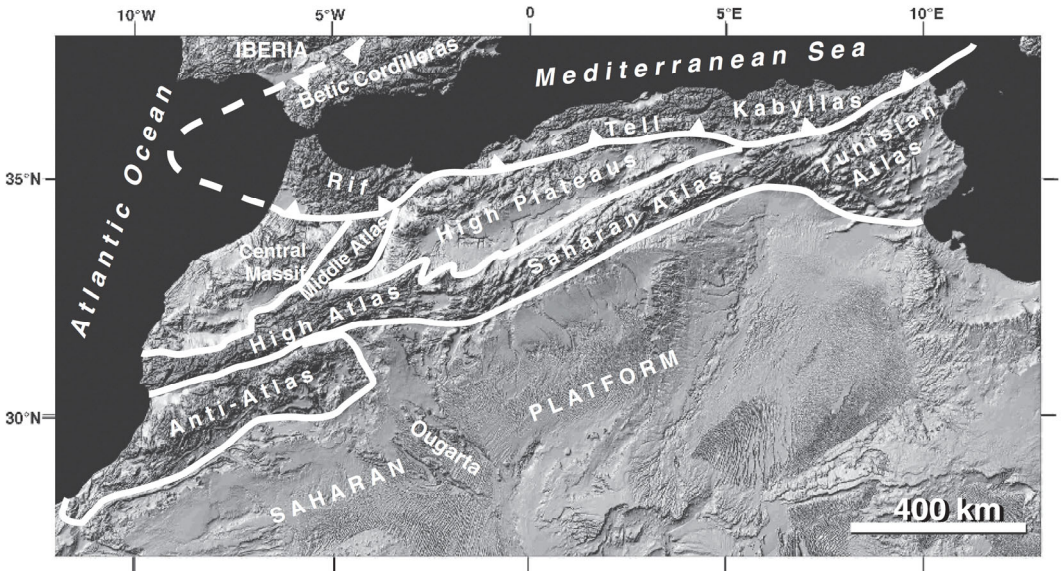

Fig. 1.2 Physiography of northwestern Africa with limits of the main natural regions and young mountain belts. Morocco extends approximately west of the meridian 2°W, and further south of the lower border of the picture (see Fig. 1.2)

of the Kabylian-Tellian belts (Maghrebides) up to the Strait of Gibraltar. South of these coastal ranges, a domain of elevated plateaus or mesetas occur (Algerian High Plateaus and Oran Meseta, Moroccan Meseta), including intramontane basins (Missour and High Moulouya basins). Then the Atlas system rises up, providing a northern boundary to the dominantly low-elevation Saharan domain.

However, Morocco differs from Algeria and Tunisia in several ways. The elevation of most of the country (except the Rif and Atlantic areas) is particularly high (Fig. 1.3). The High Atlas displays several massifs close to 4000 m high, including the highest peak of northern Africa (Jebel Toubkal). A branch of the Atlas system extends obliquely across the mesetan domain, namely the Middle Atlas, which exceeds 3000 m in elevation. The northern, sub-Saharan border of the main Saharan domain also rises and forms a massive mountain belt, the Anti-Atlas, achieving up to 2700 m in Jebel (J.) Saghro and even more in the J. Siroua (Sirwa) recent

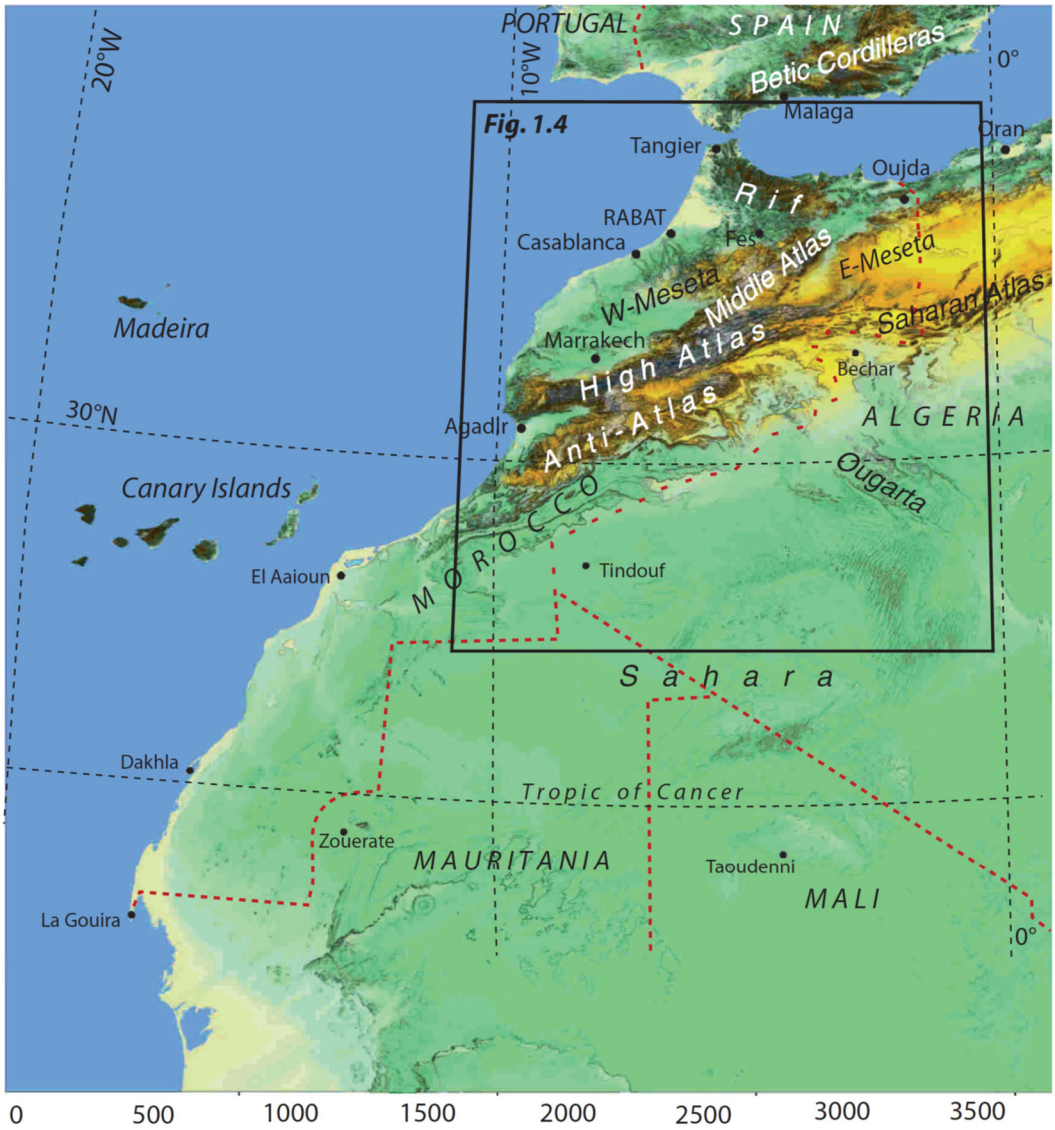

Fig. 1.3 Elevation map of Morocco and neighbouring countries from GTOPO30 database. State borders are indicative

volcano (3300 m). The elevation decreases westward, away from the Middle Atlas mountains to the Central Massif of the Moroccan Meseta, towards the Atlantic coastal basins and finally to the Atlantic abyssal plains. South of the Anti-Atlas and Saghro mountains, in the Saharan "hamadas" (plateaus), elevation decreases both southward, from ca. 1000 m to less than 400 m (Tindouf Basin), and westward to less than 200 m, close to the Atlantic (Tarfaya Basin). Neogene basins are shown along the High Atlas borders (Haouz-Tadla and Bahira Basins to the north, Souss and Ouarzazate Basins to the south) or north and east of the Middle Atlas (Guercif and Missour Basins), whereas a large foredeep basin (Gharb) extends southwest of the Rif belt.

In contrast with Algeria and Tunisia, the continental basement of North Africa is more uplifted in Morocco than in the countries further east, causing Paleozoic and Precambrian rocks to outcrop extensively (Fig. 1.4). Paleozoic rocks form large

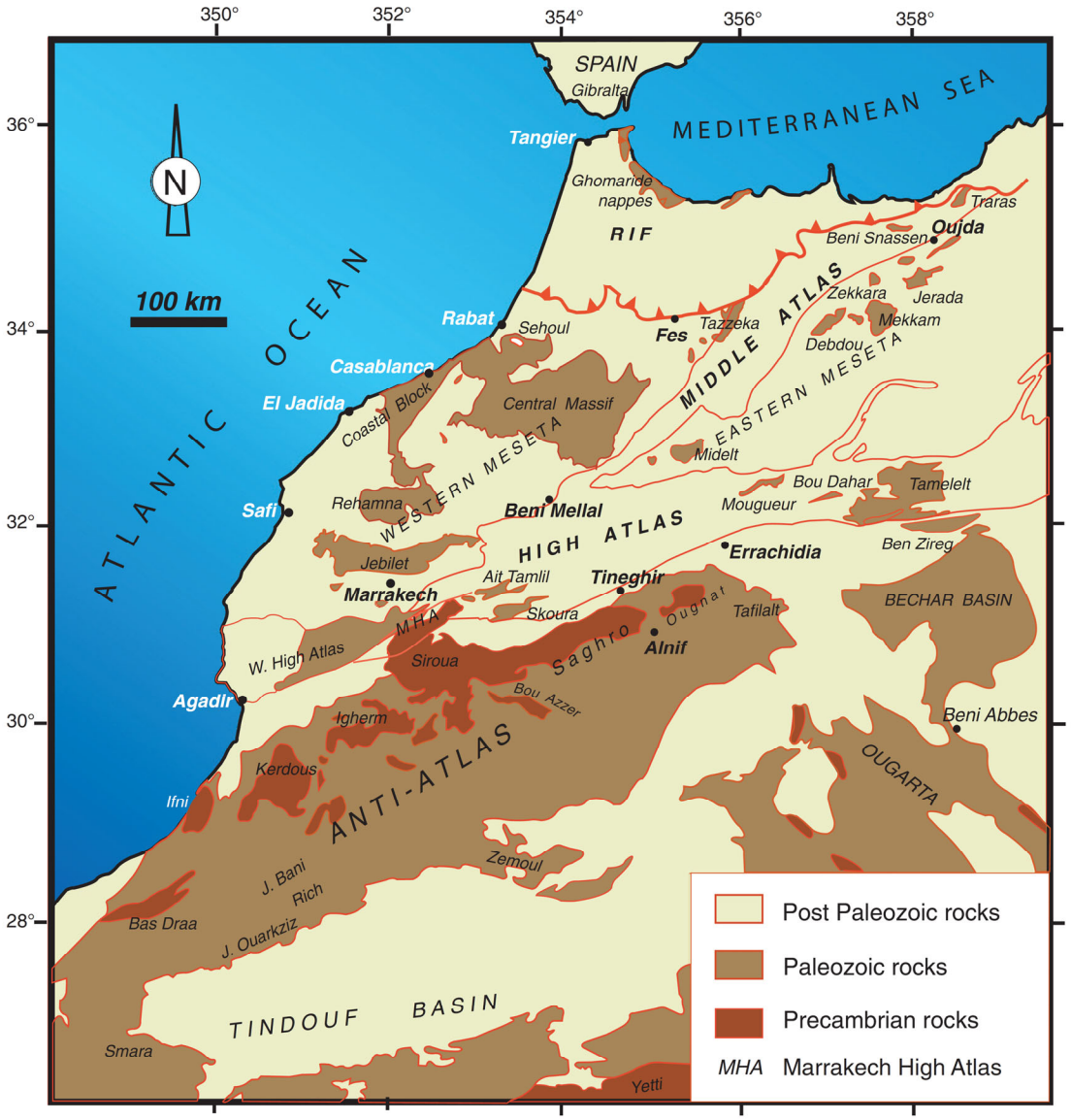

Fig. 1.4 Extension of the Paleozoic and Precambrian oucrops in Morocco (Northern Provinces) and westernmost Algeria (Traras, Ben Zireg, Béchar), modified from Piqué and Michard (1989)

culminations within the Mesozoic Atlas domain, whereas Precambrian rocks form similar culminations ("boutonnières") in the middle of the Anti-Atlas Paleozoic terranes. Paleozoic units also occur in the Maghrebide internal zones, similarly developed in Morocco (Alboran domain) and Algeria (Kabylias), but they belong to a disrupted allochthonous terrane ("AlKaPeCa") and not to the African basement itself.

1.2 Mesozoic-Cenozoic Plate Tectonic Setting

References: The most general works concerning the Alpine Tethys/Central Atlantic plate tectonics are those by Dercourt et al. (1993), Rosenbaum et al. (2002), and Stampfli & Borel (2002). More specific references for Morocco are Piqué & Laville (1995), Frizon de Lamotte et al. (2000), Le Roy & Piqué (2001), Michard et al. (2002), Olsen et al. (2003), Sahabi et al. (2004), Knight et al. (2004), Marzoli et al. (2004), Verati et al. (2007), with references therein.

All the geographic and geological peculiarities of Morocco mentioned above are related to its particular location at the northwestern corner of Africa during the ultimate Wilsonian cycle of plate tectonics. This Mesozoic-Cenozoic cycle begins with the Pangea break-up, goes on with the opening of the Central Atlantic and Alpine Tethys Oceans, and ends with the Tethys closure and Alpine belt formation (Fig. 1.5).

The rifting stage is initially recorded during the Middle-Late Triassic by the development of evaporite basins on both sides of the Central Atlantic rift, as well as in the Atlas and external Maghrebides areas (Tethyan basins). The climax of the rifting stage is marked by a short-lived, but voluminous basaltic magmatism, which defines the Central Atlantic Magmatic Province (CAMP), and probably caused the major climatic and biologic crisis of the Triassic-Jurassic boundary. Magmatism was particularly developed on the African side of the rift where it is recorded by dikes, sills and lava flows, mostly dated at 200 ± 1 Ma (Figs. 1.6A–B, 1.7). Rifting was asymmetric, with a SW-dipping main detachment (Fig. 1.6C) that caused a strong uplift of the Moroccan shoulder of the rift. This setting resulted in the extreme reduction of the Mesozoic cover in west Morocco, except in the Atlantic margin itself and Atlas rift basins, and the extensive exposures of Paleozoic and even Precambrian rocks (Fig. 1.4).

The relative position of Africa with North America by the end of the rifting process – with Morocco opposite Nova Scotia, and the age of the earliest spreading stage have recently been better constrained by fitting the east American and west African margin anomalies (Fig. 1.8), and by dating these oceanic magnetic anomalies to the end of the evaporite deposition (Sinemurian, 195–190 Ma). After this earliest, post break-away stage, spreading developed during the Jurassic in the Central Atlantic and Ligurian (Alpine) Tethys – both connected through a transform fault system north of Morocco (Fig. 1.9A). During the Cretaceous, the onset of spreading in North Atlantic resulted in Iberia's eastward displacement, and eventually brought about its anticlockwise rotation (Fig. 1.9B). At that time

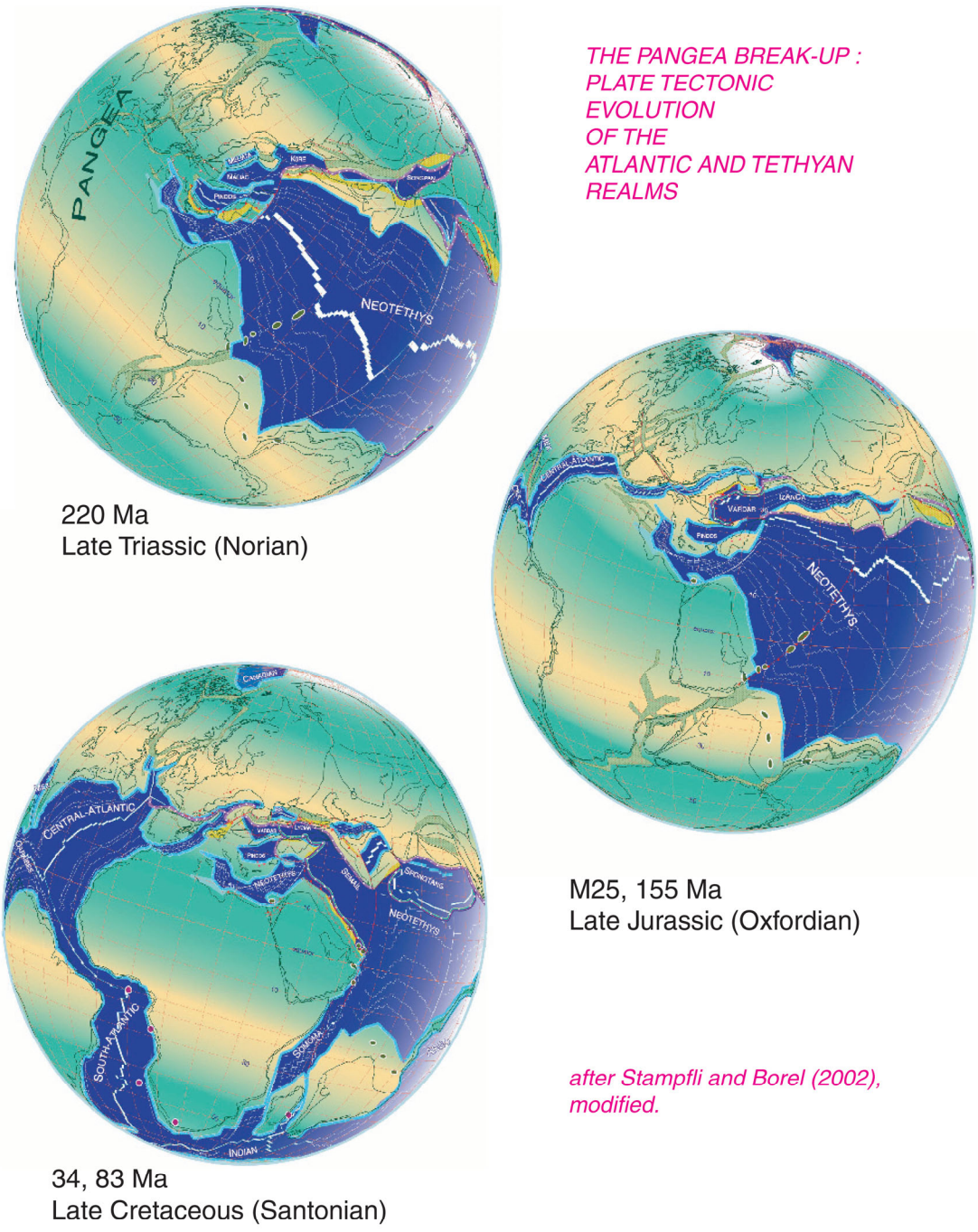

Fig. 1.5 The break-up of the Pangea super-continent and further plate tectonics of the Atlantic and Tethyan domains, after Stampfli & Borel (2002), modified. M25, 34: oceanic anomalies. Rifts are shown as yellow-greenish strips; passive margins are underlined in light blue, active margins in red. Seamounts are shown as large red spots

(Late Cretaceous), due to the opening of the South Atlantic, Africa ceased to translate parallel to southern Eurasia and began to converge with it. This resulted in the Pyrenean-Alpine and Maghrebide-Atlasic shortening events (Figs. 1.9B–D), i.e. in the closure of the Tethyan basins and correlative building of the mountain belts that characterize Morocco. The latter stage (Fig. 1.9D) is also the onset of the

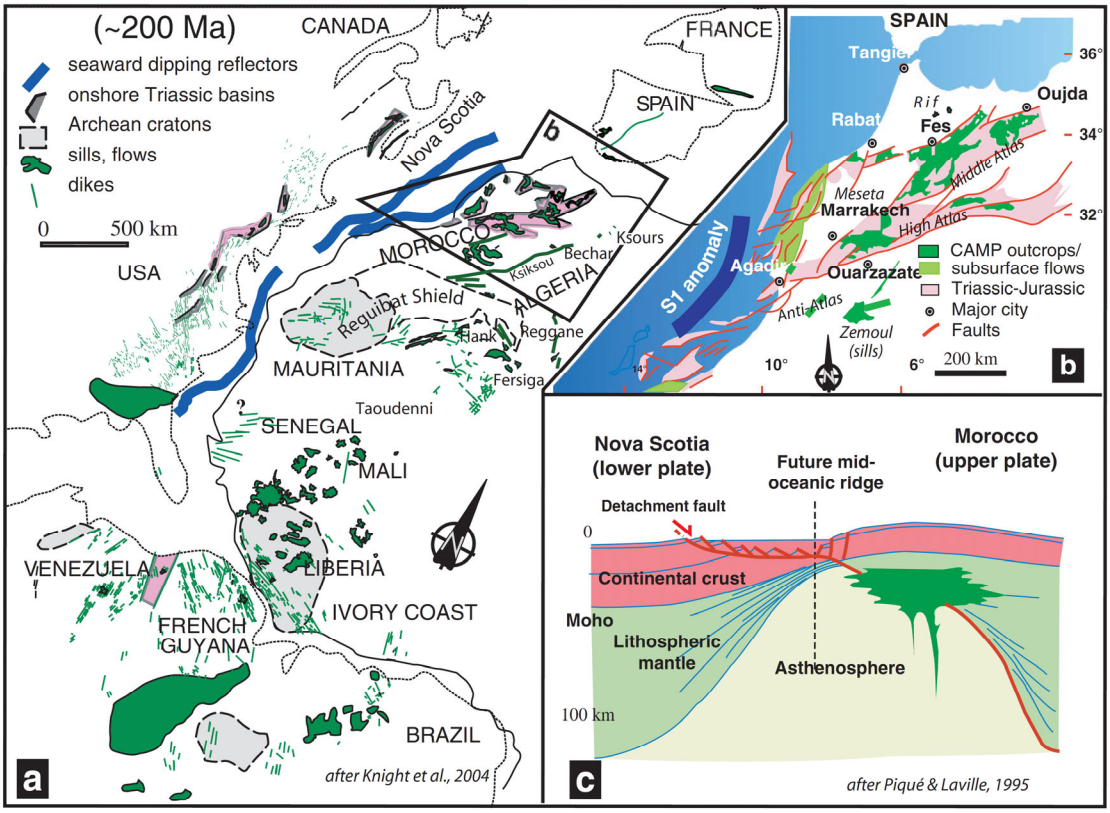

Fig. 1.6 The Atlantic and Neo-Tethyan rifting at the Triassic-Jurassic boundary. **A**: Extension of the Central Atlantic Magmatic Province (CAMP) across four Gondwanan continents (A), and zoom on the Moroccan area (B), after Knight et al. (2004), modified after Chabou et al. (2007) for SW Algeria. **C**: Asymmetric rifting resulted in strong uplift of the rift shoulder on the African side; schematic restoration after Piqué & Laville (1995), modified

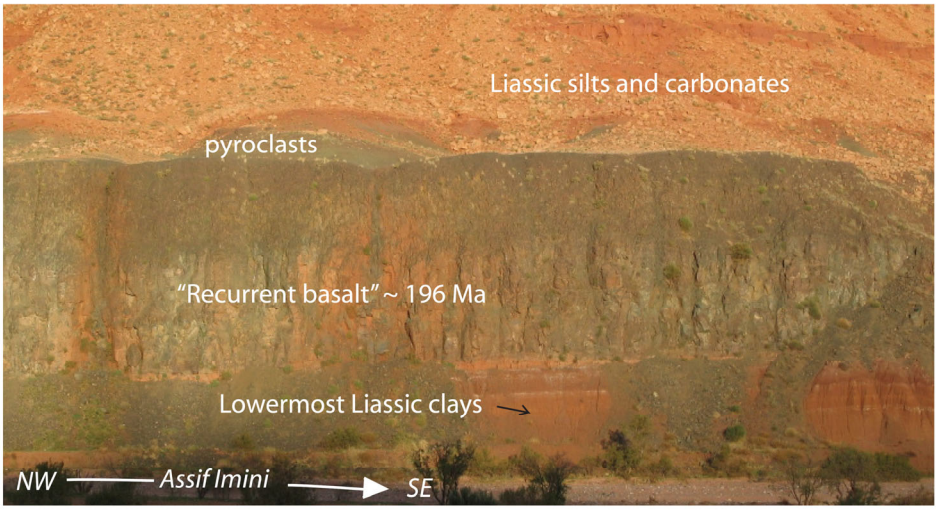

Fig. 1.7 Basaltic trapp on top of (Rhaetian)-Hettangian red clays south of the Marrakech High Atlas. Note the rough prismatic structure within the flow, and the thin pyroclastic level on its top. This is the latest basalt flow ("recurrent basalt") of the High Atlas rift, dated at ~196 Ma (Verati et al., 2007). The pinky deposits above are poorly dated Liassic dolomitic limestones and sandy marls of the post-rift sequence. Tiourjdal, Assif Imini valley, SE of Agouim, 70 km west of Ouarzazate

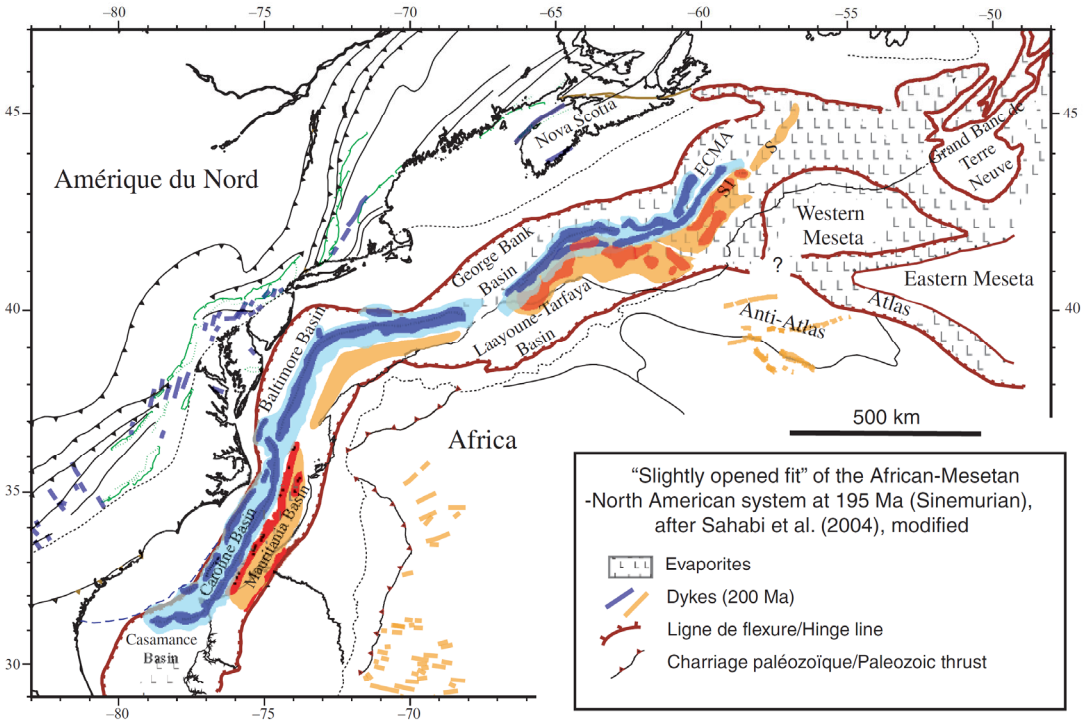

Fig. 1.8 Slightly opened fit of the Africa-Moroccan Meseta-America system at 195 Ma (Sinemurian), after Sahabi et al. (2004), modified. American structures in blue, African ones in red. Large fitted stripes: magnetic anomalies (MA), ECMA (East Coast MA) and S1-S' (West African Coast MA). The evaporite basins on both sides of these anomalies and in the Atlas domain are limited by the hinge lines. Also shown: Triassic-Jurassic dikes (thick bars) and Paleozoic structures (black lines with teeth). The Moroccan Meseta is slightly disconnected from the West African Craton in order to take into account the Atlasic shortening

Ligurian ocean subduction whose roll-back controlled the opening of the Neogene west Mediterranean basins. As Morocco was pinned against Iberia throughout the Late Cretaceous-Cenozoic (whereas wide oceanic areas still occurred to the east), convergence occurred later and at a slower rate in the Moroccan transect than in the Lybian and Egyptian ones (Fig. 1.10). This must be kept in mind to understand the lateral changes in the Alpine belt system from east (Hellenides, Alps) to west (Rif-Betic or Gibraltar Arc), and in particular, the scarcity of oceanic crust remnants in the latter orogen.

Thus, the particular position of Morocco at the NW corner of Africa accounts for the striking differences between its Mediterranean and Atlantic margins. The latter continued up to present being a passive margin. Subsidence allowed sediments to accumulate from the Triassic onward along this margin in the Moroccan Coastal Basins, which were only partially deformed and emergent during the Neogene. The high level seas of the Late Cretaceous-Eocene flooded the majority of Morocco, giving birth to the marly limestones of the Saharan hamadas and eastern Atlas domain, and more interestingly, to the phosphate deposits next to the continental slope ("Plateau des Phosphates" of the western Meseta, Tarfaya Basin). In contrast, the Tethyan margin was associated to a transform system during the Mesozoic, and changed into an oblique subduction-collision margin during the Eocene. The present

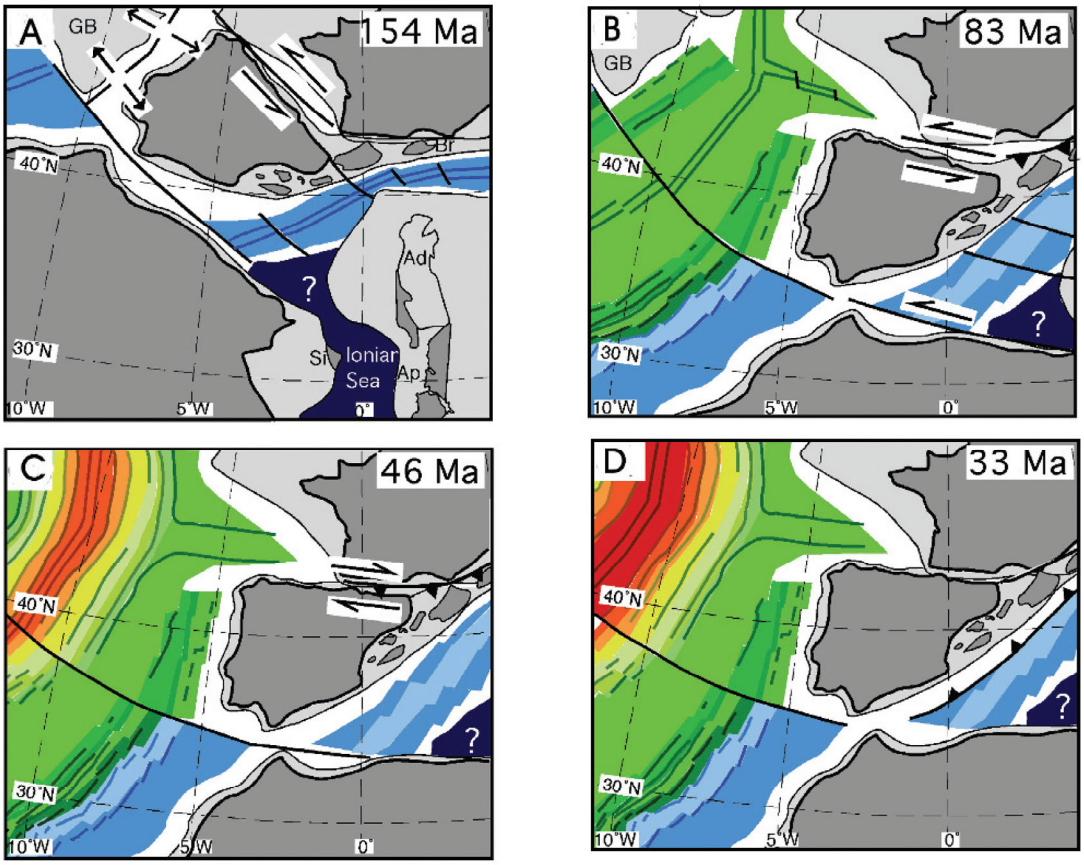

Fig. 1.9 Restoration of the evolution of Central-Northern Atlantic and western Tethys regions, after Rosenbaum et al. (2002), modified. **A**: Late Jurassic; **B**: Late Cretaceous; **C**: Middle Eocene; **D**: Early Oligocene. Ad: Adria; Ap: Apulia; Br: Briançonnais; GB: Grand Banks; Si: Sicily

Mediterranean margin formed during the Neogene, and displays the characteristics of an active margin.

1.3 Continental Growth: The Successive Fold Belts

References: Fundamentals concerning this section are available in Michard (1976), whereas some of the recent references used hereafter are as follows: (i) concerning the Archean, Eburnian and Pan-African belts, Bertrand & de Sá (1990), Black et al. (1994), Villeneuve and Cornée (1994), Dalziel (1997), Ennih and Liégeois (2001, 2003, 2008), Cordani et al. (2003), Fabre (2005), Gasquet et al. (2005), Liégeois et al. (2005), Scholfield et al. (2006), Scholfield & Gillespie (2007); (ii) concerning the Phanerozoic belts, Frizon de Lamotte et al. (2004), and Simancas et al. (2005).

Looking at the overall structure of Morocco in NW Africa (Fig. 1.11) and at the main events of its geological evolution allows us to approach and discuss the concept of continental growth. Morocco displays large parts of the orogenic systems or fold belts that developed around the 2 Ga-old continental nucleus of north-western Africa, i.e. the West African Craton (WAC). These successive

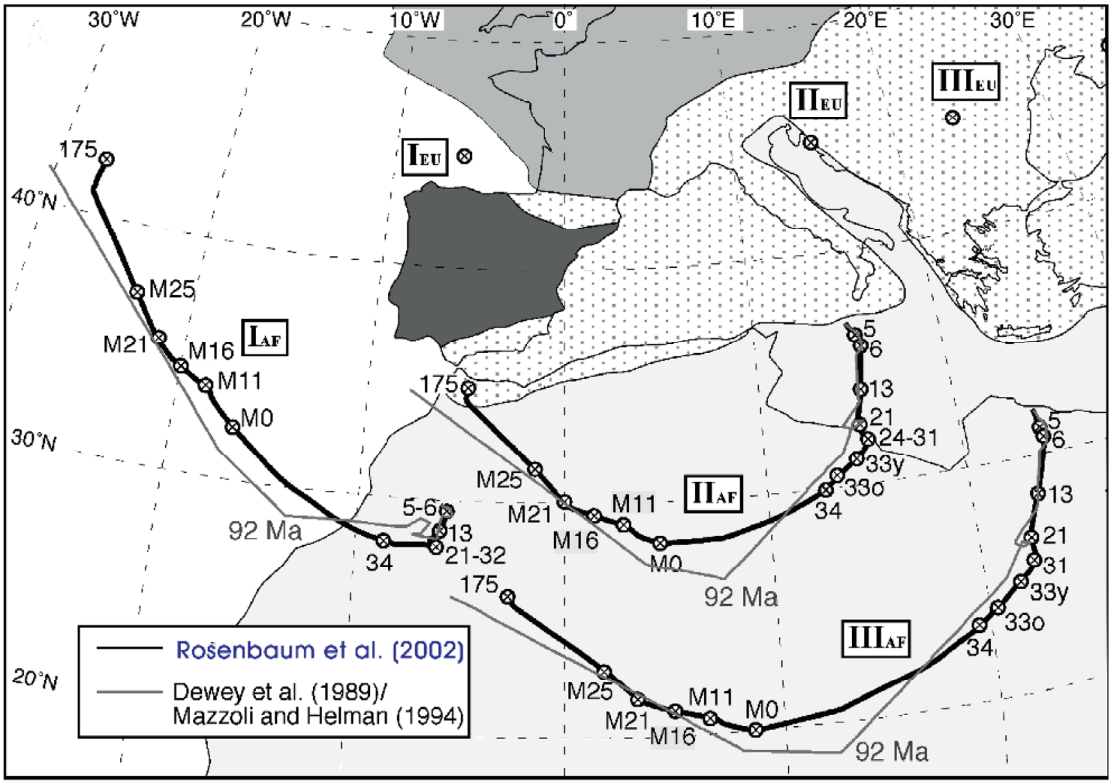

Fig. 1.10 Trajectories of three points of northern Africa relative to fixed points of Europe, plotted as a function of time since 175 Ma, and comparison with previous published trajectories, after Rosenbaum et al. (2002), modified. Each step along the trajectories corresponds to an oceanic magnetic anomaly. The most important dates are M25: 154 Ma; M0: 120.2 Ma; 34: 83 Ma; 31: 67.7 Ma; 21: 46 Ma; 13: 33.1 Ma; 6: 19.2 Ma; 5: 9.9 Ma. Stippled areas are regions of strong Mesozoic-Cenozoic deformation

belts are the Pan-African (Cadomian, Avalonian), Caledonian-Variscan (Hercynian, Alleghanian) and Alpine belts (Fig. 1.11), which are briefly presented hereafter and described in details in Chaps. 2–7. In contrast, the much older belts which constitute the basement of the WAC are presented only (and shortly) in the following section.

1.3.1 The Archean and Eburnian Terranes of the West African Craton (WAC)

1.3.1.1 Definition of the WAC

The WAC extends over millions of square kilometres in the Sahara desert (Figs. 1.11, 1.12). The crystalline basement crops out in the Reguibat Shield or Arch whereas it is hidden beneath thick piles of undeformed sediments in the Tindouf, Reggane and Taoudenni Basins. The age of these sedimentary deposits spans the whole Neoproterozoic-Cenozoic times (about 1 Ga) without any internal unconformity,

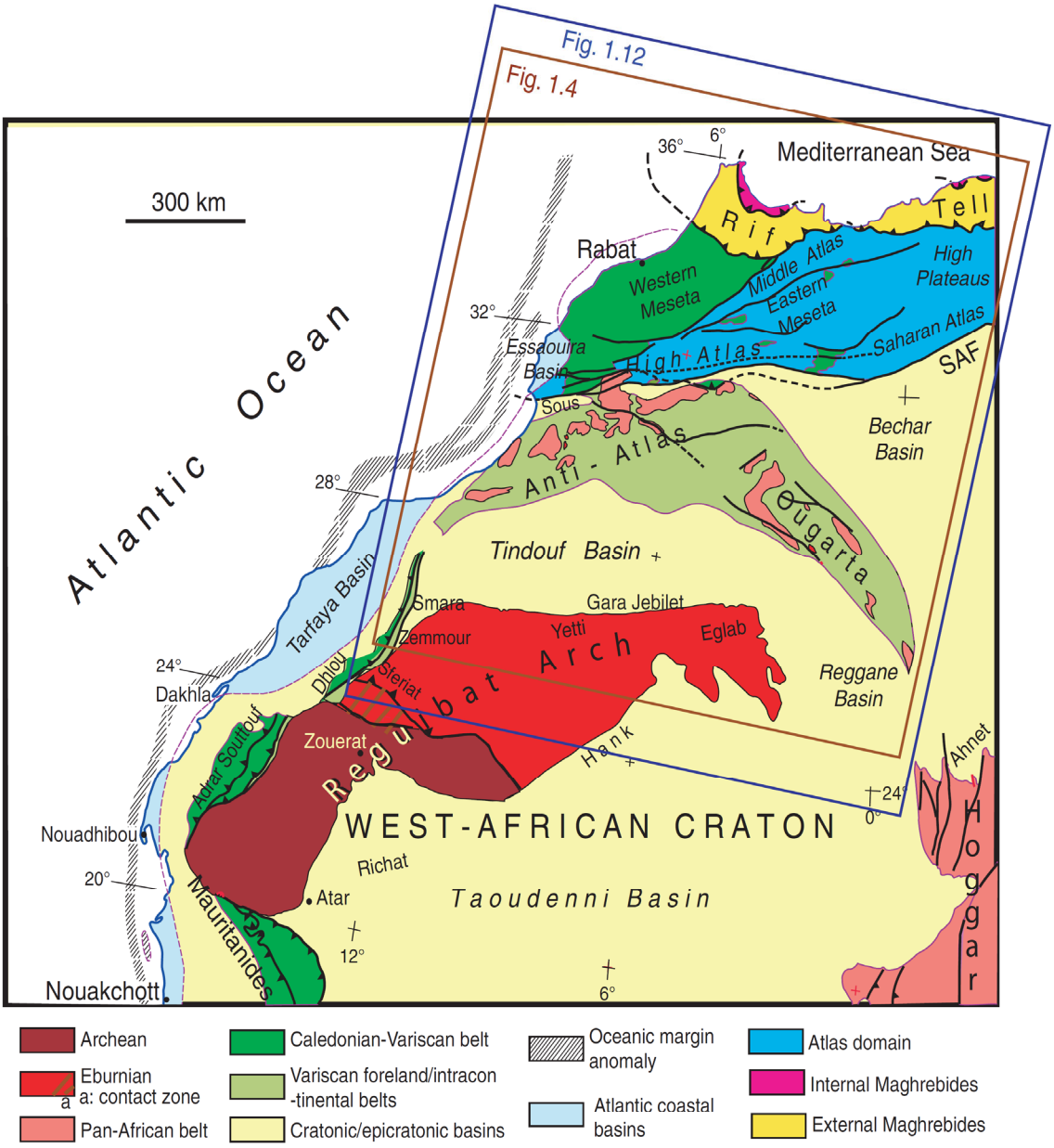

Fig. 1.11 Tectonic map of north-westernmost Africa showing the northern part of the West African Craton (WAC) and the adjoining fold belts, with location of Figs. 1.12 and 1.14 (framed). After Fabre (1976, 2005), Villeneuve & Cornée (1994), Ennih & Liégeois (2001), Villeneuve et al. (2006), Schofield et al. (2006), Schofield & Gillespie (2007). Location of the oceanic margin anomaly after Sahabi et al. (2004). SAF: South Atlas fault

which defines a typical cratonic area. The Neoproterozoic onlap is exposed on the southern border of the Reguibat Shield and in the Zemmour region, consisting of quartzites and stromatolitic limestones 1000–700 Ma in age. By contrast, at the southern border of the Tindouf basin, the base of the sedimentary succession is made up of Upper Ordovician sandstones similar to the Tassilis sandstones north of the Hoggar (or Tuareg) Shield. The thickness of the sedimentary pile in these intracratonic basins reaches 8 km at Taoudenni and up to 10 km at Tindouf.

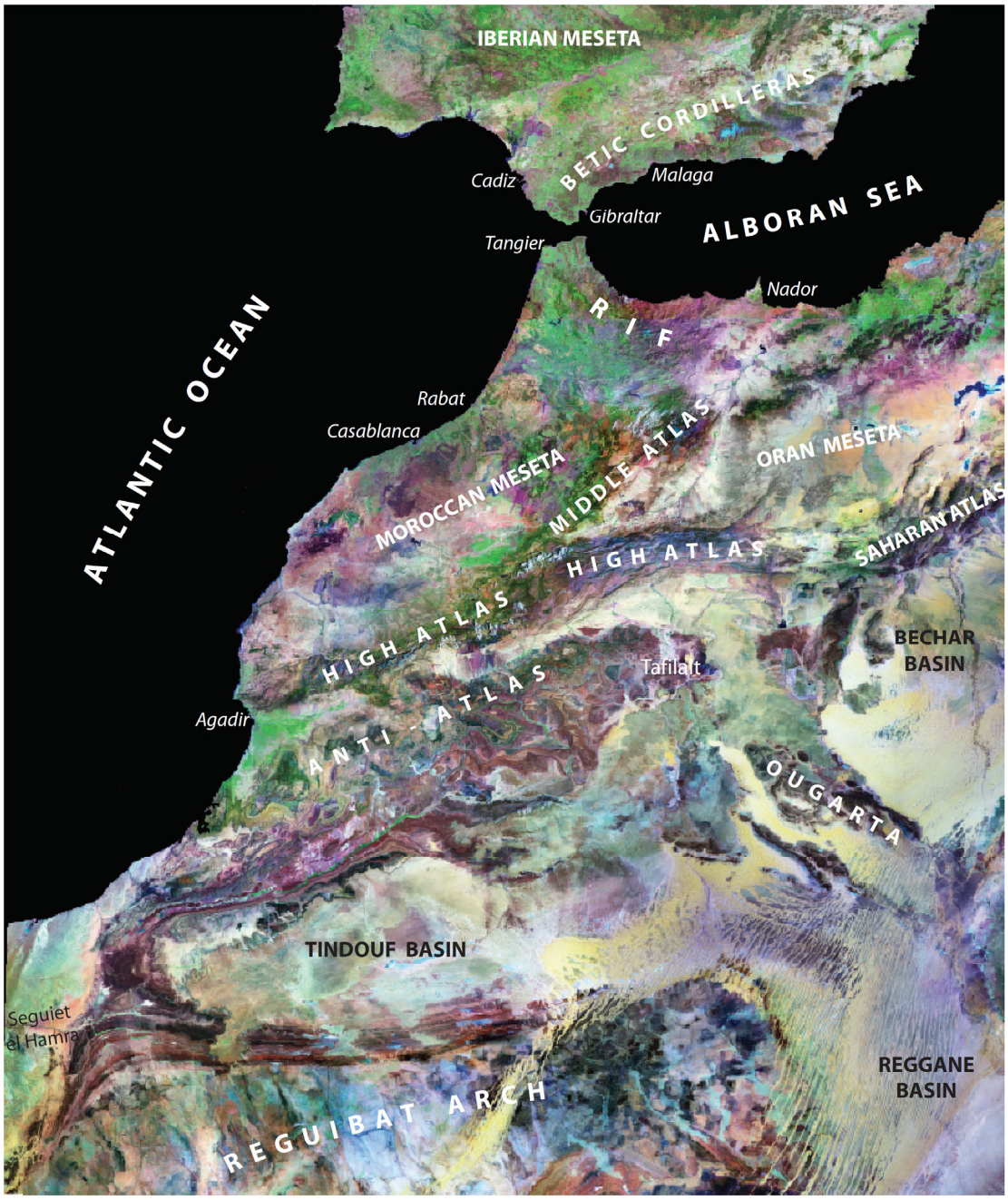

Fig. 1.12 Landsat image of Morocco (see Fig. 1.11 for location). See Fig. 1.4 for the interpretation of the different regions. More detailed Landsat images are also shown in the following chapters

1.3.1.2 The Reguibat Arch

The cratonic basement exposed in the Reguibat Arch (or Reguibat Shield) comprises two contrasting crustal domains, i.e. a western Archean terrane and an eastern Eburnian (or Eburnean) terrane (Fig. 1.11).

The *Archean terrane* is dominated by gneisses and granitic rocks with scattered lenses of metagabbros and serpentinites, and supracrustal rocks including

laminated, ferruginous quartzites, felsic gneisses interlayered with pyroxene-rich gneisses, cherts and impure marbles. Younger ages correspond to 3.04–2.83 Ga and were obtained from intrusive granitoids (Lahondère et al., 2003), suggesting a Mesoarchean age of continental crust formation.

In contrast, the *Eburnian terrane* of the eastern Reguibat Shield is largely made up of Paleoproterozoic granitic and metasedimentary rocks such as mylonitic paragneisses with calcsilicate nodules, abundant amphibolites and cherts (bimodal metavolcanic rocks), and ridges of ferruginous quartzites and marbles. The protoliths of the supracrustal rocks indicate a shallow marine basin dominated by clastic sediments, with local development of calcareous nodules and limestones (Schofield et al., 2006). The banded iron-rich formations, widely exploited in Mauritania (Zouerat area), are thought to represent chemical sediments precipitated in the presence of high concentrations of exhalative iron in relation with the activity of cyanobacteriae in an aerobic setting. Together with the associated limestones, they record the increase of the biological productivity during the Paleoproterozoic.

The granitoids plutons which intrude the metamorphic supracrustal rocks have been interpreted as formed during a cycle of subduction and subsequent accretion onto the adjacent Archean continental margin (Lahondère et al., 2006). In the Sfariat region, the Paleoproterozoic continental margin succession has been intruded with synorogenic granitoids and transported SW onto the Archean foreland during sinistral oblique collision (Schofield et al., 2006; Schofield & Gillespie, 2007). U-Pb geochronology reveals that anatexis and sinistral transpression took place between 2.12 and 2.06 Ga. Timing and kinematics of the Eburnian Orogeny in this region are similar to those for the Man Shield in equatorial West Africa.

1.3.1.3 Pre-Gondwana Supercontinents (a reminder)

The Eburnian Orogeny is thought to represent a major tectonic pulse of crustal growth (Bertrand & de Sá, 1990) related to the assembly of a pre-Rodinia, Paleo- to Mesoproterozoic supercontinent termed *Columbia* (Rodgers & Santosh, 2002). However, it must be emphasized that Mesoproterozoic terranes comparable to the 1 Ga-old Grenville terrane of the Laurentian Shield (and also present in the Avalonia basement) are not known in NW Africa.

As for *Rodinia*, it was initially defined as a long-lived supercontinent that assembled all the continental fragments around Laurentia and remained stable from 1000 up to 750 Ma (Dalziel, 1997; Weil et al., 1998, Meert & Lieberman, 2007, with references therein). Nonetheless, recent work has cast doubt on the Rodinia palaeogeography and even on the timing of its assembly and break-up. According to Cordani et al. (2003), a Braziliano Ocean separated most of the South American and African cratons from the Laurentia-Amazonia-West Africa margin. This ocean was closed between 940 and 630 Ma along the Pampean–Paraguay–Araguaia–Pharusian (Pan-African) mobile belts. Moreover, accretion along the South American and African platforms was a diachronous and long-lived process that involved several intra-oceanic and continental magmatic arcs and microcontinents. This evolution

started at around 1000 Ma and ended at around 520 Ma with the final assembly of *Gondwana* (Meert et al., 2007, with ref. therein) and, according to some authors (Dalziel, 1997), to *Pannotia*, i.e. the assembly of Gondwana, Laurentia, Baltica and Siberia.

1.3.2 The Pan-African Belt: Gondwana Assemblage

The WAC is surrounded by the Neoproterozoic Pan-African belt that first formed between ~750 and 660 Ma, then between 630 and 560 Ma (Chap. 2). The Pan-African events s.l. are responsible for the building of the supercontinent Gondwana. On the eastern side of the WAC, the Pan-African orogeny is clearly related to the convergence between the East Sahara metacraton and the WAC itself, with building of the Trans-Saharan belt including the Hoggar (Tuareg) Shield. The western part of the Hoggar was essentially built by the Pan-African Orogeny, whereas its central and eastern metacratonic parts were variably reactivated during the Neoproterozoic. The Hoggar massif includes metamorphic terranes and ophiolitic units thrust both eastward and westward. Ultra-high-pressure metamorphism (with coesite relics) has been observed in the Pan-African nappes from Gourma to Mali. In contrast, the Pan-African belt is poorly exposed in the Moroccan Anti-Atlas domain, and displays only low-pressure metamorphic units. It is currently believed that subduction-collision tectonics also occurred along the northern boundary of the WAC, but the Pan-African mobile belts of this region would be now situated elsewhere in the exotic peri-Gondwanan (Avalon) terranes. The unconformities which can be seen beneath the Anti-Atlas Cambrian formations record the end of the Pan-African geodynamic evolution (Fig. 1.13).

1.3.3 The Phanerozoic Belts: from Gondwana to Africa

The *Caledonian-Variscan belt* extends essentially along the northwestern side of Africa, and results from the collision of Gondwana with Laurentia, Baltica and intervening terranes (Avalonia, Armorica etc.) previously detached from the Gondwana continent. The belt developed through repeated oceanic closures and collisional events from about 460–420 Ma (Caledonian, Taconic or Sardic events) to 360–300 Ma (Variscan = Hercynian or Alleghanian events). This is a major orogen associated with several ophiolitic sutures and high- to ultra-high-pressure metamorphism. Only the southern external parts of the belt, devoid of ophiolite and high-pressure metamorphism, are preserved in northern Morocco (Meseta Block, including most of the Atlas basement). East-verging thrusts of "reworked" Precambrian material emplaced upon the western margin of the Reguibat Shield (Adrar Souttouf-Dhlou = Ouled Dhlim) during the Carboniferous, in the northern continuation of the Mauritanide belt. Late Paleozoic deformation remains moderate in the Moroccan Anti-Atlas and Algerian

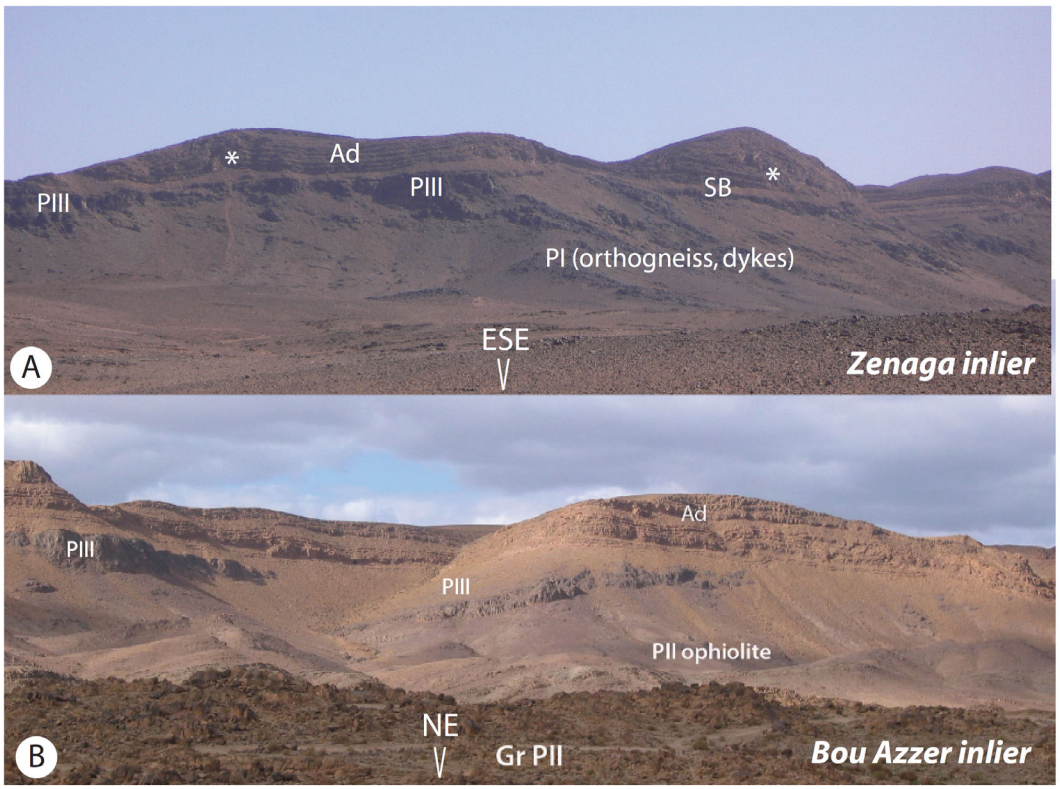

Fig. 1.13 Unconformities on top of the eroded Pan-African belt in the Central Anti-Atlas. **A**: Unconformable Ediacaran volcanites ("PIII") and late Ediacaran conglomerates ("Série de base" SB) on top of the Eburnian granite and pegmatites (Gr PI, c. 2000 Ma) in the eastern Zenaga "boutonnière". The Ediacaran-Cambrian "Adoudounian" dolomites (Ad) are virtually conformable on top of the PIII-SB formations. Asterisks (*): hinges of NE-verging Variscan folds in the detached Adoudounian layers. View from the Tazenakht-Bou Azzer road, 6 km west of Tazenakht (see Chap. 2, Fig. 2.5). – **B**: At the northwest border of the Bou Azzer inlier, the Adoudounian dolomites (Ad) unconformably overlie the tilted Ediacaran volcano-sedimentary formations (PIII) and the underlying Neoproterozoic rocks of the Pan-African belt (PII serpentinite and intrusive granitoid Gr PII). View from the same road as (A), about 20 km further east

Ougarta – both mountains being moulded around the WAC border. In contrast, the Atlas-Meseta domain is strongly deformed, more or less metamorphic, and intruded by varied granite massifs. The Late Permian or, more generally, Triassic unconformity marks the end of the Variscan evolution (Fig. 1.14).

Finally, the youngest orogenic system, i.e. the *Cenozoic Alpine belt*, extends north of the northern boundary of the WAC – being obliquely superimposed onto the Variscan belt and its putative Avalonian-Cadomian basement. The broad organisation of these young mountain belts is directly visible in the topography (Fig. 1.2). The High and Middle Atlas are autochthonous, intracontinental belts, developed by inversion of Triassic-Jurassic aborted rifts. In contrast, the Maghrebides include both parautochthonous, external units originating from the African Mesozoic passive margin, and allochthonous terranes coming from the Maghrebian-Ligurian Tethys and the continental Alboran-Kabylia-Calabria block. In both the Atlas and Maghrebide systems, deformation and mountain building span from the Late Eocene to Present times, i.e. during the last 40 My (e.g. Fig. 1.15).

Fig. 1.14 The Triassic unconformity on top of a Variscan granite from the High Moulouya massif south of Zeida. Transgression of Triassic arkosic sandstones (240–230 Ma?) on top of the 300 Ma-old Boumia granite, emplaced at ca. 10 km depth within the Paleozoic schists of the Eastern Meseta orogen. The post-Triassic oblique fractures are mineralized with barite (cf. Zeida mines)

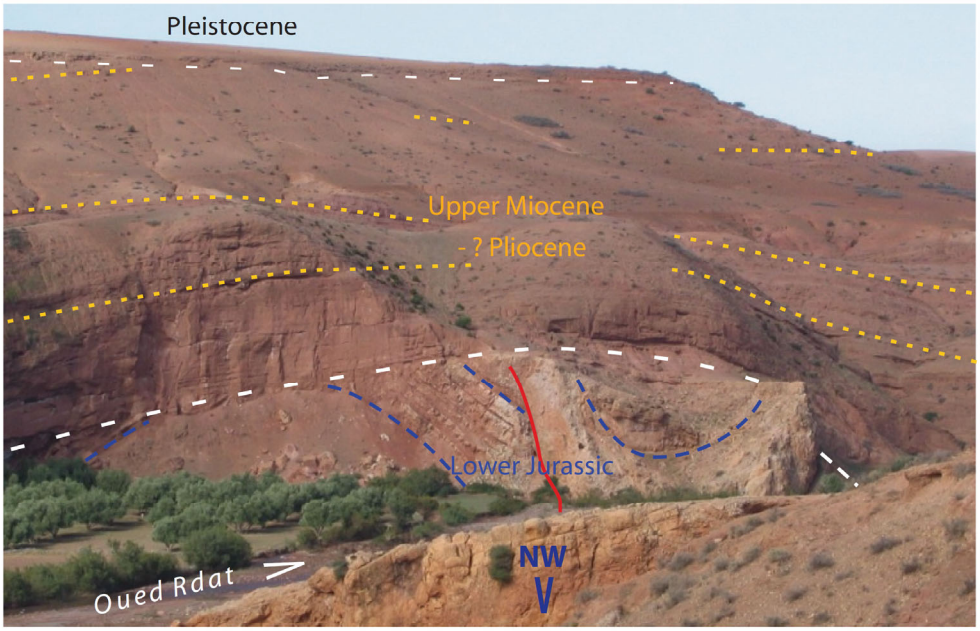

Fig. 1.15 Superimposed unconformities at the northern border of the Marrakech High Atlas, Oued Rdat valley upstream Sidi Rahal (40 km east of Marrakech). Folding of the Lower Jurassic dolomitic limestones initiated during the Late Eocene-Oligocene as the Middle Eocene limestones nearby (Ait Ourir) are also folded. The unconformable Upper Miocene conglomeratic sandstones are deformed into a large anticline which is in turn unconformably overlain by Early Pleistocene torrential conglomerates

1.3.4 Continental Growth, Continental Reworking, and Structural Inheritance

Successive orogenic belts, amalgamated against the WAC, constitute a remarkable case study for the concept of continental growth. However, it must be kept in mind that continental breakdown (rifting) also occurs, at least since the Neoproterozoic, prior to each orogenic (convergent) episode. Rifted terranes were drifted away from the Paleo-Gondwana margin, and finally accreted to Laurentia during the Early Paleozoic (Taconic-Caledonian-Acadian events). Part of the continental material was also lost by erosion, and subsequent sedimentation in remote oceanic realms (Variscan and Alpine belts). Moreover, instead of being juxtaposed as crystalline growth zones, the successive orogens are mostly superimposed. As a result, a large part of the rock material of any orogen originated from a previous one. The Pan-African Belt is superimposed onto the border of the WAC and includes rejuvenated schists and granites from the Eburnian Orogen; the Variscan Belt widely extends onto the Pan-African, including Precambrian material in the Anti-Atlas and Mauritanides; and finally, the Atlas and Rif Belts in turn deeply encroach on the Variscan Meseta Domain.

A most important outcome of the addition of superimposed orogens is that old structures (which are mechanical discontinuities) at least partially control the younger ones. A magnificent example of this fact is the *South Atlas Fault*. This Mesozoic-Cenozoic fault system which limits the Atlas Belt to the south (Fig. 1.11) reused a major Variscan fault system, the *Atlas Paleozoic Transform Zone*, which separates the highly-deformed Meseta domain from the mildly deformed Anti-Atlas. Moreover, during the Neoproterozoic this structure apparently corresponded to the northern boundary of the WAC.

1.4 Active Tectonics

References: For both this section and the next one, the sources are essentially Buforn et al. (1995), Morel and Meghraoui (1996), Gutscher et al. (2002), Negredo et al. (2002), Contrucci et al. (2004), Frizon de Lamotte et al. (2004), Spakman & Wortel (2004), Fullea Urchulutegui et al. (2005), Missenard et al. (2006), Sébrier et al. (2006), Stich et al. (2006), and Fernández-Ibáñez et al. (2007) with references therein.

Due to its position at the northwest border of the African plate (Fig. 1.16A), Morocco still exhibits significant tectonic activity, especially in its younger parts. This is clearly shown by the density map of seismicity in the Atlantic-Mediterranean transition zone (Fig. 1.16B).

The most active seismic zone is localized in the Rif and Alboran Sea. This is consistent with the fact that this region corresponds to the contact zone between the two converging plates, Eurasia and Africa. The movement of the African (Nubian)

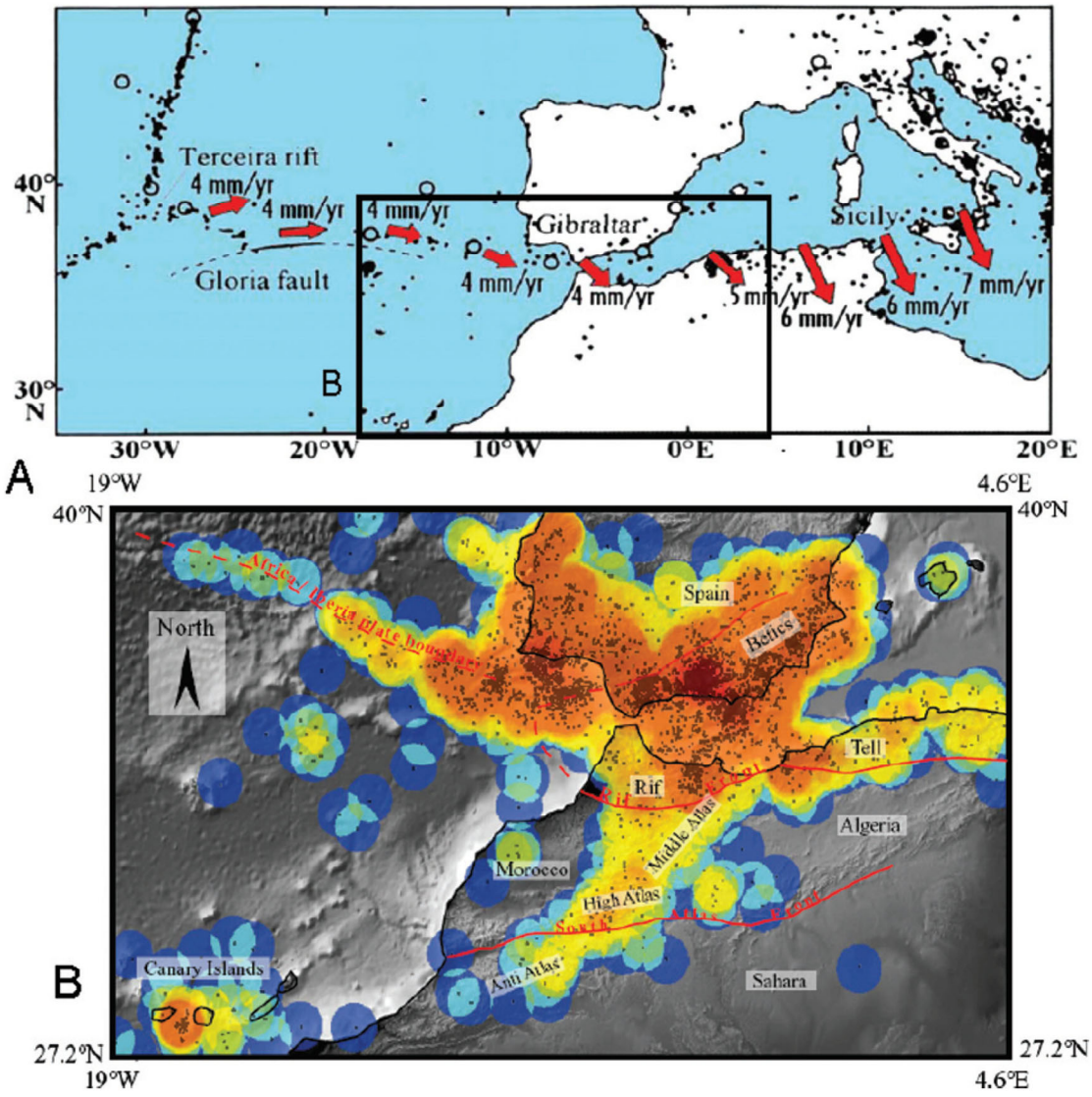

Fig. 1.16 Moroccan seismicity and plate tectonics. **A**: Direction and mean recent rate of the Europe-Africa convergence deduced from global geodetic NUVEL-1 model (DeMets et al., 1994; Morel & Meghraoui, 1996). Black dots: epicentres (1965–1985). The N-S trending seismic lineament on the left is the Mid-Atlantic ridge. The boundary between the Eurasian and African (Nubian) plates trends E-W, being diffuse in the Gibraltar area and Mediterranean Sea. – **B**: Density map of seismicity in the Mediterranean-Atlantic transition zone calculated from ISC database for the 1995–2000 time interval, after Missenard et al. (2006). Grey points indicated epicentres

plate relative to Eurasia which trended N during the Late Cretaceous-Paleogene interval (Fig. 1.10), trends approximately NW, i.e. oblique to the African margin, during the Miocene to Present interval (Fig. 1.16A). The convergence rate decreases from 6 to 4 mm/year from the longitude of Tunisia to that of Morocco due to the actual position of the pole of rotation that imposes an anti-clockwise rotation of Africa with respect to Eurasia.

The vectors of relative displacements for the African and Eurasian plates, deduced from the oceanic geophysical dataset and geodetic observations (e.g., NUVEL-1A model), fit relatively well with more recent GPS observations (Fig. 1.17).

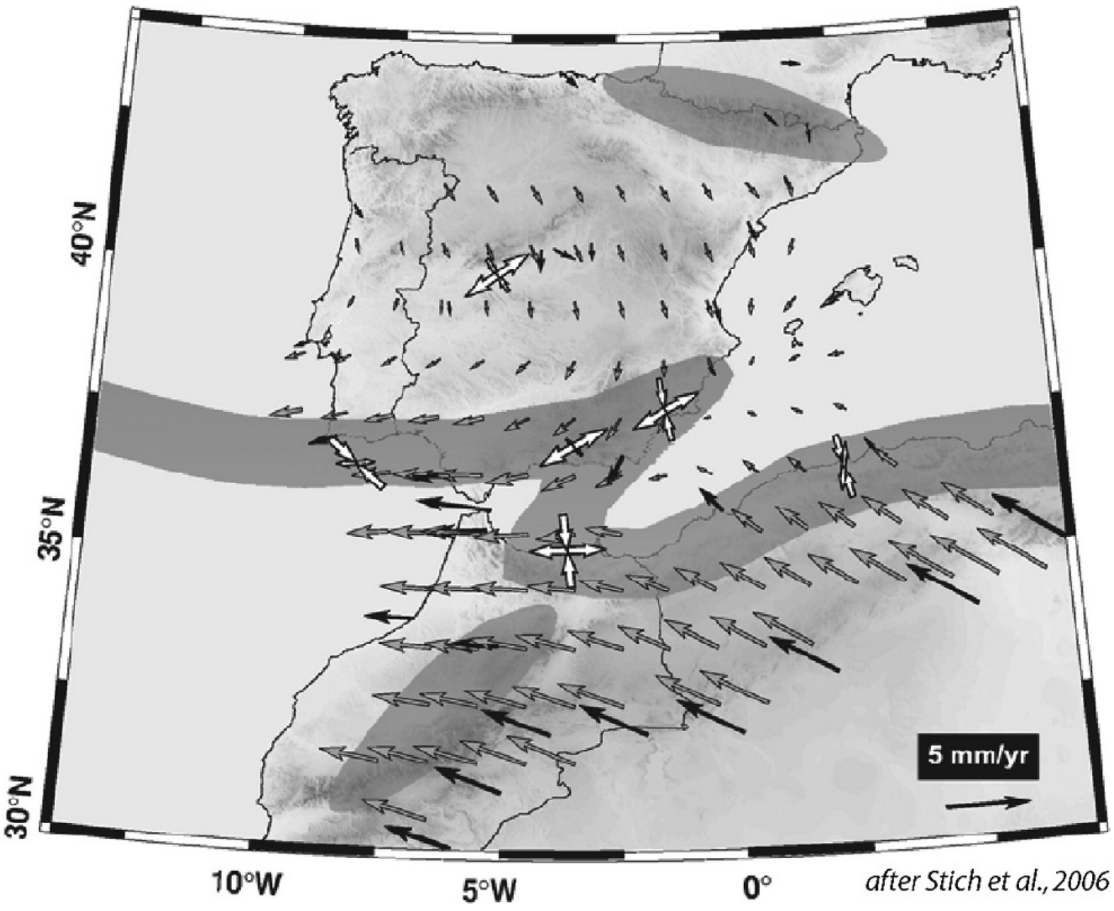

Fig. 1.17 Direction and rate of present-day motion of NW Africa and Spain relative to stable Europe after Global Positioning System (GPS) observations. *Black arrows*: velocities measured in the area or predicted from the dataset. *Grey arrows*: interpolated velocity field. The mean stress tensors deduced from the seismic focal mechanisms (*large white arrows*) are plotted on the Mediterranean seismic belt (*light grey*). After Stich et al. (2006), modified

Discrepancies between the convergence rate and direction predicted among the different global geodetic models occur. Moreover, GPS data also reflect motions by active faulting which induce local motions that deviate from the overall pattern of plate convergence. However, the available data would reflect changes in the last 3 Ma of Africa-Eurasia relative motions, related to the effects of the ongoing collision. Moreover, the overall converging movement is combined with a regional extension in the Alboran area, trending E-W to ENE-WSW, and associated with the building of the Gibraltar Arc since ~20 Ma.

The Maghreb-Alboran-Southern Spain area is characterized by frequent earthquakes, sometimes of great magnitude, resulting in appalling disasters (Al Hoceima, 24 February 2004, M 6.3). Seismic activity may be controlled by the strong spatial gradients in the velocity field. Most epicentres of shallow earthquakes are distributed in a Z-shaped area (Figs. 1.16B, 1.17) that follows the Algerian coast, crosses obliquely the Alboran basin from Eastern Rif to Eastern Betic Cordilleras (Trans-Alboran Seismic Zone, TASZ), and continues further to the west in the Atlantic Ocean. Focal mechanisms indicate a predominance of reverse faulting in

the Algerian margin that passes westward to predominant strike-slip mechanisms. Maximum horizontal stresses are consistent with NNW-SSE plate convergence, although it is observed moderate clockwise stress rotation along the TASZ. Within the TASZ relevant seismicity is characterized by predominantly sinistral strike-slip faulting associated with some normal faulting, revealing a left-lateral (transtensive) regime. The compressional deformation in the plate boundary resumes in the west-trending segment of the seismic zone up to the Gorringe Bank west of SW Spain (Fig. 1.3, 348 °E – 37 °N). Intermediate depth earthquakes (60–160 km) also occur beneath southern Spain and in the western Alboran basin, east of the Gibraltar Arc, and some deep events (~600 km) are also reported beneath southern Spain. These features should be related to the east-dipping subduction of a narrow oceanic slab, as discussed in Sect. 1.5 (Sect. 1.5.7).

South of the Mediterranean area, seismicity is scarce and occurs concentrated in a narrow, NE-SW trending zone covering the Middle Atlas, Central High Atlas and part of western Anti-Atlas (Fig. 1.16B). This seismicity mostly corresponds to $M < 5$ events in the last decades, except the appalling 29 February 1960 Agadir earthquake ($M = 5.7$), and two events in easternmost Anti-Atlas ($M = 5.5$). The earthquakes show shallow hypocentres and dominantly strike-slip or reverse mechanisms. It is worth noting that this seismic strip follows the zone where the lithosphere is thin (see below, Fig. 1.18B). Active tectonics along the South Atlas Fault, as evidenced by the deformation of the Quaternary surfaces, suggests the occurrence of an intra-crustal

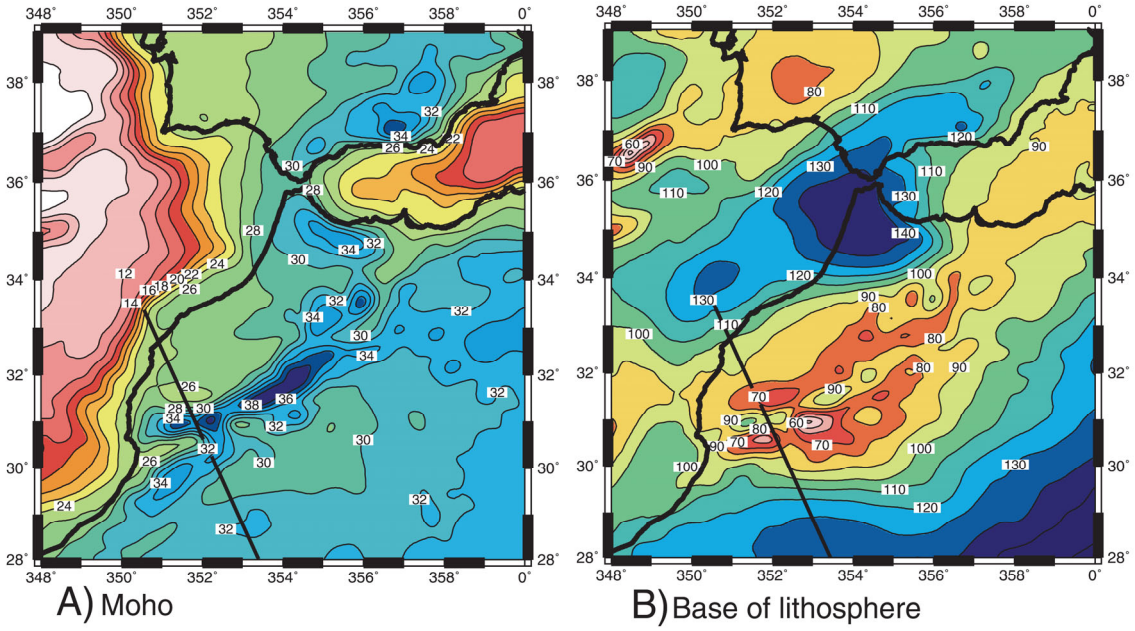

Fig. 1.18 Structure of the lithosphere of the Moroccan-south Iberian region derived from elevation and geoid anomaly modelling, after Fullea Urchulutegui et al. (2006), modified. **A**: Map of the Moho depths. Isolines every 2 km. Note the shallow root beneath High Atlas. **B**: Depth of the lithosphere-asthenosphere boundary. Contour interval is 10 km. Note thin lithosphere (asthenosphere uplift) beneath High and Middle Atlas, thick lithosphere beneath cratonic area to southeast, and decoupling of crustal and mantle lithosphere thicknesses beneath Gibraltar-NW Moroccan margin area. *Bold line*: trace of profile Fig. 1.19

décollement seismically active, which has the potential to create big earthquakes (see Chap 4). Seismicity vanishes further south in the Saharan domain, as well as further east in the Saharan Atlas.

1.5 Lithosphere Structure

References: See section above, particularly Frizon de Lamotte et al. (2004) and Missenard et al. (2006).

The crust beneath inland Morocco is not precisely imaged due to lack of deep seismic profiling. However, modelling of crustal and lithospheric thicknesses was recently performed that integrates elevation, geoid anomalies, surface heat flow, gravity, and seismic data. The resulting map of Moho isobaths (Fig. 1.18A) shows a moderately thick crust underneath the Rif and Betics (~32–34 km), whereas the Alboran Basin in between shows a continental crust (~20–22 km) that thins progressively toward the east, achieving less than 16 km at the transition with the young South-Balearic and Algerian oceanic basins. Inland Morocco, the crust thickness increases to 38 km below the most elevated parts of High Atlas, then decreases southeastward down to the normal thickness of continental crust, 30–32 km.

Remarkably, this High Atlas crustal root is not thick enough to isostatically support such a high topography. Modelling of the lithosphere thickness has led to an explanation of this discrepancy. The map of the base of the lithosphere (Fig. 1.18B) shows a prominent, NE-trending zone of thinned lithosphere, in other words an asthenosphere uplift which reaches ca. 60 km depth underneath the Western High Atlas, central Anti-Atlas and Middle Atlas ranges. Thus, thermal doming accounts for the elevation of the area, in addition to the moderate shortening and crustal thickening. In particular, this explains the high elevation of the Siroua Plateau located in the Anti-Atlas south of the High Atlas between the Sous and Ouarzazate Basins (Fig. 1.19). Moreover, the uplift of hot, asthenospheric mantle accounts for the scatter of Pliocene-Quaternary alkaline volcanoes from J. Siroua to J. Saghro, and to Middle Atlas. This uplift would correspond to the trend of a hot line similar to the Cameroon Hot Line (Deruelle et al., 2007), extending at least from the Canary Islands to southeast Spain and referred to hereafter as the *Morocco Hot Line* (see Chap. 4).

A general description of the lithosphere structure along the southern Iberia-Alboran Sea-Morocco N-S transect has been recently compiled by a large panel of scientists (Frizon de Lamotte et al., 2004). The southern part of this transect crosses the geological domains of Morocco (Fig. 1.20A, B) from the young Alboran Basin and Alpine Rif belt in the north up to the Anti-Atlas in the south. In the latter area, the lithosphere thickness attains ca. 130 km. It thins down to ca. 80 km beneath the Siroua-High Atlas area, in relation with the asthenosphere uplift already discussed (cf. Fig. 1.18B). The lithosphere again thickens beneath the Meseta and Rif domains, before its dramatic thinning beneath the Alboran Basin. These domains of irregular and relatively thin continental lithosphere corresponding to the

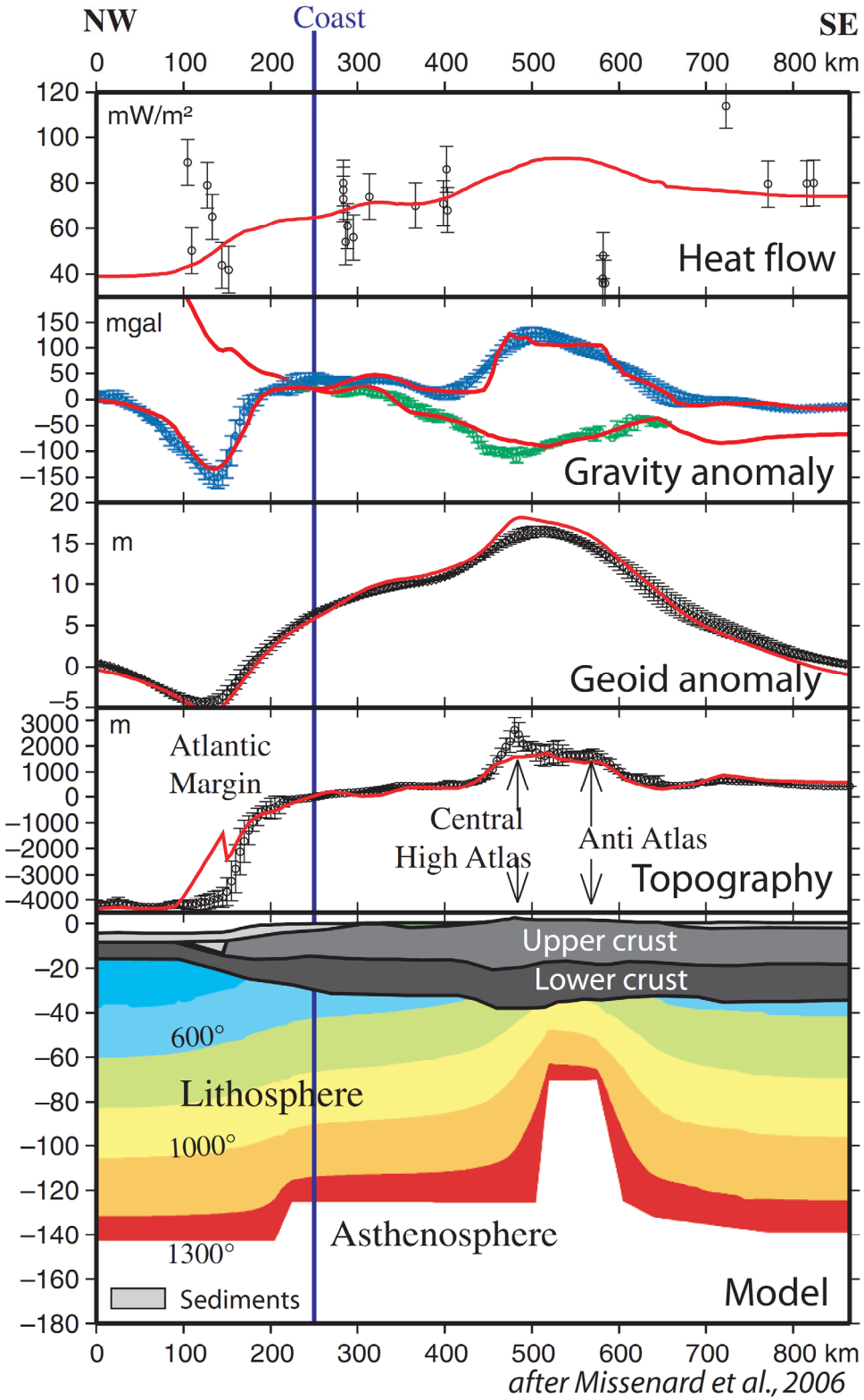

Fig. 1.19 2D lithosphere model across the western High Atlas and Siroua massifs (see Fig. 1.18 for location), with observed (*dots with error bars*) and calculated (*coloured solid lines*) physical properties along the section, after Missenard et al. (2006), modified. The model shows an asthenosphere upwelling up to ca. 60 km depth. Note the strong vertical exaggeration

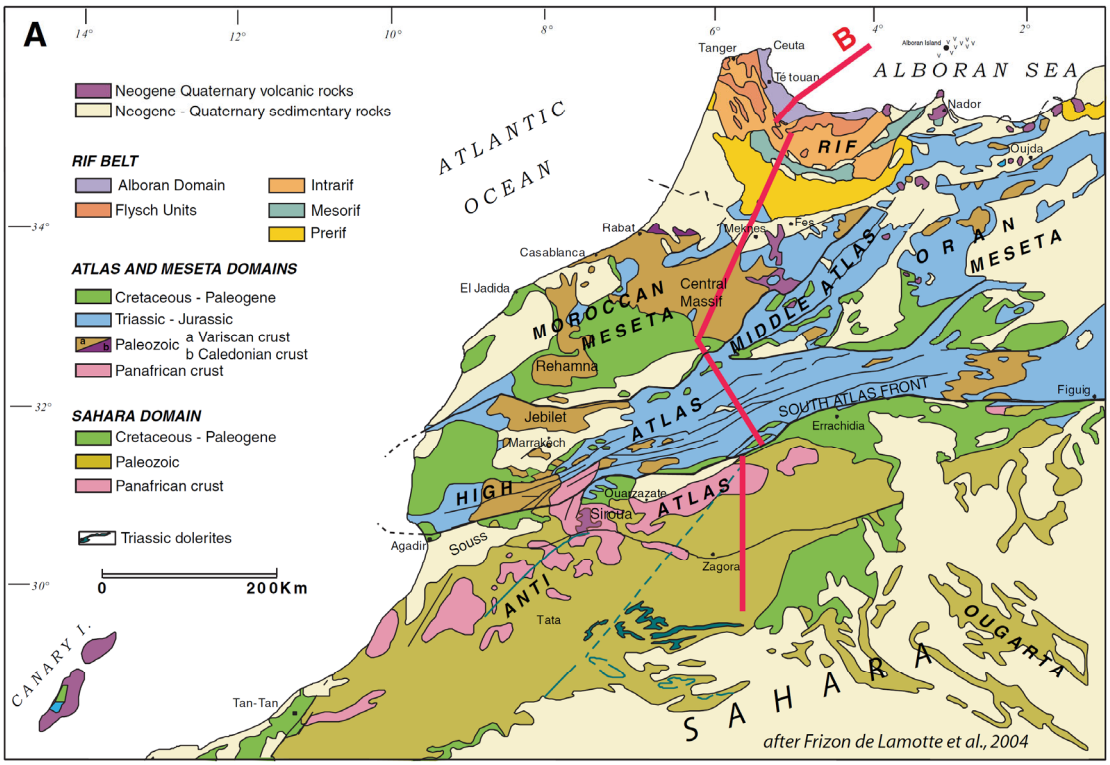

Fig. 1.20 The southern part of TRANSMED I Profile, after Frizon de Lamotte et al. (2004), modified. **A**: Location on the geological map of Morocco (Northern Provinces). – **B**: Lithospheric profile across the different geological domains. For more details see the corresponding figure at greater enlargement on the original CD-rom included in the Transed volume (Cavazza et al., Eds., 2004). The southernmost part of the profile is shown enlarged in Chap. 2

Neoproterozoic-Phanerozoic mountain belts contrast with the WAC domain which displays a remarkably thick (ca. 250 km) lithosphere (Fig. 1.21). The peripheral domain at the border of the craton, deformed during the Pan-African orogeny, then broadly stable and displaying a 130–150 km thick lithosphere are labelled "metacratonic areas".

Toward the Atlantic Ocean, the Moroccan land is bordered by a 50–100 km-wide marine continental plateau. This shallow marine plateau is limited westward by a large continental slope, about 3000 m-high and 100 km-wide, which leads to the abyssal plains. Depending of the segment considered, this margin shows either active sedimentary progradation or dominant destructional processes such as slumps and slides affecting the seafloor (e.g. Fig. 1.22). The continental slope corresponds to the eastern passive margin of the Central Atlantic Ocean, conjugate to the Nova Scotia margin of North America (Fig. 1.6, 1.8). Its deep structure is better imaged than that of inland Morocco based on offshore seismic reflection profiles combined with wide-angle seismic and gravity data (Fig. 1.23). The shallow structure shows a thick sedimentary cover (up to 6 km at the base of the continental slope) deformed by salt diapirs (see Chap. 6). Basement structures include tilted blocks and a transition zone to the oceanic crust. The crust thins from 35 km underneath the continent to approximately 7 km in the oceanic domain.

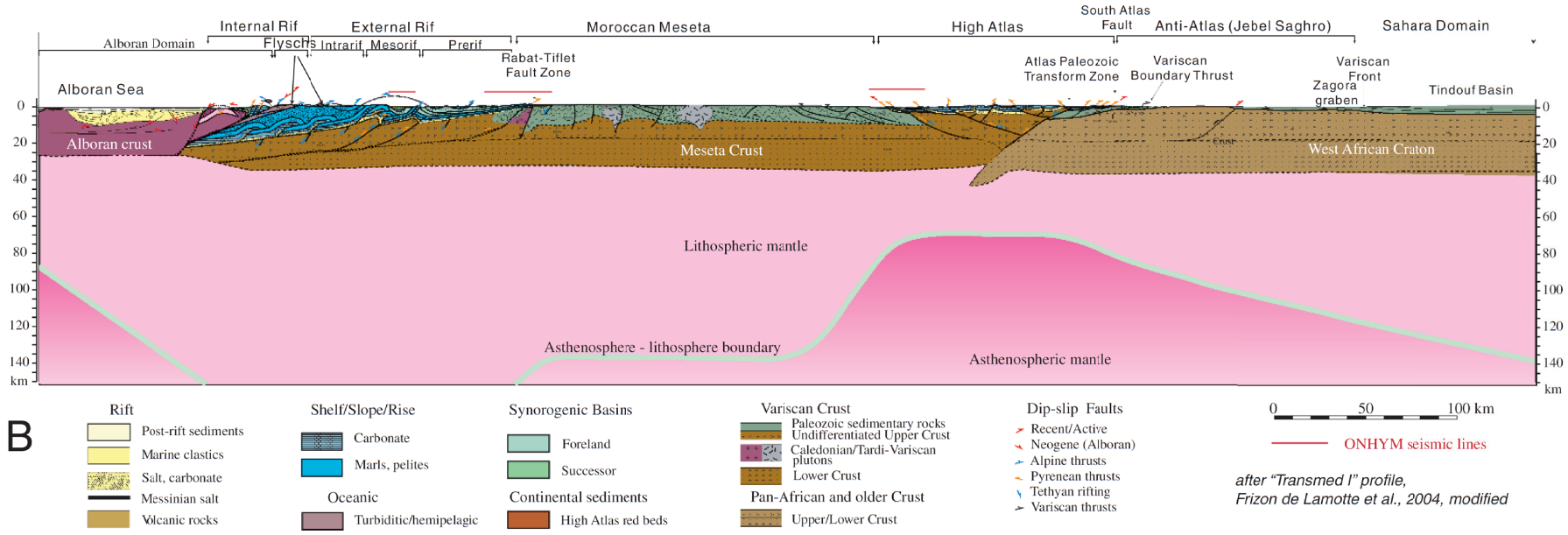

Fig. 1.20 (continued)

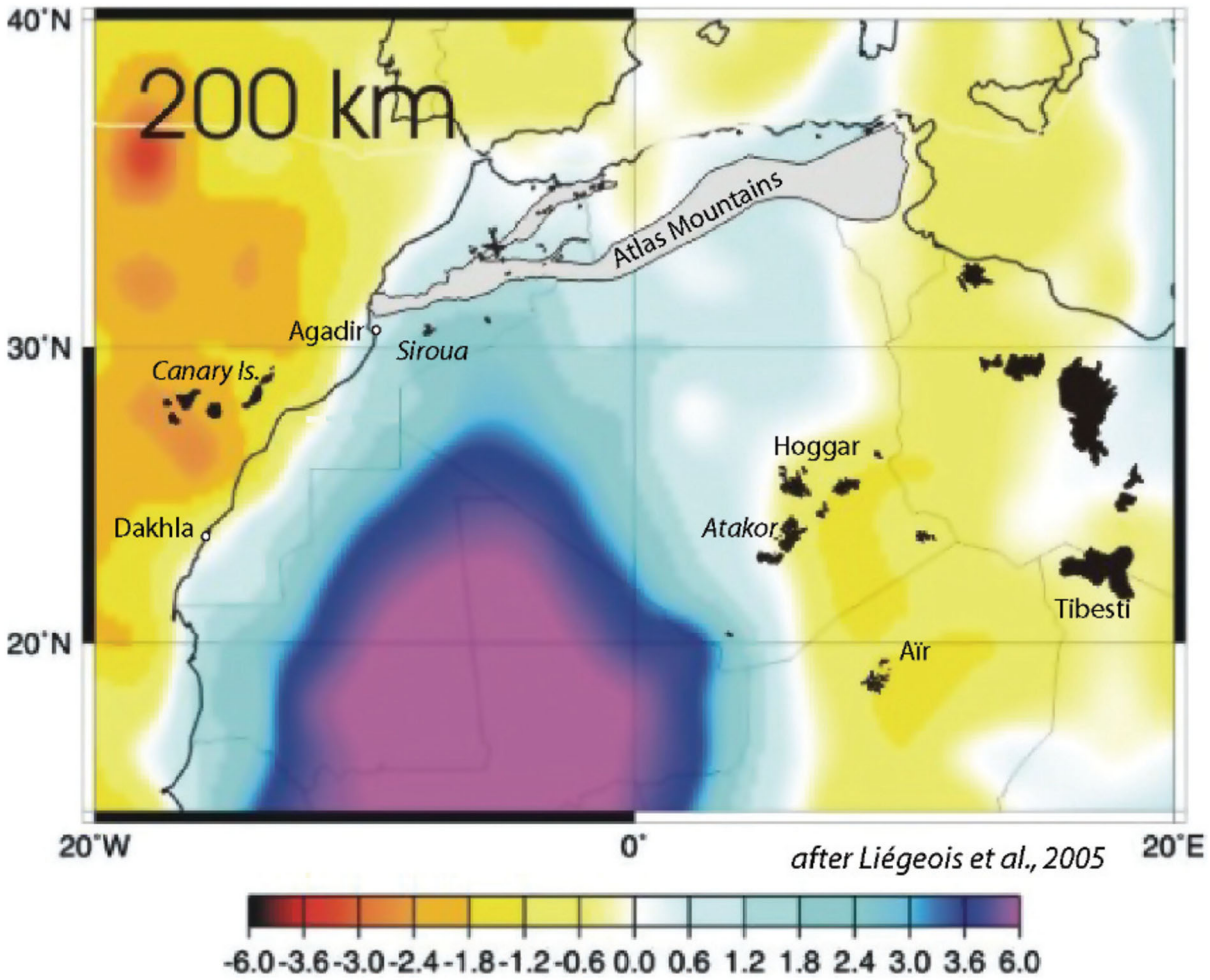

Fig. 1.21 Horizontal cross-section at 200 km depth in a 3D shear-wave velocity tomographic model of North-Western Africa, after Liégeois et al. (2005). Color scale shows the shear wave velocity as % perturbation relative to the reference value that is 4.494 km/s at that depth. *Black*: Cenozoic volcanism; *grey*: Atlas Mountains; fine lines: state borders. The West African Craton is characterized by very high shear-wave velocities which are recognized even at 250 km depth, which indicates a quite thick lithosphere. Cenozoic volcanism is lacking in the cratonic domain, whereas it is abundant in the metacratonic areas further east (Hoggar, etc.)

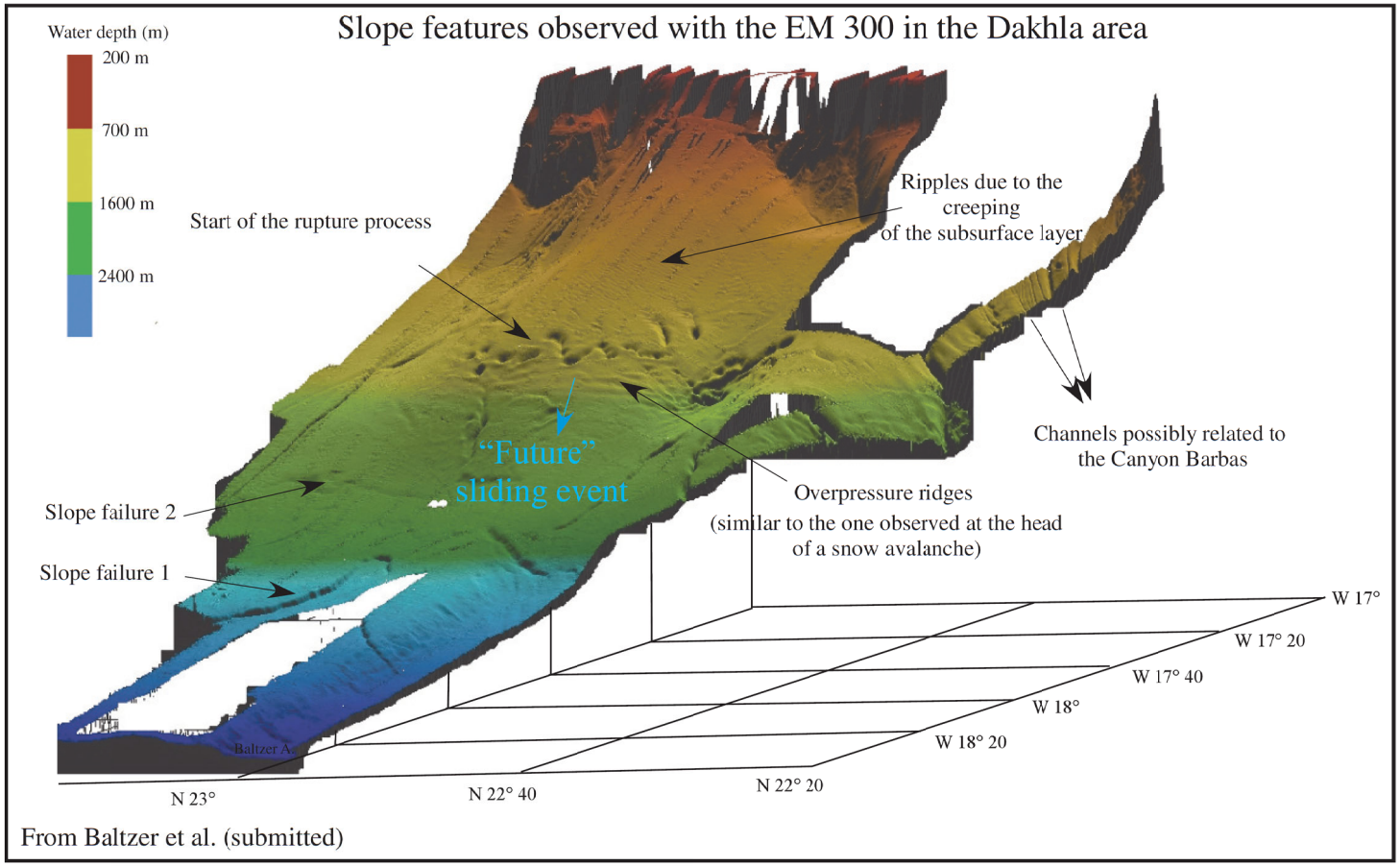

Fig. 1.22 Swath bathymetric data (Simrad EM 300 multibeam echo sounder) on a portion of the West African margin offshore Dakhla, south-western Morocco around 23°N (see Figs. 1.21 or 1.11 for approximate location). The Dakhla cruise (2002) acquired this bathymetric mosaic together with very high resolution seismic data (CHIRP). These complementary data give a 3D view of the shallow sedimentary structures such as creeping processes, slope failures, the initiation of a new failures outlined by overpressure ridges, and channels possibly related to an inactive (?) canyon. Courtesy of A. Baltzer and D. Aslanian (Baltzer et al., submitted)

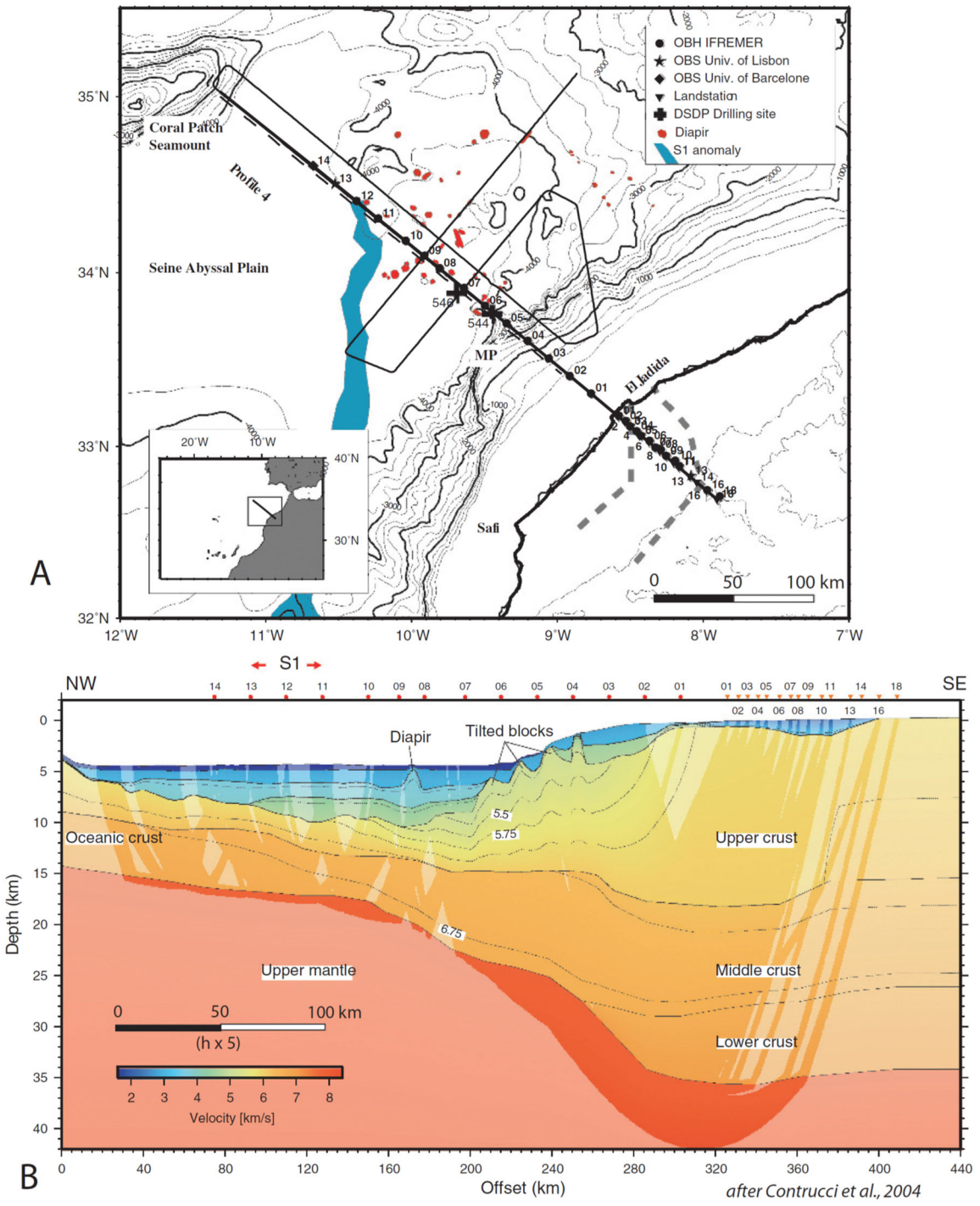

Fig. 1.23 Crustal structure of the NW Moroccan continental margin, after Contrucci et al. (2004), modified. **A**: Location of deep reflection seismic profiles (*dashed line* and *thin lines*) and crustal-scale profile shown in B (*bold line*). The map includes bathymetry. *Thick, broken grey lines* in the vicinity of the land stations indicate the extension of the El Jadida Cretaceous basin. – **B**: Final velocity model deduced from offshore seismic reflection, and both onshore and offshore wide-angle seismic data, integrating the model boundaries used during inversion (*solid lines*) and isovelocity contours every 0.25 km sec^{-1} (*thin lines*). Darker shaded areas show ray paths from the modelling and hence regions of the model that are constrained. Cross-point of the profile with the S1 magnetic anomaly is indicated above the profile, as well as the ocean bottom hydrophones/seismometres (OBH/OBSs) and land stations

Acknowledgments We are grateful to Pr. Michel Faure (Univ. Orléans) for his critical review of an early draft of this chapter. Thanks are also due to Dr. Serge Bogdanoff (Univ. Paris-Orsay), René Maury (Univ. Brest) and Dr. Juan I. Soto (Univ. Granada) for their careful readings and to Bruce Purser (Univ. Paris-Orsay) and Tan Say Biow (PETRONAS, Malaysia) for improving our English writing. Thanks are also due to all the colleagues who kindly provided the original files of many of the figures of this chapter, and kindly reviewed the corresponding paragraph.

References

Geological maps

Hollard H., Choubert G., Bronner G., Marchand J., Sougy J., Carte géologique du Maroc, scale 1:1,000,000.– *Serv. Carte géol. Maroc*, 1985, 260 (2 sheets).

Suter G.: Carte géologique de la chaîne rifaine, scale 1:500,000.– *Serv. Carte géol. Maroc*, 1980, 245a.

Other maps: see Catalogue 2004, Ministère de l'Energie et des Mines, Direction de la Géologie, Service Documentation et Publications.

Books and special issues

Note: The ancient books or special issues available in digitized versions are referenced in Chap. 9.

Anonymous, Maroc, mémoire de la Terre. *Ed. Muséum nat. Hist. Nat. Paris*, 1999, 236 p., nombreuses illustrations.

Anonymous, Minéraux du Maroc. *Ministère Energie et Mines, Rabat*, 1992, 182 p.

Anonymous, Géologie des gîtes minéraux du Maroc. – Tome I, Substances métalliques et non métalliques associées. *Notes Mém. Serv. Géol. Maroc* 276 (1980) 318 p.

Cavazza W., Roure F., Spakman W., Stampfli G.M., P.A. Ziegler (Eds), *The TRANSMED Atlas – the Mediterranean region from crust to mantle*, Springer, Berlin, 2004.

Cherotzky G., Pétrographie du Maroc (roches éruptives et métamorphiques), *Notes Mém. Serv. Géol. Maroc* 266, 1978, 152 p.

Fabre J., Introduction à la géologie du Sahara algérien, S.N.E.D., Alger, 1976, 422 p.

Fabre J., Géologie du Sahara occidental et central, *Tervuren Afric. Geosci. Coll.* 108, 2005, 572 p.

Frizon de Lamotte D., Michard A., Saddiqi O. (Eds.), Recent Developments on the Maghreb Geodynamics. *C. R. Geoscience* 338/1–2, 2006, 151 p.

Michard A., Eléments de géologie marocaine, *Notes Mém. Serv. Géol. Maroc* 252, 1976, 408 p.

Moratti G., Chalouan A. (Eds): Geology and active tectonics of the Western Mediterranean Region and North Africa, *Geol. Soc. London Spec. Publ.* 262, 2006.

Piqué A., Géologie du Maroc, *Editions Pumag*, Casablanca, 1994, 284 p.

Piqué A., Bouabdelli M.: Histoire géologique du Maroc, découverte et itinéraires. *Notes Mém. Serv. Géol. Maroc* 409, 2000, 115 p.

Piqué A., Geology of northwest Africa, Borntraeger, Berlin, 2001, 310 p.

Piqué A., Soulaimani A., Hoepffner C., Bouabdelli M., Laville E., Amrhar M., Chalouan A., Géologie du Maroc, Ed. Géode, Marrakech, 2007, 280 p.

Papers

Note: As a general rule, the references proposed in this volume correspond to the last three decades only, being dated from the 80s to early 2008, except in Chap. 9. Previous references can be found in the cited papers or in the books quoted above.

Baltzer A., Aslanian D., Rabineau M., Germond F., Loubrieu B., CHIRP and bathymetric data: a new approach of the Western Sahara continental margin offshore Dakhla. Submitted, nov. 2007.

Bertrand J.M., Jardim de Sá E.F., Where are the Eburnian-Transamazonian collisional belts? *Can. J. Earth Sci*. 27 (1990) 1382–1393.

Black R., Latouche L., Liégeois J.-P., Caby R., Bertrand J.M., Panafrican displaced terranes in the Tuareg shield (central Sahara). *Geology* 22 (1994) 641–644.

Buforn E., Sanz de Galdeano C., Udías A., Seismotectonics of the Ibero-Maghrebian region, *Tectonophysics* 248 (1995) 247–261.

Cavazza W., Roure F., Ziegler P.A., The Mediterranean area and the surrounding regions: active processes, remnants of former Tethyan oceans and related thrust belts, in: W. Cavazza, F. Roure, W. Spakman, G.M. Stampfli and P.A. Ziegler (Eds), The TRANSMED Atlas – the Mediterranean region from crust to mantle, Springer, Berlin, 2004.

Chabou M.C., Sebai A., Féraud G., Bertrand H., Datation ^{40}Ar-^{39}Ar de la province magmatique de l'Atlantique Central dans le Sud-Ouest algérien, *C. R. Geoscience* 339 (2007) 970–978.

Contrucci I., Klingelhöfer, F., Perrot J., Bartolome R., Gutscher M.A., Sahabi M., Malod J., Rehault J.P., The crustal structure of the NW Moroccan continental margin from wide-angle and reflection seismic data, *Geophys. J. Intern*. 159 (2004) 117–128.

Cordani U.G., D'Agrella-Filho M.S., Brito-Neves B.B., Trindade R.I.F., Tearing up Rodinia: the Neoproterozoic palaeogeography of South America cratonic fragments. *Terra Nova* 15 (2003) 350–359.

Dalziel I.W.D., Neoproterozoic-Paleozoic geography and tectonics; review, hypotheses, environmental speculation, *Geol. Soc. Am. Bull*. 109 (1997) 16–42.

DeMets C., Gordon R.G., Argus D.F., Stein S., Effects of recent revisions to the geomagnetic reversal time scale on estimate of current plate motions, *Geophys. Res. Lett*. 21 (1994) 2191–2194.

Dercourt J., Ricou L.E., Vrielinck B. (Eds.), Atlas Tethys environmental maps, Gauthier-Villars Paris, 1–307, 14 maps, 1 pl.

Deruelle B., Ngounouno I., Demaiffe D., The "Cameroon Hot Line" (CHL): A unique example of active alkaline intraplate structure in both oceanic and continental lithospheres, *C. R. Geoscience* 339 (2007) 589–600.

Ennih, N., Liégeois, J.P., The Moroccan Anti-Atlas: the West African craton passive margin with limited Pan-African activity. Implications for the northern limit of the craton, *Precambrian Res*. 112 (2001) 289–302

Ennih, N., Liégeois, J.P., Reply to comments by E.H Bouougri, *Precambrian Res*. 120 (2003) 185–189.

Ennih N., Liégeois J.-P., The boundaries of the West African craton, with a special reference to the basement of the Moroccan metacratonic Anti-Atlas belt. In: Ennih, N. & Liégeois, J.-P. (Eds.) The Boundaries of the West African Craton, *Geol. Soc., London Spec. Publ*. 297 (2008) 1–17. DOI: 10.1144/SP297.1

Fernández-Ibáñez F., Soto J.I., Zoback M.D., Morales J., Present-day stress field in the Gibraltar Arc (western Mediterranean), *J. Geophys. Res*. 112 (2007) B08404, doi 10.1029/2006JB004683.

Frizon de Lamotte, D., Saint Bezar, B., Bracène, R., Mercier, E., The two main steps of the Atlas building and geodynamics of the western Mediterranean, *Tectonics* 19 (2000) 740–761.

Frizon de Lamotte, D., Crespo-Blanc, A., Saint-Bézar, B., Comas, M. Fernadez, M., Zeyen, H., Ayarza, H., Robert-Charrue, C., Chalouan, A., Zizi, M., Teixell, A., Arboleya, M.L., Alvarez-Lobato, F., Julivert, M., Michard, A., TRASNSMED-transect I [Betics, Alboran Sea, Rif, Moroccan Meseta, High Atlas, Jbel Saghro, Tindouf basin], in: W. Cavazza, F. Roure,

W. Spakman, G.M. Stampfli and P.A. Ziegler (Eds), The TRANSMED Atlas – the Mediterranean region from crust to mantle, Springer, Berlin, 2004.
Fullea Urchulutegui J, Fernàndez M., Zeyen H., Lithospheric structure in the Atlantic-Mediterranean transition zone (southern Spain, northern Morocco): a simple approach from regional elevation and geoid data, in: D. Frizon de Lamotte, O. Saddiqi, A. Michard (Eds.), Some recent Developments on the Maghreb Geodynamics. *C. R. Geoscience* 338 *(2006)* 140–151.
Gasquet D., Levresse G., Cheilletz A., Azizi-Samir M.R., Mouttaqi A., Contribution to a geodynamic reconstruction of the Anti-Atlas (Morocco) during Pan-African times with the emphasis on inversion tectonics and metallogenic activity at the Precambrian-Cambrian transition, *Precambr. Res*. 140 (2005) 157–182.
Gradstein F.M. et al., International stratigraphic chart, http://www.stratigraphy.org/chus.pdf, Stratigraphy I.C.O. Ed. 2004.
Gutscher M.-A., Malod J.A., Réhault., J.P., Contrucci I., Klingelhöfer F., Spakman W., Sismar scientific team, Evidence for active subduction beneath Gibraltar, *Geology* 30 (2002) 1071–1074.
Knight K.B., Nomade S., Renne P.R., Marzoli A., Bertrand H., Youbi N., The Central Atlantic Magmatic Province at the Triassic-Jurassic boundary: paleomagnetic and $^{40}Ar/^{39}Ar$ evidence from Morocco for brief, episodic volcanism, *Earth Planet. Sci. Lett*. 228 (2004) 143–160.
Lahondère D., Thiéblemont D. et al., Notice explicative des cartes géologiques à 1/200.000 et 1/500.000 du nord de la Mauritanie, DMG, Ministère Mines Industrie, Nouakchott.
Le Roy P., Piqué A., Triassic-Liassic Western Morocco synrift basins in relation to the Central Atlantic opening, *Marine Geol*. 172 (2001) 359–381.
Marzoli A., Bertrand H., Knight K.B., Cirilli S., Buratti N., Vérati C., Nomade S., Renne P.R., Youbi N., Martini R., Allenbach K., Neuwerth R., Rapaille C., Zaninetti L., Bellieni G., Synchrony of the Central Atlantic magmatic province and the Triassic-Jurassic boundary climatic and biotic crisis, *Geology* 32 (2004) 973–976.
Meert J.G., Lieberman B.S., The Neoproterozoic assembly of Gondwana and its relationship to the Ediacaran-Cambrian radiation, *Gondwana Res*. 2007, in press.
Michard A., Chalouan A., Feinberg H., Goffé B., Montigny R., How does the Alpine belt end between Spain and Morocco? *Bull. Soc. géol. Fr*. 173 (2002) 3–15.
Missenard, Y., Zeyen H., Frizon de Lamotte D., Leturmy P., Petit C., Sébrier M., Saddiqi O., Crustal versus asthenospheric origin of the relief of the Atlas mountains of Morocco, *J. Geophys. Res*. 111 (B03401) (2006) doi:10.1029/2005JB003708.
Morel J.L., Meghraoui M., Gorringe-Alboran-Tel tectonic zone: A transpression system along the Africa-Eurasia plate boundary, *Geology* 24 (1996) 755–758.
Negredo A.M., Bird P, Sanz de Galdeano C. & Buforn E., Neotectonic modelling of the Ibero-Maghrebian region. *J. Geophys. Res*. 107 (2002) B11, 2292, doi:10.1029/2001JB000743.
Olsen P.E., Kent D.V., Et-Touhami M., Puffer J., Cyclo-, magneto-, and bio-stratigraphic constraints in the duration of the CAMP event and its relationship to the Triassic-Jurassic boundary, in W.H. Hames, J.G. McHone, P.R. Renne & C. Ruppel (Eds.), The Central Atlantic Magmatic Province: Insight from fragments of Pangea, *Geophys. Monogr. Ser*. 136 (2003), doi 10.1029/136GM01.
Piqué A., Laville E., L'ouverture initiale de l'Atlantique central, *Bull. Soc. géol. Fr*. 166 (1995) 725–738.
Piqué A., Michard A., Moroccan Hercynides, a synopsis. The Paleozoic sedimentary and tectonic evolution at the northern margin of west Africa, *Am. J. Sci*. 289 (1989) 286–330.
Rodgers J.J.W., Santosh M., Configuration of Columbia, a Mesoproterozoic supercontinent, *Gondwana Res*. 5 (2002) 5–22.
Rosenbaum G., Lister G.S., Duboz C., Relative motion of Africa, Iberia and Europe during Alpine orogeny, *Tectonophysics* 339 (2002) 117–126.
Sahabi M., Aslanian D., Olivet J.-L., Un nouveau point de départ pour l'histoire de l'Atlantique central, *C.R. Geosci*. 336 (2004) 1041–1052.
Schofield D.I., Gillespie M.R., A tectonic interpretation of "Eburnean terrane" outliers in the Reguibat Shield, Mauritania, *J. Afr. Earth Sci*. 49 (2007) 179–186.

Schofield D.I., Horstwood M.S.A., Pitfield P.E.J., Crowley Q.G., Wilkinson A.F., Sidaty H.Ch.O., Timing and kinematics of Eburnean tectonics in the central Reguibat Shield, Mauritania, *J. Geol. Soc. London* 163 (2006) 549–560.

Sébrier M., Siame L., Zouine E., Winter T., Missenard Y., Letourmy P., Active tectonics in the Moroccan High Atlas, in: D. Frizon de Lamotte, O. Saddiqi, A. Michard (Eds.), Some recent Developments on the Maghreb Geodynamics. *C. R. Geoscience* 338 *(2006)* 65–79.

Simancas J.F., Tahiri A., Azor A., Lodeiro F.G., Martinez Poyatos D.J., El Hadi H., The tectonic frame of the Variscan-Alleghanian orogen in Southern Europe and Northern Africa, *Tectonophysics* 398 (2005) 181–198.

Spakman W., Wortel R., A tomographic view on Western Mediterranean geodynamics, in], in: W. Cavazza, F. Roure, W. Spakman, G.M. Stampfli and P.A. Ziegler (Eds), The TRANSMED Atlas – the Mediterranean region from crust to mantle, Springer, Berlin, 2004.

Stampfli G.M., Borel G.D., A plate tectonic model for the Paleozoic and Mesozoic constrained by dynamic plate boundaries and restored synthetic oceanic isochrons, *Earth Planet. Sci. Let*. 196 (2002) 17–33.

Stich D., Serpelloni E., Mancilla F., Morales J., Kinematics of the Iberia-Maghreb plate contact from seismic moment tensors and GPS observations, *Tectonophysics* 426 (2006) 293–317.

Verati C., Rapaille C., Féraud G., Marzoli A., Marzoli H., Bertrand H., Youbi N., Ar-Ar ages and duration of the Central Atlantic magmatic province volcanism in Morocco and Portugal and its relation to the Triassic-Jurassic boundary. *Paleogeogr. Paleoclim. Paleoecol*. 244 (2007) 308–325.

Villeneuve M., Cornée J.J., Structure, evolution and paleogeography of the West African craton and bordering belts during the Neoproterozoic, *Precambrian Res*. 69 (1994) 307–326.

Villeneuve M., Bellon H., El Archi A., Sahabi M., Rehault J.-P., Olivet J.-L., Aghzer A.M., Evénements panafricains dans l'Adrar Souttouf (Sahara marocain), *C.R. Geosci*. 338 (2006) 359–367.

Weil A.B., Van der Voo R., Mac Niocaill C., Meert J.G., The Proterozoic supercontinent Rodinia: Paleomagnetically derived reconstructions for 1100 to 800 Ma, *Earth Planet. Sci. Lett*. 154 (1998) 13–24.

DETAILED ITINERARY

Day 1: Friday, March 6th, 2026 – Fly to Morocco

Find your way to Washington Dulles International Airport

You are responsible for getting to and from the airport. Car pools, taxi, Uber, whatever.

Our flight details:

Departure: Royal Air Maroc, AT219, Friday, March 6, 2026, 8:45PM, Washington DC (Dulles – IAD) to Casablanca (CMN)

Arrival: Casablanca on Saturday, March 7, 2026 at 8:50AM

Try to arrive at Dulles approximately 2 hrs prior to flight departure. When arriving at Dulles go to the Royal Air Maroc check-in counter, they will issue tickets to you, just show them your passport.

Again, you are allowed one checked bag and a carry-on bag for this trip. Do not exceed this allowance, please.

Day 2: Saturday, March 7th, 2026 – Arrive in Marrakech

We have a connection through Casablanca

Departure: Royal Air Maroc, AT411, Saturday, March 7, 2026, 10:55AM, Casablanca (CMN) to Marrakech (RAK)

Arrival: Marrakech on Saturday, March 7, 2026, 11:45AM

12:00 PM: Arrive in Marrakech
Afternoon: Get to the Hotel and tour around Marrakech

Hotel information: Kennedy Hospitality Resort – Marrakech
Av. du Président Kennedy, Marrakech 40000, Morocco
https://www.kennedyhospitalityresort.com/

From the Guide:
After we meet you in Marrakech airport, our private tour from Marrakech starts after we offer you a meal. Depending on the time of your arrival, we might explore some of the landmarks of Marrakech; Jemaa el fna Square, the Medina and Market. After that, we will go to your hotel.

Marrakech

This introduction is from the following guide book:

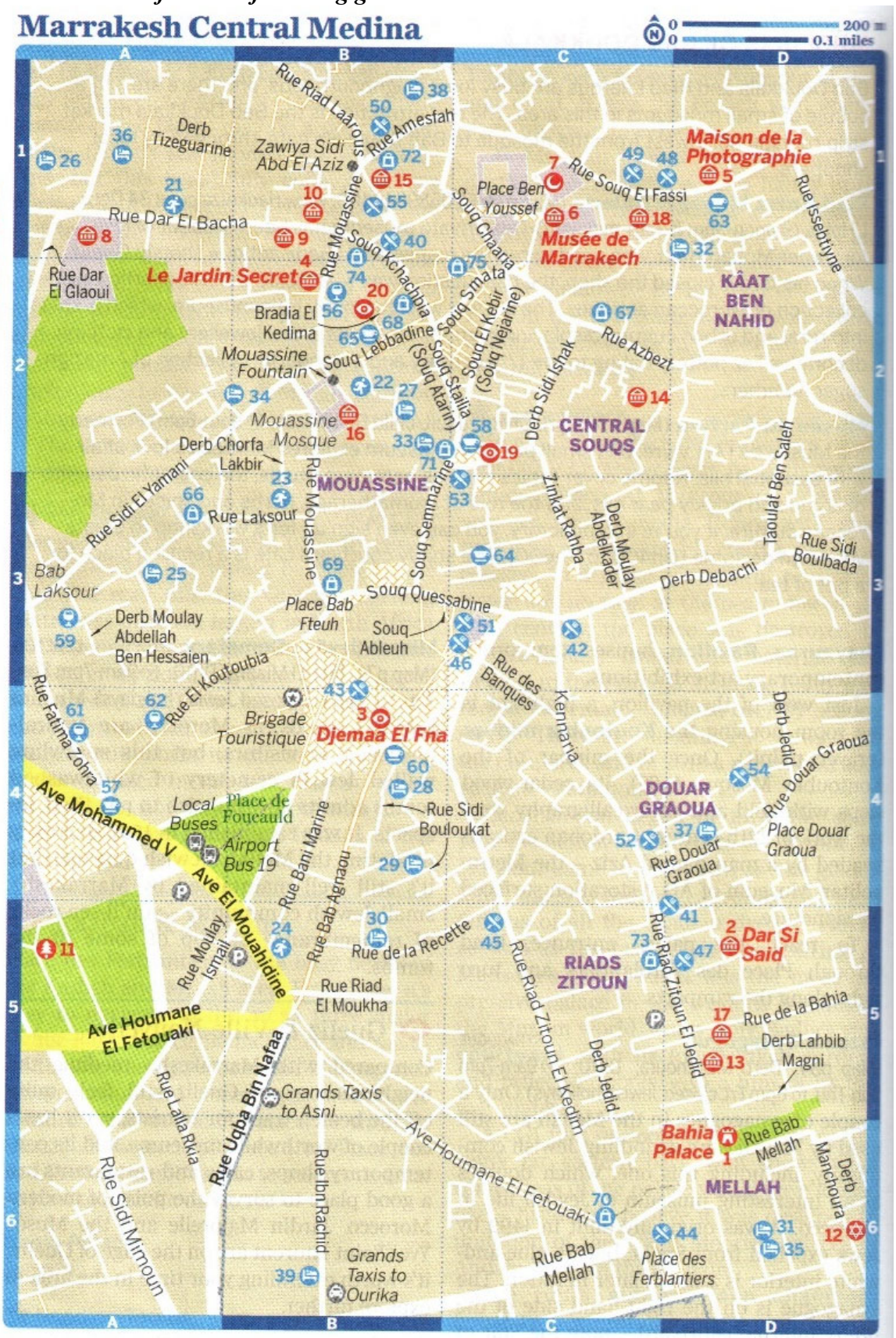

Marrakesh Central Medina

Top Sights
1 Bahia Palace D6
2 Dar Si Said D5
3 Djemaa El Fna B4
4 Le Jardin Secret B2
5 Maison de la Photographie D1
6 Musée de Marrakech C1

Sights
7 Ali Ben Youssef Medersa C1
8 Dar El Bacha A1
9 Funduq El Amri B1
10 Funduq El Mizen B1
11 Koutoubia Gardens A5
12 Lazama Synagogue D6
13 Moroccan Culinary Arts Museum D5
14 Musée Boucharouite C2
15 Musée de la Femme B1
16 Musée de Mouassine B2
17 Musée Tiskiwin D5
18 Orientalist Museum C1
19 Rahba Kedima C2
20 Souq des Teinturiers B2

Activities, Courses & Tours
21 Hammam de la Rose A1
22 Hammam Mouassine B2
23 Le Bain Bleu B3
24 Marrakech Roues B5

Sleeping
25 Dar Attajmil A3
26 Dar Baraka & Karam A1
27 Equity Point Hostel B2
28 Hôtel Cecil B4
29 Hotel du Trésor B4
30 Le Gallia B5
31 Riad Azoulay D6
32 Riad Berbère D1
33 Riad Le J B2
34 Riad L'Orangeraie B2
35 Riad Noos Noos D6
36 Riad Tizwa A1
37 Riad UP D4
38 Rodamón B1
39 Villa Verde B6

Eating
40 Beats Burger B1
41 BlackChich D5
42 Corner Cafe C3
43 Djemaa El Fna Food Stalls B4
44 Earth Cafe D6
45 Earth Café C5
46 Hadj Mustapha C3
47 La Famille D5
48 Le Foundouk C1
Le Jardin ..... (see 15)
49 Le Trou Au Mur C1
50 Max & Jan B1
51 Mechoui Alley C3
52 Naranj C4
53 Nomad C3
54 PepeNero D4
55 Souk Kafé B1

Drinking & Nightlife
Bacha Coffee ..... (see 8)
56 Café Arabe B2
57 Café El Koutoubia A4
58 Chichaoua C2
59 El Fenn A3
60 Grand Balcon du Café Glacier B4
61 Kabana A4
62 Les Jardins de la Koutoubia A4
63 Maison de la Photographie Terrace D1
64 Riad Yima C3
65 Terrasse des Teinturiers B2

Shopping
66 Al Nour A3
67 Anamil C2
Arganino ..... (see 74)
68 Cooperative Artisanale des Femmes de Marrakesh B2
69 Funduq El Ouarzazi B3
70 Kaftan Queen C6
71 L'Art du Bain Savonnerie Artisanale B2
72 Max & Jan B1
73 Naturom C5
Sissi Morocco ..... (see 71)
74 Souq Cherifia B1
75 Souq Haddadine C2

Day 3: Sunday, March 8th, 2026 – Marrakech – Sidi Rahal – High Atlas – Ait ben Haddou – Ouarzazate

STOP 3.1 – Sidi Rahal Agate Mine
STOP 3.2 – Fault near Zerkten
Lunch Stop
STOP 3.3 – Col du Tichka
STOP 3.4 – Telouet Salt Mine
STOP 3.5 – Ounila Valley
STOP 3.6 – Ait-Ben-Haddou
STOP 3.7 – Ouarzazate

Hotel Details:
Les Jardins de Ouarzazate
13 N9, Tarmigt 45000, Morocco
http://www.lesjardinsdeouarzazate.com/

From our Guide:

The tour starts by leaving the historic city of Marrakech and heading to the High Atlas Mountains. Our first stop is the Sidi Rahal agate mine which lies very close to the North Atlas Fault. The fault separates the flat plain (which Marrakech lies upon) from the High Atlas Mountains which abruptly ascend south of the fault. The agate mine is in Triassic lava that erupted as the North Atlantic began to rift open and here we can find our own agates with a pink outer layer of opal, as well as having the opportunity of buying prize specimens from the local miners. We then start to ascend the mountains, stopping near the village of Zerkten to see a major transform fault. The next stop is at a restaurant for lunch. A short distance further on we stop for panoramic views and to see Ediacaran rocks thrusting over Cambrian rocks. This is followed by the Col du Tichka which, at 2,260m above sea level, is the highest point on the road. Here a double unconformity can be seen: Ordovician rocks lie unconformably over Middle Cambrian rock, which in turn lies unconformably over Ediacaran aged rocks. A short distance from this stop, a recent road-cut beautifully reveals a fault from the South Atlas fault zone. After this stop, our route leaves the main road and travels along the beautiful Telouet Valley to reach the Telouet salt mine. The mine exploits salt deposits that lie on the Triassic/Jurassic boundary and were deposited during the initial rifting of the North Atlantic. The mine is very old and it lies on the original Marrakech-Timbuktu camel caravan route. In the 11th century its salt was worth more than its weight in gold! Our route then passes through Cretaceous and Palaeogene rocks in the Ounila Valley where we stop to view an impressive fold. Our final stop of the day is for a panoramic view of the Ait-Ben-Haddou World Heritage Site. The kasbah (fortified settlement) was founded in the seventeenth century and has been used as a film set for several movies. The night is spent in a comfortable hotel just outside the city of Ouarzazate.

STOP 3.1 – Sidi Rahal Agate Mine

The following publication is as follows:

Dumanska-Slowik, M., Natkaniec-Nowak, L., Weselucha-Birczynska, A., Gawel, A., Lankosz, M., and Wrobel, P., (2013) Agates from Sidi Rahal, in the Atlas Mountains of Morocco: Gemological Characteristics and Proposed Origin. gems and Gemology, vol. 49, no. 3, pp. 148-159.

AGATES FROM SIDI RAHAL, IN THE ATLAS MOUNTAINS OF MOROCCO: GEMOLOGICAL CHARACTERISTICS AND PROPOSED ORIGIN

Magdalena Dumańska-Słowik, Lucyna Natkaniec-Nowak, Aleksandra Wesełucha-Birczyńska, Adam Gaweł, Marek Lankosz, and Paweł Wróbel

Moroccan agates from Sidi Rahal occur within Triassic basaltoids as lens-shaped specimens in sizes up to 25 cm. Their coloration and internal structure are quite specific and characteristic for this region. The pink outer rim is composed of opal-CT. The layer within it, usually red or red-brown, contains a significant concentration of Fe compounds (hematite and goethite) that are responsible for this zone's color. The nodules' interior, usually blue-gray or white-gray, is formed of fibrous low-α quartz (a low-temperature polymorph of quartz) with minor amounts of moganite. The presence of moganite and Fe compound inclusions suggests that the agate's formation was induced by Fe^{3+} activity in silica-rich fluids. Other solid inclusions such as Cu sulfides, Ti oxides, calcite, and an organic substance were incorporated during post-magmatic, hydrothermal, or hypogenic conditions.

Agate is a unique natural wonder, with no two identical specimens: Each has a different pattern and color. It occurs in various volcanic and sedimentary rocks in nearly all countries on earth, with the most famous gems found in Brazil, India, and Madagascar (e.g., Ball and Burns, 1975; Breiter and Pasava, 1984; Priester, 1999; Moxon et al., 2006; Strieder and Heemann, 2006; Cross, 2008; Götze et al., 2009). Agates consist mainly of fibrous microcrystalline low-α quartz—i.e., macroscopic banded chalcedony (Götze, 2000). Graetsch et al. (1987), Heaney and Post (1992), and Heaney (1995) noted that in agates and other microcrystalline silica phases, low-α quartz commonly forms intergrowths with moganite, a monoclinic silica phase first described by Flörke et al. (1976, 1984) and approved as a new mineral by the International Mineralogical Association in 1999 (Grice and Ferraris, 2000).

Agates are a microcrystalline variety of silica, generally defined as banded chalcedony, but they also contain a variety of other silica polymorphs (Götze et al., 2001). The mechanism of rhythmic bands that produces agate is still not completely understood (Beaster, 2005). A number of explanations have been proposed for this banded texture and the rhythmic segregation of the silica polymorphs (see French et al., 2013). The prevailing hypothesis is that voids in volcanic rock are filled in cycles, from the rim to the center. Silica-rich fluids are believed to have penetrated the rocks through microfissures or infiltration canals. The shape and width of the zones and the general pattern of the agate all depend on the concentration of silica in the fluids, as well as the temperature, pressure, and timing of the fluid influxes. Other elements found in the fluids (Fe, Ti, Mn, and others) affect only the coloration of the agate zones. At the final stage of formation, mainly in the center of the void, idiomorphic quartz of different colors—brown, smoky quartz, amethyst, and rock crystal—can crystallize, sometimes accompanied by calcite, hematite, goethite, barite, and other minerals (Heaney, 1993; Götze et al., 2001; Moxon and Rios, 2004; French et al., 2013).

Moroccan agates from the Atlas Mountains were first described in the 1940s (Jahn et al., 2003), but only recently have they drawn the interest of collectors worldwide. The specimens are commonly white-gray, blue-gray, red-gray, and brown-gray, and are found in sizes up to 25 cm in diameter (Zenz, 2005a). The scientific literature has dealt mainly with the geology of the deposits (e.g., Jahn et al., 2003; Zenz, 2005b, 2009; Gottschaller, 2012; Mayer, 2012; Mohr, 2012; Schwarz, 2012). This paper focuses instead on the gemological characteristics of these agates.

The town of Sidi Rahal is located about 60 km east of Marrakesh. The agate outcrops occur nearby in an

See end of article for About the Authors and Acknowledgments.
GEMS & GEMOLOGY, Vol. 49, No. 3, pp. 148–159,
http://dx.doi.org/10.5741/GEMS.49.3.148.

Figure 1. The Moroccan agate nodules investigated in this study showed a wide variety of patterns, including landscape, stalactite, and pipe forms. These samples range from 4 to 15 cm wide. Photo by Małgorzata Klimek.

area approximately 40–50 km long and 5 km wide. Although the region is abundant with these gems, it is not being worked on a commercial scale. Every day locals look for agate to sell to gem collectors from around the world. The most spectacular specimens are used for carvings and cabochons.

In the present study, we investigate the distribution of different silica phases within agate from Sidi Rahal and provide initial characterization of solid inclusions found in the colored zones. Observations of the samples' microtextures, and chemical and mineralogical analysis of the solid inclusions found in the matrix, are considered with regard to how the agates formed.

GEOLOGICAL SETTING

Morocco's largest agate deposits are found in Tizi-n-Tichka, Asni, and Sidi Rahal, in the northwestern part of the Atlas Mountains; detailed geological maps of this region are presented by Jahn et al. (2003). The Atlas Mountains consist mainly of Paleozoic crystalline schists, quartzites, limestones, and Paleogene volcanic rocks associated with Alpine orogenic tectonic movements (Babault et al., 2013). The upper part of the mountains is covered with folded Jurassic and Cretaceous limestone and lower Paleogene flysch rocks (schists-sandstone).

Triassic basaltoids as thick as 3 km outcrop in the vicinity of Sidi Rahal. This semicircular volcanic outcropping covers a 110 × 70 km area. The basaltoids frequently contain spherical or lens-shaped geodes filled with SiO_2 minerals (Verdier, 1971). Agates from Sidi Rahal are mainly gray-white or red-gray, with a red-orange or pink external rim. In the inner part of the geode, white-gray chalcedony coexists with colorless quartz. Cutting and polishing reveal landscape, stalactite, or pipe-shaped patterns (figure 1). Yet some are also monocentric (see the classification proposed by Campos-Venuti, 2012), with a void in the center or filled with the youngest generation of silica polymorph.

MATERIALS AND METHODS

Ten agate samples were provided by Polish gem collectors Jacek Szczerba and Remigiusz Molenda, who personally gathered the nodules in 2010 and 2011. Mineralogical characterization of selected nodules was carried out with a transmission microscope, a scanning electron microscope (SEM-EDS and SEM-CL), X-ray fluorescence (XRF) microspectroscopy, and Raman microspectroscopy.

The specimens were examined with an Olympus BX 51 polarizing microscope with a magnification range of 40× to 400×. Backscattered electron observations were performed on polished, carbon-coated sections using an FEI Quanta 200 field emission gun scanning electron microscope equipped with energy-dispersive spectroscopy and cathodoluminescence detectors. The system was operated at 20 kV accelerating voltage in high-vacuum mode. Scanning electron microscopy provides information on the quantity of solid inclusions and their general chemical composition. Combined with Raman spectroscopy, it enables the user to identify all mineral and organic phases found within an agate's matrix.

Raman spectra of silica phases and solid inclusions were recorded with a Renishaw InVia Raman microspectrometer coupled with a Leica microscope featuring 20×, 50×, and 100× magnification objectives. Two selected samples were excited with a 785 nm high-power near-infrared (HP NIR) laser. The laser

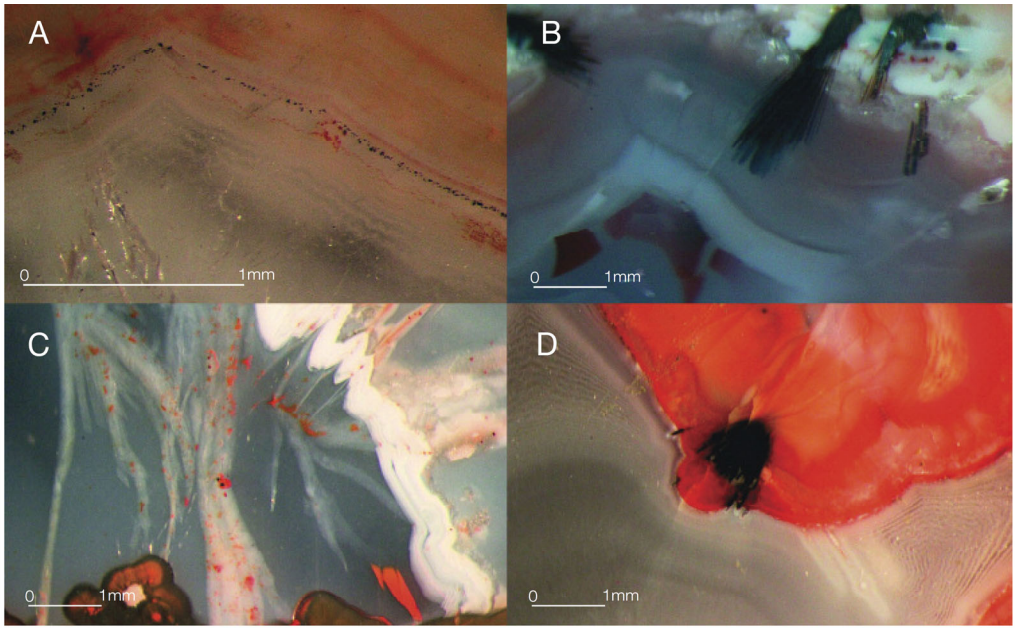

Figure 2. Solid inclusions of Fe compounds found in the agates can form tiny laminae (A), needle-like inclusions (B, D) or euhedral crystals irregularly scattered within silica (C, D). Photomicrographs by Tomasz Toboła.

power and excitation time were optimized to the optic character of the samples. The laser focus diameter was approximately 1–2 µm. It should be noted that almost no sample preparation was performed. The two samples were broken with a geological hammer, and the fractured surface was cleaned carefully with distilled water and acetone before measurements were made to avoid any contamination.

Raman maps were recorded with a Thermo Scientific DXR Raman microscope on selected areas (190 × 150 µm), using a step size of 3 µm. The agate sample was excited with a 780 nm laser. We recorded the most intense bands for quartz (460 cm^{-1}), opal (412 cm^{-1}), and moganite (501 cm^{-1}) in each point of the analytical grid.

Two-dimensional maps of elemental abundance were created with a laboratory setup consisting of a low-power X-ray tube with a molybdenum anode and a silicon drift detector, or SDD (Wróbel et al., 2012). The measurements were performed in typical 45°/45° geometry, where the angles between impinging beam, sample normal, and detector axis equaled 45°. The X-ray tube voltage and current were 50 kV and 1 mA, respectively. Primary radiation from the X-ray tube was focused with a polycapillary lens into a Gaussian-shaped beam with a spot size of at least 16.4 µm full width at half maximum (FWHM). The sample surface was placed out of focus of the primary radiation beam, which had an effective size of approximately 50 µm FWHM. The samples were mounted between two 2.5 µm thick Mylar films stretched across a plastic holder. Mounting the holder onto a motorized stage allowed the sample to be rotated in three directions with micrometer resolution.

For the mapping of agate samples 1 and 2, the step size (pixel size) equaled 150 µm in the horizontal and vertical directions. The first map measured 128 × 134 pixels, equal to 19.05 × 19.95 mm^2. The second map was 108 × 134 pixels, or 16.05 × 19.95 mm^2. The sample acquisition times were 2 seconds per pixel and 3 seconds per pixel, respectively.

The net intensities of the characteristic lines were calculated with AXIL-QXAS software using nonlinear least-squares fitting for peak deconvolution. Due to the number of measured points, we evaluated the spectra automatically using batch mode. Using our own LabVIEW scripts, we reconstructed maps of characteristic line intensities.

RESULTS

The vast majority of agate from Sidi Rahal exhibits two rim layers: pink-orange (outer) and red-brown (inner). Their thickness ranges from 0.1 to 1.0 cm. The color of the inner zone likely results from fine Fe-bearing pigments such as oxides and hydroxides scattered within the silica matrix (figures 2A, 2C, and 2D). Internally, the nodules are mostly gray-blue or white. Sometimes these regions are intersected by coarse groups of thin needle-like inclusions, either red-brown or black, that we initially attributed to Fe compounds (figures 2B and 2D). Within each zone, numerous infiltration canals called *osculum* were observed with the unaided eye.

Under the polarizing microscope in transmitted

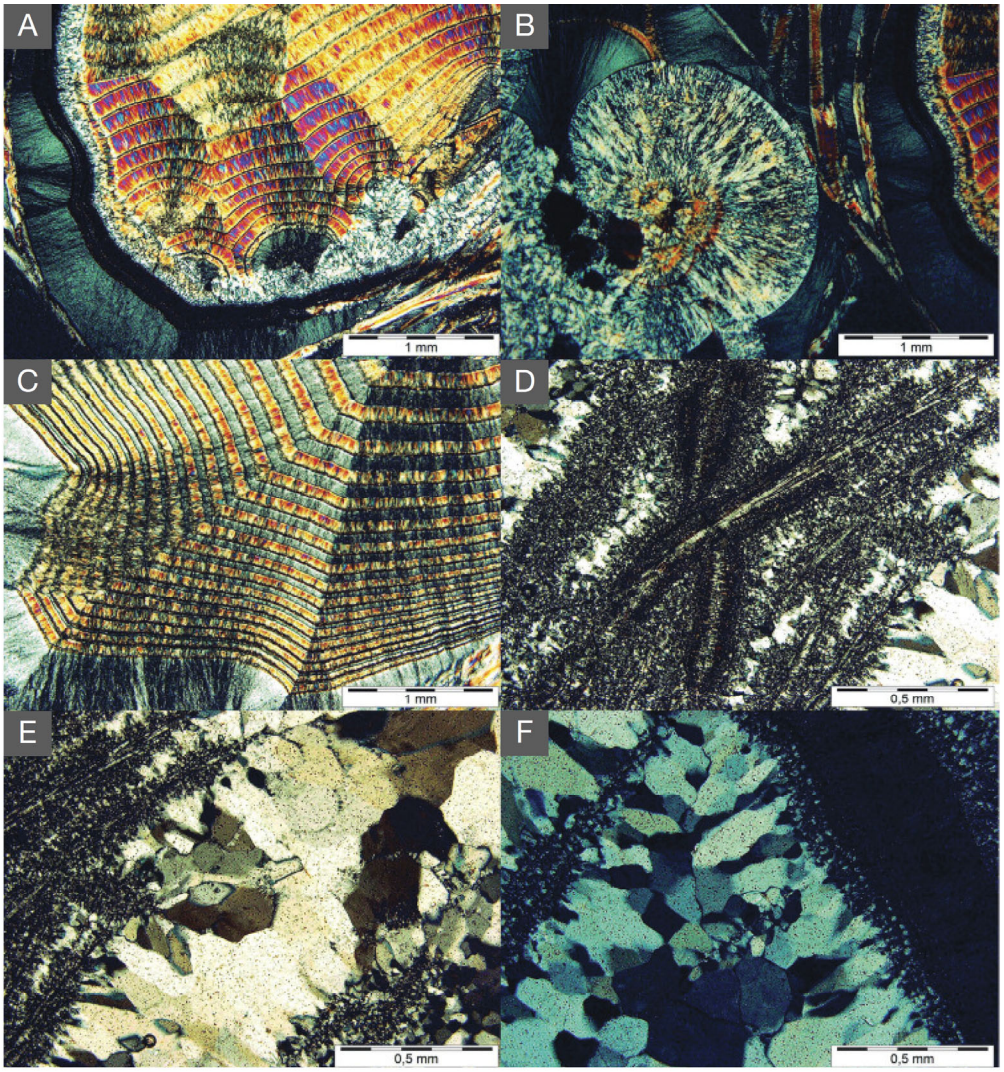

Figure 3. Between crossed polarizers, microtextures can be observed in the agates' various zones: external (A, B), middle (C, D), and internal (E, F). Photos by Małgorzata Klimek.

light, the gray-blue region inside the nodule appeared to be composed of a microcrystalline silica phase, while the internal white crustal zones contained idiomorphic quartz crystals. The microcrystalline silica phase crystallized as twisted crystals forming fibrous radial and fan-like (spherulitic) microtextures (figure 3). In the external part of the agates, the distinct boundaries between the microlayers were emphasized by thin laminae of nontransparent phases. Internally, the boundaries were almost invisible, indicating a continuous and even supply of silica-bearing water solutions. The dark brown zigzag-like inclusions consisted of an organic substance that luminesced under a long-wave UV lamp (figure 4).

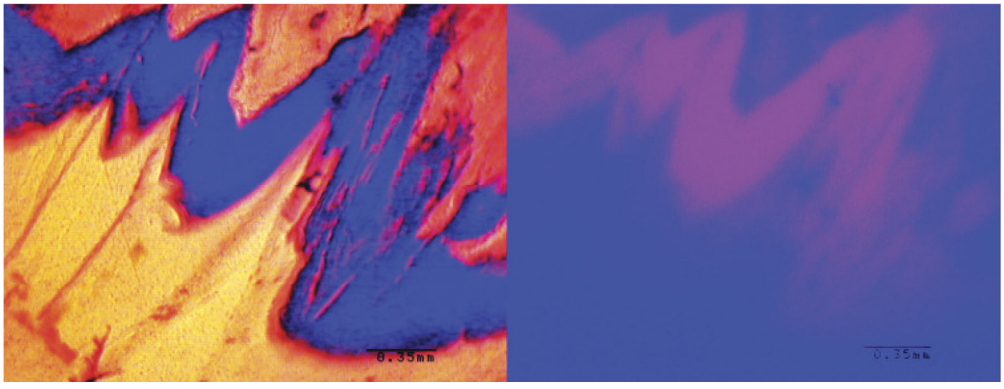

Figure 4. This agate shows organic matter in its middle region between crossed polarizers (left) and characteristic fluorescence under UV light (right). Photomicrographs by Tomasz Toboła.

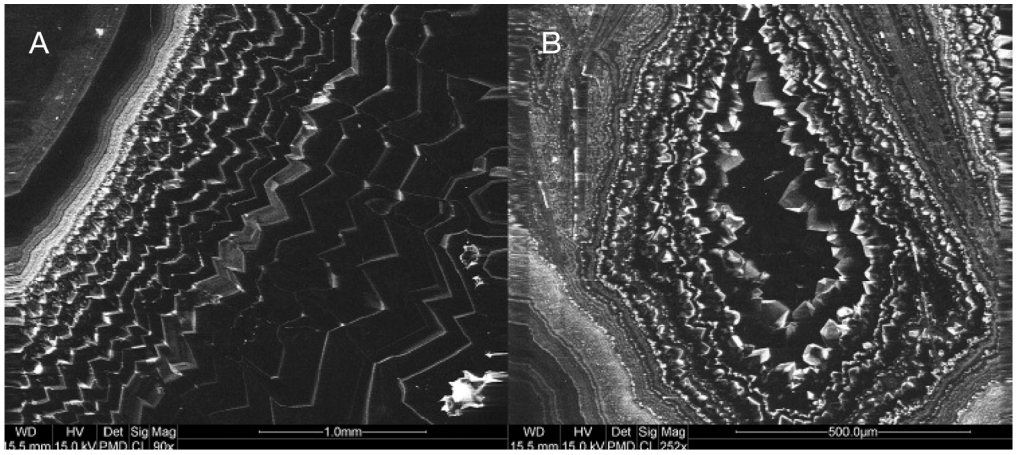

Figure 5. These SEM-CL images of agate from Sidi Rahal show the crystals' growth direction: outward from left to right (A) and inward to the center (B).

Using SEM-EDS and SEM-CL, we easily observed the various silica generations forming mosaic microtextures with different luminescence colors. The SEM-CL images revealed not only the sequence of the silica phases but also the growth direction of the crystals from the rim to the center of the agate void (figure 5). Solid mineral inclusions found in the silica matrix were comprised mainly of (1) pyroxene, typically occurring in the contact zone between the agate and the basaltoid host rock; (2) Fe compounds forming regular round crystals arranged into thin layers between silica zones; or (3) xenomorphic heterogeneous crystals scattered randomly within the matrix. Some Fe compounds, possibly hydroxides, also formed needle-like inclusions. In the central part of the nodule, tiny single crystals of Cu sulfides were accompanied by idiomorphic quartz (figure 6).

The Raman spectra of different silica polymorphs, measured from selected areas of the agates, are presented in figure 7. Band assignments and comparisons with references are listed in table 1. The distinctive 460 and 501 cm^{-1} marker bands are related to symmetric stretching-bending vibrations of low-α quartz and moganite, respectively (Götze et al., 1998). The interior of the agate nodules from Sidi Rahal is a mix-

In Brief

- Agates from Sidi Rahal have a specific coloration, with a pink rim and a blue-gray core.
- They are composed of three silica phases: opal-CT, low-α quartz, and moganite.
- The main solid inclusions found within agate matrix include goethite, hematite, Ti- and Cu compounds, plagioclase, and carbonaceous matter.

TABLE 1. Raman band positions (cm^{-1}) and assignments of agate from Sidi Rahal, Morocco.

Point 1: Opal-CT	Point 2: Low quartz + moganite	Point 3: Low quartz + moganite	Point 4: Low quartz + moganite	Point 5: Low quartz + moganite	Mode symmetry (Kingma and Hemley, 1994; Götze et al., 1998)	Interpretation
	122	121	123	126	$F_{(LO+TO)}$	Quartz/moganite
	199	197	200	207	A1	Low quartz
222						Opal-CT
346	346	344	347		A1	Quartz
412						Opal-CT
	460	460	460	461	A1	Low quartz/moganite
	483	476	475		A1	
	501	501	501	501	A1	Moganite
782	786	786		781		Low quartz

A1= symmetric stretching-bending vibrations

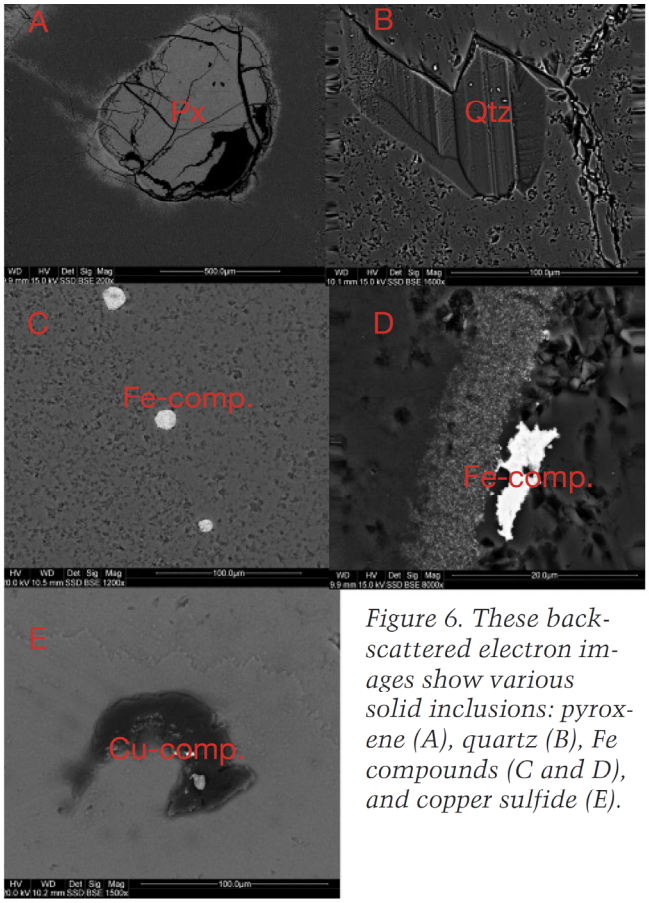

Figure 6. These backscattered electron images show various solid inclusions: pyroxene (A), quartz (B), Fe compounds (C and D), and copper sulfide (E).

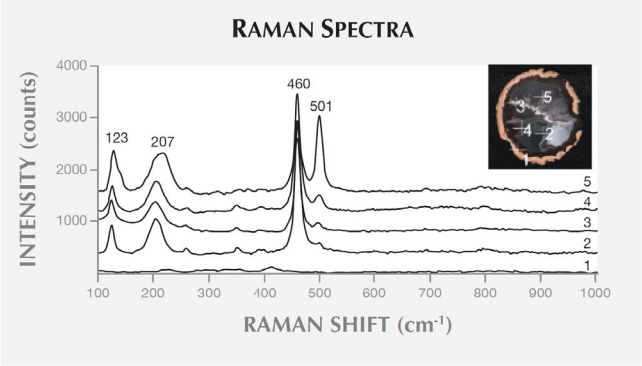

Figure 7. Raman spectra collected from various portions of agate from Sidi Rahal (points 1–5) demonstrated the presence of opal-CT (1) and low-α quartz with an admixture of moganite (2–5).

ture of these two silica polymorphs. The Raman spectrum of the external pink-orange layer revealed the presence of opal-CT with the characteristic band at 410 cm^{-1} (Pop et al., 2004). 2D mapping measurements showed that the opal-CT occurs almost exclusively in the rim, whereas the distribution of low-α quartz and moganite varies within each agate and also between samples (figure 8). The low-α quartz seems to predominate over the moganite, which occurs only in the nodules' visible white regions.

Interesting accumulations of dark brown inclusions (figure 9) were identified with Raman microspectroscopy. These complex heterogeneous inclusions consist of several different phases. Points 2–4 have very similar spectra, with the predominant band at approximately 500 cm^{-1} attributed to feldspar. Curve fitting of the wide 534 cm^{-1} band gives two components: 519 and 549 cm^{-1}, originating from anorthite and bytownite, respectively (Mernagh, 1991). In the first spectrum, the high-frequency

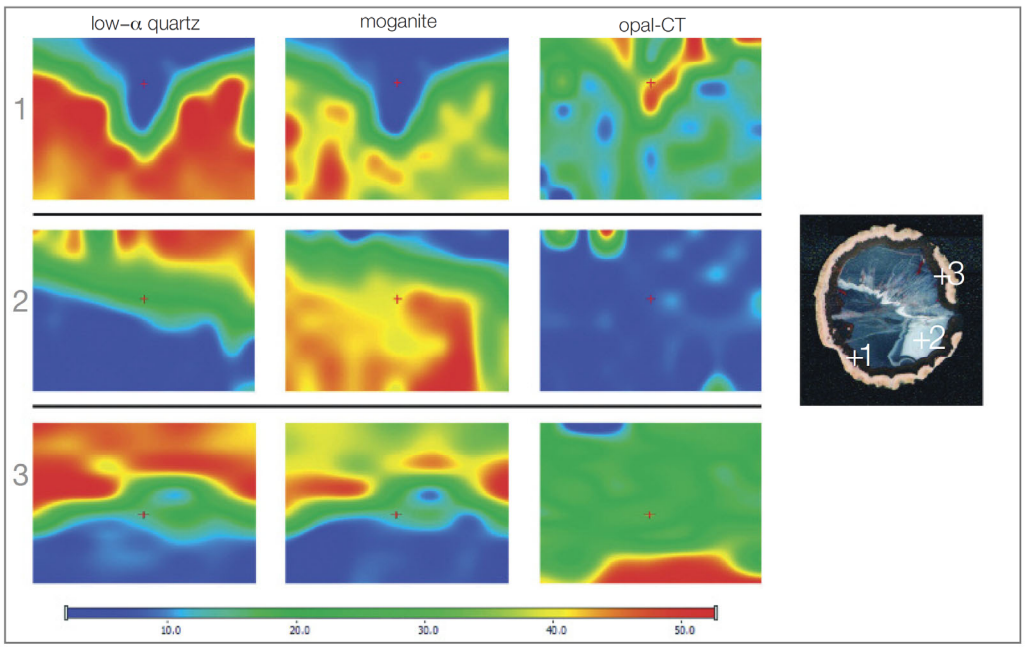

Figure 8. Non-linear Raman mapping of an agate nodule recorded in three regions shows the relative proportions of the silica polymorph. Bands characteristic of quartz (460 cm^{-1}), opal (412 cm^{-1}), and moganite (501 cm^{-1}) were chosen.

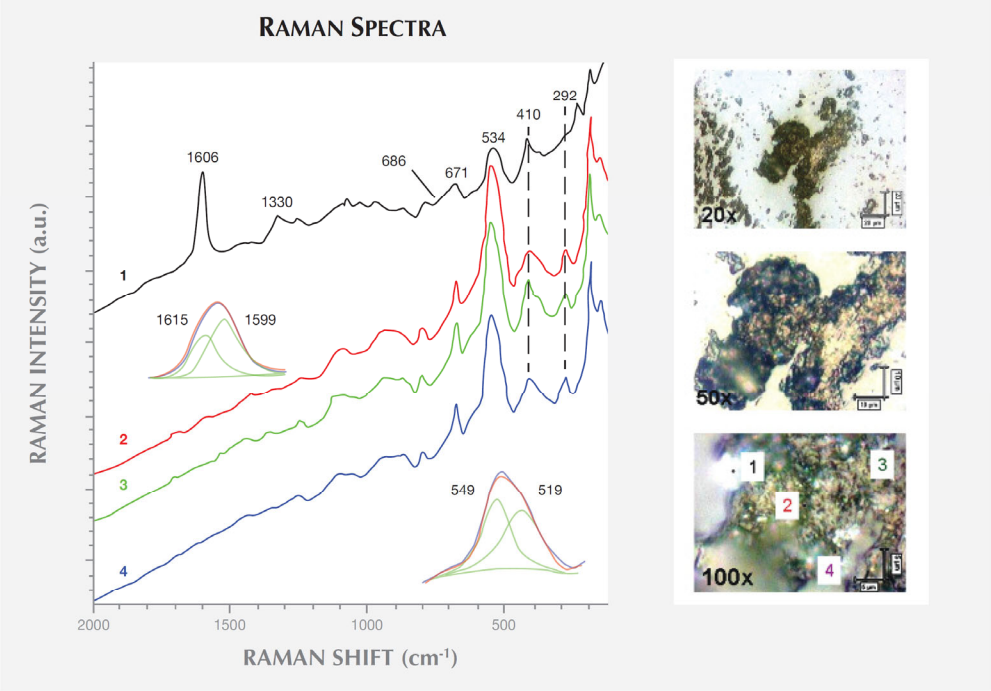

Figure 9. Photomicrographs of dark brown inclusions and Raman spectra (collected from points 1–4) in the 2000–200 cm^{-1} range show the presence of feldspars, goethite, hematite and titanium oxide.

shoulder of the 410 cm^{-1} band located at approximately 434 cm^{-1} and the broad, weak band at 686 cm^{-1} likely indicate the presence of nanocrystalline TiO_2 (figure 10).

The presence of carbonaceous matter is very clearly marked by 1330 and 1606 cm^{-1} bands (again, see figure 10). Resolving this second band gives two bands: one at 1599 cm^{-1}, the other a D1 band at 1615 cm^{-1}, forming a shoulder on the G band. These bands are characteristic for graphite and carbonaceous matter. The 1330 cm^{-1} band (called the D band) is due to disorder-induced first-order Raman mode, and the 1599 cm^{-1} band to first-order E_{2g} Raman mode (G band); the 1615 cm^{-1} band is called the D1 band (figure 10, inset, and figure 11; see Beyssac et al., 2003). The D1 band always occurs with the D band, and its intensity increases with a decreasing degree of organization. In the second-order region (2200–3400 cm^{-1}) there also appear weaker peaks, representing poorly organized carbonaceous matter, attributed to overtone or combination scattering (table 2).

Another component of this complex inclusion is goethite, indicated by the characteristic band at 387 cm^{-1} (390 cm^{-1}) observed in points 2–4. This band is caused by symmetric stretching vibrations of Fe-O-Fe-OH (Legodi and de Waal, 2006). Hematite in the agate matrix is evidenced by marker bands at 292, 410, and 610 cm^{-1} (again, see figure 10). These bands are attributed to symmetric bending vibrations of Fe-O (Legodi and de Waal, 2006).

Figure 11 presents another example of characteristic carbonaceous matter bands within an agate ma-

Figure 10. The baseline-corrected Raman spectra for points 1 and 3 (see figure 9), collected in the 2000–200 cm^{-1} range, reveal the presence of anorthite, bytownite (inset), carbonaceous matter, and titanium oxide within the dark brown complex inclusions.

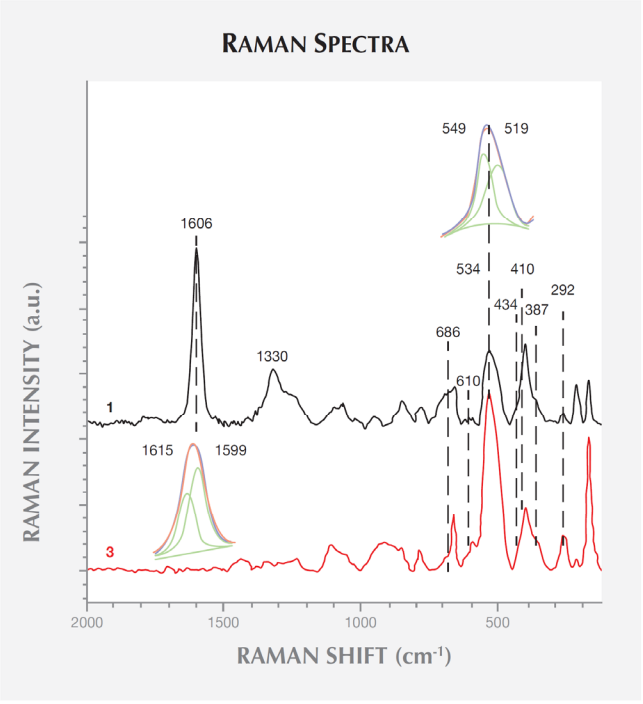

TABLE 2. Raman bands (cm^{-1}) observed in spectra shown in figures 9, 10, and 11.

Band	Assignment	References
180	Bytownite	Mernagh (1991)
225	Opal	Pop et al. (2004)
273	Goethite	Antunes et al. (2003); de Faria et al. (1997)
292	Hematite	Legodi and de Waal (2006)
387	Goethite	Legodi and de Waal (2006)
410	Opal, hematite	Pop et al. (2004); Legodi and de Waal (2006)
434	TiO_2 (nm crystallite size)	Swamy et al. (2006)
534 (519, 549)	Bytownite, anorthite, magnetite	Mernagh (1991); Antunes et al. (2003), de Faria et al. (1997)
610	Hematite	Legodi and de Waal (2006)
671	Bytownite, magnetite	Mernagh (1991); Antunes et al. (2003), de Faria et al. (1997)
686	Anorthite, TiO_2	Mernagh (1991); Swamy et al. (2006)
769	Anorthite	Mernagh (1991)
1076	Anorthite, SiO_2	Mernagh (1991); Pop et al. (2004)
1240	Anorthite	Mernagh (1991)
1330	Carbonaceous matter	Beyssac et al. (2003)
1606 (1599, 1615)	Conjugated C=C, carbonaceous matter: G and D1 mode	Beyssac et al. (2003)
2924	ν as CH_2, carbonaceous matter	Beyssac et al. (2003)
2935	ν as CH_2 in rings, carbonaceous matter	Beyssac et al. (2003)

trix (Beyssac et al., 2003). The 1585 cm^{-1} peak (E_{2g} mode) corresponding to the stretching vibration in the aromatic layers is another example of the G band. The additional band for poorly organized carbonaceous matter, the D band, appears in the first-order region around 1330 cm^{-1}. Positions and half-widths of the G and D bands in this example indicate the different degree of ordering of carbonaceous matter compared to figure 10, spectrum 1. Greater intensity of the D band (1330 cm^{-1}) with respect to the G band (1585 cm^{-1}) indicates a significant carbonaceous matter disorder in this inclusion. It is believed that organized carbonaceous matter is developed from the less homogenous organic precursors in the process of solidification of fluid inclusions (Wopenka and Pasteris, 1993). This process may lead to the formation of graphite in rocks, as we have observed in Afghan tourmalines (Wesełucha-Birczynska and Natkaniec-Nowak, 2011).

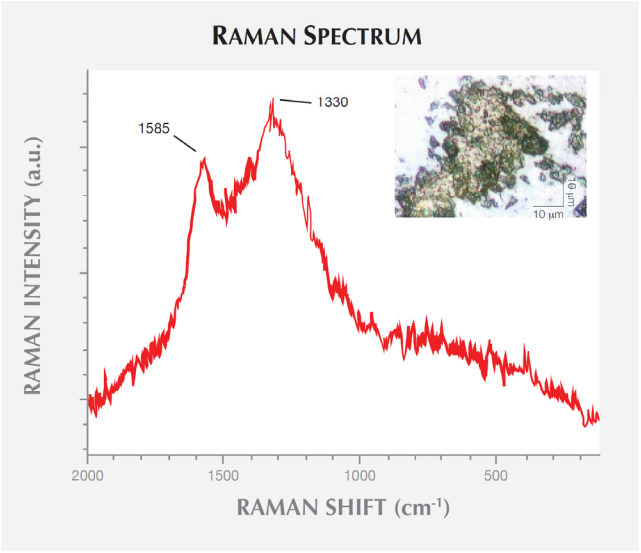

Figure 11. The Raman spectrum of the dark brown inclusions in the 2000–200 cm^{-1} is typical of carbonaceous matter. Photomicrograph by Aleksandra Wesełucha-Birczynska.

The XRF spectrum taken from sample 1 (figure 12) shows characteristic lines for Si, Cl, K, Ca, Fe, and Cu. Figures 13 and 14 present the microscopic view of the measured samples and maps of characteristic Kα X-ray intensities of Si, Ca, Cl, Cu, and Fe

Figure 12. The XRF spectrum taken from a selected area of sample 1 shows the presence of Si, Ca, Cu, Fe, and Cl.

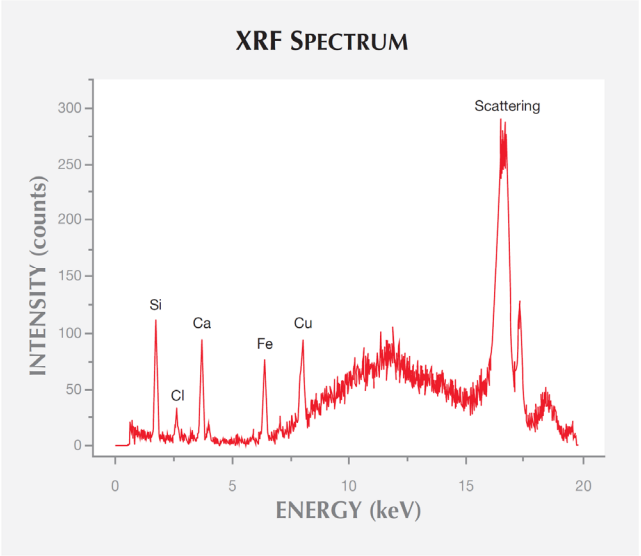

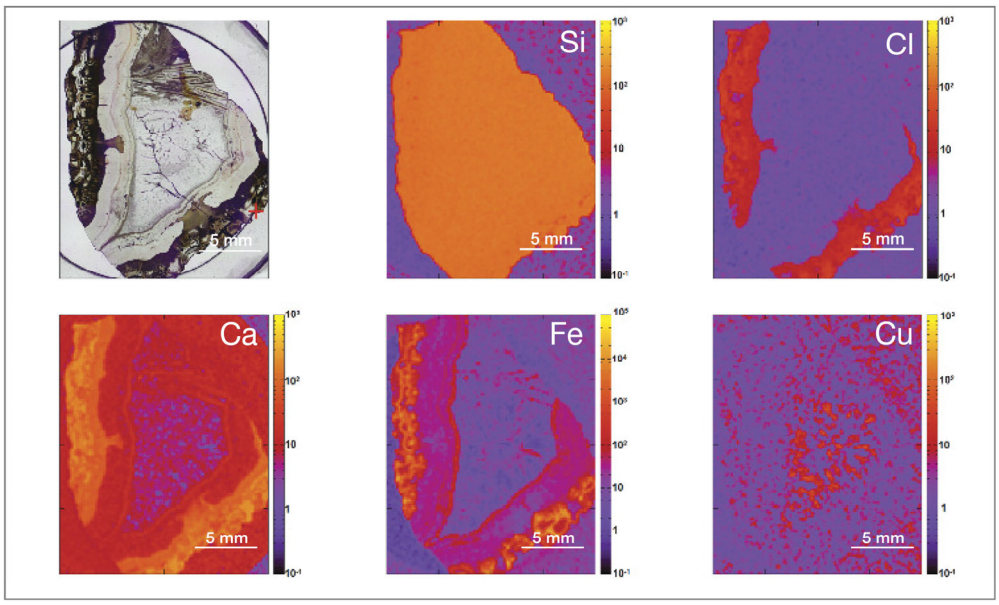

Figure 13. The microscopic view of sample 1 and maps of characteristic Kα X-ray intensities (the red cross marks the analytical point where the XRF spectrum was recorded) show the distribution of Si, Cl, Ca, Fe, and Cu.

in samples 1 and 2. As would be expected, silicon is uniformly distributed in both samples. The other elements are distributed unevenly. In both agates the highest concentrations of Cl, Ca, and Fe are distributed close to the edges. Whereas the inner part of sample 1 shows a very low abundance of Ca and Fe, these elements are evenly distributed throughout sample 2. It is worth noting that fragments containing large amounts of Cl, Ca, and Fe are quite narrow, and concentrations of these elements decrease toward the center of both samples. The varying elemental concentration within the mineral can result from the scattering of Ca, Cl, and Fe during crystal growth. Cu, on the other hand, is deposited in irregular structures measuring about 2 mm or less (sample 1) or in single points less than 0.5 mm in diameter (sample 2). For both samples, Cl and Ca show a very similar pattern; the correlations between Cl-Kα and Ca-Kα intensities are shown in figure 15. The positive correlation coefficients (R) calculated for these elements were 0.94 and 0.89 for samples 1 and 2, respectively.

DISCUSSION

Moroccan agates from Sidi Rahal occurring within Triassic basaltoids are composed mainly of low-α quartz only locally intergrown with moganite. The maturation of cryptocrystalline silica phases (the

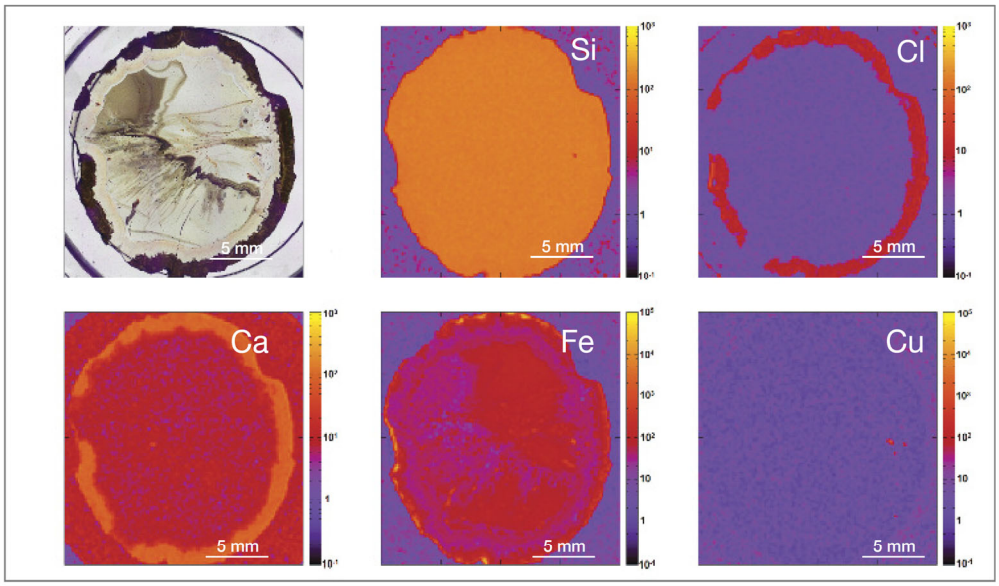

Figure 14. The microscopic view of sample 2 and the maps of characteristic Kα X-ray intensities indicate the distribution of Si, Cl, Ca, Fe, and Cu. Photomicrograph by Piotr Wróbel.

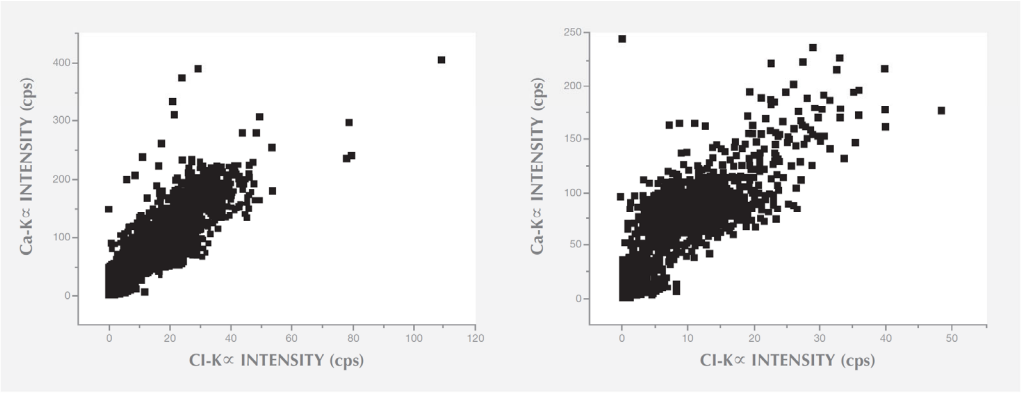

Figure 15. Positive correlations between Ca and Cl concentrations are found in agate samples 1 (R=0.94) and 2 (R=0.89).

transformation of metastable moganite into low-α quartz) generally lowers the moganite content (Moxon and Rios, 2004) over tens of millions of years (Heaney, 1995). Thus, Pop et al. (2004) proposed moganite content as a tool for age evaluation and noted no direct correlation with the geological age of the agate's host rock. Nevertheless, their investigation of the oldest (Cretaceous) microcrystalline samples showed only minor moganite content, while the youngest chalcedony had a relatively high concentration of it. Moganite has generally been identified as an indicator of evaporative sedimentation, although non-evaporitic rocks often contain 5.0–15.0 wt.% moganite (Heaney, 1995). The results of our Raman studies are consistent with these observations, as Triassic agates from Sidi Rahal contain only minor amounts of moganite (figures 7 and 8; table 1).

Pop et al. (2004) noted that moganite crystallization is favored by alkaline fluid composition combined with the high activity of ferric iron. As a result, the absence of moganite in weathered and hydrothermally altered silica samples may be a useful measure of fluid-rock interactions (Heaney, 1995). Agates from Sidi Rahal often contain thin layers with an orange-red, red, or brown-red color, and these are associated with the presence of Fe compounds. Some Fe-bearing phases form linear aggregates, suggesting a continuous supply of iron-bearing fluids to the basaltoid nodule. Hence, the occurrence of both Fe compounds strongly suggests that the crystallization of these agates was induced by Fe^{3+}-rich fluids.

The most widespread inclusions found in the samples were hematite and goethite, which probably formed during hydrothermal conditions of post-magmatic activities. The presence of Cu sulfides and Ti oxides scattered within the agate matrix might also be attributed to hydrothermal fluids. Only traces of titanium phases could have occurred, as XRF analyses did not detect their presence in the agate matrix. In a few instances, the agates' voids or some of their microfissures were filled with idiomorphic calcite crystals. The formation of this carbonate phase is associated with a *hypogenic* process (referring to a mineral deposit formed from aqueous solutions that originated at depth and ascended through the crust). Other solid inclusions occurring within the silica matrix are pyroxene, plagioclase, and an organic substance forming irregularly scattered aggregates. Pyroxene and plagioclase occur only in the outer portions, and these are typical components of the basaltoids' host rock. The organic substance was probably incorporated into the agate under late hydrothermal, hypogenic conditions by exposure to groundwater, or it might be of algal-marine origin. To determine the exact origin of the organic substance, we plan to carry out stable carbon isotope analyses in the next stage of our investigations, as we did with the "bituminous" agates from Nowy Kościół, Poland (Dumańska-Słowik et al., 2008).

In XRF maps of agate from Sidi Rahal, the location and distribution of Ca and Cl are mutually correlated (figure 15). Such a strong correlation indicates that the concentration of these elements may be related to the same mechanism. They could have been incorporated into the nodules from a marine environment. Similarly, the presence of moganite, the silica phase typical of evaporative sedimentation, and some organic components found in the agates supports the thesis that a marine environment affected the formation of these beautiful gems. Undoubtedly, the crystallization of agates from Sidi Rahal lasted millions of years and took place in stages, influenced by various geochemical processes of terrestrial and marine environments.

CONCLUDING REMARKS

Agates from Sidi Rahal are composed of three silica phases: low-α quartz, moganite, and opal-CT. The

latter occurs mainly in the nodules' pink outer zone, while the interior consists of low-α quartz and moganite. The nodules' red or brown-red layer results from linearly scattered Fe compounds (hematite). Goethite usually appears as rusty brown forms in a characteristic coarse grouping of needles.

The most common solid inclusions found within the agate matrix include pyroxene, calcium-rich plagioclase, hematite, goethite, and Ti and Cu compounds. Hydrothermal fluids seem to be responsible for the formation of iron, copper, and titanium phases within the agate's microfissures. An organic substance forms tiny irregularly scattered or zigzag-like aggregates, mainly concentrated in the external and middle zones. The substance formed under hydrothermal, hypogenic conditions and may be of algal marine origin. Similarly, the presence of calcite, mainly filling the void, is connected to hypogenic processes.

The presence of red and brown-red external nodule layers enriched with scattered Fe pigments, as well as isolated aggregates of Fe oxides and hydroxides (hematite and goethite) in the whole mass of the nodules, suggests that agate crystallization was associated with the activity of Fe^{3+} in silica-bearing fluids. The higher moganite concentration in the inner part of the agate also indicates the alkaline character of the silica fluids. The significant concentration of Ca, Cl, and Fe in the nodules suggests that the formation of agates from Sidi Rahal was affected by both marine and terrestrial geochemical processes.

Similar patterns of silica polymorph growth within banded agate were observed by French et al. (2013), who attributed these gems' formation to aqueous silica-rich fluid influxes, consistent with our observations of agates from Sidi Rahal.

REFERENCES

Antunes R.A., Costa I., De Faria D.L.A. (2003) Characterization of corrosion products formed on steels in the first months of atmospheric exposure. *Materials Research*, Vol. 6, No. 3, pp. 403–408, http://dx.doi.org/10.1590/S1516-14392003000300015.

Babault J., Teixell A., Struth L., Van Den Driessche J., Arboleya M.L., Tesón E. (2013) Shortening, structural relief and drainage evolution in inverted rifts: Insights from the Atlas Mountains, the Eastern Cordillera of Colombia and the Pyrenees. *Geological Society, London, Special Publications*, Vol. 377, http://dx.doi.org/10.1144/SP377.14.

Ball R.A., Burns R.L. (1975) Agate part 1: A review—Genesis and structure. *Australian Gemmologist*, Vol. 12, No. 5, pp. 143–150.

Beaster T.J. (2005) Agates: A literature review and electron backscatter diffraction study of Lake Superior agates. B.A. thesis, Carleton College, www.carleton.edu/departments/geol/Resources/comps/CompsPDFfiles/2005/Beaster2005.pdf

Beyssac O., Goffe B., Petitet J-P., Froigneux E., Moreau M., Rouzaud J-N. (2003) On the characterization of disordered and heterogeneous carbonaceous materials by Raman spectroscopy. *Spectrochimica Acta Part A*, Vol. 59, No. 10, pp. 2267–2276, http://dx.doi.org/10.1016/S1386-1425(03)00070-2.

Breiter K., Pasava J. (1984) Agates from Horni Halze, Czechoslovakia. *Lapidary Journal*, Vol. 37, No. 11, pp. 1556–1557.

Campos-Venuti M. (2012) *Genesis and Classification of Agates and Jaspers: A New Theory*. Published by the author, 160 pp.

Cross B.L. (2008) Classic agate deposits of northern Mexico. *Mineralogical Record*, Vol. 39, No. 6, pp. 69–88.

de Faria D. L. A., Venaüncio Silva S., de Oliveira M. T. (1997) Raman microspectroscopy of some iron oxides and oxyhydroxides. *Journal of Raman Spectroscopy*, Vol. 28, No. 11, pp. 873–878, http://dx.doi.org/10.1002/(SICI)1097-4555(199711)28:11<873::AID-JRS177>3.3.CO;2-2.

Dumańska-Słowik M., Natkaniec-Nowak L., Kotarba M., Sikorska M., Rzymełka J.A., Łoboda A., Gaweł A. (2008) Mineralogical and geochemical characterization of the "bituminous" agates from Nowy Kościół (Lower Silesia, Poland). *Neues Jahrbuch für Mineralogie Abhandlungen*, Vol. 184, No. 3, pp. 255–268, http://dx.doi.org/10.1127/0077-7757/2008/0098.

Flörke O.W., Jones J.B., *Schmicke* H-U. (1976) A new microcrystalline silica from Gran Canaria. *Zeitschrift für Kristallographie*. Vol. 143, pp. 156–165.

Flörke O.W., Flörke U., Giese U. (1984) Moganite, a new microcrystalline silica mineral. *Neues Jahrbuch für Mineralogue Abhandlungen*. Vol. 149, pp. 325–336.

French M.W., Worden R.H., Lee D.R. (2013) Electron backscatter diffraction investigation of length-fast chalcedony in agate: Implications for agate genesis and growth mechanism. *Geofluids*, Vol. 13, pp. 32–44, http://dx.doi.org/10.1111/gfl.12006.

Gottschaller S. (2012) Wichtige Mineralfundstellen in Marokko. In *Marokko*, extraLapis No. 42, Weise Verlag, Munich, pp. 76–98.

Götze J. (2000) Cathodoluminescence microscopy and spectroscopy in applied mineralogy. *Freiberger Forschungshefte*, C.485, 128 pp.

Götze J., Nasdala L., Kleeberg R., Wenzel M. (1998) Occurrence and distribution of "moganite" in agate/chalcedony: A combined micro-Raman, Rietveld, and cathodoluminescence study. *Contributions to Mineralogy and Petrology*, Vol. 133, No. 1-2, pp. 96–105, http://dx.doi.org/10.1007/s004100050440.

Götze J., Tichomirowa M., Fuchs H., Pilot J., Sharp Z.D. (2001) Geochemistry of agates: A trace element and stable isotope study. *Chemical Geology*, Vol. 175, No. 3–4, pp. 523–542, http://dx.doi.org/10.1016/S0009-2541(00)00356-9.

Götze J., Mockel R., Kempe U., Kapitonov I.,Vennemann T. (2009) Characteristics and origin of agates in sedimentary rocks from the Dryhead area, Montana, USA. *Mineralogical Magazine*, Vol. 73, No. 4, 673–690, http://dx.doi.org/10.1180/minmag.2009.073.4.673.

Graetsch H., Flörke O.W., Miehe G. (1987) Structural defects in microcrystalline silica. *Physics and Chemistry of Minerals*, Vol. 14, No. 3, pp. 249–257, http://dx.doi.org/10.1007/BF00307990.

Grice J.D., Ferraris G. (2000) New minerals approved in 1999 by the Commission on New Minerals and Mineral Names, International Mineralogical Association. *Canadian Mineralogist*,

Vol. 38, No. 1, pp. 245–250, http://dx.doi.org/10.2113/gscanmin.38.1.245.
Heaney P.J. (1993) A proposed mechanism for the growth of chalcedony. *Contributions to Mineralogy and Petrology*, Vol. 115, No. 1, pp. 66–74, http://dx.doi.org/10.1007/BF00712979.
——— (1995) Moganite as an indicator for vanished evaporates: A testament reborn? *Journal of Sedimentary Research A: Sedimentary Petrology and Processes*, Vol. 65, pp. 633–638.
Heaney P.J., Post J.E. (1992) The widespread distribution of a novel silica polymorph in microcrystalline quartz varieties. *Science*, Vol. 255, No. 5043, pp. 441–443, http://dx.doi.org/10.1126/science.255.5043.441.
Jahn S., Bode R., Lyckberg P., Medenbach O., Lierl H-J. (2003) *Marokko – Land der schönen Mineralien und Fossilien*. Bode Verlag. 536 pp.
Kingma K.J, Hemley R.J. (1994) Raman spectroscopic study of microcrystalline silica. *American Mineralogist*, Vol. 79, pp. 269–273.
Legodi M.A., de Waal D. (2006) The preparation of magnetite, goethite, hematite and maghemite of pigment quality from mill scale iron waste. *Dyes and Pigments*, Vol. 74, pp. 161–168, http://dx.doi.org/10.1016/j.dyepig.2006.01.038.
Mayer D. (2012) "Nicht nur" Achate in Marokko. In *Marokko*, extraLapis No. 42, Weise Verlag, Munich, pp. 22–25.
Mernagh T. P. (1991) Use of the laser Raman microprobe for discrimination amongst feldspar minerals. *Journal of Raman Spectroscopy*, Vol. 22, No. 8, pp. 453–457, http://dx.doi.org/10.1002/jrs.1250220806.
Mohr C. (2012) Zur aktuellen Achat-Fundsituation in Marokko. *Mineralien Welt*, Vol. 23, No. 3, pp. 82–89.
Moxon T., Rios S. (2004) Moganite and water content as a function of age in agate: an XRD and thermogravimetric study. *European Journal of Mineralogy*, Vol. 16, No. 2, pp. 269–278, http://dx.doi.org/10.1127/0935-1221/2004/0016-0269.
Moxon T., Nelson D.R. and Zhang M. (2006) Agate recrystallization: Evidence from samples found in Archaean and Proterozoic host rocks, western Australia. *Australian Journal of Earth Sciences*, Vol. 53, No. 2, pp. 235–248.
Pop D., Constantina C., Tatar D., Kiefer W. (2004) Raman spectroscopy on gem-quality microcrystalline and amorphous silica varieties from Romania. *Studia Universitatis Babes-Bolyai Geologia*, Vol. 49, No. 1, pp. 41–52.
Priester M. (1999) Der Achat- und Amethystbergbau in der Region Medio Alto Uruguai in Rio Grande do Sul, Brasilien: Eine geologische und technische Betrahtung. *Zeitschrift der Deutschen Gemmologischen Gesellschaft*, Vol. 48, No. 4, pp. 211–222.
Schwarz D. (2012) Marokko - und dieses Mal keine Achate. *Mineralien Welt*, Vol. 23, No. 2, pp. 85–88.
Strieder A.J., Heemann B. (2006) Structural considerations on Parana basalt volcanism and their implications on agate geode mineralization (Salto do Jacui, RS, Brazil). *Pesquisas em Geociencias*, Vol. 33, No. 1, pp. 37–50.
Swamy V., Muddle B.C., Dai Q. (2006) Size-dependent modifications of the Raman spectrum of rutile TiO_2. *Applied Physics Letters*, Vol. 89, No. 163118, pp. 1–3, http://dx.doi.org/10.1063/1.2364123.
Wesełucha-Birczynska A., Natkaniec-Nowak L. (2011) A Raman microspectroscopic study of organic inclusions in "watermelon" tourmaline from the Paprok mine (Nuristan, Afghanistan). *Vibrational Spectroscopy*, Vol. 57, No. 2, pp. 248–253, http://dx.doi.org/10.1016/j.vibspec.2011.08.001.
Wopenka B., Pasteris J.D. (1993) Structural characterizations of kerogens to granulite-facies graphite; applicability of Raman microprobe spectroscopy. *American Mineralogist*, Vol. 78, pp. 533–557.
Wróbel P., Czyzycki M., Furman L., Kolasiński K., Lankosz M., Mrenca A., Samek L., Wegrzynek D. (2012) LabVIEW control software for scanning micro-beam X-ray fluorescence spectrometer. *Talanta*, Vol. 93, pp. 186–192, http://dx.doi.org/10.1016/j.talanta.2012.02.010.
Verdier J. (1971) Etude géologique des basalts doléritiques du Trias du barrage de Moulay-Yussef au site des Aït-Aadel sur l'oued Tessaout, Haut Atlas. *Notes et Mémoires du Service Géologique du Maroc*, Vol. 31, No. 237, pp. 241–272.
Zenz J. (2005a) *Achat-Schätze*. Edition Mineralien Welt, Salzhemmendorf, 160 pp.
——— (2005b) *Achate*. Bode Verlag, Haltern, Germany, 656 pp. (in German).
——— (2009) *Achate II*. Bode Verlag, Haltern, Germany, 656 pp. (in German).

ABOUT THE AUTHORS

Drs. Dumańska-Słowik (dumanska@uci.agh.edu.pl) and Natkaniec-Nowak are assistant professor and associate professor, respectively, in the Faculty of Geology, Geophysics, and Environmental Protection at the AGH University of Science and Technology in Krakow, Poland. Mr. Gaweł is a researcher at the Laboratory of Phase, Structural, Textural and Geochemical Analyses at the Faculty of Geology, Geophysics and Environmental Protection at the AGH University. Prof. Lankosz is a professor, and Mr. Wróbel a Ph.D. student, in the Faculty of Physics and Applied Computer Science at the AGH University. Dr. Wesełucha-Birczyńska is an associate professor in the Faculty of Chemistry at Jagiellonian University in Krakow.

ACKNOWLEDGMENTS

The authors would like to thank Jolanta and Jacek Szczerba and Remigiusz Molenda for providing several samples. Tomasz Toboła and Małgorzata Klimek are acknowledged for their help with microscopic observations and initiation of this research, respectively. The reviewers made helpful and constructive comments on the manuscript. This work was supported by research statutory grant 11.11.140.319 from the AGH University of Science and Technology.

STOP 3.2 – Fault near Zerkten

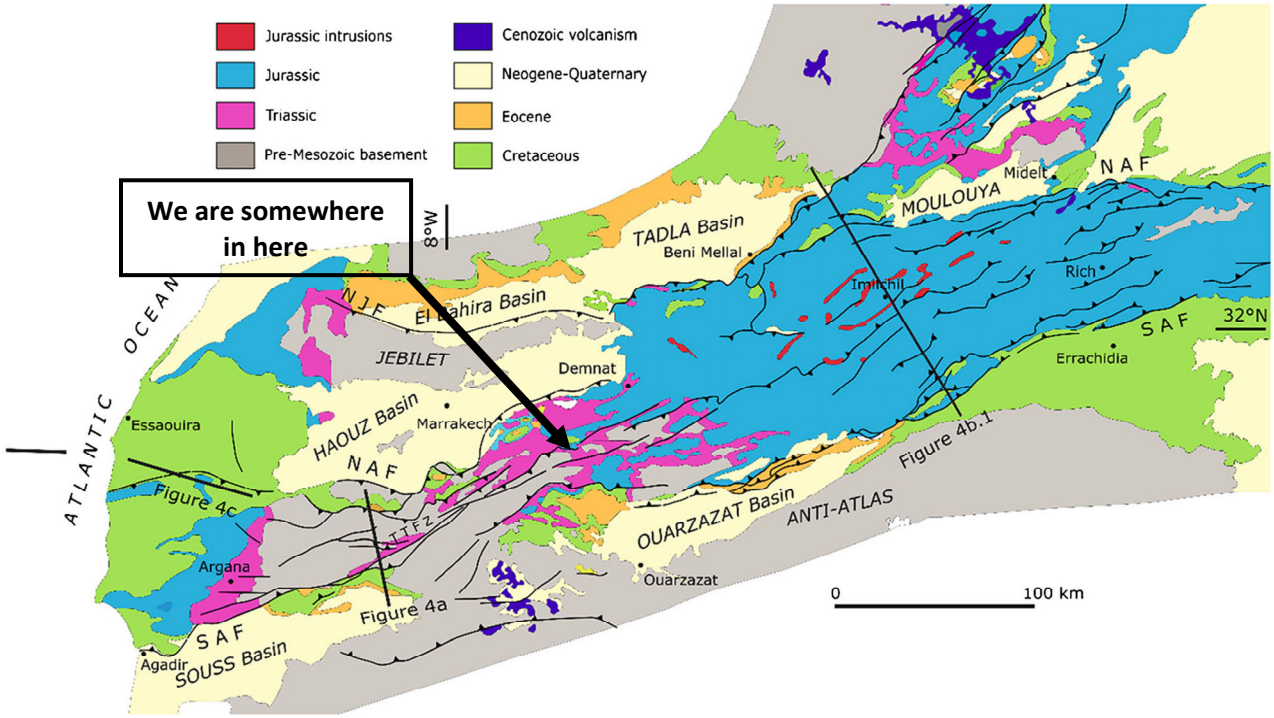

Fig. 3 Simplified geological map of the High Atlas Mountains showing the main geological exposures and structural features of the range (redrawn from Teixell et al. 2007)

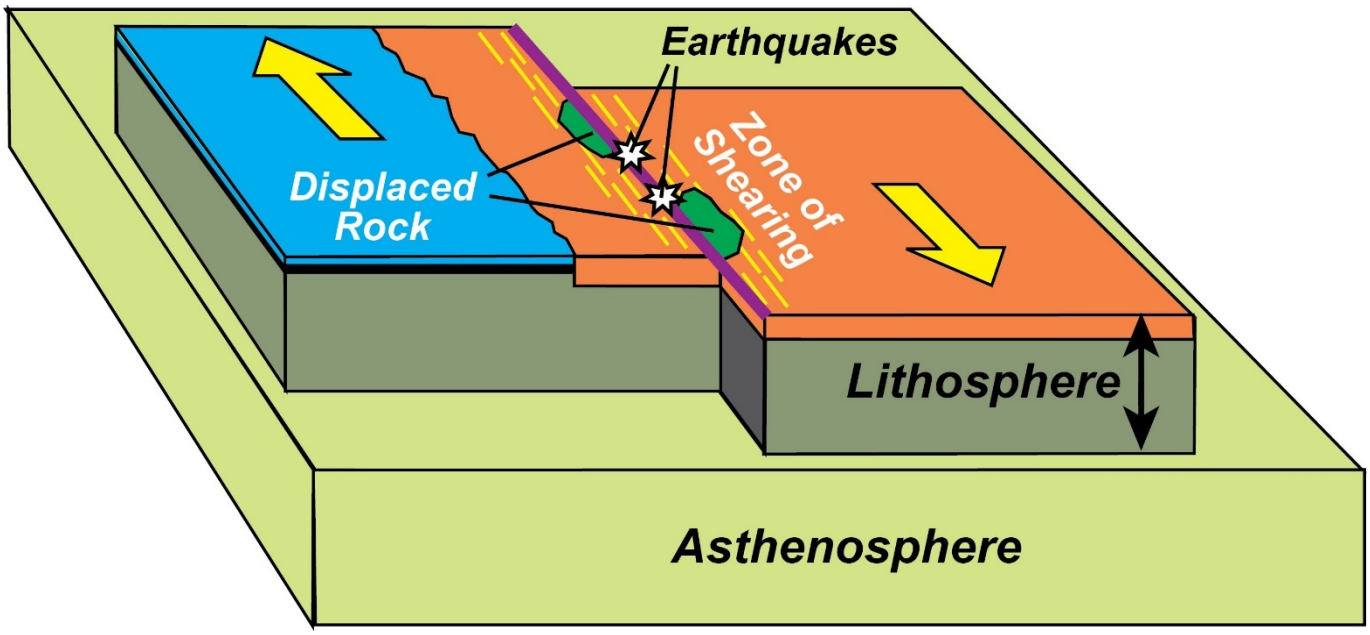

2023 Al Haouz Earthquake
This is from Wikipedia

Introduction

On 8 September 2023 at 23:11 DST (22:11 UTC), an earthquake with a moment magnitude of 6.9 and maximum Mercalli intensity of IX (Violent) struck Morocco's Al Haouz Province. The earthquake's epicenter was 73.4 km (45.6 mi) southwest of Marrakesh, near the town of Ighil and the Oukaïmeden ski resort in the Atlas Mountains. It occurred as a result of shallow oblique-thrust faulting beneath the mountain range. At least 2,960 deaths were reported, with most occurring outside Marrakesh. Damage was widespread, and historic landmarks in Marrakesh were destroyed. The earthquake was also felt in Spain, Portugal, and Algeria.

It is the strongest instrumentally recorded earthquake in Morocco, the deadliest in the country since the 1960 Agadir earthquake, and the second-deadliest earthquake of 2023 after the Turkey–Syria earthquakes. Its magnitude also makes it the largest earthquake on the African continent since the 2006 Mw 7.0 Mozambique earthquake and the largest in North Africa since the 1980 Mw 7.1 El Asnam earthquake. Over 2.8 million people from Marrakesh and areas surrounding the Atlas Mountains were affected, including 100,000 children. Following the earthquake, many countries offered humanitarian assistance, and Morocco announced a three-day period of national mourning.

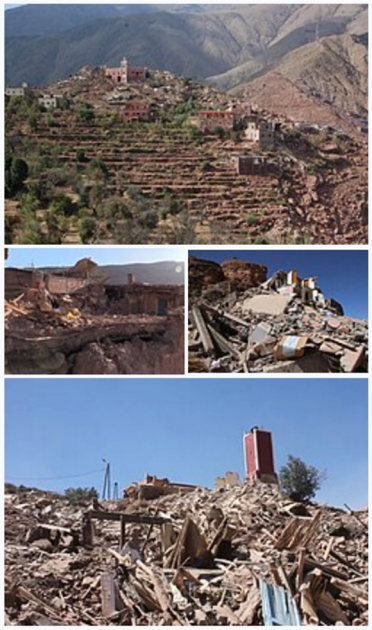

Clockwise from top: Imi N'Tala, Moulay Brahim, Tizi N'Test and Tansghart after the earthquake

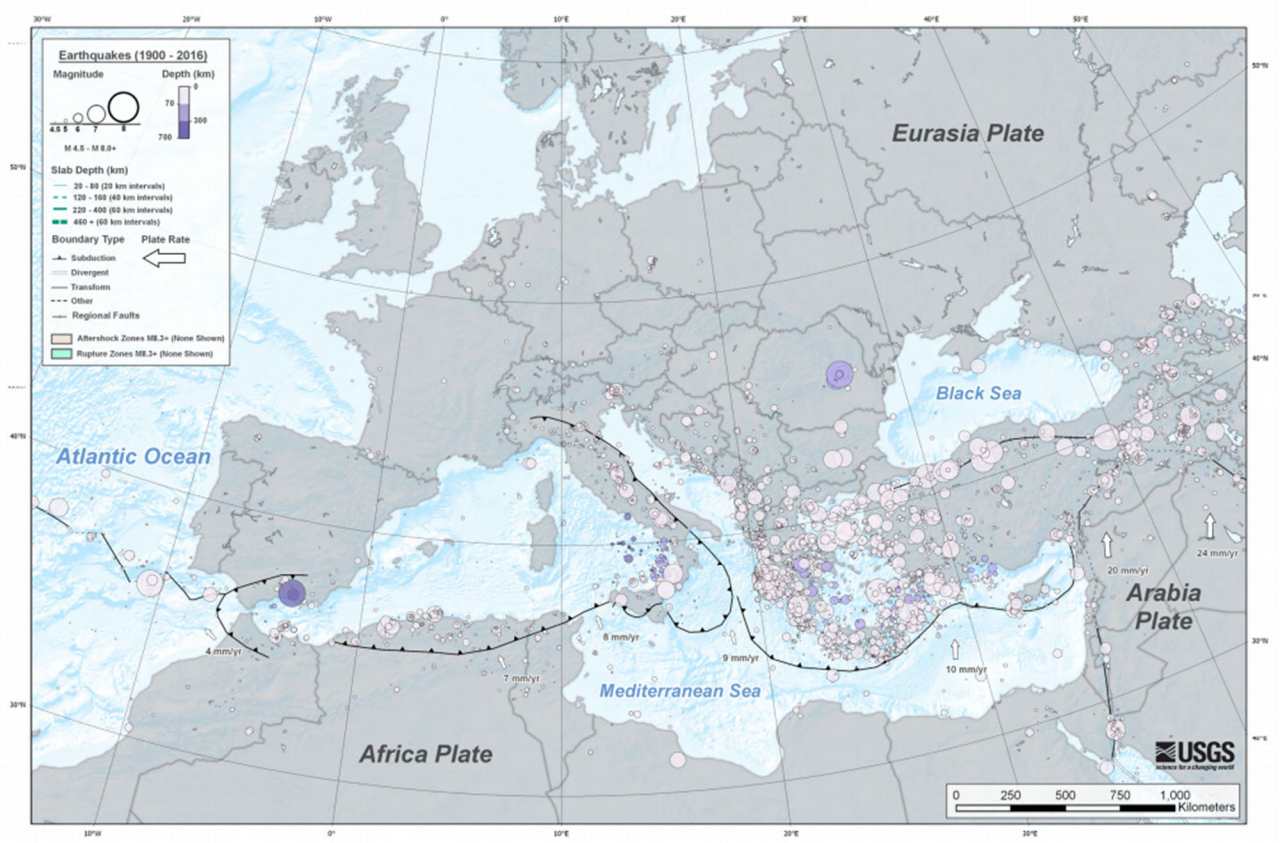

UTC time	2023-09-08 22:11:01
ISC event	626740945
USGS-ANSS	ComCat
Local date	8 September 2023
Local time	23:11 DST
Magnitude	6.9 M_w[1]
Depth	19.0 km (11.8 mi)[1]
Epicenter	31.073°N 8.407°W
Type	Oblique-thrust
Areas affected	Morocco
Total damage	US$7 billion
Max. intensity	MMI IX (*Violent*)
Casualties	2,960 killed, 5,674 injured

Tectonic Setting

Morocco lies south of a major tectonic boundary between the African and Eurasian plates, the Azores–Gibraltar transform fault. This major fault stretches from the Azores to Gibraltar Strait where it is dominated by right-latera strike-slip movement. In the Gibraltar Arc and Alboran Sea, at the eastern end of the fault it becomes transpressional with the development of large thrust faults. East of the Strait of Gibraltar, in the Alboran Sea, the boundary becomes collisional in type. Most of the seismicity in Morocco is related to movement on that plate boundary, with the greatest seismic hazard in the north of the country close to the boundary. In 2004, the coastal province of Al Hoceima was struck by a magnitude 6.3 earthquake that left 628 people dead and 926 injured. In nearby Algeria, magnitude 7.3 earthquake occurred in 1980 that killed 2,500 people.

The Atlas Mountains are an intracontinental mountain belt that extends 2,000 km (1,200 mi) from Morocco to Tunisia. These mountains formed from a collision during the Cenozoic. The mountain range reaches its highest elevation to the west, in Morocco. The High Atlas, a subrange, formed when an ancient Triassic rift was reactivated. However rather than resuming the rifting process, the reactivation compressed the rift due to the collision in the north. Due to the unusually high topography of the Atlas range, mantle upwelling may have played a role in its orogeny. The crust beneath the Atlas range from 32–40 km (20–25 mi), considered thin and physically impossible to support high elevations exceeding 4,000 m (13,000 ft). Typically, a crustal thickness of 50 km (31 mi) is required, hence mantle upwelling raises the overlying crust.

The seismicity of Morocco is concentrated in its northern region and the Alboran Sea. South of the Rif, seismic activity is sparse but widely distributed across the Middle Atlas, High Atlas, and Anti-Atlas. Seismicity in the Saharan Atlas is limited, and is absent in the Saharan region south of the belt; it is also less active eastwards in Algeria and Tunisia. Previously, the largest earthquake recorded in the Atlas Mountains was a Mw 5.9 earthquake that struck Agadir in 1960. Earthquakes in the Atlas Mountains display focal mechanisms of strike-slip, thrust or a combination of both (oblique-slip).

Earthquake

Measuring Mw 6.9 at a depth of 19 km (12 mi), it is the strongest earthquake recorded by a seismograph with an epicenter in Morocco. Morocco's seismic agency reported a Mwp of 7.2 and focal depth of 8 km (5.0 mi). The tremors were detected by monitoring stations as far away as Egypt.

Mechanism

The earthquake had a focal mechanism indicating oblique-thrust faulting beneath the High Atlas. The rupture occurred on a steep-dipping oblique-reverse fault striking northwest or a shallow-dipping oblique-reverse fault striking east. The USGS estimated the fault rupture area to be 30 km (19 mi) by 25 km (16 mi) on an east-northeast striking, north–northwest dipping fault. Slip was generally observed at 15 km (9.3 mi) to 35 km (22 mi) depth, but mostly concentrated around the hypocentre within an elliptical

Macroseismic Intensity Map USGS
ShakeMap: 52 km WSW of Oukaïmedene, Marrakesh-Safi, MA
Sep 08, 2023 22:11:01 UTC M6.8 N31.06 W8.38 Depth: 19.0km ID:us7000kufc

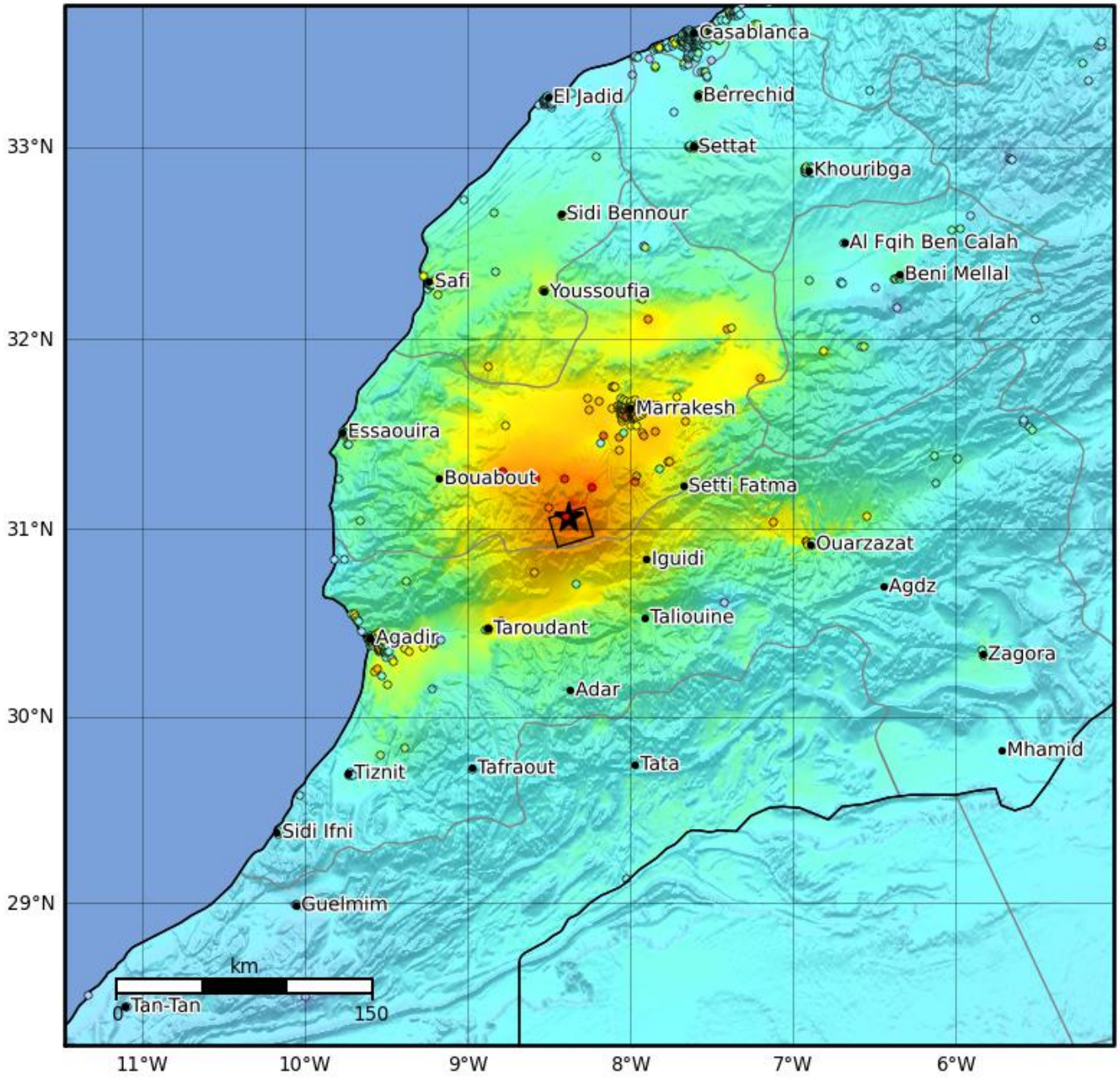

SHAKING	Not felt	Weak	Light	Moderate	Strong	Very strong	Severe	Violent	Extreme
DAMAGE	None	None	None	Very light	Light	Moderate	Moderate/heavy	Heavy	Very heavy
PGA(%g)	<0.0464	0.297	2.76	6.2	11.5	21.5	40.1	74.7	>139
PGV(cm/s)	<0.0215	0.135	1.41	4.65	9.64	20	41.4	85.8	>178
INTENSITY	I	II-III	IV	V	VI	VII	VIII	IX	X+

Scale based on Worden et al. (2012)
Version 12: Processed 2023-10-20T03:40:58Z
△ Seismic Instrument ○ Reported Intensity ★ Epicenter ▭ Rupture

slip patch 30 km (19 mi) long by 25 km (16 mi) wide. A maximum displacement of 1.9 m (6 ft 3 in) was observed at 25 km (16 mi) depth while there was little to no slip above 15 km (9.3 mi) depth. Many east-west and northeast–southwest strike-slip and thrust faults occur in the High Atlas. Since 1900, there has not been a Mw 6.0 or larger earthquake within 500 km (310 mi) of the recent earthquake's epicenter; but nine Mw 5.0 and larger events have occurred to its east. In another finite fault model published by Italy's National Institute of Geophysics and Volcanology, the focal depth was determined at 24.7 km (15.3 mi) beneath the High Atlas. The focal mechanism of this model displayed rev erse and left-lateral faulting. Slip occurred in an elliptical area along an east-northeast–west-southwest trending fault dipping 69° north–northwest. A peak slip of 2 m (6 ft 7 in) occurred at 23.3 km (14.5 mi).

Geodetic modeling suggests the earthquake originated from within the lower crust and ruptured up to the middle crust. The deeper depth and greater remoteness from populated areas compared to the earthquake that struck Agadir in 1960 meant it caused fewer casualties and damage. The range of depth where slip occurred is unusually deep for crustal earthquakes as they tend to occur shallower than 15 km (9.3 mi) depth. Fluid and magma associated with the mantle plume beneath the High Atlas may have intruded via a fault and pervade across, bringing it closer to rupture.

No surface faulting occurred hence the causative fault responsible could not be identified, however the focal mechanism suggests rupture on a steep north-dipping plane or shallow south-dipping plane. The USGS finite fault is aligned with the former solution. Two dominant shallow-dipping thrust systems, the North and South Atlas faults, occur in the western High Atlas. Their fault geometries contradict that of the USGS finite fault's preferred steep-dipping plane. Other unmapped faults within the range, including the Tizi n'Test Fault, have surface projections that match closer to the USGS finite fault. If the rupture occurred on the shallow south-dipping plane, a possible source is a low-angle detachment beneath the High Atlas. Geologists have previously interpreted low-angle faults in the region in past studies. For the steep north-dipping plane, the possible source are unmapped or blind thrust faults. The Tizi n'Test Fault, a north-dipping fault where no recent activity has been recorded, may be a possible source of the earthquake. Cornell University geologist Judith Hubbard said the fault was active 300 million years ago during the formation of Pangaea and later, its fragmentation. Ancient faults, such as the Tizi n'Test Fault, create zones of strain within the crust and could reactivate, such as the case in Morocco.

Ground effects

Vertical movement of the land surface detected by repeat observations of the Sentinel-1 satellite is consistent with movement on a blind thrust fault dipping north. An analysis of satellite data obtained from Daichi-2 by the Geospatial Information Authority of Japan revealed a 20 cm (7.9 in) surface uplift around the epicenter and 7 cm (2.8 in) of subsidence to the south. Surface deformation was observed around the epicenter across a 50 km (31 mi) area trending east–west, and 100 km (62 mi) trending north–south.

According to the United States Geological Survey's PAGER service, the earthquake had a maximum Modified Mercalli intensity of IX (Violent). Intensity VIII (Severe) shaking was felt by approximately 157,000 residents, including the town of Azgour and villages surrounding the Atlas Mountains. Intensity VII (Very Strong) shaking was felt by over 811,000 people, with intensity VI (Strong) shaking felt by 3.2 million residents, including in the cities of Marrakesh, Taroudant and Ouarzazate. Shaking of intensity V (Moderate) was felt in Agadir, Beni Mellal, and Safi, with intensity IV (Light) shaking being felt in Casablanca. According to the European-Mediterranean Seismological Centre, it was also felt in Portugal, Spain, Mauritania, Algeria, Western Sahara and along the coast of the Strait of Gibraltar.

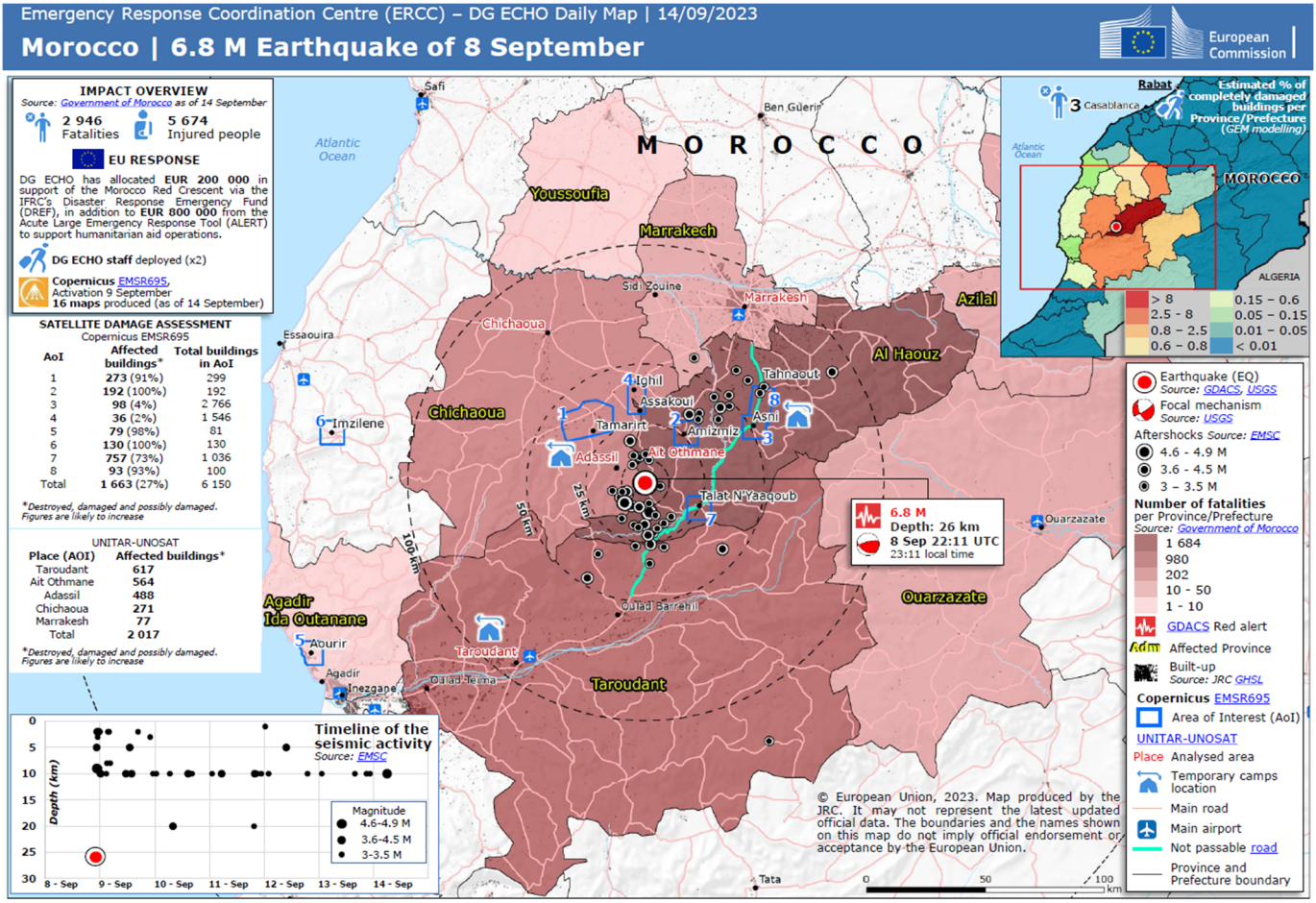
Emergency Response Coordination Centre (ERCC) – DG ECHO Daily Map | 14/09/2023
Morocco | 6.8 M Earthquake of 8 September
European Commission
IMPACT OVERVIEW
Source: Government of Morocco as of 14 September
2 946 Fatalities
5 674 Injured people
EU RESPONSE
DG ECHO has allocated EUR 200 000 in support of the Morocco Red Crescent via the IFRC's Disaster Response Emergency Fund (DREF), in addition to EUR 800 000 from the Acute Large Emergency Response Tool (ALERT) to support humanitarian aid operations.
DG ECHO staff deployed (x2)
Copernicus EMSR695, Activation 9 September
16 maps produced (as of 14 September)
SATELLITE DAMAGE ASSESSMENT
Copernicus EMSR695
AoI | Affected buildings* | Total buildings in AoI
1 | 273 (91%) | 299
2 | 192 (100%) | 192
3 | 98 (4%) | 2 766
4 | 36 (2%) | 1 546
5 | 79 (98%) | 81
6 | 130 (100%) | 130
7 | 757 (73%) | 1 036
8 | 93 (93%) | 100
Total | 1 663 (27%) | 6 150
*Destroyed, damaged and possibly damaged. Figures are likely to increase
UNITAR-UNOSAT
Place (AOI) | Affected buildings*
Taroudant | 617
Ait Othmane | 564
Adassil | 488
Chichaoua | 271
Marrakesh | 77
Total | 2 017
*Destroyed, damaged and possibly damaged. Figures are likely to increase
Timeline of the seismic activity
Source: EMSC
Depth (km)
Magnitude
4.6-4.9 M
3.6-4.5 M
3-3.5 M
8 - Sep
9 - Sep
10 - Sep
11 - Sep
12 - Sep
13 - Sep
14 - Sep
MOROCCO
Atlantic Ocean
Safi
Ben Guerir
Youssoufia
Marrakech
Sid Zouine
Marrakesh
Azilal
Chichaoua
Essaouira
Al Haouz
Tahnaout
Ighil
Assakoul
Asni
Amizmiz
Tamarirt
Adassil
Ait Othmane
Talat N'Yaaqoub
Imzilene
Chichaoua
Agadir Ida Outanane
Aburir
Agadir
Inezgane
Oulad Berrehil
Taroudant
Oulad Teima
Taroudant
Ouarzazate
Ouarzazate
Tata
6.8 M
Depth: 26 km
8 Sep 22:11 UTC
23:11 local time
25 km
50 km
100 km
© European Union, 2023. Map produced by the JRC. It may not represent the latest updated official data. The boundaries and the names shown on this map do not imply official endorsement or acceptance by the European Union.
0
50
100
km
Rabat
3 Casablanca
Estimated % of completely damaged buildings per Province/Prefecture (GEM modelling)
MOROCCO
ALGERIA
> 8
2.5 - 8
0.8 - 2.5
0.6 - 0.8
0.15 - 0.6
0.05 - 0.15
0.01 - 0.05
< 0.01
Earthquake (EQ)
Source: GDACS, USGS
Focal mechanism
Source: USGS
Aftershocks Source: EMSC
4.6 - 4.9 M
3.6 - 4.5 M
3 - 3.5 M
Number of fatalities
per Province/Prefecture
Source: Government of Morocco
1 684
980
202
10 - 50
1 - 10
GDACS Red alert
Affected Province
Built-up
Source: JRC GHSL
Copernicus EMSR695
Area of Interest (AoI)
UNITAR-UNOSAT
Place Analysed area
Temporary camps location
Main road
Main airport
Not passable road
Province and Prefecture boundary

Lunch Stop
STOP 3.3 – Col du Tichka

Tizi n'Tichka (*from Wikipedia*)

Elevation 2,205 m (7,234 ft)
Atlas Mountains, Morocco
Coordinates 31° 17′ 9″ N 7° 22′ 51″ W

Tizi n'Tichka (Berber languages: ⵜⵉⵣⵉ ⵏ ⵜⵉⵛⴽⴰ, romanized: Tizi en Ticka; Arabic: تيزي ن تيشكا) is a mountain pass in Morocco, linking the south-east of Marrakesh to the city of Ouarzazate through the High Atlas mountains. It lies above the great Marrakesh plains, and is a gateway to the Sahara.

Climate and elevation

From November through March, snow can often fall on the pass, but it can be warm all year round in the strong sun. It has been believed for a long time that it reaches an elevation of 2,260 metres (7,415 ft) above the sea level (this is also indicated on a sign at the top of the pass), but a gps-measurement by Hans Mülder on 30 November 2022 indicated it is only 2,205 metres (7,234 ft) high, which was confirmed by Google Earth, on which the highest altitude of the pass is 2,207 metres (7,241 ft). It is the highest major mountain pass in North Africa. The road was constructed along the old caravan trail by the French military in 1936, and is now part of National Route 9 (formerly Route P-31).

Fauna

The last known wild Barbary lion in Morocco was shot near Tizi n'Tichka in 1942.

STOP 3.4 – Telouet Salt Mine

From ChatGPT:

1. Setting in the High Atlas Mountains

The Telouet salt mine is located in the High Atlas mountain range of Morocco, a major intracontinental mountain belt formed by the collision of the African and Eurasian Plates and inversion of earlier rift basins. This tectonic compression reactivated older faults and folded older sedimentary rocks into the impressive relief seen today.

2. Salt Formation: Evaporites from Triassic Seas

The salt deposit exploited in the Telouet mine is part of evaporite sequences that formed during the Late Triassic period, when rifting associated with the opening of the Central Atlantic created isolated basins that repeatedly flooded with seawater and then dried out. This produced thick layers of evaporites — halite (rock salt) and associated minerals like gypsum — as seawater evaporated.

These evaporite-bearing Triassic formations are typically layered with red silts and clays and occur near other Triassic rocks in the High Atlas, which helps explain the salt's geological context.

3. Geological Age and Stratigraphy

The mine lies close to the Triassic–Jurassic boundary in the regional rock record, meaning salt and associated sediments were laid down just before the Jurassic period — around 200 million years ago. Above or nearby in the landscape are Jurassic marine rocks that contain fossils like brachiopods, indicating a shift from arid basins to shallow marine environments over time.

4. Structural and Tectonic Context

The broader High Atlas region has a complex structural history: Rifting and deposition in the Triassic to Early Jurassic created basins where sediments, including evaporites, accumulated. Cenozoic compression from plate convergence folded and uplifted these sequences into the High Atlas ranges seen today, bringing salt deposits into accessible positions at elevation.

5. Local Characteristics of Salt

The Telouet salt itself is halite-rich (sodium chloride) and historically was a highly prized commodity. The color and texture of the local salt can vary (including pink hues), influenced by trace minerals and the conditions of deposition. In some accounts, local salt is described as having a "living salt" quality with traditional medicinal uses, although that's more cultural than strictly geological.

Why It's Geologically Interesting

Evaporite deposition in a rift setting — The Telouet salt deposit is a classic example of large evaporite layers associated with restricted basins during continental breakup.

Proximity to major stratigraphic boundaries — Its position near the Triassic–Jurassic transition makes it a useful marker for understanding how environments changed from continental arid basins to marine conditions in northern Africa.

Mountain uplift and exposure — Regional tectonics uplifted these otherwise buried salts to elevations where they could be mined historically and observed at the surface.

If you want, I can also point you to specific academic papers or maps that show the rock units around Telouet and their ages in detail.

STOP 3.5 – Ounila Valley

from ChatGPT

The Ounila Valley (Vallée de l'Ounila) in southern Morocco lies on the southern flank of the High Atlas Mountains, extending roughly from the old salt-rich headwaters near Telouet down to Aït Benhaddou and the edges of the Ouarzazate region. It's a dramatic mountain valley cut by the seasonal river Oued (Assif) Ounila, carving through layered sedimentary rocks and creating steep slopes and colorful cliffs as it descends toward lower, more arid terrain.

Regional Geological Context: High Atlas Mountains

The Ounila Valley is part of the broader High Atlas orogenic belt — a mountain range formed by ancient tectonic events. These key points apply to the valley's geology:

Plate Tectonics & Uplift: The High Atlas Mountains formed during Cenozoic (from ~66 Ma to present) tectonic compression as the African plate interacted with the Eurasian plate. Older sedimentary rocks deposited over hundreds of millions of years were folded and uplifted, exposing them at the surface.

Sedimentary Rock Dominance: Much of the rock exposed in the High Atlas — including in the Ounila Valley — is sedimentary (e.g., sandstones, mudstones, marls, limestones) that accumulated in marine and continental basins before later mountain building. Exposures often have striking ochre, red, brown, and gray colors reflecting differences in composition and oxidation.

Rocks & Stratigraphy in the Ounila Valley Area

Although there isn't a detailed published strata column specifically for the valley widely available online, the general geology of this part of the High Atlas suggests the valley cuts through a section of the southern High Atlas rock sequences, including:

Mesozoic sedimentary rocks — including Triassic and Jurassic age formations (sandstones, siltstones, and marls). These were originally deposited in rift basins and shallow seas before being uplifted during later tectonic events.

Triassic red beds and evaporites: In nearby areas of the High Atlas (including close to Telouet and the headwaters of Ounila), Triassic terrestrial red sandstones and shales, sometimes with evaporite layers (salt and gypsum), are known — reflecting deposition in arid basins during breakup of Pangea.

Jurassic marine sediments: Further up the Atlas and across much of the High Atlas region, Jurassic limestones and marls reflect a period when the region was submerged under shallow seas. These rocks are often fossil-rich in other parts of the High Atlas (e.g., fossil footprints, marine faunas) and likely form part of the broader stratigraphic context.

Valley Geomorphology and Erosion

River incision: The Oued Ounila has cut a narrow, steep-sided valley/canyon into these sedimentary rocks. With limited perennial flow (the river often dries outside winter and early spring), the valley's shape reflects episodic flash floods that quickly erode and transport sediments.

Colorful cliffs: The characteristic ochre and reddish hues of the valley sides come from weathering and oxidation of iron-rich sedimentary rocks (e.g., red beds or ferruginous sandstones).

Alluvial deposits: Within the valley floor, sediments transported by the river (gravels, sands, silts) buildup along terraces and floodplain areas, often supporting fertile soils and the palm groves and gardens that contrast with the arid uplands.

STOP 3.6 – Ait-Ben-Haddou
From Wikipedia

Aït Benhaddou (Arabic: آيت بن حدّو) is a historic ighrem or ksar (fortified village) along the former caravan route between the Sahara and Marrakesh in Morocco. It is considered a great example of Moroccan earthen clay architecture and has been a UNESCO World Heritage Site since 1987.

History

Mosque in the modern village where most residents now live, across the valley from the old ksar (*is a type of fortified village in North Africa, usually found in the regions predominantly or traditionally inhabited by Berbers (Amazigh)*)

The site of the ksar has been fortified since the 11th century during the Almoravid period. None of the current buildings are believed to date from before the 17th century, but they were likely built with the same construction methods and designs as had been used for centuries before. The site's strategic importance was due to its location in the Ounila Valley along one of the main trans-Saharan trade routes. The Tizi n'Tichka pass, which was reached via this route, was one of the few routes across the Atlas Mountains, crossing between Marrakech and the Dra'a Valley on the edge of the Sahara. Other kasbahs and ksour were located all along this route, such as the nearby Tamdaght to the north.

Today, the ksar itself is only sparsely inhabited by several families. The depopulation over time is a result of the valley's loss of strategic importance in the 20th century. Most local inhabitants now live in modern dwellings in the village on the other side of the river, and make a living off agriculture and especially off the tourist trade. In 2011 a new pedestrian bridge was completed linking the old ksar with the modern village, with the aim of making the ksar more accessible and to potentially encourage inhabitants to move back into its historic houses.

The site was damaged by the September 2023 earthquake that struck southern Morocco. An early assessment of the damage reported cracks and partial collapses, with risk of further collapses.

Description

Layout of the site

The agadir (granary) at the top of the hill

The ksar is located on the slopes of a hill next to the Ounila River (Asif Ounila). The village's buildings are grouped together within a defensive wall that includes corner towers and a gate. They include dwellings of various size ranging from modest houses to tall structures with towers.

Some of the buildings are decorated in their upper parts with geometric motifs. The village also has a number of public or community buildings such as a mosque, a caravanserai, multiple kasbahs (castle-like fortification) and the Marabout of Sidi Ali or Amer. At the top of the hill, overlooking the ksar, are the remains of a large fortified granary (agadir). There is also a public square, a Muslim cemetery, and a Jewish cemetery. Outside the ksar's walls was an area where grain was grown and threshed.
A kasbah (fortified dwelling) in the lower part of the village

Building materials

The ksar's structures are made entirely out of rammed earth, adobe, clay bricks, and wood. Rammed earth (also known as pisé, tabia, or al-luh) was a highly practical and cost-effective material but required constant maintenance. It was made of compressed earth and mud, usually mixed with other materials to aid adhesion. The structures of Ait Benhaddou and of other kasbahs and ksour throughout this region of Morocco typically employed a mixture of earth and straw, which was relatively permeable and easily eroded by rain over time. As a result, villages of this type can begin to crumble only a few decades after being abandoned. At Ait Benhaddou, taller structures were made of rammed earth up to their first floor while the upper floors were made of lighter adobe so as to reduce the load of the walls.

Preservation

The ksar has been significantly restored in modern times, thanks in part to its use as a Hollywood filming location and to its inscription on the UNESCO list of World Heritage Sites in 1987. UNESCO reports that the ksar has "preserved its architectural authenticity with regard to configuration and materials" by continuing to use traditional construction materials and techniques and by largely avoiding new concrete constructions. A local committee is in charge of monitoring and managing the site.

Films shot at Aït Benhaddou

A large number of films shot in Morocco have used Aït Benhaddou as a location, including:

Lawrence of Arabia (1962)
Sodom and Gomorrah (1963)
Oedipus Rex (1967)
The Man Who Would Be King (1975)
The Message (1976)
Jesus of Nazareth (1977)
Time Bandits (1981)
Marco Polo (1982)
The Jewel of the Nile (1985)
The Living Daylights (1987)
The Last Temptation of Christ (1988)
The Sheltering Sky (1990)
Kundun (1997)
The Mummy (1999)
Gladiator (2000)
Alexander (2004)
Kingdom of Heaven (2005)
Babel (2006)
One Night with the King (2006)
Prince of Persia (2010)
Son of God (2014)
Queen of the Desert (2015)
A Life on Our Planet (2020)
The Odyssey (2026)

Aït Benhaddou was also used in parts of the TV series Game of Thrones.

STOP 3.7 – Ouarzazate
From Wikipedia

Ouarzazate (/ˌwɑːrzəˈzæt, -ˈzɑːt/; Berber languages: ⵡⴰⵔⵣⴰⵣⵜ Arabic: ورزازات, romanized: Warzāzāt, IPA: [warzaːˈzaːt]) is a city and capital of Ouarzazate Province in the region of Drâa-Tafilalet, south-central Morocco.

Ouarzazate is a primary tourist destination in Morocco during the holidays, as well as a starting point for excursions into and across the Draa Valley and the desert. The fortified village Aït Benhaddou west of the city is a UNESCO World Heritage Site.

Front view (north side) of the Kasbah Taourirt

The Ouarzazate area is a noted film-making location, with Morocco's biggest studios inviting many international companies to work here. Films such as Lawrence of Arabia (1962), The Man Who Would Be King (1975), The Living Daylights (1987), The Last Temptation of Christ (1988), The Mummy (1999), Gladiator (2000), Kingdom of Heaven (2005), Kundun (1997), Legionnaire (1998), The Hills Have Eyes (2006), Salmon Fishing in the Yemen (2011) and The Wages of Fear (2024) were shot here, as was part of the TV series Game of Thrones. It was the filming location for the fictional city of Agapenta in the fourth season of the Netflix series Outer Banks.

History

For a long time, Ouarzazate was a small crossing point for African traders on their way to northern Morocco and Europe. In the 16th century, Sheikh Abu al-'Abaas Ahmed bin Abdellah al-Wizkiti al-Warzazi, emir of the qasba of Ouarzazate and father of Lalla Masuda, helped establish Saadi control over the Sous-Dra'a region.

Ouarzazate was home to a thriving Jewish community. In 1954, about 170 Jews lived in the Mellah. The "Old Synagogue", a synagogue said to be nearly 300 years old, is located in Ouarzazate. There is also a Jewish cemetery, which is no longer in use.

During the French period, Ouarzazate expanded considerably as a garrison town, administrative centre and customs post and a church (Eglise Saint Therese) was built in 1931. It is home to the Kasbah Taourirt, which was the kasbah of the former caïd and later owned by T'hami El Glaoui. The Krupp field gun which secured Glaoui power is displayed outside the kasbah today.

Geography

Ouarzazate is at an elevation of 1,151 metres (3,776 ft)[citation needed] in the middle of a bare plateau south of the High Atlas Mountains, with a desert to the city's south.

Climate

Ouarzazate has a hot desert climate (Köppen climate classification BWh).[citation needed] The city is hot and dry in summer, but can be very cold in winter, with icy winds coming from the High Atlas Mountains.

Day 4: Monday, March 9th, 2026 – Ouarzazate – Anit-Atlas Stromatolites – Draa Valley – Alnif Fossils

STOP 4.1 – Ediacaran Stromatolites
STOP 4.2 – Tizi-n-Tinififfft Pass
STOP 4.3 – Agdz and The Draa Valley
STOP 4.4 – Orthoceras Quarry near Tazzarine
STOP 4.5 – Trilobite Preparation Workshop near Alnif
Hotel Information:

Auberge Kasbah Meteorites
Ksar Tighirna à 13 km d'Alnif BP138, Alnif 52452, Morocco
http://www.kasbah-meteorites.com/

From our guide

We begin the day in the Anti-Atlas Mountains with a visit to an exceptional palaeontological site featuring vast areas of Ediacaran-aged stromatolites, dating back around 600 million years and representing some of the earliest evidence of life on Earth. We then continue across the Anti-Atlas, stopping at the Tizi-n-Tinififfft Pass, the highest point on this mountain crossing, where we can observe Lower Cambrian sedimentary rocks and the Precambrian–Cambrian boundary, a key moment in Earth's geological history. Descending from the mountains, we reach the town of Agdz for a short coffee break before following the scenic route through the date palm oases of the Draa Valley, one of Morocco's longest and most picturesque river valleys. In the afternoon, we continue toward the Saredrar area near Tazzarine to visit the famous Orthoceras quarry, where Silurian-aged straight-shelled cephalopods, ancestors of later ammonites, are extracted and fashioned into decorative fossil stone objects seen in galleries around the world. We then drive on to the Alnif region, renowned for its rich fossil heritage, where we visit a Devonian trilobite preparation workshop to observe the meticulous techniques used by skilled preparators to extract and prepare trilobites from the rock. Overnight in Alnif.

STOP 4.1 – Ediacaran Stromatolites

This image is from our guide

The following is an excerpt from: Beraaouz, M., Macadam, J., Bouchaou, L., Ikenne1, M., Ernst, R., Tagma, T., and Masrour, M. (2019) An Inventory of Geoheritage Sites in the Draa Valley (Morocco): a Contribution to Promotion of Geotourism and Sustainable Development. Geoheritage, vol. 11, pp. 241-255.

Stromatolite Geosite of Amane-n'Tourhart

The stromatolites of Amane-n'Tourhart outcrop on both sides of the national road P31 connecting Ouarzazate to Zagora cities (Fig. 1). The site is located about 25 km south-east of Ouarzazate at N 30° 47′ 33.0″ and W 06° 43′ 19.7″. These stromatolite limestones were reported first by Raguinin 1948 (in Choubert and Faure-Muret 1970). They form an outcrop which has proved to be the most spectacular Conophyton site in the Anti-Atlas (Choubert et al. 1952a, 1952b) with an exposure extending over about 0.04km^2 (4 ha) and a thickness of 10–20 m. Stromatolite limestone units are interbedded with andesite, rhyolite, tuff, and conglomerate of Jbel Tinghouy in the east, and andesite, tuff, and sandstone of Jbel Tissouktai in the west. The sequence belongs to the Ouarzazate Supergroup of the upper Neoproterozoic (Fig. 2a); the three separate limestones "benches" with stromatolites are clearly shown on the lithological log (Fig. 2b) for the Amane-n'Tourhart site.

Stromatolite domes outcrop in limestone deposited in a shallow sedimentary basin, most likely in a lacustrine environment. They take the form of a lamellar structure that developed from the accumulation of carbonates or sand grains by felting of cyanobacteria. Stromatolite colonies are grouped into sub-circular or sometimes elliptical domes which are 5–60 cm in diameter and up to 1 m in height (Fig. 3a), with well-preserved lamellar structure (Fig. 3b). The domes are outlined in shiny black patina and have regularly spaced fractures filled with red ochre. The importance of the site is both in its wonderful visual appearance and for its scientific importance. This site can be related to the role of stromatolites in early life on Earth.

The Formation of Stromatolites

Stromatolites are interpreted as organo-sedimentary structures resulting from lithified microbial mats where cyanobacteria are the main contributors; most Proterozoic stromatolites probably accreted by microbial trapping and/or binding (Knoll 2008). Because of morphological similarity, most described Precambrian microfossils have been attributed to cyanobacterial activities (Golubic 1991; Golubic et al. 2000; Knoll 2008).

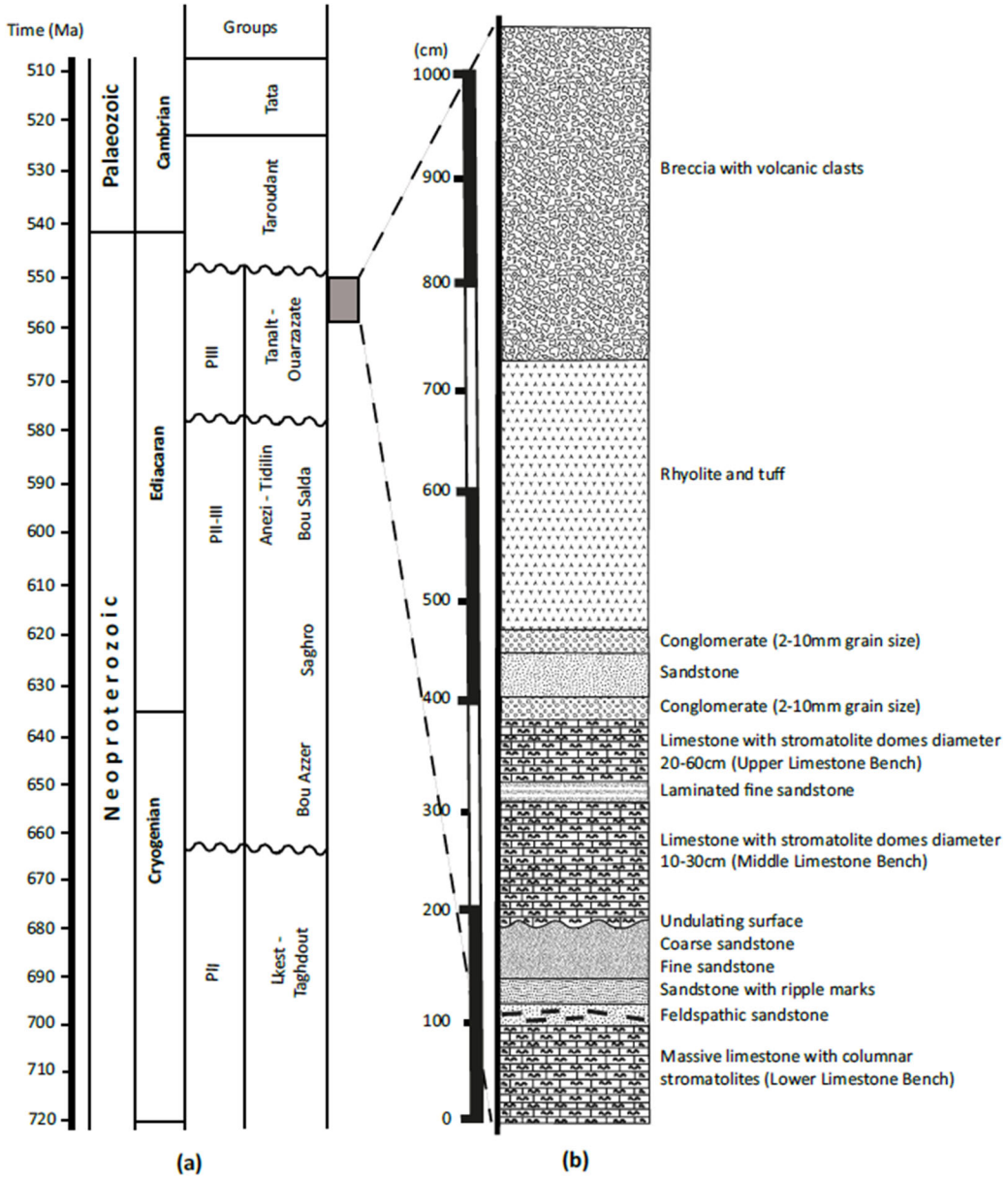

Fig. 2 **a** Generalized stratigraphic column for the Anti-Atlas Pan-African orogen. PII and PIII are the classic stratigraphic symbols used on Anti-Atlas geological maps. Modified from Gasquet et al. (2008). **b** Lithological log for the Amane-n'Tourhart geosite

In the Amane-n'Tourhart geosite, the cyanobacteria have developed as follows: initially, some precipitation of calcareous concretions occurred at irregularities (bumps) in the muddy sediment, caused by a cyanobacteria species (this forms the lower limestone "bench"). Subsequently, the intense growth of this cyanobacteria species, or invasions by other species, leads to growth of encrusting forms and lamellar tubes because of their biological activity during the day and inactivity during the night. Indeed, after sunset, the cyanobacteria bend over, and suspended sediment, particularly fine-grained sands and silts, settle on these cyanobacteria forming crusts, which then alternate to produce laminations. Regular growth builds both small and large domes. Lake shores receive mud that can disrupt the development of crusts and so cyanobacteria typically flourish in the middle of lakes where waters are sufficiently non-turbid. The role of stromatolites in the appearance of life on earth is very important: cyanobacteria display significant morphological and metabolic versatility (Stal 1991), two attributes that confer on them a great adaptive capacity that positions them as key precursors of early ecosystems. Whether cyanobacteria were also present in the Archean (>2500 million years ago) is still subject to discussion, but their geobiological impact on Earth history has been crucial. At some point in the Precambrian, oxygen released by cyanobacterial activity

changed from being poisonous to becoming vital and thus changed forever the course of geobiological evolution on Earth (Chacón et al. 2011).

Unlike any other biological group, cyanobacteria triggered major evolutionary events that shaped the biosphere that we see today: cyanobacteria were the first organisms to employ oxygenic photosynthesis, being responsible for the transition of the Earth's atmosphere from anoxic to oxic (Ehrlich 1981). The interpretation and promotion of this stromatolite geosite are important for two main reasons: first, because it can be easily integrated into sustainable geotourism development, since it is located near the road between Ouarzazate and Zagora; and second, because the history of the primitive micro-organisms tells an important story about the history of life on Earth.

This section is taken from Wikipedia as a general intro to stromatolites

Stromatolites or stromatoliths (from Ancient Greek στρῶμα (strôma), GEN στρώματος (strṓmatos) 'layer, stratum' and λίθος (líthos) 'rock') are layered sedimentary formations (microbialite) that are created mainly by photosynthetic microorganisms such as cyanobacteria, sulfate-reducing bacteria, and Pseudomonadota (formerly proteobacteria). These microorganisms produce adhesive compounds that cement sand and other rocky materials to form mineral "microbial mats". In turn, these mats build up layer by layer, growing gradually over time.

This process generates the characteristic lamination of stromatolites, a feature that is hard to interpret, in terms of its temporal and environmental significance. Different styles of stromatolite lamination have been described, which can be studied through microscopic and mathematical methods. A stromatolite may grow to a meter or more. Fossilized stromatolites provide important records of some of the most ancient life. As of the Holocene, living forms are rare.

Definition

Paleoproterozoic oncoids from the Franceville Basin, Gabon, Central Africa. Oncoids are unfixed stromatolites ranging in size from a few millimeters to a few centimeters

Stromatolites are layered, biochemical, accretionary structures formed in shallow water by the trapping, binding and cementation of sedimentary grains in biofilms (specifically microbial mats), through the action of certain microbial lifeforms, especially cyanobacteria.

Ancient stromatolites - *Morphology*

Fossilized stromatolites exhibit a variety of forms and structures, or morphologies, including conical, stratiform, domal, columnar, and branching types. Stromatolites occur widely in the fossil record of the Precambrian but are rare today. Very few Archean stromatolites contain fossilized microbes, but fossilized microbes are sometimes abundant in Proterozoic stromatolites.

While features of some ancient apparent stromatolites are suggestive of biological activity, others possess features that are more consistent with abiotic (non-biological) precipitation. Finding reliable ways to distinguish between biologically formed and abiotic stromatolites is an active area of research in geology. Multiple morphologies of stromatolites may exist in a single local or geological stratum, depending on specific conditions at the time of their formation, such as water depth.

Most stromatolites are spongiostromate in texture, having no recognisable microstructure or cellular remains. A minority are porostromate, having recognisable microstructure; these are mostly unknown from the Precambrian but persist throughout the Palaeozoic and Mesozoic. Since the Eocene, porostromate stromatolites are known only from freshwater settings.

Fossil record

Some Archean rock formations show macroscopic similarity to modern microbial structures, leading to the inference that these structures represent evidence of ancient life, namely stromatolites. However, others regard these patterns as being the result of natural material deposition or some other abiogenic mechanism. Scientists have argued for a biological origin of stromatolites due to the presence of organic globule clusters within the thin layers of the stromatolites, of aragonite nanocrystals (both features of current stromatolites), and of other microstructures in older stromatolites that parallel those in younger stromatolites that show strong indications of biological origin.

Stromatolites are a major constituent of the fossil record of the first forms of life on Earth. They peaked about 1.25 billion years ago (Ga) and subsequently declined in abundance and diversity, so that by the start of the Cambrian they had fallen to 20% of their peak. The most widely supported explanation is that stromatolite builders fell victim to grazing creatures (the Cambrian substrate revolution); this theory implies that sufficiently complex organisms were common around 1 Ga. Another hypothesis is that protozoa such as foraminifera were responsible for the decline, favoring formation of thrombolites over stromatolites through microscopic bioturbation.

Proterozoic stromatolite microfossils (preserved by permineralization in silica) include cyanobacteria and possibly some forms of the eukaryote chlorophytes (that is, green algae). One genus of stromatolite very common in the geologic record is Collenia.

The connection between grazer and stromatolite abundance is well documented in the younger Ordovician evolutionary radiation; stromatolite abundance also increased after the Late Ordovician mass extinction and Permian–Triassic extinction event decimated marine animals, falling back to earlier levels as marine animals recovered. Fluctuations in metazoan population and diversity may not have been the only factor in the reduction in stromatolite abundance. Factors such as the chemistry of the environment may have been responsible for changes.

Fossilized stromatolites in the Hoyt Limestone (Cambrian) exposed at Lester Park, near Saratoga Springs, New York

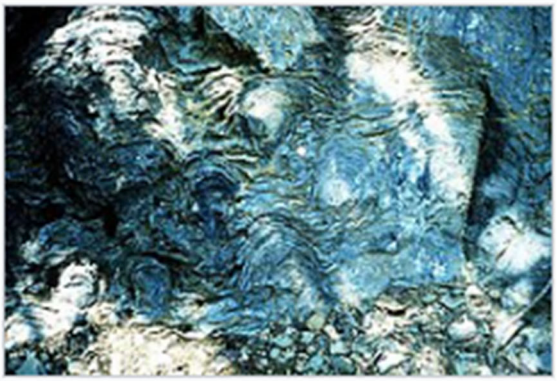

Precambrian fossilized stromatolites in the Siyeh Formation, Glacier National Park

Fossilized stromatolites (Pika Formation, middle Cambrian) near Helen Lake, Banff National Park, Canada

While prokaryotic cyanobacteria reproduce asexually through cell division, they were instrumental in priming the environment for the evolutionary development of more complex eukaryotic organisms. They are thought to be largely responsible for increasing the amount of oxygen in the primeval Earth's atmosphere through their continuing photosynthesis (see Great Oxygenation Event). They use water, carbon dioxide, and sunlight to create their food. A layer of polysaccharides often forms over mats of cyanobacterial cells. In modern microbial mats, debris from the surrounding habitat can become trapped within the polysaccharide layer, which can be cemented together by the calcium carbonate to grow thin laminations of limestone. These laminations can accrete over time, resulting in the banded pattern common to stromatolites. The domal morphology of biological stromatolites is the result of the vertical growth necessary for the continued infiltration of sunlight to the organisms for photosynthesis. Layered spherical growth structures termed oncolites are similar to stromatolites and are also known from the fossil record. Thrombolites are poorly laminated or non-laminated clotted structures formed by cyanobacteria, common in the fossil record and in modern sediments. There is evidence that thrombolites form in preference to stromatolites when foraminifera are part of the biological community.

The Zebra River Canyon area of the Kubis platform in the deeply dissected Zaris Mountains of southwestern Namibia provides a well-exposed example of the thrombolite-stromatolite-metazoan reefs that developed during the Proterozoic period, the stromatolites here being better developed in updip locations under conditions of higher current velocities and greater sediment influx.

Modern occurrence

Stromatolites at Lake Thetis, Western Australia

Stromatolites at Highborne Cay, in the Exumas, The Bahamas

Formation

Time lapse photography of modern microbial mat formation in a laboratory setting gives some revealing clues to the behavior of cyanobacteria in stromatolites. Biddanda et al. (2015) found that cyanobacteria exposed to localized beams of light moved towards the light, or expressed phototaxis, and increased their photosynthetic yield, which is necessary for survival. In a novel experiment, the scientists projected a school logo onto a petri dish containing the organisms, which accreted beneath the lighted region, forming the logo in bacteria. The authors speculate that such motility allows the cyanobacteria to seek light sources to support the colony.

In both light and dark conditions, the cyanobacteria form clumps that then expand outwards, with individual members remaining connected to the colony via long tendrils. In harsh environments where mechanical forces may tear apart the microbial mats, these substructures may provide evolutionary benefit to the colony, affording it at least some measure of shelter and protection.

Lichen stromatolites are a proposed mechanism of formation of some kinds of layered rock structure that are formed above water, where rock meets air, by repeated colonization of the rock by endolithic lichens.

STOP 4.2 – Tizi-n-Tinififfft Pass

This is from ChatGPT

Overview

Tizi-n-Tinififfft (also spelled Tizi n'Tinifift) is a mountain pass in the Atlas Mountains of southeastern Morocco (Drâa-Tafilalet region) at about 1,693 m (5,554 ft) above sea level on National Route 9 between Ouarzazate and Zagora/Agdz.

While there are few detailed academic sources focused specifically on the pass's geology, its broader geological context can be explained from our understanding of the Atlas Mountain system.

Geological Setting: Atlas Mountains

The Atlas Mountains — including the range that contains Tizi-n-Tinififfft — are a young intracontinental mountain belt formed primarily during the Cenozoic (last ~66 million years) as a result of tectonic compression and uplift of older sedimentary and basement rocks.

Key tectonic processes:

- The Atlas arose far inland from the main African–Eurasian plate boundary, and its uplift is linked to inversion tectonics (compression that reactivates older extensional basins).
- Thick-skinned deformation (involving basement rocks) and thrust faulting elevated the region.
- Quaternary (recent) and older faults continue to shape the relief, producing valleys and rugged passes typical of the High Atlas.
- The mountain belt includes a complex stack of rocks ranging from Precambrian crystalline basement to Paleozoic, Mesozoic and Cenozoic sedimentary cover, though exact exposures vary locally.

Likely Rock Types Near Tizi-n-Tinififfft

In the Drâa-Tafilalet sector of the High Atlas, the geology generally includes:

- Folded and faulted sedimentary rocks (sandstones, shales, limestones) originally deposited in ancient basins before being uplifted.
- Older metamorphic and crystalline rocks at deeper structural levels of the range (common in High Atlas backbone).
- Red-bed continental sequences (e.g., Triassic rift deposits) often visible in outcrop on southern Atlas flanks.
- The pass and surrounding plateaus likely reflect this mix of uplifted, tilted sedimentary strata and older basement rocks that have been deeply eroded and faulted as a result of Atlas-building tectonics.

Topography & Surface Geology

The terrain around Tizi-n-Tinififfft — a high plateau interrupted by erosion, canyons, and rocky outcrops — reflects the interplay of tectonic uplift and surface processes:

Erosional landforms: The descents from the pass cut through valleys and canyons, shaped by long-term water and wind erosion acting on uplifted rocks.

Steep relief: The Atlas landscape in this region is characterized by abrupt elevation changes, a signature of tectonic uplift and differential erosion typical of mountain belts.

STOP 4.3 – Agdz and The Draa Valley

The image is from: Beraaouz, M., Macadam, J., Bouchaou, L., Ikenne1, M., Ernst, R., Tagma, T., and Masrour, M. (2019) An Inventory of Geoheritage Sites in the Draa Valley (Morocco): a Contribution to Promotion of Geotourism and Sustainable Development. Geoheritage, vol. 11, pp. 241-255.

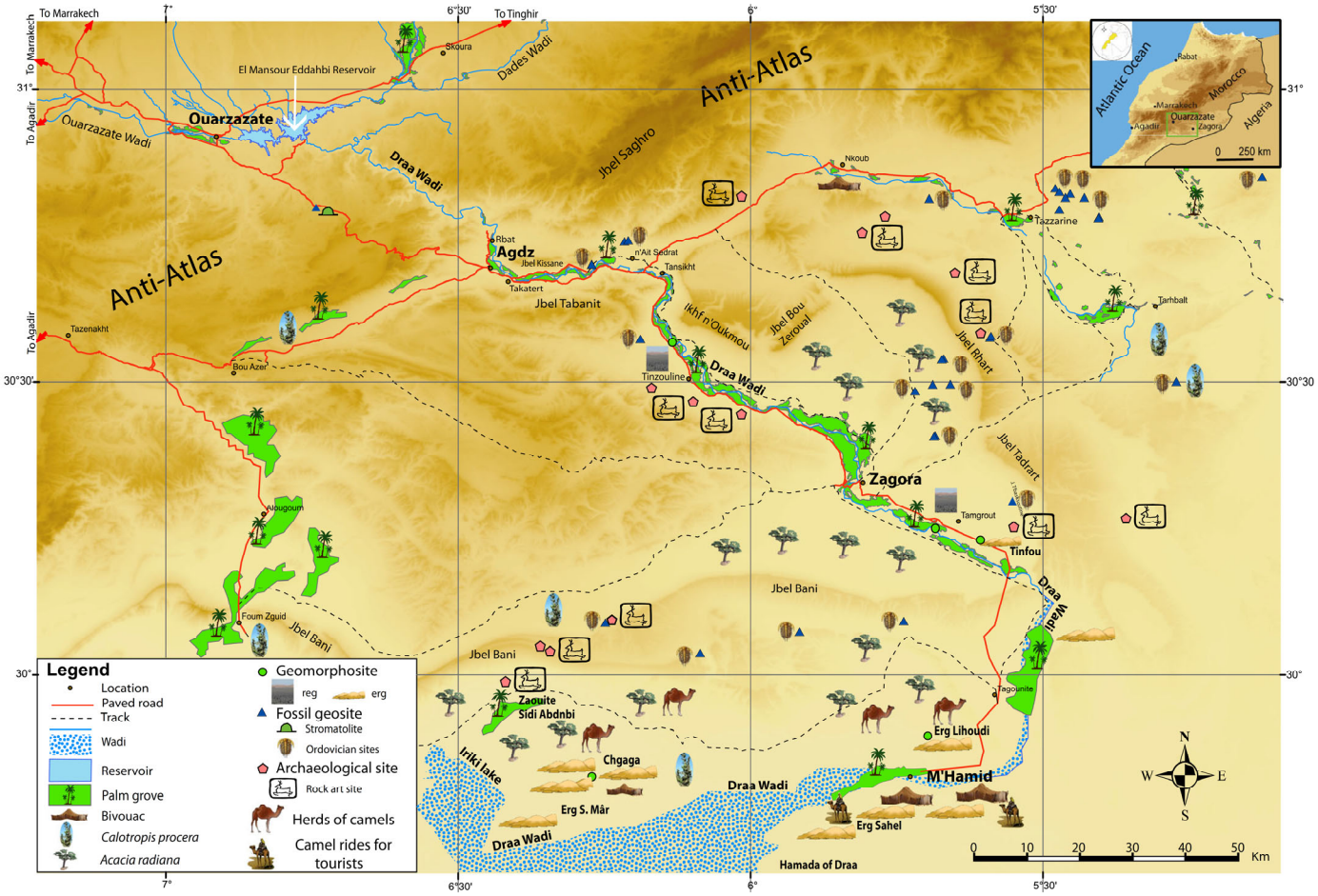

Fig. 1 Map of proposed geosite locations

The Following writing is taken from: Becker, T.R., Jansen, U., Plodowski, G., Schindler, E., Aboussalam, S.Z., and Weddige, K., (2004) Devonian litho- and biostratigraphy of the Dra Valley area – an overview - Devonian of the western Anti Atlas: correlations and events. Doc. Inst. Sci, Rabat, vol. 19, pp. 3-18.

The Dra or Drâa Valley is a main valley running over a distance of almost 600 km in parallel to the overall strike direction of the Anti-Atlas Palaeozoic, from about Zagora in the NE to Tan-Tan near the Atlantic Ocean in the SW. From Zagora a significant branch of the valley cuts in northwestern direction through the Palaeozoic and Precambrian towards Ouarzazate, creating spectacular outcrops. The main Oued Dra runs over wide distance in parallel to the topmost Devonian and prominent Tournaisian Jebel Tazout, mostly very close to the Moroccan-Algerian border, and partly has become inaccessible for security reasons. However, the Dra Valley has given its name to the wide stretch of Devonian outcrops (HOLLARD & JAQUEMONT 1956, HOLLARD 1978) which forms the northern limb of the extensive Tindouf Basin (Fig. 1). This stretches into former Spanish Sahara and northern Mauritania in the SW (forming the Zemmour as an appendix) and into large parts of Algeria in its southern, central and eastern parts, including the poorly studied Menakeb in the SE. The basin has recurrently attracted interest in potential hydrocarbon reservoirs. Thermal maturation was strongly influenced by the lack of a post-Variscan cover until a late

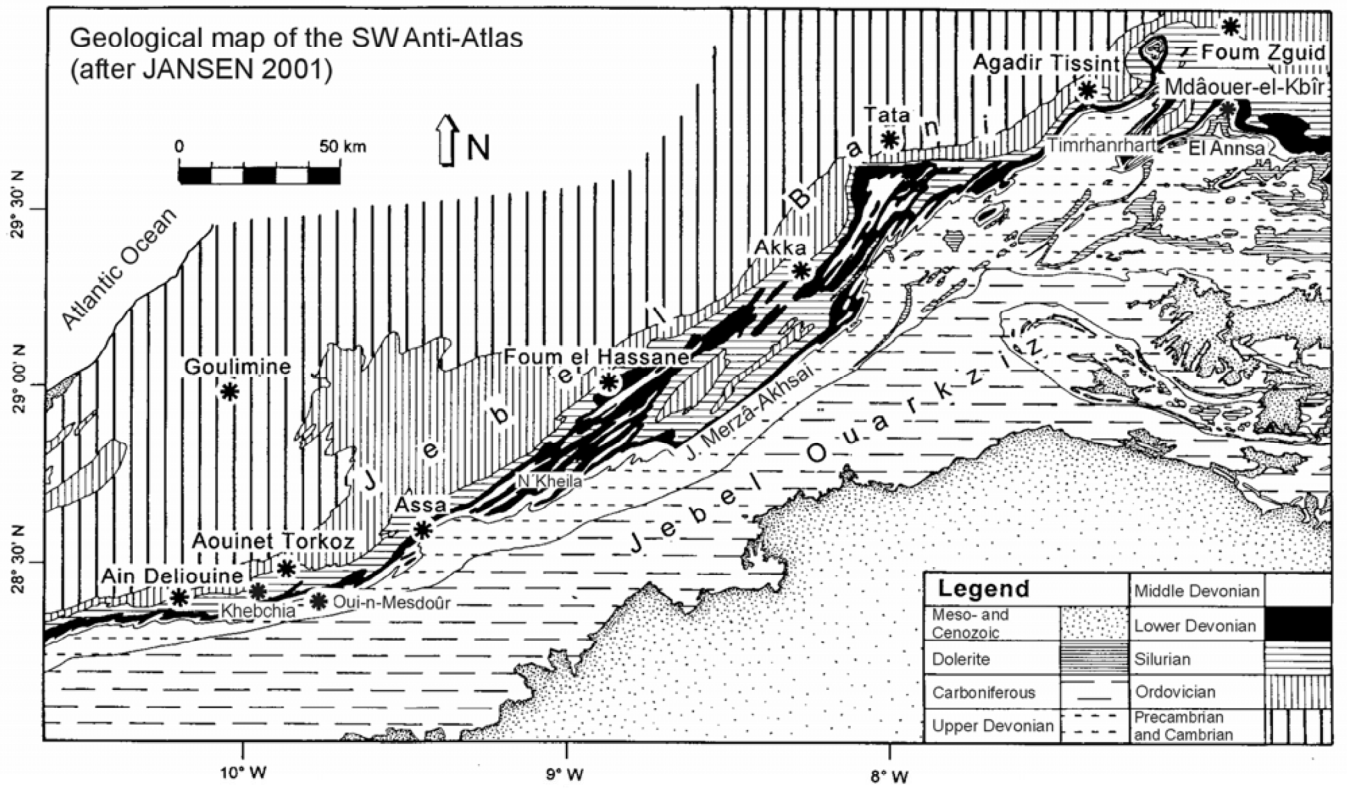

Fig. 1 : Geological map of the SW Anti Atlas (based on HOLLARD & JAQUEMONT 1956, modified after JANSEN 2001).

Cretaceous transgression. The Zemoul is an anticline and syncline of Palaeozoic rocks which runs from south of Tata in NW-E direction towards Tinfouchy and today mostly belongs to Algeria. Recent Devonian studies presented in this guidebook concentrate on accessible Moroccan sections, between the S of Foum Zguid and the area S of Torkoz, allowing correlations over almost 400 km on strike. The relative continuity of exposures enables an outstanding reconstruction of facies and faunal changes along the Devonian palaeoshelf of northwestern Gondwana, with little influence (only folding and some faulting) of subsequent deformation by the Variscan Orogenesis which affected all the Palaeozoic north of the South Atlas fault. The overall increasing thickness of sedimentary rocks towards the SW indicates a predominant provenance of siliciclastic supply and the presence of erosive land masses towards the SW and W. However, there are also thick clastic wedges (e.g., the Rich 3 sandstones) which fade out from NE to SW. This confirms (see cross-sections in HOLLARD 1967) that a combination of subsidence variation and changing supply directions needs to be considered in palaeogeographic reconstructions.

The scientific investigation of the Devonian of the Dra Valley area started later and led to much fewer detailed studies of faunas and sedimentology than in other parts of Morocco. Almost thirty years ago, in 1975, Henry HOLLARD led SDS members during an excursion which covered during 11 field days localities from the eastern Dra Valley to the Tafilalt. It is intriguing how few detailed section logs have been published since. Rather detailed compilations in a post-mortem publication by HOLLARD (1981b) are partly difficult to follow. Research is still in an exploration stage. The first reports of Dra Valley Devonian faunas go back to GENTIL (1929), DESCOSSY & ROCH (1934), BONDON & CLARIOND (1934), and BOURCART (1938). CHOUBERT et al. (1948) reported on the first Emsian and Famennian goniatites of the area, discovered earlier in 1938 to 1941. Recently, BULTYNCK & WALLISER (2000) gave reference to the Dra Valley in their overview of the Moroccan Anti-Atlas that otherwise is more focused on the (hemi)pelagic successions in the Tafilalt and Maider areas.

Thick, partly quartzitic sandstone units have resisted erosion and today form extensive and elevated ridges stretching along strike. As widespread marker units they provide easy landmarks for

lithostratigraphical correlation and give evidence for huge open marine sandbars bordering the ancient Gondwana coastline. Starting with CHOUBERT (1948, 1951, 1956) they were named in the Lower Devonian as “Rich”. Later the term “Rich” was used for successive formations based on complete rhythothemes, numbering 1 to 4 (HOLLARD 1963a, 1981a, see Fig. 2). Late Devonian and Early Carboniferous massive sand sheets formed the Jebel Tazout and Jebel Ouarkziz, the latter also including limestones. Despite the gradual wedging out of some units over very long distances, our recent research confirmed their high correlation value and invariable stratigraphic position between well-dated pelagic levels with ammonoids and conodonts. This also applies to some thinner marker limestones which form low hills. Rich 1 to 4 sandstones represent the upper part of shallowing upwards cycles with subsequent transgressions linked to global eustatic pulses and events. The definition of formations should follow this natural division, with formation boundaries to be placed at the top of the regressive Rich sandstone units which represent late highstand system tracts and filling up successions. Sequence boundaries and paraconformities have to be sought near the very tops. Thinning and fading of Rich 4 sandstones (of the SW Dra Valley) towards the NE do not form an obstacle since the subsequent early Eifelian transgression allows an easy recognition of T-R cycles and correlation. The same applies to Rich 3 sandstones which are restricted to the NE succession, but are apparently followed by a late Emsian transgression throughout the Dra Valley.

The Dra Valley Devonian is generally characterized by high sedimentation rates, a predominance of fine and coarse clastics and by an alternation of fossiliferous, neritic and pelagic intervals reflecting the oscillation of relative sea-level caused by basin subsidence, infilling, and/or eustatics. Successions of the Maider and Tafilalt, which SDS has visited on previous occasions, are much more condensed by comparison, up to a factor of 200 on the pelagic carbonate platforms. Due to the high input of clastic material, reefs and biostromes are mostly missing in the Dra Valley. Rare exceptions were mentioned by HOLLARD (1967). Extensive Middle and early Upper Devonian carbonate platforms re-appear towards the SW in the Western Sahara (DUMESTRE & ILLING 1967, KÖNIGSHOF et al. 2003) and at the southern margin of the Tindouf Basin. Biostratigraphy is currently based on the interfingering of faunas with ammonoids, conodonts, brachiopods, tentaculitids and trilobites but some studies have not yet left the level of preliminary identifications. The alternation of neritic and pelagic units makes the Dra Valley a significant region for the often difficult correlation of the so-called Rhenish and Hercynian facies realms (see discussion and correlations in HOLLARD 1978, JANSEN 2001). In addition, neritic faunal elements may enter assemblages gradually from NE to SW whilst pelagic taxa, such as Lower Emsian, uppermost Famennian or basal Carboniferous goniatites (e.g., Gattendorfia faunas, HOLLARD 1956) fade out completely. Many faunal groups are still insufficiently studied and new discoveries are to be expected in the future. Knowledge of brachiopods (HOLLARD & DROT 1958, DROT 1964, 1971 etc., BRICE & NICOLLIN 2000, NICOLLIN & BRICE 2000, AIT MALEK et al. 1999, JANSEN 1999, 2000, 2001), ammonoids (HOLLARD 1960, BENSAID 1974, KLUG 2003, and articles in this volume), trilobites (HOLLARD 1963b, ALBERTI & HOLLARD 1963, MORZADEC 1988, 2001, SCHRAUT 1998a, 1998b, 2000a, 2000b), and ostracods (G. BECKER et al. 2003, in press) is at an advanced stage, but nautiloids, pelecypods, gastropods, corals, Bryozoa, palynomorphs, fish (LEHMAN 1976) and ichnofossils have hardly been described. Work on tentaculitoids by G.K.B. ALBERTI is still mostly unpublished. This guidebook for the first time will clearly outline the regional event stratigraphy, with sometimes preliminary data on the Daleje, Chotec, pumilio, Taghanic, Rhinestreet, semichatovae, Lower and Upper Kellwasser, and Hangenberg Events. Of special interest is the discovery of “pumilio Beds” (EBBIGHAUSEN et al., this vol., R.T. BECKER et al., this vol.) which are much older than the two well-established Givetian pumilio Events.

STOP 4.4 – Orthoceras Quarry near Tazzarine

I don't think this article covers the specific Orthoceras quarry we are visiting, but it is definitely covers cephalopod quarry very close to where we will be!!!

Kroger, B. and Lefebvre, B. (2012) Palaeogeography and palaeoecology of early Floian (Early Ordovician) cephalopods from the Upper Fezouata Formation, Anti-Atlas, Morocco. Fossil Record, vol. 15, no. 2, pp. 61-75.

Palaeogeography and palaeoecology of early Floian (Early Ordovician) cephalopods from the Upper Fezouata Formation, Anti-Atlas, Morocco

Received 9 September 2011
Accepted 28 December 2011
Published 3 August 2012

Abstract

In the central Anti-Atlas (Morocco), the Early Ordovician succession consists of about 1000 m of fossiliferous argillites and siltstones. The Upper Fezouata Formation (Floian) contains a comparatively rich and abundant cephalopod association. A small collection of these cephalopods is described herein for the first time. The cephalopods are interpreted as autochthonous or parautochthonous, representing a fauna, which originally lived nektobenthically in the open water above the sediments or related to the sea bottom. The cephalopod associations of the Upper Fezouata Formation are similar to other contemporaneous assemblages known from higher palaeolatitudes and associated with deeper depositional settings and in siliciclastically dominated deposits. They are composed almost exclusively of slender orthocones, in this case predominantly of *Destombesiceras zagorense* n. gen., n. sp., which is interpreted as an early discosorid. *Bathmoceras australe* Teichert, 1939 and *Bathmoceras taichoutense* n. sp. from the Upper Fezouata Formation are at present the earliest unambiguous occurrences of bathmocerid cephalopods. Epizoans on the shell of a specimen of *Rioceras* are the earliest evidence of bryozoans growing as potential hitchhikers on cephalopod shells, indicating an early exploitation of a pseudoplanktonic lifestyle in this phylum.

Key Words

Gondwana
Palaeozoic
cephalopod diversity
bryozoan epizoans

Introduction

This is the first description of Ordovician cephalopods from Morocco. Although their occurrence has been known for a long time, only a poorly preserved conch from the late Katian of Ikhf n'Ouzerg (central Anti-Atlas) was described as "*Orthoceras hastile* Barrande" by Termier & Termier (1950). In some cases Ordovician cephalopods were mentioned within faunal lists without classification (e.g., Gutiérrez-Marco 2003; Destombes 2006a; Van Roy et al. 2010). Indeed, the lack of earlier works on Moroccan cephalopod assemblages does not reflect their absence or rarity. It rather is an expression of a neglect of the group by many palaeontologists working in the region. Generally, the Ordovician cephalopods of the high latitude margins of Gondwana are poorly known and, where known, often are in need of revision. Of those high latitudinal assemblages most recently revised or newly described in detail (Marek et al. 2000; Gnoli & Pillola 2002; Evans 2005; Kröger & Evans 2011), all seem to be characterized by the presence (often in abundance) of specific forms that are rare or absent in low palaeolatitude regions.

Contrary to the situation in most other high latitude (peri-)Gondwanan regions (e.g., Algeria, Bohemia, France, Spain), the first reports of Ordovician faunas in the Anti-Atlas, Morocco are relatively recent (Bigot & Dubois 1931; Choubert 1952; Choubert et al. 1953). Intensive field work achieved by Jacques Destombes between 1959 and 1985 during the campaign of 1 : 200,000 mapping of the whole Anti-Atlas lead to a much improved stratigraphic framework, and to the collection of abundant fossil material (Destombes 1962, 1971; Destombes et al. 1985). In particular, extremely

rich and diverse Early Ordovician marine assemblages were described from the Anti-Atlas, based on Destombes' material, including acritarchs and chitinozoans (Deunff 1968a, b; Elaouad-Debbaj 1984, 1988), bivalves and rostroconchs (Destombes & Babin 1990), brachiopods (Havlicek 1971; Mergl 1981), echinoderms (Ubaghs 1963; Chauvel 1966, 1969, 1971a, b; Donovan & Savill 1988), gastropods (Horny 1997), graptolites (Destombes & Willefert 1959), hyolithids (Marek 1983), and trilobites (Destombes 1972; Vidal 1998a, b). Early Ordovician faunas from the Anti-Atlas exhibit strong affinities with other high-latitude assemblages, and in particular with those from the Montagne Noire (Southern France).

In the early 2000s, intensive field work in the Early Ordovician succession of Zagora area (central Anti-Atlas) lead to the discovery of several horizons yielding exceptionally preserved assemblages (Van Roy et al. 2010). This so-called Fezouata Biota contains not only fully articulated remains of skeletonised organisms (e.g., echinoderms: Lefebvre 2007; Noailles et al. 2010; Sumrall & Zamora in press), but also extremely abundant and diverse remains of soft-bodied to lightly sclerotised invertebrates (e.g., annelids, anomalocaridids, machaeridians, marrellomorphs, sponges: Van Roy 2006; Van Roy & Tetlie 2006; Botting 2007; Vinther et al. 2008; Van Roy & Briggs 2011). These Lagerstätten provide an unprecedented opportunity to document the onset of the Great Ordovician Biodiversification Event (Servais et al. 2010), and the transition from the Cambrian Evolutionary Fauna to the Palaeozoic Evolutionary Fauna. They also offer for the first time the possibility to compare the well-known Early to Mid-Cambrian marine communities (e.g., Chengjiang, Burgess Shale) with similarly preserved Ordovician assemblages.

The description of the Fezouata Formation cephalopods, which are generally considered as the top free swimming predators, will provide new information on this important element of the food web of the Fezouata Biota. A comparison with contemporaneous Gondwanan cephalopod assemblages will deepen our knowledge on the as yet poorly documented cephalopod faunas in high latitude regions in Early Ordovician times.

Material and methods

Most of the material described herein was collected in situ during two successive field campaigns (January 2003 and January 2004) in the Early Ordovician succession of the Zagora area. This material (marked as AA) is now deposited in the collections of Cadi Ayyad University, Marrakech (Faculté des Sciences et Techniques, Guéliz). In the early 2000s, additional specimens were collected by Roland and Véronique Reboul (Saint-Chinian). Their material is now deposited in the palaeontological collections of Lyon 1 University, Villeurbanne (FSL), the Musée des Confluences, Lyon (ML), and the Natural History Museum of Marseille (MHNM).

After taxonomic determination of the specimens, we estimated the diversity measures of the assemblage with the software Estimates Version 8.20 (Colwell 2009) and with the R-software package Vegan Version 1.15–2 (Oksanen et al. 2011).

Geological setting and stratigraphic framework

The study material was collected in situ from six different localities, all located within the central part of the Anti-Atlas, Morocco (Fig. 1). In the Zagora area, the Early Ordovician succession is weakly folded, and about 1000 m thick (Destombes et al. 1985; Destombes 2006b). Its lower part, the Lower Fezouata Formation (Tremadocian) consists of approximately 430 m of blue to greenish fine argillites resting unconformably over sandstones of the Azlag Formation (Tabanite Group, Middle Cambrian). The detailed stratigraphy of the Lower Fezouata Formation is relatively well constrained, based on its acritarch, chitinozoan, and graptolite assemblages (Destombes & Willefert 1959; Deunff 1968a, b; Elaouad-Debbaj 1988). The overlying Upper Fezouata Formation (Floian) corresponds to about 570 m of yellow to greenish siltstones, containing (in its upper part) several levels with alumino-siliceous concretions. The uppermost part of the Upper Fezouata Formation was assigned to the late Floian (time slice

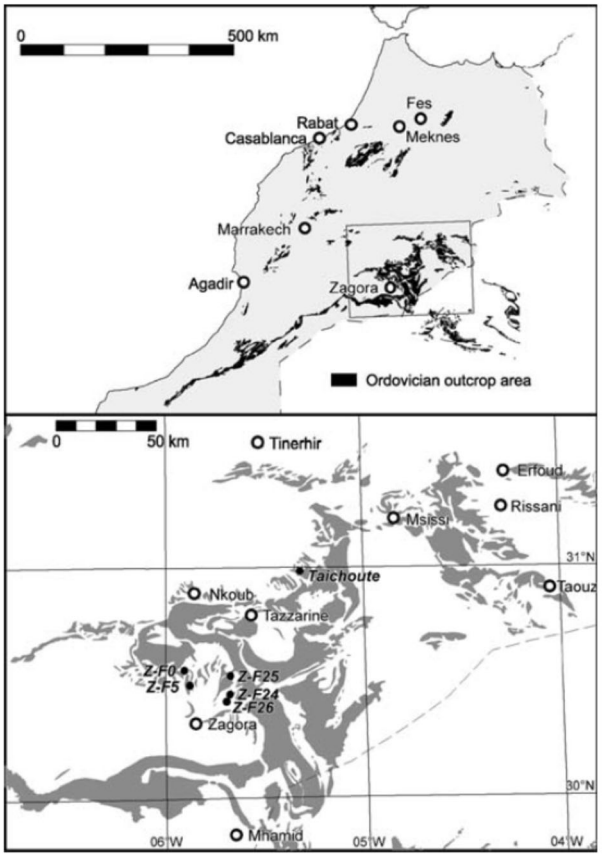

Figure 1. Generalized maps showing Ordovician outcrops in Morocco (top), and in central and eastern Anti-Atlas (bottom), with location of the six main cephalopod localities mentioned in text (modified from Lefebvre & Botting 2007).

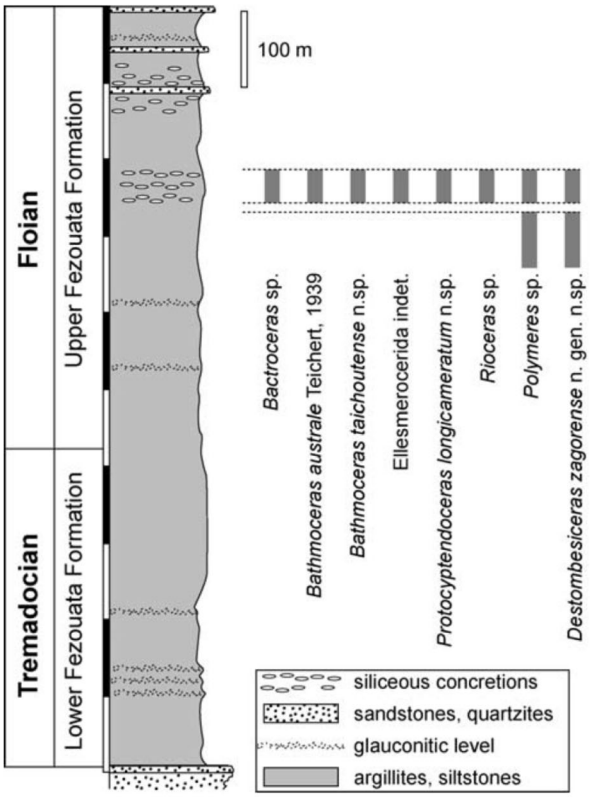

Figure 2. Stratigraphic ranges of cephalopods in the Early Ordovician of central Anti-Atlas (Zagora area). Stippled lines mark the two sampled stratigraphic intervals. Section modified from Vidal (1998a) and Destombes (2006b).

2c) based on the presence of the chitinozoan *Eremochitina baculata brevis* (Elaouad-Debbaj 1984). All fossils described herein were collected from two distinct stratigraphic intervals, both located within the Upper Fezouata Formation (Fig. 2).

The lower stratigraphic interval corresponds to micaceous siltstones located between 680 and 750 m above the base of the Ordovician succession. Graptolites (*Baltograptus geometricus*, *B. vacilllans*) are suggestive of an early Floian age (J. C. Gutiérrez-Marco, pers. comm., May 2003). The associated benthic fauna is particularly abundant and diverse, including various arthropods (e.g., aglaspidids, cheloniellids, *Zagoracaris fezouataensis*), bivalves (*Babinka*, *Coxiconcha*, *Redonia*), echinoderms (eocrinoids, rhombiferans, solutans, somasteroids, cornute and mitrate stylophorans), gastropods (*Carcassonnella*, *Deshyolites*, *Lesueurilla*, *Thoralispira*), hyolithids, machaeridians, rostroconchs (*Ribeiria*), trilobites (e.g., *Agerina*, *Ampyx*, *Asaphellus*, *Colpocoryphe*, *Euloma*, *Harpides*, *Parabathycheilus*, *Prionocheilus*, *Selenopeltis*, *Toletanaspis*), as well as "soft-bodied" organisms (e.g., various "worms") (Destombes et al. 1985; Van Roy et al. 2010). This assemblage occurs in the following four localities: Jbel Bou Zeroual (noted as "Z-F0" on specimen labels), Oued Beni Zoli ("Z-F5"), N. of Toumiat ("Z-F24"), and Toumiat ("Z-F26"). The most diverse benthic assemblages were collected in the yellow, micaceous siltstones of both Jbel Bou Zeroual (small quarry, about 26 km NNW of Zagora, W of Jbel Bou Dehir) and Toumiat (low cliff on the bank of a dried oued, about 18 km NE of Zagora, E of Jbel Bou Dehir). The green micaceous siltstones of Oued Beni Zoli (low cliff on the bank of Oued Beni Zoli, about 17 km NNW of Zagora, W of Jbel Bou Dehir) have yielded a less diverse assemblage, dominated by gastropods and the rhombiferan *Macrocystella bohemica* (B. Lefebvre, pers. obs.). The fourth locality, N. of Toumiat (low cliff on the bank of a dry oued, about 2 km NE of Z-F26), corresponds to a relatively small lens containing abundant fragments of a low diversity assemblage dominated by isolated steles (stems) of the solutan *Plasiacystis mobilis*, associated with pieces of large asaphid trilobites, hyolithids, and disarticulated eocrinoid stems (B. Lefebvre, pers. obs.).

The second stratigraphic interval corresponds to concretion-bearing siltstones, about 750 to 790 m above the base of the Ordovician succession. In the absence of graptolites, the age can be estimated roughly as late early to mid Floian, based on the associated trilobite assemblage (e.g., *Ampyx* sp., *Asaphellus fezouataensis*, *Basilicus* (*Basiliella* ?) aff. *destombesi*) (Vidal 1998a, b). Other elements of the fauna include bivalves, brachiopods, echinoderms (asterozoans, crinoids, edrioasteroids, eocrinoids, solutans, cornute and mitrate stylophorans), gastropods (e.g., *Carcassonnella*, *Lesueurilla*, *Thoralispira*), hyolithids (e.g., *Cavernolites* ?), and machaeridians (B. Lefebvre, pers. obs.). This assemblage occurs in fossiliferous concretions collected in two localities. The first one, Bou Chrebeb, is located about 29 km NE of Zagora, E of Jbel Bou Dehir. It was previously mentioned in the literature either as locality "1687" (Vidal 1998a, b; Destombes 2006b), "Z-5" (Van Roy 2006), or as "Z-F25" (Sumrall & Zamora 2011). It corresponds to two main trenches (Z-F25b, Z-F25c), several hundred meters long, excavated by local fossil traders looking for complete, three-dimensionally preserved trilobites occurring in the alumino-siliceous concretions. This site has generally yielded the most diverse fossil assemblage. The second locality, Taichoute, was also exploited by local fossil traders. It is about 90 km NE of Zagora (37 km NE of Tazzarine, and 16 km SW of Alnif). Its faunal content is less diverse, and largely dominated by echinoderms (the solutan *Plasiacystis mobilis*, associated with the rhombiferan *Macrocystella bohemica*) (B. Lefebvre, pers. obs.).

Preservation and taphonomy

The study material consists of impressions and moulds of original shells, which are dissolved and preserved as empty spaces. Most specimens are fragmented, sometimes with septa imploded.

In the lower fossiliferous interval, three localities (Jbel Bou Zeroualm Z-F0; Oued Beni Zoli, Z-F5; Toumiat, Z-F26) have yielded exquisitely preserved, though

strongly compressed, specimens of cephalopods. Taphonomic features of the associated fauna (e.g., abundant remains of soft-bodied organisms, preservation of fully articulated portions of the delicate brachioles of eocrinoids) suggest both the rapid burial (smoothering) of living communities by a sudden influx of sediment (e.g., turbidite, heavy storm), and a limited or no transport of the assemblage (Van Roy et al. 2010).

In Bou Chrebeb and Taichoute, cephalopods of the second stratigraphic interval are preserved in three dimensions within alumino-siliceous concretions. Most individuals show parts of the siphuncular mould with no traces of the chambers or of the phragmocone wall (e.g. Fig. 5K). This type of preservation is interpreted as the result of conch implosion during sinking of the dead shells, herein. A similar taphonomic scenario was interpreted in the same way by Hewitt & Westermann (1996, fig. 8, scenario 2b) and in Kröger & Evans (2011) for Ordovician and Silurian orthocone dominated environments. The frequent fragmentation of the conchs indicates some reworking or transport of the dead shells. This interpretation accords well with sedimentological data and taphonomic features observed on other elements of the fauna: In Ordovician times, alumino-siliceous concretions are generally associated with cold, relatively deep environmental conditions (below storm wave base), and a low rate of sedimentation (Loi & Dabard 1999, 2002). Due to their prolonged exposure on the sea-floor, fossils preserved in concretions are often slightly disarticulated or collapsed, and encrusted by various kinds of epibionts (Bruthansova & Kraft 2003; Vidal 1998b; Sumrall & Zamora in press).

In locality Z-F24 cephalopod conchs and hyolithids are both clearly aligned with their apices in one direction (Fig. 3). Taphonomic features of this assemblage indicate some current influence (with a limited transportation), and probably local accumulation of material (e.g., cephalopod conchs, disarticulated specimens of solutans and large trilobites) within channels or depressions. On one specimen of *Rioceras*? sp. (MHNM 15690.216 c; Fig. 4) epizoans (probably ceramoporid bryozoans of the order Cystoporata; pers. comm. Andrej Ernst, Kiel) are preserved on the outer surface of the phragmocone shell. Along with a specimen of *Bactroceras sandbergeri* (Barrande, 1867), figured in Evans (2005, pl. 4, fig. 1) from the Dapingian Pontyfenni Formation, this is the earliest known evidence of a bryozoan overgrowth on cephalopod shells. The pores of the bryozoans are aligned in subparallel direction along the growth axis and a growth direction toward the aperture of the cephalopod shell can be identified. This is similar to the situation described in specimens from the Upper Ordovician (Kröger et al. 2009 and references therein) and potentially is evidence for a syn-vivo growth of the bryozoans on the shell. However, more material is needed in order to verify this interpretation. Nevertheless, considering a latest Cambrian origin of bryozoans, this occurrence indicates an early exploitation of the niche of potentially floating cephalopod shells early in the evolutionary history of bryozoans.

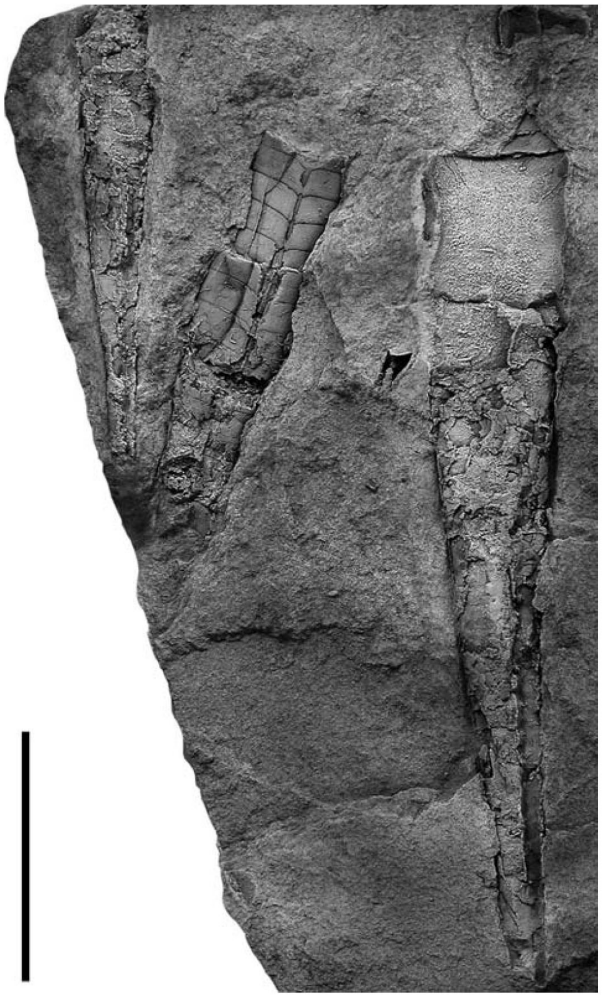

Figure 3. Aligned oriented orthoconic cephalopods from Upper Fezouata Formation, early Floian, locality Z-F24, Toumiat, near Zagora, Anti-Atlas. Specimen on the right (MHNM 15690.216a) and left (MHNM 15690.216b) are *Destombesiceras zagorense* n. sp., n. gen., specimen in the middle is *Rioceras?* sp. (MHNM 15690.216c). Scale bar 30 mm.

Faunal composition and depositional setting

The small collection (25 determinable specimens) of cephalopods from the Upper Fezouata Formation consists exclusively of longiconic orthocones. Fifty-six percent (14 specimens) are *Destombesiceras zagorense* n. gen., n. sp. This genus is a very distinctive endemic orthocone with partially expanded siphuncles and characteristic endosiphuncular deposits. The remaining cephalopods are two species of bathmocerids (3 specimens), the orthoceratoid *Polymeres* Murchison, 1839 (3 specimens), *Rioceras* Flower, 1964 (2 specimens), an unidentifiable ellesmerocerid, the orthocerid *Bactroceras* Holm, 1898 (1 specimen), and one specimen of the endocerid *Protocyptendoceras* Cecioni, 1965.

Figure 4. Internal surface of impression of *Rioceras?* sp., specimen MHNM 15690.216c, from Upper Fezouata Formation, early Floian, locality Z-F24, Toumiat, near Zagora, Anti-Atlas with overgrowth of probably ceramoporid bryozoans of the order Cystoporata (pers. comm. Andrej Ernst, Kiel). Scale bar 5 mm.

Of these genera *Destombesiceras*, the bathmocerids and the polymerids have siphuncles with thick endosiphuncular deposits, and/or strongly thickened connecting rings. Both characters can be interpreted as beneficial for rapid buoyancy change and sensitive buoyancy regulation (see e.g., Mutvei & Dunca, in press). It can be assumed that these forms lived as vertical migrants in open water environments. The longiconic shell indicates a relatively high strength against hydrostatic pressure (see discussion and review in Kröger et al. 2009). Based on the morphology of the cephalopods an open water association with relatively great water depths must be assumed. The occurrence of septal implosion in many shells is an additional evidence of a relatively deep, probably deeper neritic, depositional environment. This interpretation is in good accordance with both sedimentological data (e.g., presence of alumino-siliceous concretions), and the composition of both echinoderm and trilobite assemblages. For example, the co-occurrence of the eocrinoid *Lingulocystis* and a diverse stylophoran assemblage (comprising cornutes, kirkocystids and mitrocystitid mitrates) suggests relatively deep palaeoenvironmental conditions (mid- to outer shelf, below storm wave base), comparable to those described in the Early Ordovician of the Montagne Noire (Saint-Chinian and Landeyran formations; Vizcaïno & Lefebvre 1999; Lefebvre 2007). The trilobite assemblage (e.g., *Ampyx*, asaphids, *Basilicus*) is typical of the raphiophorid biofacies (Vidal 1998a, b). This biofacies was originally described in the Early Ordovician of Wales (Carmarthen Formation; Fortey & Owens 1978), and later documented also in the Early Ordovician of Montagne Noire (Saint-Chinian Formation; Vidal 1996). The raphiophorid biofacies is generally interpreted as typical of soft substrates in relatively deep, outer shelf palaeoenvironmental conditions. Finally, the occurrence of a rich concomitant benthic fauna (e.g., bivalves, brachiopods, gastropods, echinoderms, hyolithids, trilobites) is indicative of good living conditions at the bottom.

The cephalopod assemblage of the Upper Fezouata Formation is interpreted here mainly as (par-)autochtho-

Table 1. Diversity estimates of the cephalopod association of the Upper Fezouata Formation (early-mid Floian), Anti Atlas, Morocco compared with the St. Chinian and La Maurerie formations (late Tremadocian–early Floian), Montagne Noire, France. Note the similarity of the evenness and richness estimates in the St. Chinian and Fezouata Formation. S_{obs}, observed species richness; S_{Chao1}, Chao 1 richness estimator; $S_{rarified}$, rarified species richness with census of 18 specimens; $D_{Simpson}$, Simpson diversity index (inverted), (Magurran 2004: 115); J evenness J = H′/log (S); where H′ is the Shannon-Wiener index of the sample.

	Upper Fezouata Fm	La Maurerie Fm	St. Chinian Fm
S_{Chao1} (lower – upper 95 % confidence)	13 (9–40)	8 (7–15)	10 (10–11)
$D_{Simpson}$ (inverted)	4.78	1.77	6.23
S_{obs}	8	7	10
$S_{rarified}$ (lower – upper 95 % confidence)	8	4 (2–6)	7 (5–9)
J	0.82	0.48	0.86

nously deposited. Potentially water currents induced local concentrations and the alignment of the dead shells (locality Z-F24). The faunal deposition and general morphology of the cephalopods, as well as the depositional environment can be best compared with both the Saint-Chinian (late Tremadocian) and La Maurerie (latest Tremadocian – early Floian) formations of Montagne Noire (Kröger & Evans 2011) (Table 1).

The diversity of the La Maurerie Formation is significantly lower, but a great similarity exists in diversity estimates and evenness between the St. Chinian Formation and the Upper Fezouata Formation, which is in concordance with the interpretation of the relatively deep depositional environments in both formations. The St. Chinian Formation is interpreted as a transgressive interval deposited below storm wave base in an outer platform environment (Álvaro et al. 2003). The same interpretation was proposed for the Upper Fezouata Formation (Vidal 1998a, b).

The taxonomic composition of the cephalopod assemblage of the Upper Fezouata Formation is distinctive and differs from that of the Montagne Noire. The dominance of the endemic *Destombesiceras* and the abundance of *Bathmoceras* is remarkable. *Bactroceras*, *Rioceras* are known from both the Montagne Noire and the Anti-Atlas. These two genera appear to be a common element of several Early Ordovician Gondwanan cephalopod associations, further supporting the so-called "*Saloceras*-realm" (Kröger & Evans 2011). Potentially, *Bathmoceras australe* Teichert, 1939, which occurs in Australia and possibly in Argentina (see below), *Polymeres*, which otherwise is known from early Floian sediments of Wales (Evans 2005), and *Protocyptendoceras*, which is known now from Morocco and Argentina (Cichowolski 2009) are additional elements of the *Saloceras*-realm.

In conclusion, our data demonstrate that taxonomically highly diverse, but morphologically monotone cephalopod associations are characteristic for high palaeolatitude Early Ordovician depositional settings. These associations appear to be most diverse in relatively deep waters. Distinctive slender orthocones dominated these associations. This is in strong contrast to the morphologically more diverse cephalopod faunas of shallow palaeotropical settings.

Systematic palaeontology

Class **Cephalopoda** Cuvier, 1797
Order **Ellesmerocerida** Flower in Flower & Kummel, 1950
Family **Bathmoceratidae** Gill, 1871

Bathmoceras Barrande, 1865

Type species. Orthoceras complexum Barrande, 1856; by monotypy.

Diagnosis. Straight or very weakly curved longicones with siphuncle on convex side of conch curvature. Conch cross-section circular, moderately depressed or slightly compressed. Shell smooth or annulate, sometimes with distinctive fine growth lines. Sutures nearly straight and almost directly transverse, forming a distinct v-shaped ventral saddle. Siphuncle c. 0.2–0.25 of phragmocone diameter and marginal in position. Septal necks suborthochoanitic to cyrtochoanitic. Connecting ring thickened, with concavo-convex segments. Endosiphuncular ridges form narrow intrusions and chevron-like forward projecting lobes within the siphuncle. Apically a solid layer of endosiphuncular deposits occurs (after Furnish & Glenister 1964, K156, Mutvei in press).

Bathmoceras australe Teichert, 1939

Figures 5F, 6

1939 *Bathmoceras australe* Teichert, p. 388, pl. 24, figs 1–4.
1984 *Bathmoceras australe*. – Stait & Laurie, p. 262, table 2.
1986 *Bathmoceras australe*. – Chen & Teichert, p. 176.

Type locality and horizon. Larapintine series, from fossiliferous strata 2.20 m below top of series Horn Valley Siltstone, Horn Valley, Glen Helen, Western Macdonell Ranges, Central Australia.

Material. Specimen AA-BCBb-OI-49 from locality Z-F25b, and AA-BCBc-OI-4 from locality Z-F25c, Bou Chrebeb, near Zagora, Anti-Atlas; Upper Fezouata Formation, late early to mid Floian.

Diagnosis. Straight conchs with apical angle of c. 10°, depressed conch cross section; smooth shell. Ratio cross section width/height c. 0.75. Adult body chamber with width of c. 31 mm and with adoral constriction. Fifteen chambers occur in a distance similar to phragmocone width. Sutures almost directly transverse and nearly straight with v-shaped saddle over the venter. Siphuncle marginal in position, with a diameter 0.25 that of the phragmocone height.

Description. The specimen AA-BCBb-OI-49 consists of an internal mould of a 48 mm long fragment of a phragmocone with a width of c. 22 mm, and a high of 15 mm (ratio width/height 0.75). The angle of expansion is difficult to measure. The height of the chamber is c. 1.2 mm. The sutures are straight and form a ventral saddle. The siphuncle is marginal. On the mould of the siphuncle the distinctive chevron-like structures are preserved; they are formed by the strong endosiphuncular ridges. The ridges form a v-shaped lobe on the ventral side of the siphuncle and are oblique in lateral view. The preserved part of the siphuncle has a maximum expansion of 5.5–6.7 mm over a length of 11 mm. The siphuncle is marginal in position and relatively narrow in diameter. Ridge directed adorally over the ventral surface of the siphuncle suggesting the presence of a short septal neck.

The second specimen is a taphonomically depressed, nearly tubular fragment of the phragmocone with a length of 46 mm a diameter of 22 mm and a siphuncle diameter of 56 mm. About 13 chambers occur in a distance similar to the corresponding conch diameter.

Discussion. These specimens are assigned to *Bathmoceras australe* based on their relatively low apical angle, and their depressed conch cross section, which is very similar to that of the holotype of the species. Specimens assigned to *Bathmoceras* cf. *australe* from the middle Tremadocian Floresta Formation of Jujuy, Argentina are synonymised with *Saloceras* cf. *sericeum* Salter in Ramsay 1866 by Cichowolski & Vaccari

(2011). However, because the internal characters of the specimen described by Cichowolski & Vaccari (2011) are very poorly known and the conch shape remains speculative, the possibility remains that the specimens from Argentina represent *Bathmoceras*.

Bathmoceras was considered a characteristic Dapingian – early Darriwilian genus (see discussion in e.g., Teichert 1939; Evans 2005). Therefore, the occurrence of *Bathmoceras australe* in the Larapintine Series led Teichert (1939) to conclude that the type horizon must be early Darriwilian. Cooper (1981) suggests a late Floian – early Dapingian age for the Horn Valley Siltstone (*Oepikodus evae* to *Baltoniodus navis/triangularis* Conodont Zones; see Zhen et al. 2003). The specimen described herein extends the range of *Bathmoceras* toward the early Floian.

Stratigraphic and geographic occurrences. Floian – early Dapingian, central Australia, Morocco.

***Bathmoceras taichoutense* n. sp.**

Figure 5D

Derivation of name. Referring to the type locality of the holotype.

Holotype. Specimen ML20-269266.

Type locality and horizon. Locality Taichoute, Anti-Atlas; Upper Fezouata Formation, late early to mid Floian.

Material. Holotype only.

Diagnosis. Slender, straight to slightly curved, annulate conchs; cross section depressed with ratio conch width/height 0.8; annulations form shallow lobe at prosiphuncular side, c. 5 annulations per distance similar to conch width; sutures directly transverse narrowly spaced c. 15 per corresponding conch width; siphuncle marginal with diameter 0.25 of conch height; siphuncle with distinctive endosiphuncular ridges that form chevron-like forward projecting lobes within the siphuncle.

Description. The holotype consists of the internal mould of a fragment of phragmocone with a total length of 46 mm. The length of the preserved internal mould is 23 mm with a maximum width of 15 mm and a minimum width of 14 mm (apical angle 3°). The conch cross-section is depressed, its width is 15 mm at height 12 mm (ratio width/height 0.8). Six annulations are present at the mould, which are nearly straight and transverse, forming a very weak and wide ventral lobe. No growth lines are visible on the impression of the outer shell. The sutures are essentially straight. A v-shaped lobe exists on the venter over the position of the siphuncle. The septa are very narrowly spaced with a distance of 1 mm at a conch width of 15 mm.

The diameter of the siphuncle is 3 mm at a conch width of 15 mm, its position is marginal. The mould of the siphuncle shows distinctive v-shaped lobes on the ventral side and deep endosiphuncular ridges.

Stratigraphic and geographic occurrences. Upper Fezouata Formation, late early to mid Floian, Anti-Atlas, Morocco.

Discussion. This new species of *Bathmoceras* is characterized by its very low apical angle and its prominent annulation. Both characters are unique within the known species of *Bathmoceras*. The deep endosiphuncular lobes form the characteristic v-shaped pattern of the siphuncle of *Bathmoceras*.

Evans (2005, pl. 4, fig. 5) figured a specimen from the Whitlandian (late Floian – early Dapingian) of the Afon Ffinnant Formation of Wales, UK that he assigned to *Semiannuloceras abbeyense* Evans, 2005 which is not in line with the diagnosis of this species. It has a very narrow septal spacing and shows a sharp, v-shaped ventral saddle of the suture. Both features are a characteristic of *Bathmoceras*. The specimen figured by Evans (2005) also has a very distinctive annulation, which resembles *Bathmoceras zagorense* n. sp., described herein, and it probably represents a fragment of the latter. However, the fragmentary character of the specimen figured by Evans (2005) allows no definite species assignation.

Family **Rioceratidae** Kröger & Evans, 2011

***Rioceras* Flower, 1964**

Type species. *Rioceras nondescriptum* Flower, 1964, by original designation. From the Victorio Formation of the El Paso Group of New Mexico, southwestern United States.

Diagnosis. Small slender orthocones expanding at rates between 5° and 25°; circular to slightly compressed or depressed cross-sections; shell smooth; sutures generally straight and directly transverse; camerae shallow, depth 0.1–0.2 dorsoventral diameter of phragmocone; body-chamber simple, tubular or faintly fusiform; septal necks loxochoanitic-orthochoanitic; siphuncle marginal, with diameter of about 0.4–0.1 of dorsoventral phragmocone diameter, segments concave with moderately thick connecting rings; endosiphuncular deposits strongly reduced or not present (from Kröger & Evans, 2011).

***Rioceras* sp.**

Figure 5K

Material. Two specimens AA-BCBb-OI-38 and FSL 711706 from locality Z-F25b, Bou Chrebeb, near Zagora, Anti-Atlas, Upper Fezouata Formation, late early to mid Floian.

Description. The specimen AA-BCBb-OI-38 consists of a portion of phragmocone increasing in diameter from 33 mm to 37 mm over a distance of 55 mm (angle of expansion 4°). The conchs of both specimens are slightly crushed and are slightly depressed in cross section. No signs of ornamentation are visible in the two specimens described. The chamber distance is narrow varying between 0.15 (AA-BCBb-OI-38) and 0.17 (FSL 711706) of the corresponding diameter. The sutures are directly transverse and straight. The siphuncle is marginal with a diameter of 0.15 (AA-BCBb-OI-38) and 0.13 (FSL 711706) of the corresponding conch diameter, respectively. The connecting ring is poorly preserved in both specimens, but a generally concave outline of the siphuncular segments and orthochoanitic septal necks are visible in both fragments.

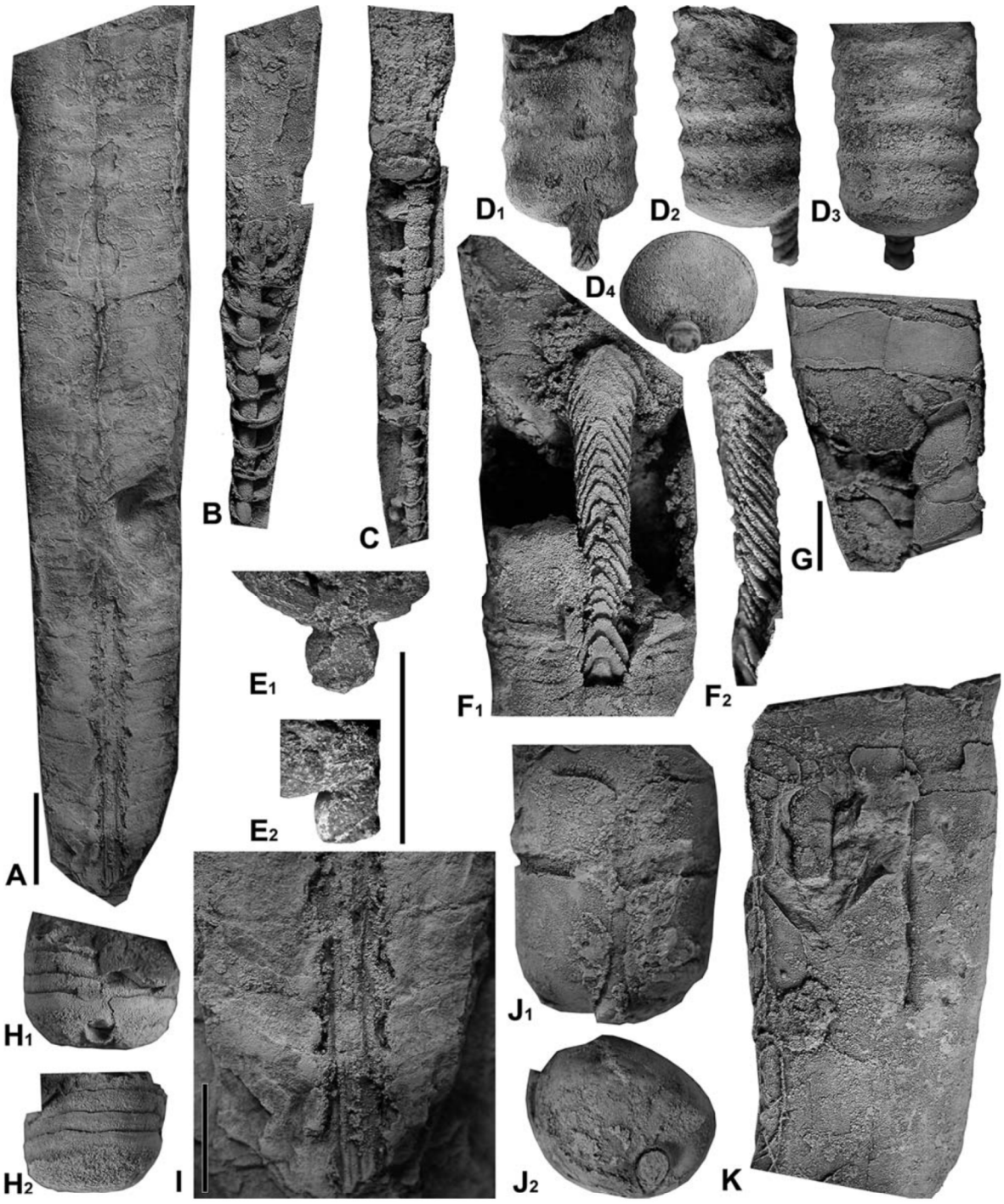

Stratigraphic and geographic occurrences. Upper Fezouata Formation, late early to mid Floian, Anti-Atlas, Morocco.

Discussion. The two specimens are assigned to *Rioceras* based on their general conch morphology and the thin empty, marginal siphuncle with concave siphuncular segments. Because details of early growth stages and detailed characters of conch cross section remain unknown in both specimens, a species-level determination is impossible.

Family, genus and species indeterminate

Figure 5H

Material. Specimen AA-BCBb-OI-39 from locality Z-F25b, Bou Chrebeb, near Zagora, Anti Atlas; Upper Fezouata Formation, early Floian.

Description. The specimen consists of a portion of phragmocone increasing in diameter from 14 mm to 15 mm over a distance of 7 mm (angle of expansion 8°). The short fragment appears to be part of a slightly curved conch; it is circular in cross section. No signs

Figure 5. Cephalopods from the Upper Fezouata Formation, late early to mid Floian, Early Ordovician of central Anti-Atlas (Zagora area). **A.** *Polymeres* sp. specimen AA-OBZ-OI-29 from locality Z-F5, Oued Beni Zoli, near Zagora, ventral view, same specimen as in I, scale bar 10 mm; **B**, **C.** *Destombesiceras zagorense* n. sp. from locality Z-F26, Toumiat, near Zagora, scale same as in A; **B.** specimen AA-BCBb-OI-42; **C.** specimen FSL 711703; **D.** *Bathmoceras taichoutense* n. sp., holotype, from Taichoute, Anti-Atlas, D_1, ventral, D_2, lateral, D_3, dorsal, D_4, adapical view, scale same as in A; **E.** *Destombesiceras zagorense* n. sp., specimen FSL 711701, external details of the mould of the siphuncle, E_1, ventral view, E_2, lateral view, note the concave connecting ring portion at the ventral side, scale bar 10 mm; **F.** *Bathmoceras australe* Teichert, 1939, specimen AA-BCBb-OI-49 from locality Z-F25b, Bou Chrebeb, near Zagora, F_1, ventral view, F_2, detail of siphuncle in lateral view, scale same as in A; **G.** *Protocyptendoceras longicameratum* n. sp., holotype, locality Z-F25b, Bou Chrebeb, near Zagora, lateral view, scale bar 10 mm; **H.** Ellesmerocerida indet., specimen AA-BCBb-OI-39 from locality Z-F25b, Bou Chrebeb, near Zagora, H_1, ventral view H_2, lateral view below, note the slightly oblique, narrowly spaced sutures, scale same as in A; **I.** *Polymeres* sp., same specimen as in A, detail of the apical part of the siphuncle, note the tubular endosiphuncular structures, scale bar 5 mm; **J.** *Bactroceras* sp., specimen FSL 711707 from locality Z-F25b, Bou Chrebeb, J_1, ventral view, J_2, adapical view, note the wide septal spacing and the tubular shape of the siphuncle, scale same as in F; **K.** *Rioceras* sp., specimen AA-BCBb-OI-38 from locality Z-F25b, Bou Chrebeb, near Zagora, near ventral view, scale same as in G.

of ornamentation are visible. Four chambers are preserved with an average distance of 0.08 of the corresponding conch diameter. The sutures are directly transverse and form shallow lateral lobes. The siphuncle is marginal with a diameter of 0.17 of the corresponding conch diameter. Traces of the connecting ring indicate a concave shape of the siphuncular segments.

Discussion. This poorly preserved small fragment has a very narrow septal spacing and a marginal siphuncle with concave siphuncular segments, both characters are indicative of the Ellesmerocerida. However, the details of the ornamentation, endosiphuncular deposits and the general outline of the conch are unknown.

Order **Discosorida** Flower in Flower & Kummel, 1950
Family **Apocrinoceratidae** Flower in Flower & Teichert, 1957

Destombesiceras n. gen.

Deriviation of name. In honor of Jacques Destombes, who mapped the whole Anti-Atlas between 1959 and 1985, established the detailed stratigraphy of the Moroccan Ordovician series, and collected the large palaeontological collections available for study.

Type species. Destombesiceras zagorense n. gen., n. sp. from the Upper Fezouata Formation, late early to mid Floian, Anti-Atlas, Morocco.

Diagnosis. Smooth, slightly curved longicones expanding at approximately 7°; sutures directly transverse, 3–4 in a distance equal to the corresponding phragmocone diameter; siphuncle marginal at concave side of conch curvature, diameter approximately 0.3 of phragmocone diameter; segments slightly concave on the side closest to the conch wall and convex on the side closest to the conch axis; septal necks suborthochoanitic with length of c. 0.3 of chamber height; parietal endosiphuncular deposits on portion directed toward conch center. In apical portions thick porous deposits on outer surface of connecting ring on side closest to conch axis.

Comparison. Destombesiceras n. gen. is unique with regard to its siphuncular shape and siphuncular wall morphology. No other orthocones with concavo-convex siphuncular segments (segments that with convex and concave sections) are known that have a similarly thickened siphuncular wall. As the calcareous thickening of the siphuncular wall extends beyond the tip of the septal neck inside the siphuncle; it must be interpreted as an endosiphuncular lining, inside the connecting ring (Fig. 6). Similar endosiphuncular deposits are known from Apocrinoceratidae such as *Glenisteroceras* Flower, 1957, and from *Bathmoceras* Holm, 1899 (Mutvei & Dunca in press, fig. 3). In contrast to *Bathmoceras* and other eothinocerids, the connecting ring is composed of siphuncular segments that are expanded, or convex facing, toward the center of the conch. This is similar to apocrinocerids in which the siphuncular segments are expanded and the septal necks are curved. Based on the connecting ring and the presence of specific endosiphuncular deposits *Destombesiceras* n. gen. is placed within the Apocrinoceratidae, herein. *Destombesiceras* n. gen. is the only known apocrinocerid with a marginal siphuncle. Its morphology is transient between eothinocerids and apocrinocerids. Because apocrinocerids are believed to be primitive discosorids (Kröger et al. 2009), it can be speculated that the latter are related to orthoconic Ellesmerocerida. Thus, the earlier notion of Flower &

Figure 6. Siphuncle of *Bathmoceras australe* Teichert, 1939, specimen AA-BCBb-OI-49 from locality Z-F25b, Bou Chrebeb, near Zagora. The endosiphuncular ridges form narrow intrusions and chevron-like forward projecting lobes within the siphuncle.

Teichert (1957: 44) that nothing suggests an ancestry of discosorids in orthoconic shells is disproved. However, this single genus *Destombesiceras* n. gen. is probably only a small section of a more diverse group of Floian Gondwanan orthocones with expanded siphuncles that probably also includes the poorly known *Belloceras* Cecioni, 1965 from Argentina. More material is needed in order to resolve the puzzle of the origin of the Discosorida and the phylogenetic relationships of the earliest Ordovician cephalopods with expanded siphuncles.

Species included. Type species only.

***Destombesiceras zagorense* n. sp.**

Figures 3, 5B, C, E, 7–10

Deriviation of name. Referring to Zagora, the largest town near the type locality.

Figure 7. Median section of details of the siphuncle of *Destombesiceras zagorense* n. gen., n. sp., holotype, Upper Fezouata Formation, early Floian, from locality Z-F25b, Bou Chrebeb, near Zagora. Note the endosiphuncular lining and the concave shape on the marginal portion of the siphuncle. Scale bar 1 mm.

Holotype. Specimen FSL 711700.

Paratypes. 9 specimens AA-BCBb-OI-42, -43, -47, FSL 711701, -702, -703, -704, -705, -708 from type locality; 3 specimens AA-TMT-OI-13, -33, -34, from locality Z-F26, Toumiat, near Zagora, Anti- Atlas; MHNM 15690.216a, -b, from locality Z-F24, N. of Toumiat, near Zagora, Anti-Atlas, all from the Upper Fezouata Formation.

Type locality and horizon. Upper Fezouata Formation, late early to mid Floian, from locality Z-F25b, Bou Chrebeb, near Zagora, Anti-Atlas, Morocco.

Diagnosis. As for genus by monotypy.

Description. The holotype is an orthoconic portion of phragmocone with a total length of 47 mm, increasing in diameter over a distance of 34 mm from 13 mm to 16 mm (angle of expansion 7°). The maximum diameter of the specimen is 15 mm. The cross section of the conch is nearly circular. Conch surface is smooth. The sutures are straight, directly transverse and distant 0.26 of the corresponding phragmocone diameter. The terminal, adoral-most septa are crowded at only 2 mm apart. The siphuncle is marginal in position with a diameter of 5 mm where the phragmocone diameter is 16 mm (or 0.31 of the phragmocone diameter). The siphuncular segments are slightly expanded into the chambers on the side closest to the axis of the conch, and concave into the lumen of the siphuncle on the side closest to the conch margin. The septal necks are suborthochoanitic with a length of c. 0.3 of the chamber height. Connecting ring relatively thick (Figs 7, 9), and simple.

Figure 8. Schematic reconstruction of details of the septa and connecting ring of *Destombesiceras zagorense* n. gen., n. sp. Note the suborthochoanitc septal necks (black), the convex shape of the connecting ring (dark grey) on side closest to the conch axis. In contrast, the side of the connecting ring closest to the conch wall is concave. Also, note the endosiphuncular lining, which extends beyond the tip of the preceding septal neck (light grey). Based on holotype, see Fig. 7.

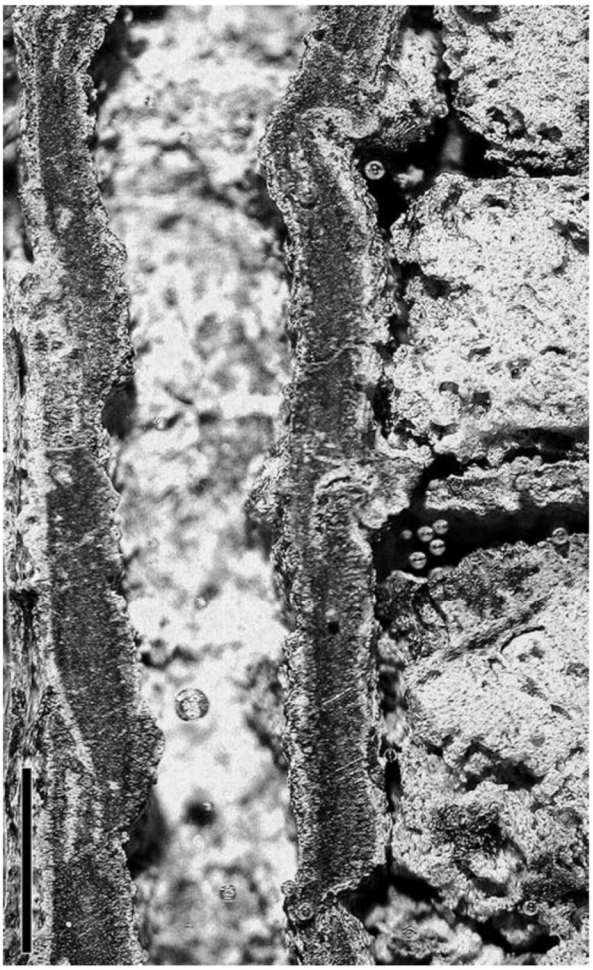

Figure 9. Median section of details of the siphuncle of *Destombesiceras zagorense* n. gen., n. sp., specimen AA-BCBb-OI-42, from locality Z-F26, Toumiat, near Zagora. Note the thick outer layer, the endosiphuncular deposit and the concave shape on the marginal portion of the siphuncle. Scale bar 1 mm.

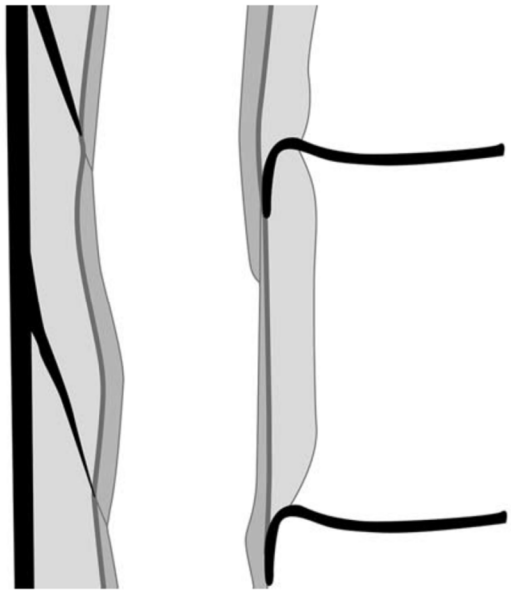

Figure 10. Schematic reconstruction of details of the septa and connecting ring of adapical part of *Destombesiceras zagorense* n. gen., n. sp. Note the suborthochoanitc septal necks (black), the convex shape of the connecting ring (dark grey) on side closest to the conch axis. In contrast, the side of the connecting ring closest to the conch wall is concave. Also, note the endosiphuncular lining, which extends beyond the tip of the preceding septal neck (medium grey) and the thick cameral deposits on the outside of the connecting ring (light grey). Based on specimen AA-BCBb-OI-42, see Fig. 9.

The endosiphuncular deposits are segmental, reaching from the tip of the septal neck toward the inner surface of the preceding one (Figs 8, 10). They are concentrated on the side of the siphuncle closest to the axis of the conch. In apical parts of the phragmocone additionally thick, porous deposits occur on the outer surface of the connecting ring (Figs 5G, 9, 10).

The angle of expansion of the five specimens measured is in the mean 7°, the chamber height of 13 measured specimens is in the mean 0.27 of the corresponding conch diameter with a clear tendency of decreasing septal distance with increasing conch diameter (Fig. 3). The maximum conch diameter of an adult specimen is 18 mm (MHNM 15690.216b). The conch of specimen FSL 711708 is slightly curved with the siphuncle at the concave side of curvature.

Stratigraphic and geographic occurrences. Upper Fezouata Formation, late early to mid Floian, Anti-Atlas, Morocco.

Subclass **Orthoceratoidea** Zhuravleva, 1994
Order **Orthocerida** Kuhn, 1940
Family **Baltoceratidae** Kobayashi, 1935

Bactroceras Holm, 1898

Type species. *Bactroceras avus* Holm, 1898, subsequent designation by Glenister (1952, p. 90).

Diagnosis. Slender, smooth orthocones with nearly circular cross sections; camerae generally deep; sutures straight and directly transverse; siphuncle marginal or slightly removed from conch margin, with diameter about 0.1 that of phragmocone, septal necks orthochoanitic, siphuncular segments tubular to slightly inflated with thin connecting rings; endosiphuncular deposits unknown (compiled from Holm, 1898; Evans 2005).

Bactroceras sp.

Figures 5J, 11

Material. Specimen FSL 711707 from locality Z-F25b, Bou Chrebeb, near Zagora, Anti- Atlas, Upper Fezouata Formation, late early to mid Floian.

Description. The specimen consists of a portion of two chambers of a phragmocone with a diameter of 23 mm. The cross section is nearly circular. No signs of ornamentation are visible. The two chambers have a height of 9 mm, respectively (0.35 of the corresponding diameter). The sutures are directly transverse and straight.

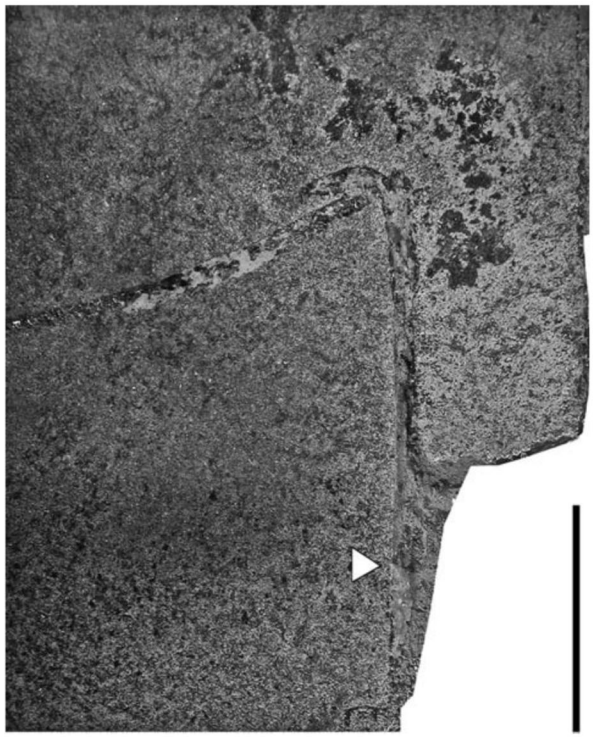

Figure 11. Median section of details of the siphuncle of *Bactroceras* sp. specimen FSL 711707 from locality Z-F25b, Bou Chrebeb, near Zagora, Anti-Atlas, Upper Fezouata Formation, late early to mid Floian. Note the tubular siphuncle and the orthochoanitic septal neck. Arrow marks the tip of the septal neck. Scale bar 5 mm.

The siphuncle is marginal with a diameter of 3 mm (0.12 of the corresponding conch cross section). The connecting ring is tubular and the septal necks are orthochoanitic with a length of 0.15 of the corresponding septal distance.

Stratigraphic and geographic occurrences. Upper Fezouata Formation, late early to mid Floian, Anti-Atlas, Morocco.

Discussion. The general conch morphology and the thin marginal, tubular siphuncle, and the wide septal spacing justify an assignment to *Bactroceras*. The relative siphuncular diameter and the relative septal distance of the specimen described above both fall within the variability of *Bactroceras angustisiphonatum* (Rüdiger, 1891), but because details of the ornamentation and conch expansion are not known, a species-level determination is impossible.

Order **Dissidocerida** Zhuravleva, 1964
Family **Polymeridae** Evans, 2005

Polymeres Murchison, 1839

Type species. *Polymeres demetarum* Murchison, 1839, by original designation.

Diagnosis. Smooth orthocones with low moderate angle of expansion of c. 5°; distance of sutures in juvenile conch portions c. 0.35 of corresponding conch cross section to 0.15 in later growth stages; sutures straight and directly transverse with deep ventral lobe over siphuncle; siphuncle marginal with diameter 0.3–0.5 of corresponding phragmocone cross-section; septal necks orthochoanitic; siphuncular segments tubular or slightly expanded with thin connecting rings; endosiphuncular deposits complex, consisting of combination of lining, annuli and a rod; episeptal hyposeptal and mural cameral deposits present, but limited to venter (compiled from Evans 2005).

Polymeres sp.

Figures 5A, I

Material. Three specimens; AA-OBZ-OI-29 from locality Z-F5, Oued Beni Zoli, near Zagora, Anti-Atlas, AA-BCBb-OI-46 from locality Z-F25b, Bou Chrebeb, near Zagora, Anti-Atlas, AA-JBZ-OI-73 from locality Z-F0, North of Beni Zoli, near Zagora, Anti- Atlas; all from Upper Fezouata Formation, late early to mid Floian.

Description. The specimen AA-OBZ-OI-29 consists of a portion of phragmocone increasing in diameter from 16 mm to 21 mm over a distance of 95 mm (angle of expansion 3°). The rate of expansion in AA-JBZ-OI-73 is slightly higher with 5°. Specimen AA-BCBb-OI-46 is essentially tubular with a diameter of c. 26 mm. All three specimens are smooth and straight, without traces of ornamentation. The chamber distances vary between 0.3 of the corresponding diameter in the smallest conch portions (c. 6 mm in diameter in specimen AA-JBZ-OI-73) and 0.13 in the largest portions (AA-BCBb-OI-46). The sutures are straight and transverse, the portions over the siphuncle are not preserved. The siphuncle is marginal in position, with a diameter of c. 0.25 of that of the phragmocone. In the apical parts of specimen AA-OBZ-OI-29 longitudinal structures in the marginal portions of exfoliated parts of the siphuncle indicate an endosiphuncular lining. The shape of the siphuncular segments is not known.

Stratigraphic and geographic occurrences. Upper Fezouata Formation, late early to mid Floian, Anti-Atlas, Morocco.

Discussion. All three specimens are poorly and fragmentarily preserved. The specimens resemble each other with respect to the low angle of expansion, narrow spacing of the septa, and the marginal siphuncle. Details of the siphuncle are not preserved except in specimen AA-OBZ-OI-29, where the shape of the siphuncular segments are not determinable. However, the tubular structures in the apical parts of the siphuncle of specimen AA-OBZ-OI-29 can be interpreted as remnants of a continuous endosiphuncular lining or a rod (Fig. 5I) similar to that of *Polymeres demetarum* Murchison, 1839 (see Evans 2005) from the early Floian deposits of Wales. The latter differs from the Moroccan specimens only in having a wider siphuncle. More, and better preserved material is needed for a definite species determination of the three specimens.

Order **Endocerida** Teichert, 1933
Family **Protocameroceratidae** Kobayashi, 1937

Protocyptendoceras Cecioni, 1965

Type species. Protocyptendoceras fuenzalidae Cecioni, 1965. By original designation. Floian stage, Early Ordovician, Sepulturas Formation, La Ciénaga, Jujuy Province, Argentina.

Diagnosis. Slender orthocones with circular or subcircular section. Sutures almost straight, directly transverse with narrow ventral lobe. Moderate to large circular siphuncle in contact with ventral wall of phragmocone. Septal necks subholochoanitic and connecting rings thick. Endocones generally droplet shaped in cross section, but sometimes simply rounded (after Cichowolski 2009).

Protocyptendoceras longicameratum n. sp.

Figure 5G

Derivation of name. Referring to the septal distance, which is wide compared with the genus type species.

Holotype. Specimen AA-BCBb-OI-40

Diagnosis. Protocyptendoceras with comparatively long chamber distance of 0.38 of the corresponding diameter and narrow siphuncle of c. 0.39 of the corresponding conch diameter.

Type locality and horizon. Locality Z-F25b, Bou Chrebeb, near Zagora, Anti-Atlas, Upper Fezouata Formation, late early to mid Floian.

Material. Type specimen only.

Description. The specimen consists of a portion of a straight phragmocone increasing in diameter from 18 mm to 26 mm over a distance of 60 mm (angle of expansion 7.5°). The fragment is diagenetically compressed. No signs of ornamentation are visible. Eight chambers are preserved with an average distance of 0.38 of the corresponding diameter. The sutures are straight and laterally slightly inclined toward the apex at the ventral and toward the aperture at the dorsal side. The siphuncle is marginal with a diameter of 0.39 of the corresponding conch diameter. The septal necks are subholochoanitic and slightly convex, forming droplet shaped siphuncular segments. The preserved part of the siphuncle displays no signs of endosiphuncular deposits.

Discussion. The position and shape of the siphuncle and septal neck indicate that this specimen must be assigned to *Protocyptendoceras.* Prior to this study, this genus was only known from its type specimen from the Sepulturas Formation from Argentina. *Protocyptendoceras longicameratum* n. sp. differs from the type species in having a clearly more widely spaced septa and a slightly narrower siphuncle.

Acknowledgements

The authors are grateful to Kathleen Histon (Modena, Italy) and David Evans (Peterborough, UK) for their constructive comments on the MS, as well as to Roland and Véronique Reboul (Saint-Chinian) for their help in the field, to Jacques Destombes (Pessac) for providing many useful informations on local geology and stratigraphy, to Joe Botting (Nanjing), Juan-Carlos Gutiérrez-Marco (Madrid), Radvan Horny (Prague), Peter Van Roy (Ghent), Muriel Vidal (Brest), and Daniel Vizcaïno (Carcassonne) for their help in the identification of the associated fauna, to Didier Berthet (Musée des Confluences, Lyon), Khadija El Hariri (FST Marrakech), Anne Médard and Sylvie Pichard (MHN Marseille), and Abel Prieur (University Lyon 1) for access to the specimens deposited in their collections. This paper is a contribution to the project of cooperation n°22593 between the universities of Marrakech and Lyon 1, and also to the team "Vie Primitive" of the UMR CNRS 5276.

References

Álvaro, J. J., González-Gómez, C. & Vizcaïno, D. 2003. Paleogeographic patterns of the Cambrian – Ordovician transition in the southern Montagne Noire (France): preliminary results. – Bulletin de la Société Géologique de France 174: 217–225

Barrande, J. 1856. Bemerkungen über einige neue Fossilien aus der Umgebung von Rokitzan im silurischen Becken von Mittel-Böhmen. – Jahrbuch der kaiserlich-königlichen geologischen Reichsanstalt 7: 355–360.

Barrande, J. 1865. Système Silurien du centre de la Bohême, I.ère partie, Recherches Paléontologiques, vol. II, Classe de Mollusques, Ordre des Céphalopodes. Prague: 804.

Barrande, J. 1867. Cephalopodes. Charles Bellman, Prague and Paris.

Bigot, A. & Dubois, J. 1931. Sur la présence de l'Ordovicien dans l'Anti-Atlas marocain. – Comptes-rendus de l'Académie des Sciences 193: 288–289.

Botting, J. P. 2007. 'Cambrian' demosponges in the Ordovician of Morocco: insights into the early evolutionary history of sponges. – Geobios 40: 737–748.

Bruthansová, J. & Kraft, P. 2003. Pellets independent of or associated with Bohemian Ordovician body fossils. – Acta Palaeontologica Polonica 48: 437–445.

Cecioni, G. 1965. Contribucion al conocimiento de los Nautiloideo-seopaleozoicos Argentinos. Parte II: Robsonoceratidae, Ellesmeroceratidae, Proterocameroceratidae, Baltoceratidae. – Boletin del Museo Nacional de Historia Natural 29: 1–24.

Chauvel, J. 1966. Echinodermes de l'Ordovicien du Maroc. Editions du CNRS, Cahiers de Paléontologie, Paris.

Chauvel, J. 1969. Les échinodermes macrocystellides de l'Anti-Atlas marocain. – Bulletin de la Société géologique et minéralogique de Bretagne 1: 21–32.

Chauvel, J. 1971a. *Rhopalocystis* Ubaghs: un échinoderme éocrinoïde du Trémadocien de l'Anti-Atlas marocain. – Mémoires du Bureau de Recherches Géologiques et Minières 73: 43–49.

Chauvel, J. 1971b. Les échinodermes carpoïdes du Paléozoïque inférieur marocain. Notes du Service géologique du Maroc 31: 49–60.

Chen, J.-y. & Teichert, C. 1986. The Ordovician cephalopod suborder Cyrtocerinina (order Ellesmerocerida). – Palaeontologia Cathayana 3: 145–229.

Choubert, G. 1952. Histoire géologique du domaine de l'Anti-Atlas. – Notes et Mémoires du Service géologique du Maroc 100: 77–194.

Choubert, G., Termier, H. & Termier, G. 1953. Présence du genre *Mimocystites* Barrande dans l'Ordovicien du Maroc. – Notes et Mémoires du Service géologique du Maroc 117: 137–143.

Cichowolski, M. 2009. A review of the endocerid cephalopod *Protocyptendoceras* from the Floian (Early Ordovician) of the Eastern Cordillera, Argentina. – Acta Palaeontologica Polonica 54: 99–109.

Cichowolski, M. & Vaccari, N. E. 2011. The oldest record of Eothinoceratidae (Ellesmerocerida, Nautiloidea): Middle Tremadocian of the Cordillera Oriental, NW Argentina. – Geological Journal 46: 42–51.

Colwell, R. K. 2009. EstimateS: Statistical estimation of species richness and shared species from samples. Version 8.2. User's Guide and application published at: http://purl.oclc.org/estimates.

Cooper, B. J. 1981. Early Ordovician conodonts from the Horn Valley Siltstone, Central Australia. – Palaeontology 24: 147–183.

Cuvier, G. 1797. Tableau élémentaire de l'histoire naturelle des animaux. no publisher recorded,

Destombes, J. 1962. Stratigraphie et paléogéographie de l'Ordovicien de l'Anti-Atlas (Maroc), un essai de synthèse. – Bulletin de la Société géologique de France 4: 453–460.

Destombes, J. 1971. L'Ordovicien au Maroc. Essai de synthèse stratigraphique. – Mémoires du Bureau de Recherches Géologiques et Minières 73: 237–263.

Destombes, J. 1972. Les trilobites du sous-ordre des Phacopina de l'Ordovicien de l'Anti-Atlas (Maroc). – Notes et Mémoires du Service géologique du Maroc 240: 1–74.

Destombes, J. 2006a. Carte géologique au 1/200000 de l' Anti-Atlas marocain. Paléozoïque inférieur. Cambrien moyen et supérieur-Ordovicien- Base du Silurien. Sommaire général sur les Mémoires explicatifs des cartes géologiques au 1/200000 de l' Anti-Atlas marocain. – Notes & Mémoires du Service géologique du Maroc 515: 1–149.

Destombes, J. 2006b. Carte géologique au 1/200000 de l'Anti-Atlas marocain. Paléozoïque inférieur: Cambrien moyen et supérieur – Ordovicien – base du Silurien. Feuille Zagora-Coude du Drâ. – Mémoire explicatif. Notes et Mémoires du Service géologique du Maroc 273: 1–5.

Destombes, J. & Babin, C. 1990. Les mollusques bivalves et rostroconches ordoviciens de l'Anti-Atlas marocain: intérêt paléogéographique de leur inventaire. – Géologie méditerranéenne 17: 243–261.

Destombes, J. & Willefert, S. 1959. Sur la présence de *Dictyonema* dans le Trémadoc de l'Anti-Atlas (Maroc). – Comptes-rendus de l'Académie des Sciences 249: 1246–1247.

Destombes, J., Hollard, H. & Willefert, S. 1985. Lower Palaeozoic rocks of Morocco. *In* Holland, C. H. (ed.). Lower Palaeozoic Rocks of the World. John Wiley & Sons, New York: pp. 91–336.

Deunff, J. 1968a. *Arbusculidium*, genre nouveau d'acritarche du Trémadocien marocain. – Comptes-rendus sommaires de la Société géologique de France 3: 101–102.

Deunff, J. 1968b. Sur une forme nouvelle d'acritarche possédant une ouverture polaire (*Veryhachium miloni*) et sur la présence d'une colonie de Veryhachium dans le Trémadocien marocain. – Comptes-rendus de l'Académie des Sciences 267: 46–49.

Donovan, S. K. & Savill, J. J. 1988. *Ramseyocrinus* (Crinoidea) from the Arenig of Morocco. – Journal of Paleontology 62: 283–285.

Elaouad-Debbaj, Z. 1984. Acritarches et chitinozoaires de l'Arenig-Llanvirn de l'Anti-Atlas (Maroc). – Revue de Paléobotanique et de Palynologie 43: 67–88.

Elaouad-Debbaj, Z. 1988. Acritarches et chitinozoaires du Trémadoc de l'Anti-Atlas central (Maroc). – Revue de Micropaléontologie 31: 85–128.

Evans, D. H. 2005. The Lower and Middle Ordovician cephalopod faunas of England and Wales. – Monograph of the Palaeontographical Society 628: 1–81.

Flower, R. H. 1964. The nautiloid order Ellesmeroceratida (Cephalopoda). – New Mexico Institute of Mining and Technology, State Bureau of Mines and Mineral Resources, Memoir 12: 1–164.

Flower, R. H. & Kummel, B. 1950. A classification of the Nautiloidea. – Journal of Paleontology 24: 604–616.

Flower, R. H. & Teichert, C. 1957. The cephalopod order Discosorida. – University of Kansas Paleontological Contributions, Art. 21 (Mollusca, Art. 6): 1–144.

Fortey, R. A. & Owens, R. M. 1978. Early Ordovician (Arenig) stratigraphy and faunas of the Camarthen district, south-west Wales. – Bulletin of the British Museum (Natural History), Geology 30: 225–294.

Furnish, W. M. & Glenister, B. F. 1964. Nautiloidea-Tarphycerida. *In* Teichert, C. (ed.). Geological Society of America and the University of Kansas Press, Boulder, Colorado: pp. K343–K368.

Gill, T. 1871. Arrangement of the families of the Mollusca. – Smithsonian Miscellaneous Collections 227: 1–49.

Glenister, B. F. 1952. Ordovician nautiloids from New South Wales. – Australian Journal of Science 15: 89–91.

Gnoli, M. & Pillola, G. L. 2002. The oldest nautiloid cephalopod of Sardinia: *Cameroceras* cf. *vertebrale* (Eichwald, 1860) from the Arenig (Early Ordovician) of Tacconis (South East Sardinia) and remarks on the associated biota. – Neues Jahrbuch für Geologie und Paläontologie, Monatshefte 2002 (1) 1: 19–26.

Gutiérrez-Marco, J. C., Destombes, J., Rabano, I., Acenolaza, G. F., Sarmiento, G. N. & San Jose, M. A. 2003. El Ordovícico Medio del Anti-Atlas marroquí: paleobiodiversidad, actualización bioestratigráfica y correlación. – Geobios 36: 151–177.

Havlicek, V. 1971. Brachiopodes de l'Ordovicien du Maroc. – Notes et Mémoires du Service géologique du Maroc 230: 1–135.

Hewitt, R. A. & Westermann, G. E. G. 1996. Post-mortem behaviour of Early Paleozoic nautiloids and paleobathymetry. – Paläontologische Zeitschrift 70: 405–424.

Holm, G. 1898. Palaeontologiska notiser II: Om ett par Bactrites-liknade Untersiluriska Orthocera-former. – Geologiska Freningens i Stockholm Frhandingar 20: 354–360.

Holm, G. 1899. Palaeontologiska notiser. Om ett par *Bactrites*-liknande Untersiluriska Orthocer-former. – Geologiska Föreningens i Stockholm Förhandlingar 20: 354–360.

Horny, R. J. 1997. Ordovician Tergomya and Gastropoda (Mollusca) of the Anti-Atlas (Morocco). – Sbornik Narodniho Muzea v Praze 53: 37–78.

Kobayashi, T. 1935. On the phylogeny of the primitive nautiloids with description of *Plectronoceras liaotungense* and *Iddingsia*? *shantungensis*, new species. – Japanese Journal of Geology and Geography 21: 17–26.

Kobayashi, T. 1937. Contribution to the study of the apical end of the Ordovician nautiloid. – Japanese Journal of Geology and Geography 14: 1–21.

Kröger, B. & Evans, D. H. 2011. Review and palaeoecological analysis of the late Tremadocian-early Floian (Early Ordovician) cephalopod fauna of the Montagne Noire, France. – Fossil Record 14 (1): 5–34.

Kröger, B., Servais, T & Zhang Yunbai. 2009. The origin and initial rise of pelagic cephalopods in the Ordovician. – PLoS ONE 4 (9): e7262. doi:10.1371/journal.pone.0007262.

Kuhn, O. 1940. Paläozoologie in Tabellen. Fischer Verlag, Jena.

Lefebvre, B. 2007. Early Palaeozoic palaeobiogeography and palaeoecology of stylophoran echinoderms. – Palaeogeography, Palaeoclimatology, Palaeoecology 245: 156–199.

Lefebvre, B. & Botting, J. P. 2007. First report of the mitrate *Peltocystis cornuta* Thoral: (Echinodermata, Stylophora) in the Lower Ordovician of central Anti-Atlas (Morocco). – Annales de Paléontologie 93: 183–198.

Loi, A. & Dabard, M. P. 1999. Stratigraphic significance of siliceous-argilaceous nodules in Ordovician formations of the Armorican massif (France) and Sardinia (Italy). – Acta Universitatis Carolinae, Geologica 43: 89–92.

Loi, A. & Dabard, M. P. 2002. Controls of sea-level fluctuations on the formation of Ordovician siliceous nodules in terrigeneous offshore environments. – Sedimentary Geology 153: 65–84.

Magurran, A. E. 2004. Measuring biological diversity. Blackwell, Malden, Mass.; Oxford.

Marek, J., Weber, B., Schönian, F., Egenhoff, S. O. & Erdtmann, D. 2000. Arenig cephalopods from Bolivia. – Palaeontology Down Under 2000 Geological Society of Australia, Abstracts, 2000: 56.

Marek, L. 1983. The Ordovician hyoliths of Anti-Atlas (Morocco). Sbornik Narodniho Muzea v Praze 39: 1–36.

Mergl, M. 1981. The genus *Orbithele* (Brachiopoda, Inarticulata) from the Lower Ordovician of Bohemia and Morocco. Vestnik Ustredniho ustavu geologickeho 56: 287–292.

Murchison, R. I. 1839. The Silurian System founded on geological researches in the counties of Salop, Hereford, Radnor, Montgomery, Caermarthen, Brecon, Pembroke, Monmouth, Gloucester, Worcester, and Stafford: with descriptions of the coalfields and overlying formations. John Murray, London.

Mutvei, H. in press. Shell structure and buoyancy regulation in the Ordovician nautiloid Bathmoceras (Cephalopoda) elucidating nautiloid evolution. Palaeontology.

Noailles, F., Lefebvre, B., Guensburg, T. E., Hunter, A. W., Nardin, E., Sumrall, C. D. & Zamora, S. 2010. New echinoderm-Lagerstätten from the Lower Ordovician of central Anti-Atlas (Zagora area, Morocco): a Gondwanan perspective of the Great Ordovician Biodiversification Event. *In* M. Reich, J. R., Roden, V. & Thuy, B. (eds). Echinoderm Research 2010. Universitätsverlag Göttingen, Göttingen: 77–78.

Oksanen, J., Kindt, R., Legendre, P., O'Hara, B., Simpson, G. L., Solymos, P., Stevens, M. H. M. & Wagner, H. 2009. vegan: Community Ecology Package. http://CRAN.R-project.org/package=vegan.

Ramsay, A. C. 1866. The Geology of North Wales, with an appendix on the fossils by J. W. Salter. – Memoir of the Geological Survey of Great Britain 3: 1–381.

Rüdiger, H. 1891. Ueber die Silur-Cephalopoden aus den Mecklenburgischen Diluvialgeschieben. – Archiv des Vereins der Freunde der Naturgeschichte Mecklenburg 1891: 1–86.

Servais, T., Owen, A. W., Harper, D. A. T., Kröger, B. & Munnecke, A. 2010. The Great Ordovician Biodiversification Event (GOBE): The palaeoecological dimension. – Palaeogeography, Palaeoclimatology, Palaeoecology 294: 99–119.

Stait, B. & Laurie, J. 1984. Ordovician nautiloids of central Australia, with a revision of Madiganella Teichert & Glenister. – BMR Journal of the Australian Geology and Geophysics 9: 261–266.

Sumrall, C. D. & Zamora, S. 2011. Ordovician edrioasteroids from Morocco: faunal exchanges across the Rheic Ocean. Journal of Systematic Palaeontology 9: 425–454.

Teichert, C. 1933. Der Bau der actinoceroiden Cephalopoden. – Palaeontographica A 77: 111–230.

Teichert, C. 1939. Nautiloid Cephalopods from the Devonian of Western Australia. – Journal of the Royal Society of West Australia 25: 103–121.

Termier, G. & Termier, H. 1950. Paléontologie marocaine. Tome 2. Invertébrés de l'Ere Primaire. Fascicule 3 – Mollusques. Hermann & Cie, Paris.

Ubaghs, G. 1963. *Rhopalocystis destombesi* n. g., n. sp. éocrinoïde de l'Ordovicien inférieur (Trémadocien supérieur) du Sud marocain. – Notes du Service géologique du Maroc 172: 25–45.

Van Roy, P. 2006. Non-trilobite arthropod from the Ordovician of Morocco. Unpublished PhD thesis, Ghent University.

Van Roy, P. & Briggs, D. E. G. 2011. A giant Ordovician anomalocaridid. – Nature 473: 510–513.

Van Roy, P. & Tetlie, O. E. 2006. A spinose appendage fragment of a problematic arthropod from the Early Ordovician of Morocco. – Acta Palaeontologica Polonica 51: 239–246.

Van Roy, P., Orr, P. J., Botting, J. P., Muir, L. A., Vinther, J., Lefebvre, B., El Hariri, K. & Briggs, D. E. G. 2010. Ordovician faunas of Burgess Shale type. Nature 465: 215–218.

Vidal, M. 1996. Quelques Asaphidae (Trilobita) de la Formation de Saint-Chinian, Ordovicien inférieur, Montagne Noire (France): systématique et paléoenvironnements. – Geobios 29: 725–744.

Vidal, M. 1998a. Le modèle des biofaciès à trilobites: un test dans l'Ordovicien inférieur de l'Anti-Atlas, Maroc. – Comptes-rendus de l'Académie des Sciences 327: 327–333.

Vidal, M. 1998b. Trilobites (Asaphidae et Raphiophoridae) de l'Ordovicien inférieur de l'Anti-Atlas, Maroc. – Palaeontographica Abteilung A 251: 39–77.

Vinther, J., Van Roy, P. & Briggs, D. E. G. 2008. Machaeridians are Palaeozoic armoured annelids. – Nature 451: 185–188.

Vizcaïno, D. & Lefebvre, L. B. 1999. Les échinodermes du Paléozoïque inférieur de Montagne Noire: biostratigraphie et paléodiversité. – Geobios 32: 353–364.

Zhen, Y.-Y., Percival, I. G. & Webby, B. D. 2003. Early Ordovician conodonts from far western New South Wales, Australia. – Records of the Australian Museum 55 (2) 2: 169–220.

Zhuravleva, F. A. 1964. New Ordovician and Silurian cephalopods from the Siberian platform. – Paleontological Journal 1964: 87–100.

Zhuravleva, F. A. 1994. The order Dissidocerida (Cephalopoda). – Paleontological Journal 28: 115–132.

STOP 4.5 – Trilobite Preparation Workshop near Alnif

https://moroccofamilyvacation.com/alnif-morocco/

Welcome to Alnif Morocco, a hidden gem in southeastern Morocco where the vast desert meets the echoes of ancient seas. Known as the "fossil capital of Morocco", Alnif draws geology enthusiasts, adventure travelers, and cultural explorers eager to uncover its rich heritage and breathtaking landscapes. From trilobite fossils dating back hundreds of millions of years to vibrant Berber markets and authentic Moroccan cuisine, Alnif offers a unique blend of history, culture, and natural beauty.

Located along the N12 highway connecting Zagora to Rissani, Alnif Morocco is a crossroads of past and present. Visitors can explore fossil-rich desert terrains, trek through rolling dunes, and experience local Berber traditions. This guide will provide everything you need to know from practical travel tips and top attractions to cultural insights and day trips ensuring your journey to Alnif is unforgettable.

Why Visit Alnif Morocco?

What Makes Alnif So Special

Fossil Heritage and Trilobite Beds

Alnif is globally renowned for its fossil deposits, particularly trilobites, which date back to the Devonian period. Fossil hunters and amateur geologists can explore these ancient terrains with guided tours, making it a must-visit for science enthusiasts.

Berber Traditions and Culture

Beyond fossils, Alnif offers a glimpse into authentic Berber life, from traditional music to vibrant markets and artisan workshops. Visitors can engage with locals, learn about customs, and even participate in cultural festivals.

Where Is Alnif Morocco? Geography & Setting

Location within Drâa-Tafilalet Province

Alnif lies in southeastern Morocco, nestled between the Sahara Desert and the Anti-Atlas mountains. Its strategic location makes it an ideal stop for travelers exploring the Moroccan desert circuit.

History of Alnif Morocco

Ancient Geological History

Millions of years ago, Alnif was part of a prehistoric sea, which explains its abundant fossil deposits. Geologists frequently visit the area to study trilobites and Devonian-era formations.

Human Settlement and Berber Culture

Berber tribes have inhabited the region for centuries, maintaining traditions and craftsmanship. Alnif's history blends natural wonders with the resilience and cultural richness of its people.

Top Attractions in Alnif Morocco

Fossil Sites & Geological Wonders

Explore the region's fossil-rich hills, guided by local experts who can identify rare trilobites and other ancient marine life.

Ihmadi Trilobites Centre

This small museum showcases fossils collected locally, providing insights into Morocco's prehistoric past.

Weekly Markets & Souks

Alnif's Sunday market is a lively spot for local crafts, spices, and Berber textiles.

Local Artisan Workshops

Witness artisans crafting traditional pottery, jewelry, and carpets, supporting the local economy while gaining cultural insights.

Day 5: Tuesday, March 10th, 2026 – Around Alnif – Trilobites of the Maider Basin – Mharch Desert Oasis

STOP 5.1 – Cambrian Trilobite Fossils
STOP 5.2 – Ordovician Trilobite Fossils
STOP 5.3 – Devonian Trilobite Fossils
STOP 5.4 – Desert Oasis in Mharch

Hotel Information:
Auberge Camping Oasis El Mharech
QC6P+4J6, Sidi Ali, Morocco

From our Guide:

After breakfast, we begin the day exploring the Anti-Atlas Mountains north of Alnif, visiting active fossil sites where large yellow Middle Cambrian trilobites are mined. These include impressive Paradoxides and Cambropellas, often found as complete specimens. We then continue to Jebel Tiskaouine, one of the most famous trilobite-mining areas in Morocco. Although commonly sold as "Calymene" trilobites, the fossils from this region actually belong to the genera Neseuretus, Colpocoryphe, and Flexicalymene, dating back to the Ordovician period (Sandbian–Katian). Later, we head toward Atchana, meaning "the dry place." Here, we meet local fossil miners working the Devonian Ihandar Formation, renowned for spectacular specimens such as Dicranurus monstrosus and Paralejurus spatuliformis. In the afternoon, we travel further south off-road through the wild landscapes of the Maider Basin, often called the "Lost World" of trilobites. By evening, we arrive at the remote desert oasis of Mharch, where we spend the night in a traditional mud-brick hotel. Though simple, the rooms are en suite, and the isolation makes it a perfect spot for stargazing beneath a spectacular night sky.

Introduction to the Maider Basin

The following is taken from: Kaufmann, B., 1998, Facies, stratigraphy and diagenesis of Middle Devonian reef- and mud-mounds in the Mader (eastern Anti-Atlas, Morocco). Acta Geologica Polonica, vol. 48, no. 1, pp. 43-106.

GEOLOGICAL SETTING AND HISTORY

The Anti-Atlas of Morocco is a NE-SW trending, about 700 km long and up to 200 km wide Variscan anticlinorium at the northern margin of the Sahara Craton (PIQUE & MICHARD 1989) (Text-fig. 1). It is separated from the highly deformed Mesozoic rocks in the north by the South-Atlas Fault. The Precambrian crystalline core of the Anti-Atlas is exposed in its northern central part and consists of granitic plutons, which are covered by sedimentary and volcanic rocks of Late Precambrian age. Mainly towards the south, the basement is overlain by a weakly folded Palaeozoic sequence, which continues in that direction towards the rather undeformed Tindouf Basin (Text-fig. 1). An almost complete succession of Palaeozoic sediments, ranging from the Lower Cambrian to the Lower Carboniferous was deposited along the NE-SW trending passive continental margin of northwestern Gondwana (Sahara Craton). Its thickness exceeds 10 km in the central Anti-Atlas and the northern flank of the Tindouf Basin, strongly decreasing towards the east (DESTOMBES & al. 1985).

In the eastern Anti-Atlas (regions of the Tafilalt and the Mader), the Palaeozoic succession generally crops out in W-E- and NW-SE trending synclines. The easternmost outcrops of the Precambrian basement of the Anti-Atlas are located at Jebel Sarhro and Jebel Ougnate in the northwestern and northern Mader area respectively (Text-fig. 2). The folded Palaeozoic succession of the eastern Anti-Atlas is overlain by undeformed, flat-lying Upper Cretaceous deposits of the Kem-Kem towards the south and Tertiary deposits of the Hamada du Guir towards the east. Palaeozoic rocks reappear in Algeria about 100 km southeast of the Tafilalt in the NW-SE-trending Ougarta fold belt and 50 km to the east in the Carboniferous Béchar Basin (Text-fig. 1).

The oldest sedimentary rocks in the eastern Anti-Atlas are terrestrial clastic deposits (conglomerates, sandstones and shales) of latest Precambrian age with considerable intercalations of calcalkaline volcanic rocks (JEANNETTE & TISSERANT 1977). The Lower to Middle Cambrian consists mainly of marine silt- and sandstones with a maximum thickness of about 700 m (eastern end of Jebel Sarhro), extremely diminishing towards the east (DESTOMBES & al. 1985). Volcanic activity as indicated by basalts, dolerites, volcanic breccias and tuffs is common in the Middle Cambrian at Jebel Ougnate (DESTOMBES & al. 1985). Upper Cambrian deposits have not been recognized in the eastern Anti-Atlas so far (Carte Géologique du Maroc, 1:200.000, sheets 'Tafilalt-Taouz' and 'Todrha-Ma'der'). The lower part of the Ordovician (Tremadoc to Llanvirn) consists of 300-800 m thick marine shales with graptolites, trilobites, brachiopods and echinoderms (DESTOMBES & al. 1985). The upper Ordovician (Llandeilo to Ashgill) consists of 300-600 m thick sandstones which, in the upper part (upper Asghillian), are supposed to be of glacial origin (DEYNOUX 1985). A post-glacial transgression with graptolite shales and siltstones marks the lower Silurian. They are followed by Ludlowian Orthoceras limestones, which are the first significant carbonate deposits in the Palaeozoic sequence of the eastern Anti-Atlas. Fine-grained sandstones and Scyphocrinites limestones represent the uppermost Silurian. Thickness of Silurian sediments in the eastern Anti-Atlas decreases from 500 m in the Mader area to 150 m in the northern Tafilalt (HOLLARD 1970).

Devonian sediments are exposed over an area of about 20000 km2 (Text-fig. 2). They were deposited in an extensive epicontinental sea, which changed its palaeogeographical position during the Devonian northward drift of Gondwana from about 45° to 30°S (SCOTESE & MCKERROW 1990). The Lower Devonian consists predominantly of shales interbedded with cephalopod limestones. In the higher part of the Lower Devonian and in the transition to the Middle Devonian, marls and nodular cephalopod

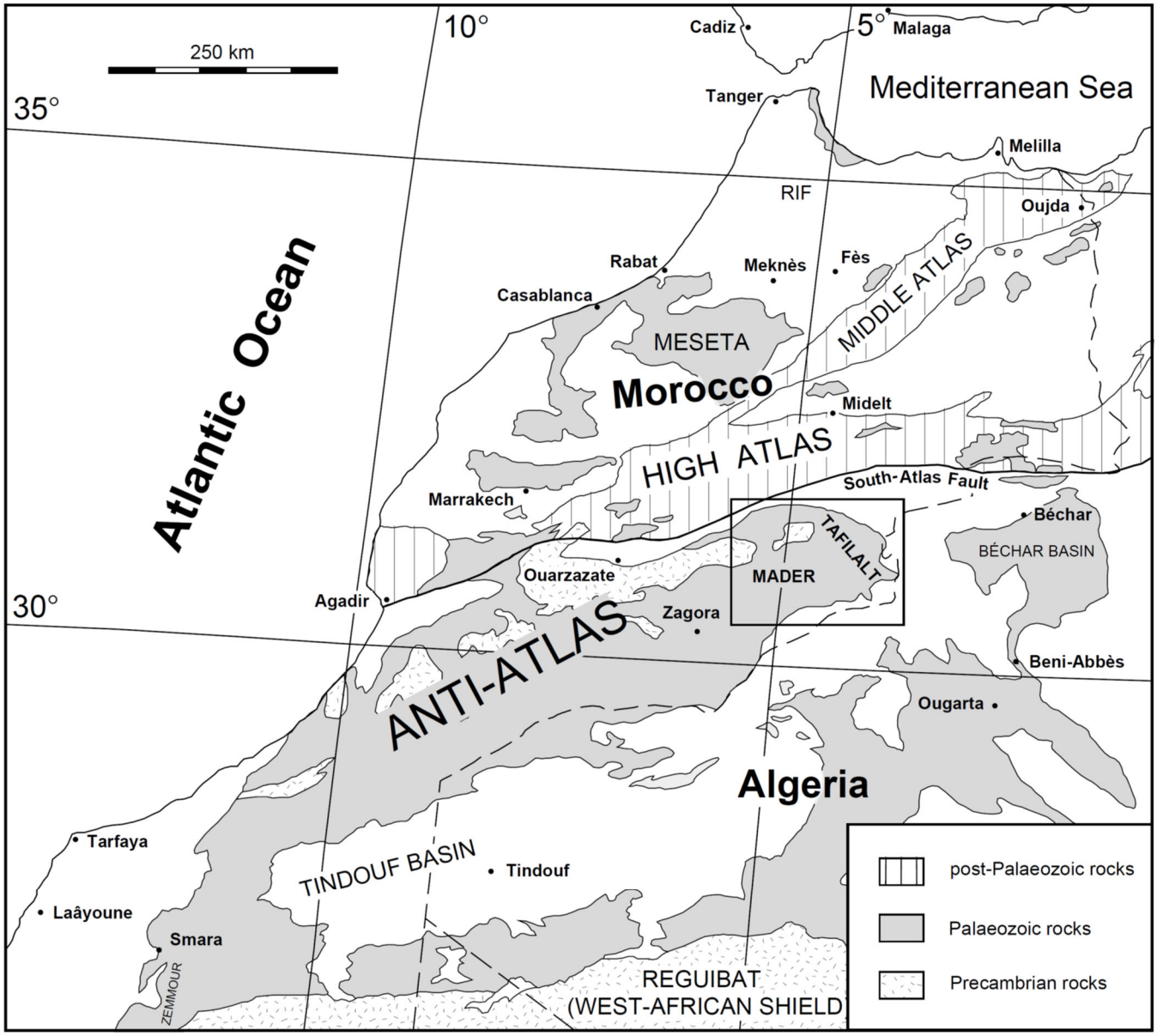

Fig. 1. Major tectonic units of Morocco (modified from PIQUE & MICHARD 1989); boxed area indicates location of the study area and fields of Text-figs 2-5

limestones become more frequent. Carbonate deposition was most widespread in Middle and Late Devonian times. At that time, a differentiated facies pattern developed in the eastern Anti-Atlas. Differential subsidence, resulting from early Variscan tensional block faulting, caused the disintegration of the formerly stable shelf into a platform and basin topography (WENDT 1985, 1988). In the Mader Basin, a 200-400 m thick neritic succession of argillaceous, fossiliferous wackestones, locally with intercalated mudmounds and coral-stromatoporoid floatstones, was deposited during Middle Devonian times (HOLLARD 1974; WENDT 1988, 1993). In the Late Devonian, the basin was filled with up to 800 m of shales interbedded with some sandstones (WENDT 1991). In contrast, only some tens of metres of condensed cephalopod limestones were deposited on the pelagic Tafilalt Platform during the Middle and Late Devonian (WENDT 1991).

During the Early Carboniferous, the whole basin and platform topography was levelled by thick deltaic sandstones. The Lower Carboniferous (Tournaisian and Viséan) clastic succession is best developed

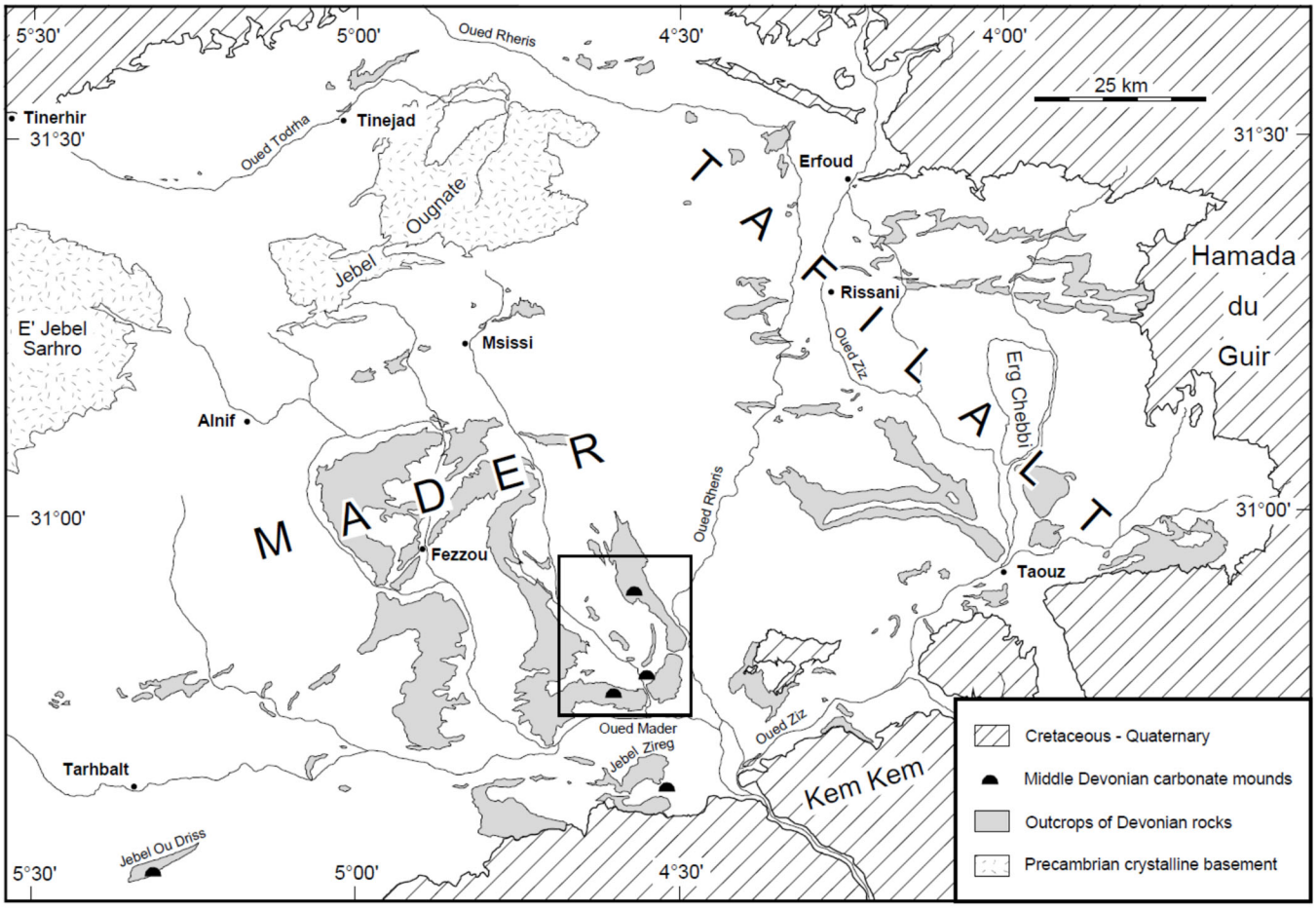

Fig. 2. Locality map of the eastern Anti-Atlas with locations of Middle Devonian carbonate mounds; boxed area indicates field of Text-fig. 9

in the southern Tafilalt where it is about 2000 m thick (BELKA 1991). Huge allochthonous mud-mound boulders (lower Viséan) occur in the southeastern Tafilalt (Jebel Bega and farther east, PAREYN 1961). The youngest preserved Palaeozoic strata of the eastern Anti-Atlas are lower Namurian shales (DELÉPINE 1941), which are exposed near the northwestern edge of Erg Chebbi. The geological history of the Anti-Atlas between the Namurian and the continental Upper Cretaceous (Cenomanian) is unknown. Variscan folding and uplift was weak and probably took place during the Late Carboniferous (Westphalian) (BONHOMME & HASSENFORDER 1985).

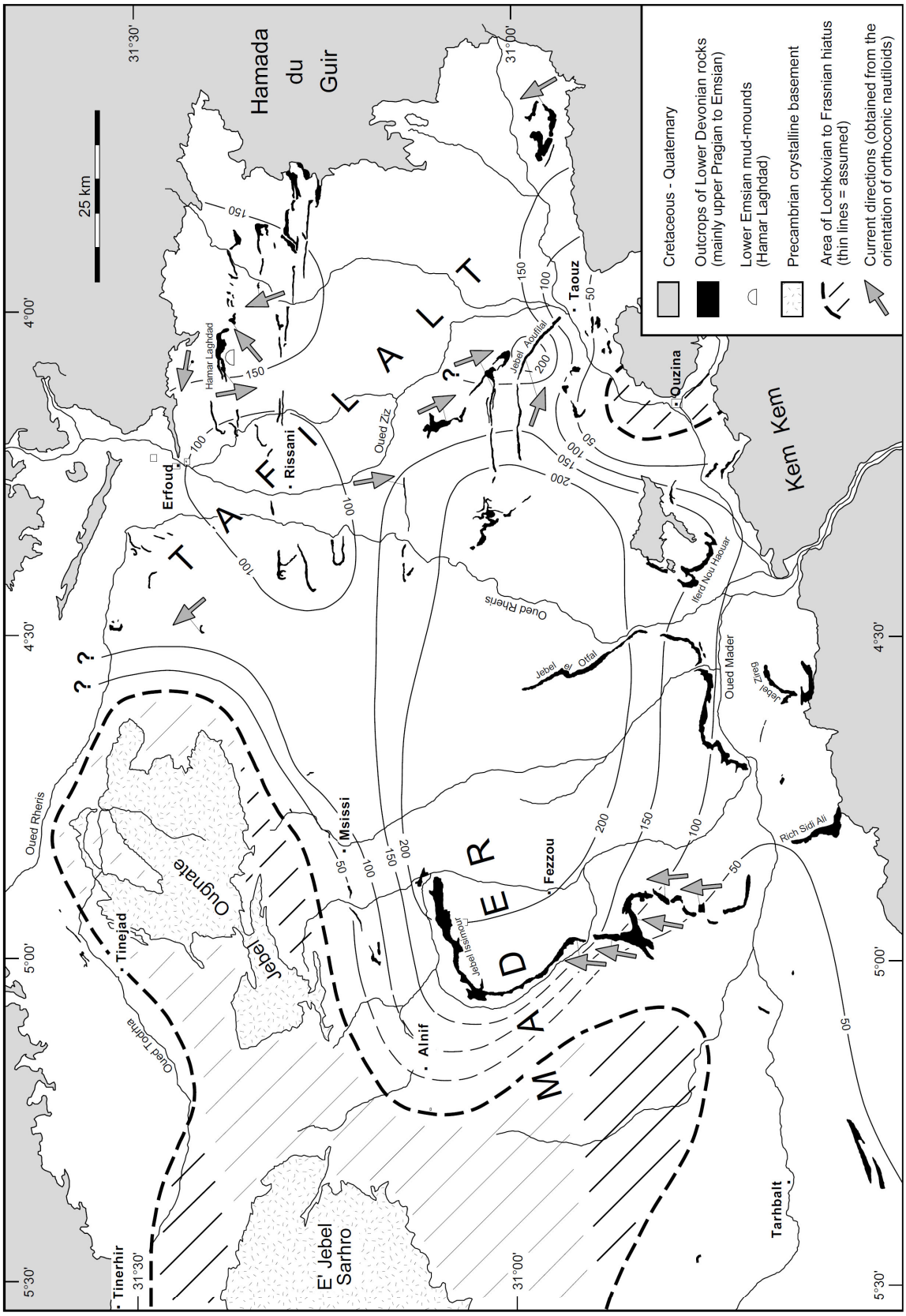

Fig. 3. Isopach map with Emsian thicknesses in metres and current directions; based on the geological map 1:200.000 (sheets 'Todrha-Ma'der' and 'Tafilalt-Taouz'), data in MASSA (1965), HOLLARD (1967, 1974), ALBERTI (1980, 1981b), BULTYNCK (1985), WENDT (1995) and own investigations

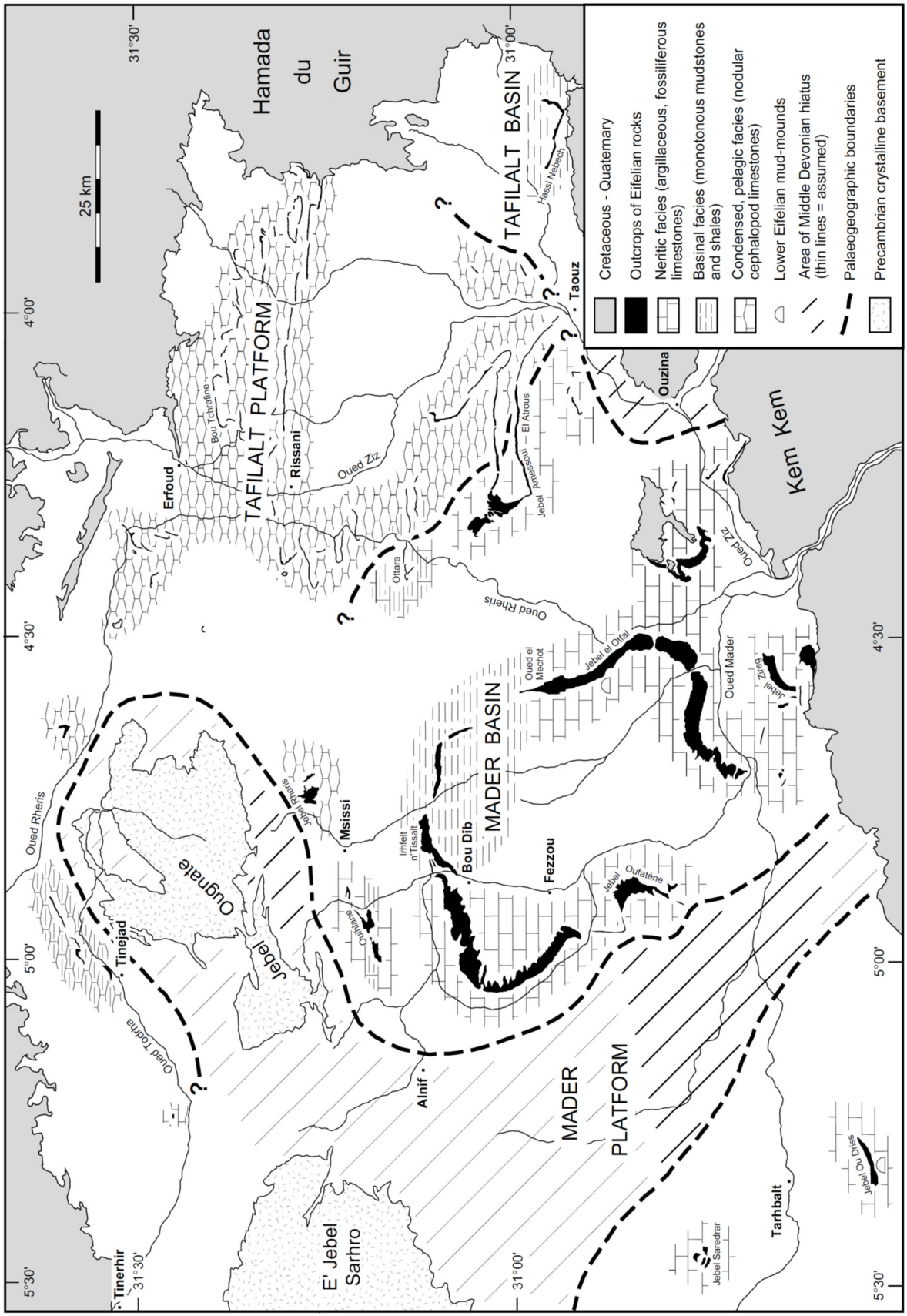

Fig. 4. Facies pattern and palaeogeography of the early Eifelian (*costatus* Zone); based on the geological map 1:200.000 sheets 'Todrha-Ma'der' and 'Tafilalt-Taouz'), data in HOLLARD (1974), WENDT (1988, 1993) and own investigations

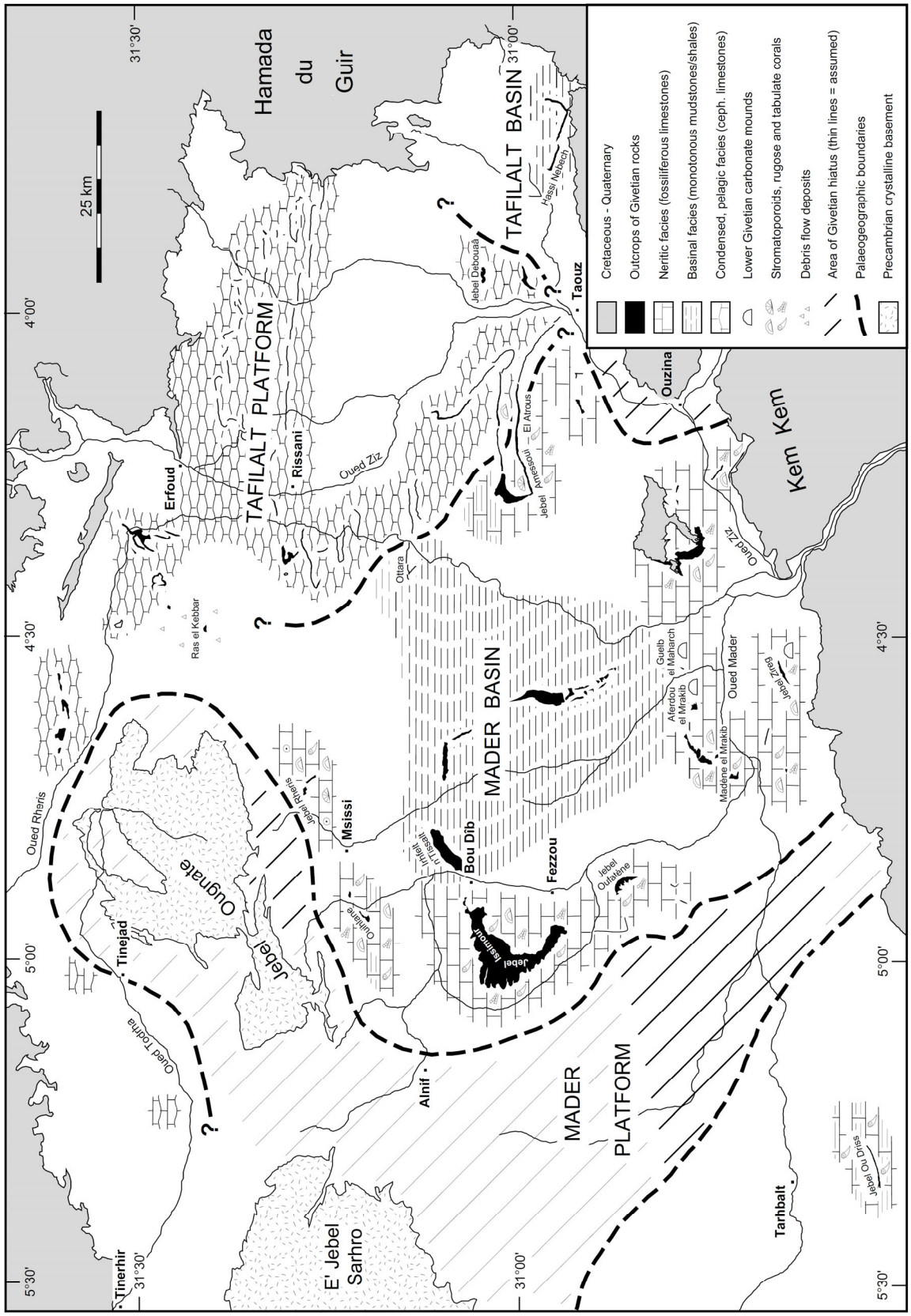

Fig. 5. Facies pattern and palaeogeography of the early Givetian (Lower *varcus* Zone); based on the geological map 1:200.000 (sheets 'Todrha-Ma'der' and 'Tafilalt-Taouz'), data in HOLLARD (1974), WENDT (1988, 1993) and own investigations

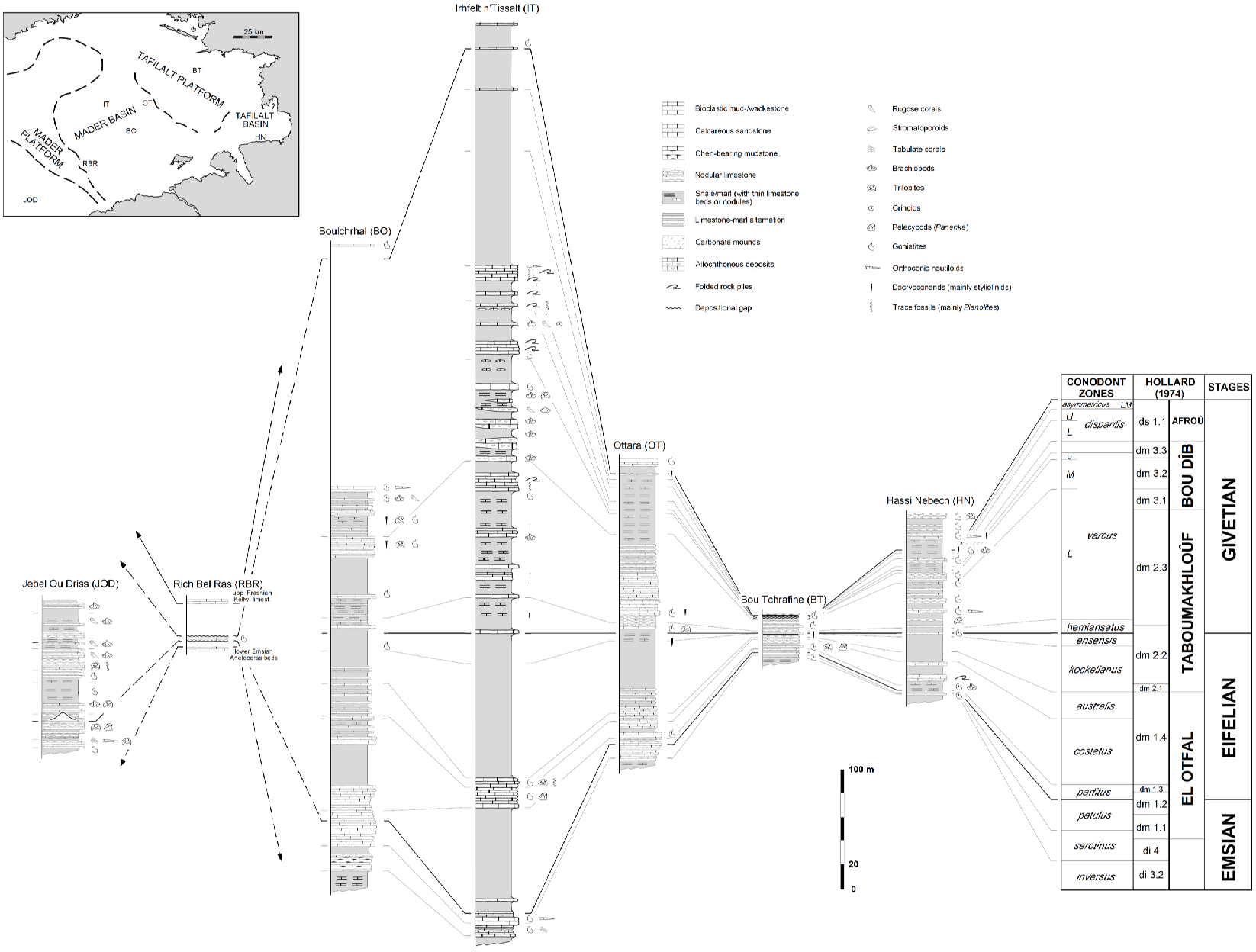

Correlation of typical upper Emsian to lower Frasnian sections of the eastern Anti-Atlas; correlation of HOLLARD's (1974) lithological units with the actual upper Emsian to Givetian conodont zonation after data in ALBERTI (1980, 1981a), BULTYNCK & HOLLARD (1980), BULTYNCK & JACOBS (1981) and own calculations; relative duration of conodont zones in the Eifelian and Givetian stage after BELKA & *al.* (in press) and HOUSE (1995) respectively; ottara and Boulchrhal sections modified and completed after HOLLARD (1974); Irhfelt n'Tissalt section modified and completed after HOLLARD (1974), BULTYNCK & JACOBS (1981) and WENDT (*written comm.*)

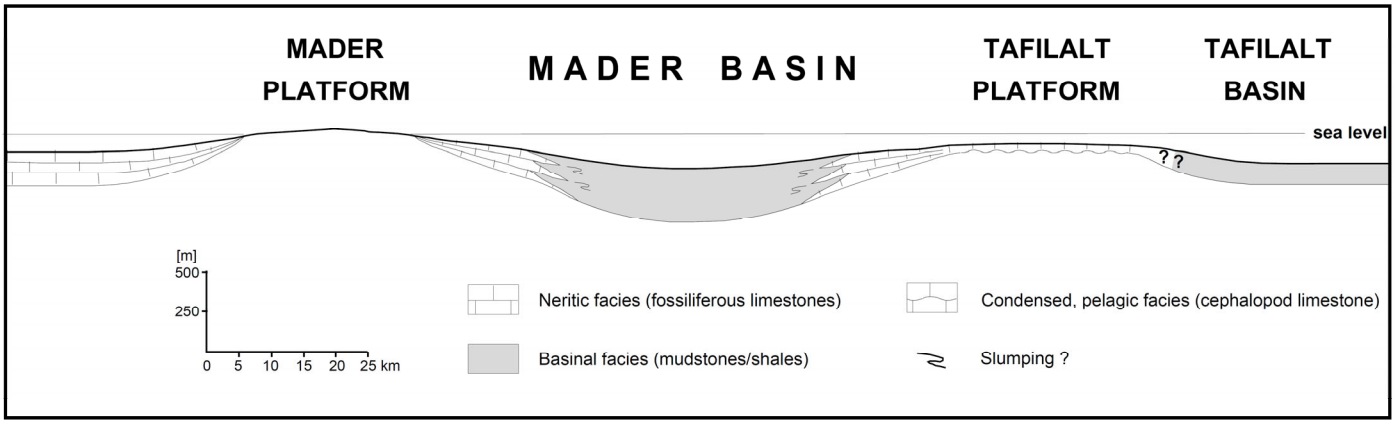

Fig. 7. Simplified lower Givetian (Lower *varcus* Zone) facies profile of the eastern Anti-Atlas, drawn along a line Tarhbalt – Fezzou – Jebel Amessoui – Jebel Debouaâ – Hassi Nebech (*see* Text-fig. 5)

STOP 5.1-5.3 Cambrian, Ordovician, and Devonian Trilobite Fossils

Introduction to Trilobites

A PICTORIAL GUIDE TO THE ORDERS OF TRILOBITES

by Samuel M. Gon III, Ph.D.

ORDER PROETIDA

Superfamily Aulacopleuroidea
Aulacopleuridae *Aulacopleura*

Superfamily Bathyuroidea
Bathyuridae *Goniotelus*

Superfamily Proetoidea
Proetidae *Cyphoproetus*

ORDER ASAPHIDA

Superfamily Anomocaroidea
Anomocarellidae *Glyphaspis*

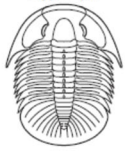

Superfamily Asaphoidea
Asaphidae *Ogygiocaris*

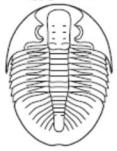

Superfamily Trinucleioidea
Trinucleidae *Cryptolithus*

Superfamily Dikelocephaloidea
Dikelocephalidae *Dikelocephalus*

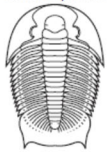

Superfamily Cyclopygoidea
Cyclopygidae *Cyclopyge*

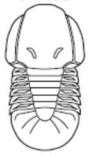

Superfamily Remopleuridoidea
Remopleuridae *Remopleurides*

ORDER HARPETIDA

Suborder Harpetina

Harpetidae *Harpes*

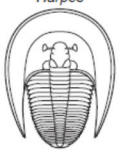

ORDER CORYNEXOCHIDA

Suborder Corynexochina

Dorypygidae *Olenoides*

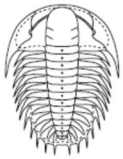

Suborder Illaenina

Illaenidae *Bumastus*

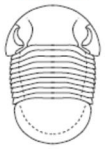

Suborder Leiostegiina

Kaolishaniidae *Mansuyia*

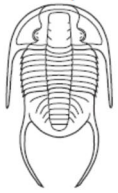

ORDER LICHIDA

Superfamily Lichoidea
Lichidae *Arctinurus*

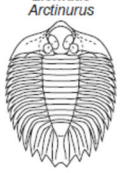

ORDER ODONTOPLEURIDA

Superfamily Dameselloidea
Damesellidae *Drepanura*

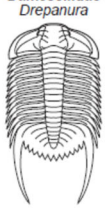

Superfamily Odontopleuroidea
Odontopleuridae *Kettneraspis*

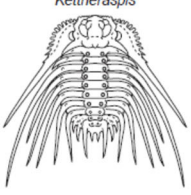

ORDER PHACOPIDA

Suborder Calymenina

Calymenidae *Calymene*

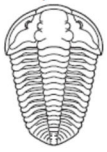

Suborder Cheirurina

Cheiruridae *Ceraurus*

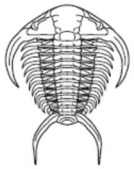

Suborder Phacopina

Phacopidae *Phacops*

Acastidae *Kayserops*

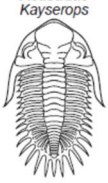

ORDER PTYCHOPARIIDA

Suborder Ptychopariina

Tricrepicephalidae *Tricrepicephalus*

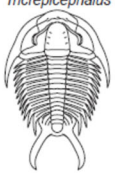

Ptychopariidae *Modocia*

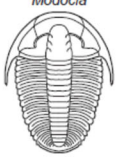

Ellipsocephalidae *Ellipsocephalus*

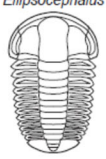

Suborder Olenina

Olenidae *Olenus*

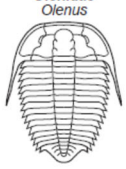

ORDER AGNOSTIDA

Suborder Agnostina

Agnostidae *Agnostus*

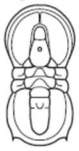

Condylopygidae *Pleuroctenium*

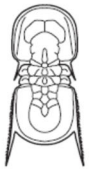

Suborder Eodiscina

Eodiscidae *Pagetia*

ORDER REDLICHIIDA

Suborder Olenellina

Olenellidae *Paedeumias*

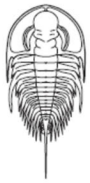

Fallotaspididae *Fallotaspis*

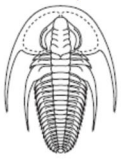

Suborder Redlichiina

Redlichiidae *Redlichia*

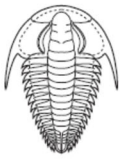

Paradoxididae *Paradoxides*

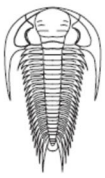

Xystriduridae *Xystridura*

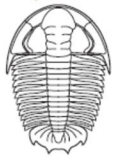

Emuellidae *Balcoracania*

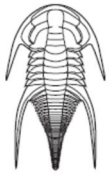

What are Trilobites?

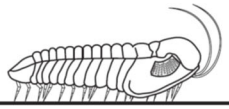

Trilobites are hard-shelled, segmented creatures that existed over 300 million years ago in the Earth's ancient seas. They went extinct before dinosaurs even existed, and are the signature creatures of the **Paleozoic** Era, the first era to generate a diversity of complex life forms, including nearly all of the phyla of today. Although dinosaurs are the most well-known fossil life forms, trilobites are also a favorite among those familiar with **paleontology** (the study of the development of life on Earth)

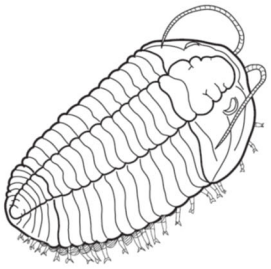

Fossil (left) and reconstruction (right) of the trilobite, *Flexicalymene meeki*

Ancient Arthropods

Trilobites were among the first of the **arthropods**, a phylum of hard-shelled creatures with multiple body segments and jointed legs. They constitute an extinct class of arthropods, the **Trilobita**, made up of nine orders, over 150 families, thousands of genera, and over 15,000 described species. New species of trilobites are unearthed and described each year. This makes trilobites the single most diverse group of extinct organisms, and within the generalized body plan of trilobites there was a great range of size and form. The smallest known trilobite is just over a millimeter long, while the largest include species from 30 to 70 cm in length (roughly a foot to over two feet long!) With such a diversity of species and sizes, thoughts on the life styles of trilobites include planktonic, swimming, and crawling forms, and we can presume they filled a varied set of ecological roles, although perhaps mostly as predators, detritivores, and scavengers. Most trilobites are about an inch long, and part of their appeal is that you can hold and examine an entire fossil animal in your hand. Try that with a dinosaur!

The 3-lobed body plan

Whatever their size, all trilobites share a similar body plan, being made up of three main body parts: a **cephalon** (head), a segmented **thorax**, and a **pygidium** (tail piece). However, the name "trilobite," meaning "three lobed," is not in reference to those three body features, but to the fact that all trilobites bear a long central axis, or **axial lobe**, flanked on each side by right and left **pleural lobes**. These three lobes that run from the cephalon to the pygidium give trilobites their name.

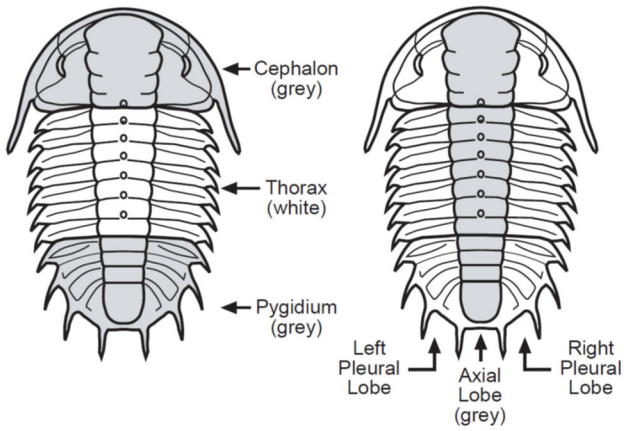

a trilobite's body can be divided into three parts both lengthwise as well as laterally.

Please explore further

Trilobites are distinguished from their sister arthropods via characters thought to be unique to trilobites, including their three-lobed structure, a dorsally calcified exoskeleton, and a specialized ventral mouthpart called a hypostome. Now that you know generally what trilobites are, please explore this illustrated guide to the orders of trilobites. You'll learn about trilobite body parts, how scientists classify trilobites, when they lived, and how to tell the major groups apart. In the end, I hope you gain a better appreciation of their amazing variety. Although they are all extinct now, they were among the first explosions of biological diversity that this amazing planet of ours has produced over the eons.

Proetidae
Cyphoproetus

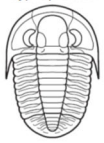

Asaphidae
Homotelus

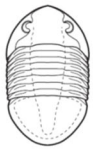

Phacopidae
Phacops

Lichidae
Arctinurus

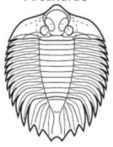

Ptychoparilidae
Modocia

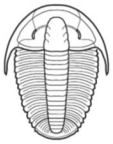

Harpetidae
Harpes

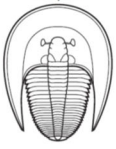

Corynexochidae
Bonnaspis

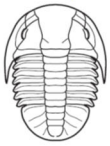

Redlichiidae
Redlichia

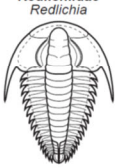

Agnostidae
Agnostus

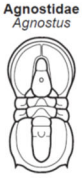

When Did Trilobites Exist?

(Geological time from a trilobite's point of view)

This chart depicts the geological periods of the **Paleozoic Era**, during which trilobites lived. Trilobites are one of the diagnostic fossils of the Paleozoic Era, the earliest era of the **Phanerozoic Epoch**. The Paleozoic portion of the geological scale at bottom left is expanded on the right as geological **periods**, and the scale indicates how many millions of years ago (mya) each period spanned.

Trilobites can be found from the Early **Cambrian** period (544 mya) to the Late **Permian** (245 mya), after which trilobites (among a large number of marine organisms) went extinct in the great catastrophe that removed an estimated 90%+ of all species on earth. The **Great Permian Extinction** marks the end of the **Paleozoic** and the start of the **Mesozoic**. Trilobites are one of the few organisms that existed from the start to the end of the Paleozoic Era.

The greatest numbers of species and forms of trilobites lived during the **Cambrian** and **Ordovician** periods, after which trilobites began to decline (see Chart of trilobite family diversity over time). There were far fewer species in the **Carboniferous** and **Permian** periods. Nevertheless, to have persisted for nearly 300 million years is a testimony to the successful design and adaptability of trilobites. Some scientists even hold faint hope that in poorly explored deep sea environments, trilobites may still exist, a holdover from truly ancient times.

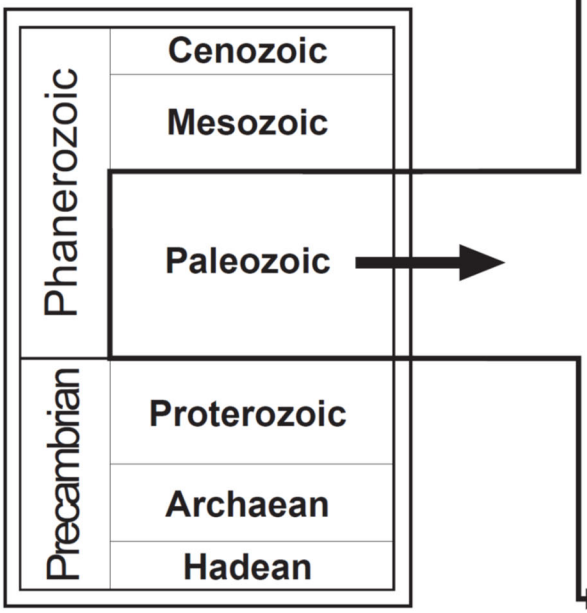

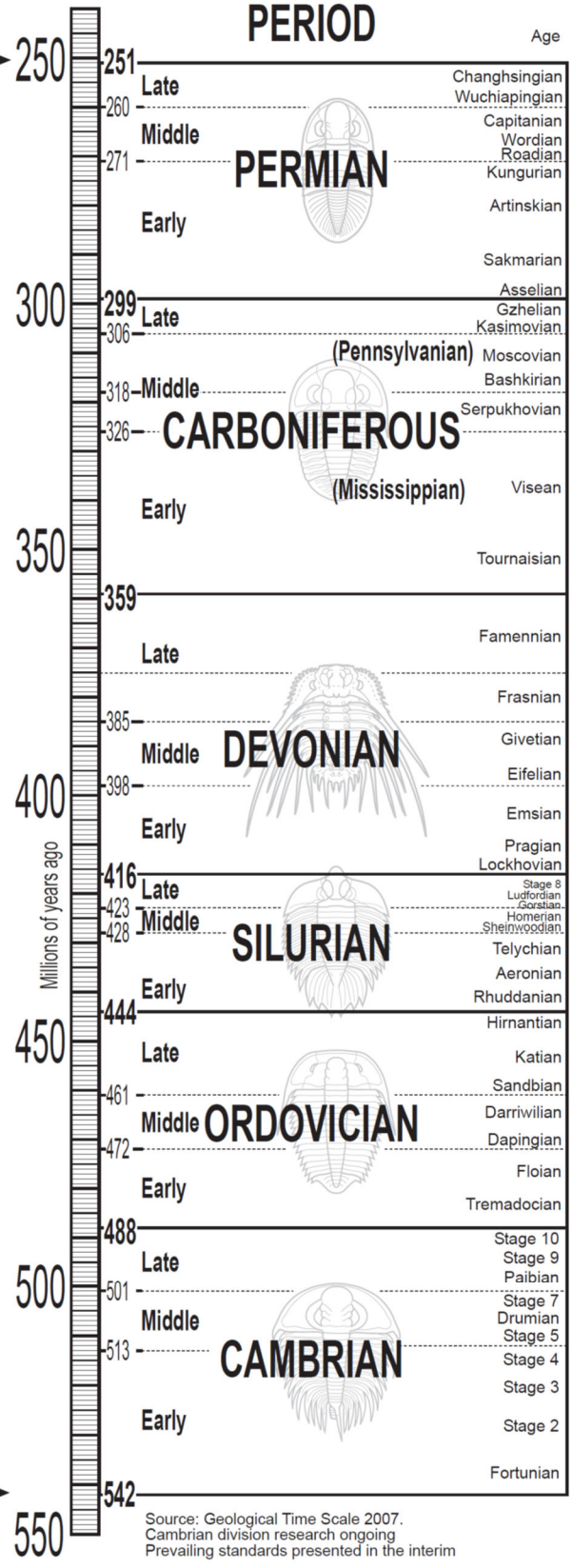

Source: Geological Time Scale 2007.
Cambrian division research ongoing
Prevailing standards presented in the interim

The Rise and Fall of Trilobites

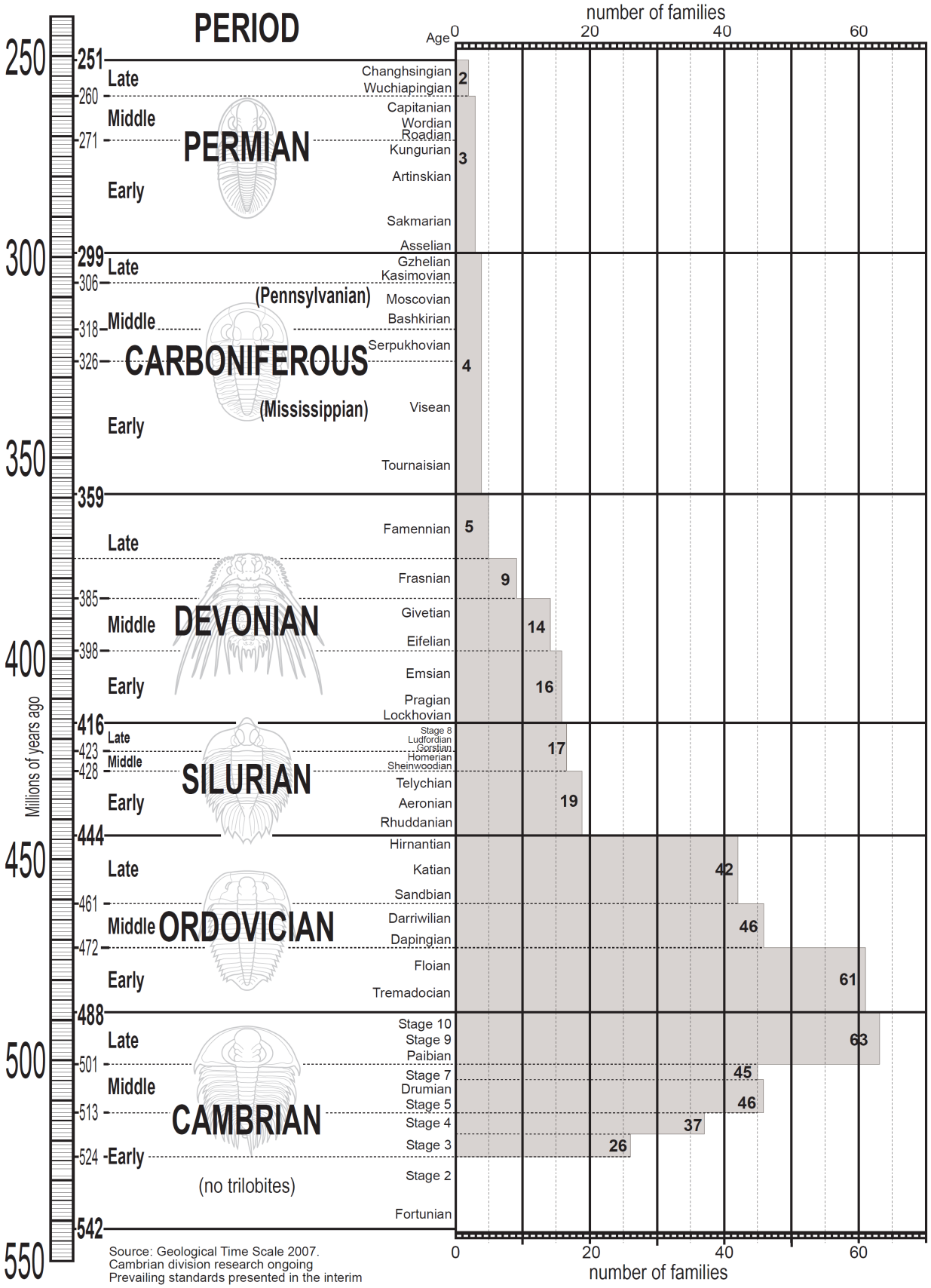

Source: Geological Time Scale 2007.
Cambrian division research ongoing
Prevailing standards presented in the interim

Systematic Relationships and Chronological Extent of the Trilobite Orders

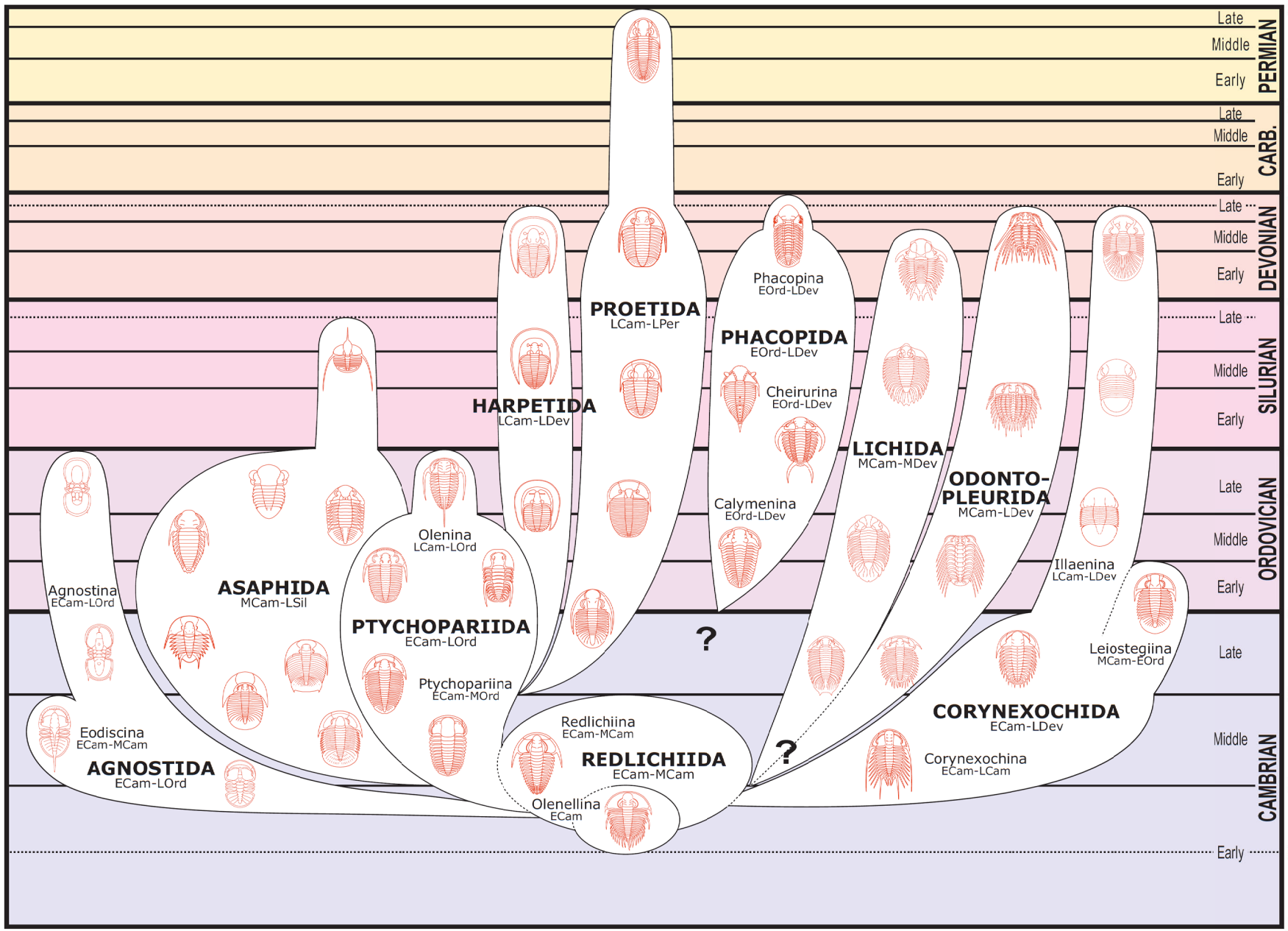

What distinguished Trilobites among Arthropods?

Trilobites are the most diverse of the extinct arthropod groups, known from perhaps 5000 genera. The classification of trilobites within the Arthropoda has generated much controversy, much of which is still not completely resolved. There are a number of characters that most workers agree distinguish trilobites from within the Arachnomorph clade, the most significant described below:

eye ridges: These are consistently present in primitive forms, connecting the front of the palpebral lobe with the axial furrow. Eye ridges are lost in many post-Cambrian trilobites)

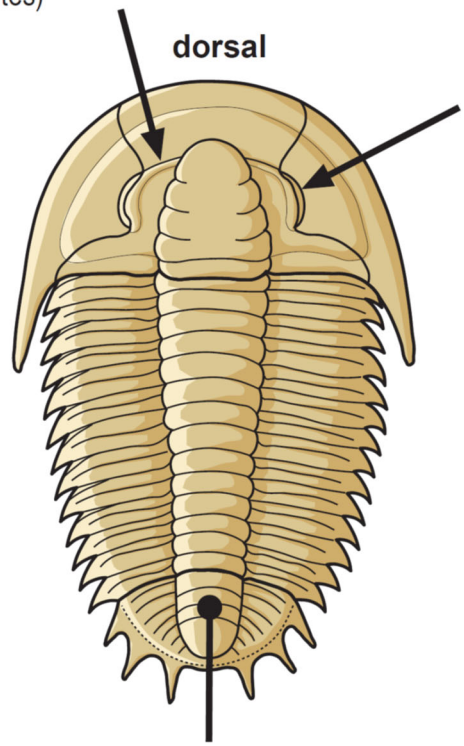

calcitic eyes: While other compound eyes are found in Cambrian arthropods, only those of trilobites have corneal surfaces composed of prismatic calcite lenses (with the crystallographic axis perpendicular to the lens surface).

circum-ocular sutures: In Cambrian holochroal trilobite eyes, a suture around the edge of the shared corneal surface assisted in molting of holaspid trilobites. In post-Cambrian trilobites this feature is secondarily lost, leaving the corneal surface attached to the fixigena.

rostral plate: A ventral anterior plate separated from the rest of the cephalic doublure by sutures is very well developed in primitive trilobites (*e.g.*, Redlichiida), narrower in other trilobite orders, and secondarily lost in some advanced forms (*e.g.*, Asaphida and Phacopida).

pygidium: The posterior tagma (body division) of >1 segment is a conspicuous feature of trilobites, primitively small (*e.g.*, in Olenellina).

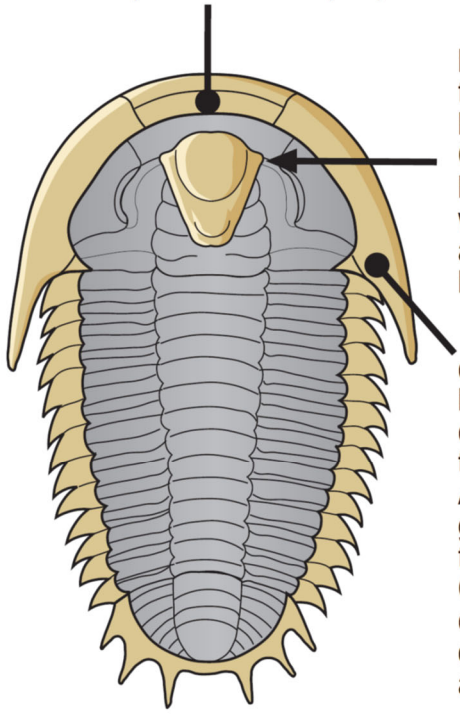

hypostomal wings: The trilobite hypostome may be homologous to the labrum in Crustacea, but only trilobite hypostoma bear anterior wings which fit in pits in the anterior axial glabellar furrows (or homologous locations).

calcified cuticle: Trilobites bear a rather pure calcareous cuticle that ends ventrally at the inner edge of the doublure. Although a few other arthropod groups calcify, none do so in the same way as trilobites. Crustacea, for example, are calcified ventrally and post-orally, so their appendages are calcified.

ventral

Together with the organization of the body into three anterior-posterior divisions (cephalon, thorax, and pygidium), and the three longitudinal lobes (axial lobe and two flanking pleural lobes), the body features on this page serve to readily distinguish trilobites from all other known Arthropod groups.

Major Trilobite Features

The major trilobite body features (those which generally distinguish trilobites from other Paleozoic arthropods) are summarized and illustrated here. Most of these terms figure prominently in trilobite descriptions. More detailed charts of trilobite dorsal and ventral morphological terms are presented elsewhere in this guide, as well as a glossary of terms.

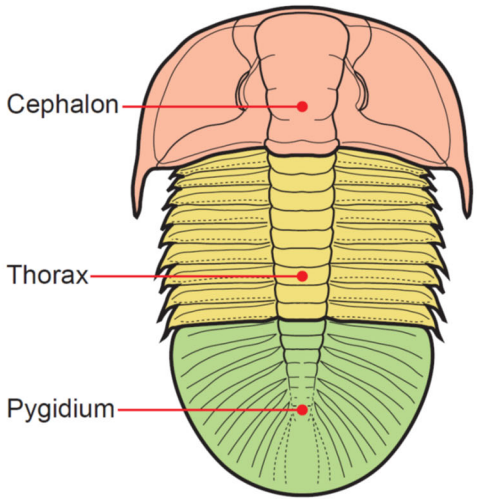

The trilobite body is divided into three major sections: a **cephalon** with eyes, mouthparts and sensory organs such as antennae, a **thorax** of multiple articulating segments (that in some species allowed enrollment), and a **pygidium**, or tail section, in which segments are fused together. These divisions are easily discerned in the dolichometopid trilobite *Bathyuriscus elegans*.

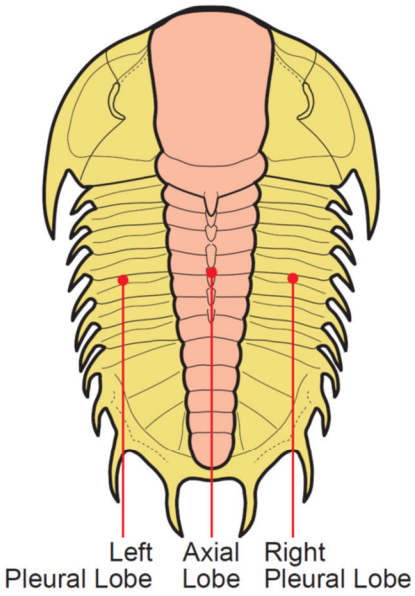

The name **"trilobite"** (meaning "**three-lobed**") is *not* based on the body sections cephalon, thorax and pygidium, but rather on the three longitudinal lobes: a central **axial lobe**, and two symmetrical **pleural lobes** that flank the axis. In the corynexochid trilobite *Dorypyge*, deep axial furrows clearly separate the axis from the two lateral lobes along the entire length of the body.

Major Trilobite Features

The major trilobite body features (those which generally distinguish trilobites from other Paleozoic arthropods) are summarized and illustrated here. Most of these terms figure prominently in trilobite descriptions. More detailed charts of trilobite dorsal and ventral morphological terms are presented elsewhere in this guide, as well as a glossary of terms.

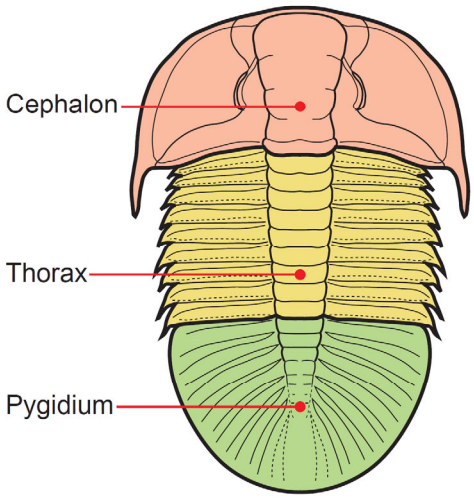

The trilobite body is divided into three major sections: a **cephalon** with eyes, mouthparts and sensory organs such as antennae, a **thorax** of multiple articulating segments (that in some species allowed enrollment), and a **pygidium**, or tail section, in which segments are fused together. These divisions are easily discerned in the dolichometopid trilobite *Bathyuriscus elegans*.

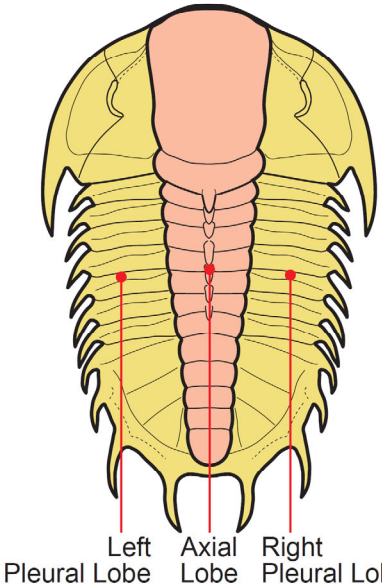

The name **"trilobite"** (meaning "**three-lobed**") is *not* based on the body sections cephalon, thorax and pygidium, but rather on the three longitudinal lobes: a central **axial lobe**, and two symmetrical **pleural lobes** that flank the axis. In the corynexochid trilobite *Dorypyge*, deep axial furrows clearly separate the axis from the two lateral lobes along the entire length of the body.

Major Trilobite Features

CEPHALIC FEATURES:
Perhaps the most important feature used to distinguish trilobite species is the cephalon, or head piece. Features of the cephalon are shown below. These are subdivisions that often assume different shapes or sizes relative to each other in different species. These are typically demarcated by the glabella, by the eyes and eye lobes, and by the facial sutures that separate the librigenae (free cheeks) from the central cranidium (see left, below).

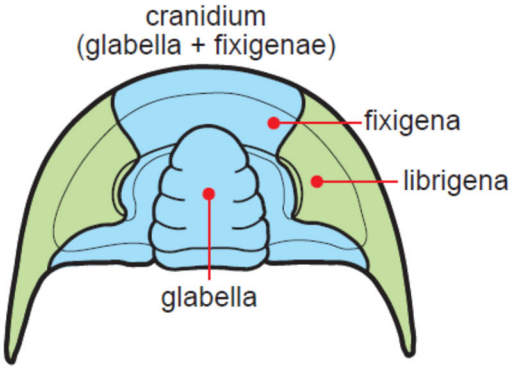

The cheeks (genae) are the pleural lobes on each side of the axial feature, the glabella. When trilobites molt or die, the librigenae (free cheeks) often separate, leaving the cranidium (glabella + fixigenae) behind.

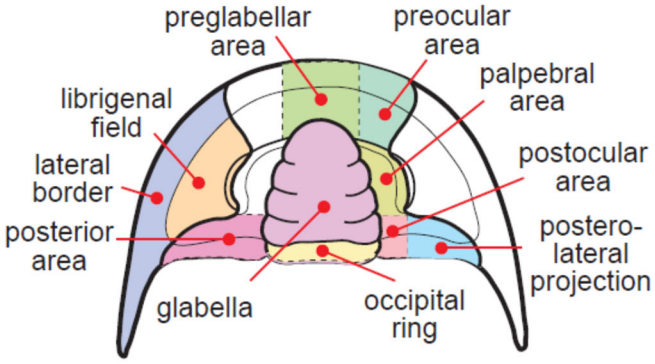

When describing distinguishing characters between different taxa of trilobites, the presence, size, and shape of the cephalic features labeled above are often described and contrasted.

THORACIC FEATURES:
In some trilobites, the thorax may be divided into an anterior **prothorax**, followed by a posterior (often many-segmented) **opisthothorax**. This is seen in some of the Order Redlichiida, such as *Balcoracania* (see figure and image to right). Sometimes, one pleural segment is prominent in size, and is referred to as a **macropleural** segment. This is seen in many species of the suborder Olenellina of the order Redlichiida.

The majority of trilobites do not show the prothorax-opisthothorax division or the presence of macropleural segments.

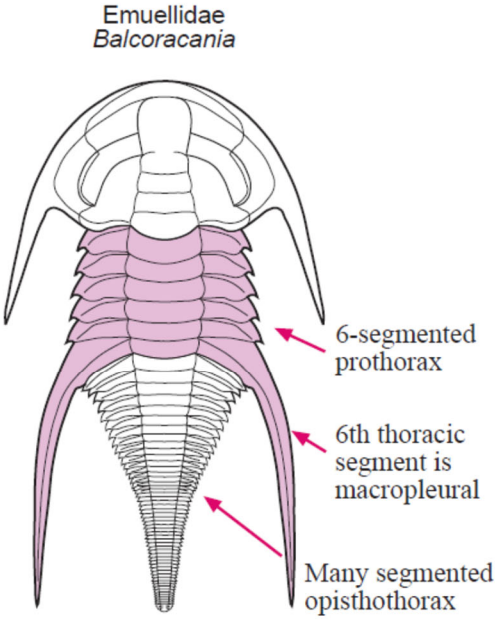

Trilobite Dorsal Morphology

The dorsal (top) structures of a trilobite are the parts typically preserved. This is presumably because the ventral (underside) exoskeleton was either much thinner, or did not include the calcite minerals that facilitated preservation of the dorsal shell. Because of this, dorsal characters are most frequently used in trilobite classification. The image below includes most of the **dorsal morphological terms** used to define trilobite taxa. **Ventral morphology** (see page 15) can also be important. For example, there are terms describing the way the **hypostome** (a hard mouthpart on the underside of a trilobite) attaches to the rest of the cephalon. There are also broader terms that refer to **major body divisions** such as cephalon, pygidium, cranidium, axis, etc. There are some terms that relate to the relative sizes of the cephalon and pygidium. **Facial sutures** (lines along which the cephalic exoskeleton split to allow molting) are also important in classifying trilobites. There was also significant variation of trilobite eyes. We don't know very much about a trilobite's **internal anatomy**, with some exceptions! More detailed definitions of most the terms in the images below are provided in the **glossary** (page 2).

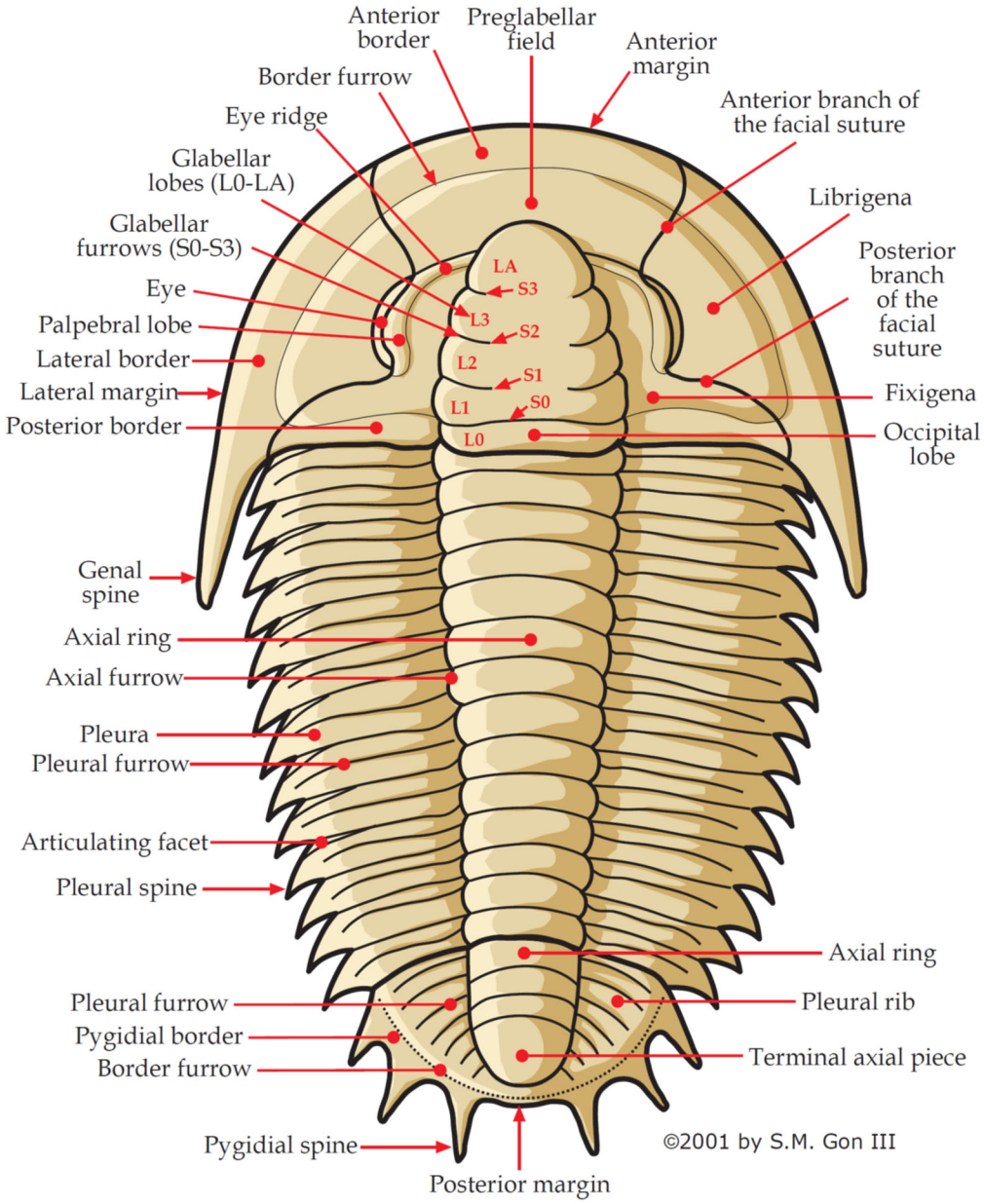

Trilobite Dorsal Morphology

Although the general terms for dorsal morphology of trilobites can be applied to all trilobites, there are some features that are only shared by specialized groups. These receive special terms designed to be used when describing these groups. Some examples of these are given below:

Some morphological terms applied to Order Lichida

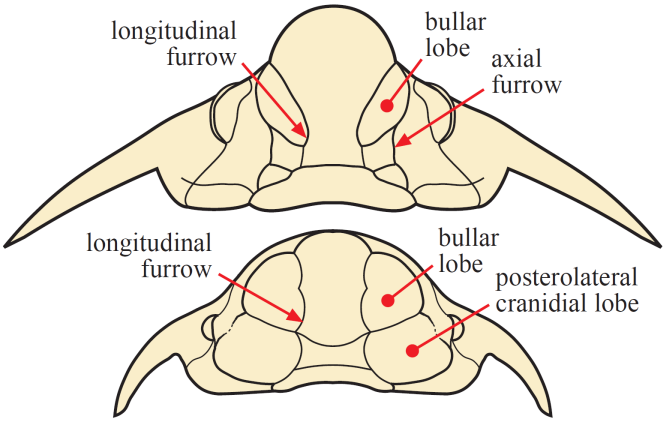

Some morphological terms applied to Order Asaphida

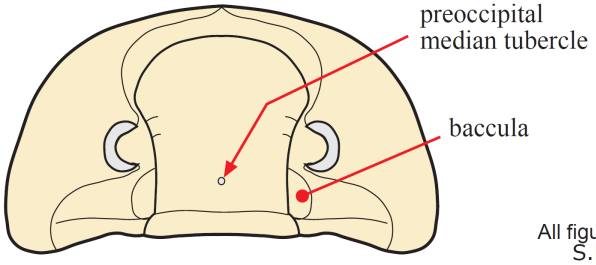

Some morphological terms applied to Order Redlichiida Suborder Olenellina

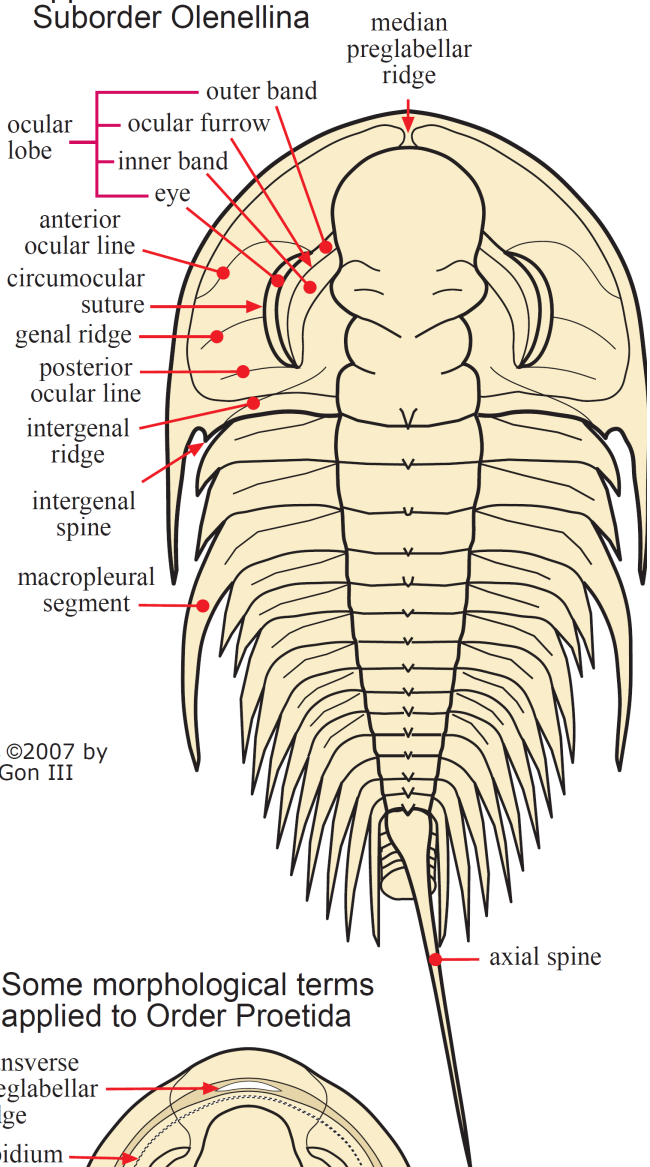

Some morphological terms applied to Order Agnostida Suborder Agnostina

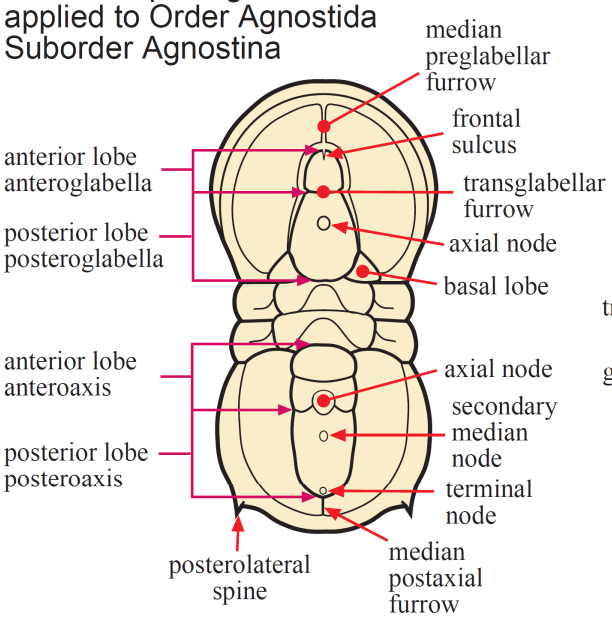

Some morphological terms applied to Order Proetida

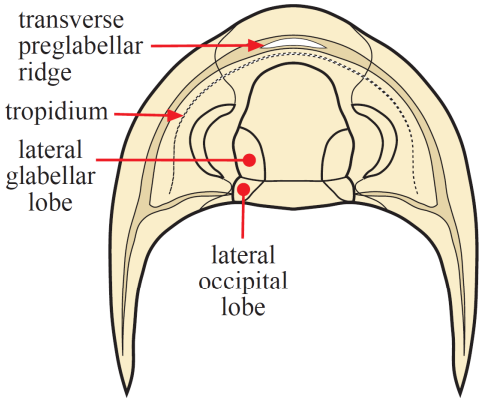

The international fossil trade from the Paleozoic of the Anti-Atlas, Morocco

JUAN CARLOS GUTIÉRREZ-MARCO[1]* & DIEGO C. GARCÍA-BELLIDO[2,3]

[1]*Instituto de Geociencias (CSIC, UCM) and Departamento de Geodinámica, Estratigrafía y Paleontología, Facultad CC. Geológicas, José Antonio Novais 12, 28040 Madrid, Spain*

[2]*School of Biological Sciences, University of Adelaide, North Terrace, Adelaide, SA 5005, Australia*

[3]*South Australian Museum, North Terrace, Adelaide, SA 5000, Australia*

J.C.G., 0000-0003-4213-6144; D.C.G., 0000-0003-1922-9836

**Correspondence: jcgrapto@ucm.es*

Abstract: The fossil trade of Paleozoic material from southern Morocco was estimated by some North American media to reach about US$ 40 million a year, and it supplies fossil shows and shops all over the world. In its initial stages of extraction, preparation and export, this trade constitutes the main source of income to more than 50 000 people in an area basically conscribed within the triangle made by Alnif–Erfoud–Taouz (eastern Anti-Atlas), and generated a true 'fossil industry'. This includes diggers and miners, artisans that prepare and restore fossils (and others dedicated to making replicas with decorative purposes), quarries working on fossiliferous ornamental rocks, and numerous middlemen and Moroccan wholesalers who annually attend the large fossil fairs of Europe and the USA. More than 25 years of intensive exploitation of fossil resources in the Anti-Atlas has also produced important scientific discoveries, such as world-renowned fossil biotas like Fezouata and Tafilalt, and hundreds of new Paleozoic fossil taxa, in parallel with a worrying destruction of outcrops and many palaeontological sites. The new mining legislation also deals with the extraction, collection and trade of geological specimens, and a future specific legal framework for fossils and geological heritage will try to manage the existing industry. It will aim to restrain the constant deterioration of the rich Moroccan geological heritage, while enabling strategies of sustainable development so that the local population is not negatively affected.

The Anti-Atlas Mountains lie in the periphery of the West African Craton, and are regarded as the common foreland fold belt of both the Mesetian Variscides and the northernmost Mauritanides. This large domain extends for more than 750 km from the Atlantic coast in the west to the coeval Ougarta belt in the east, the latter entering Algerian territory. Basement rocks forming more or less faulted antiforms crop out in the Anti-Atlas as Precambrian inliers affected by the Pan-African Orogeny. They are surrounded by extensive Cambrian–early Carboniferous outcrops belonging to a thick pre-Variscan Paleozoic succession, which was slightly to moderately folded during the Late Carboniferous–Early Permian and then eroded during the next 125 myr or more. In the Cretaceous–Paleocene, the Variscan basement was partially overlain by a thin continental to marine sedimentary cover which formed the Hamada plateau. Finally, the entire Anti-Atlas was uplifted and slightly tilted contemporaneously with the High Atlas Mountains during the Neogene (Piqué *et al.* 1991; Michard *et al.* 2008, 2010; Soulaimani & Burkhard 2008).

The fossil richness of the Paleozoic of the Anti-Atlas is well known from the first general palaeontological compilations of Termier & Termier (1950*a*, *b*, *c*), mainly based on the stratigraphic work of the French geologist Georges Choubert (1908–86). From the late 1950s to the late 1990s, the vast geological mapping work done by another French geologist, Jacques Destombes (1926–2018), allowed him to find thousands of fossil localities during the fieldwork carried out for nine geological maps (1:200 000 scale) covering the whole Anti-Atlas. His maps and the numerous palaeontological publications derived from his fossil material (see Destombes 2006) are still the most valuable source of information when planning new geological and palaeontological detailed explorations in this whole region.

The search and commercial exploration of fossils in the south of Morocco started in the late 1970s, as a

From: Hunter, A. W., Álvaro, J. J., Lefebvre, B., Van Roy, P. & Zamora, S. (eds) 2022. *The Great Ordovician Biodiversification Event: Insights from the Tafilalt Biota, Morocco*.
Geological Society, London, Special Publications, **485**, 69–96.
First published online October 23, 2018, https://doi.org/10.1144/SP485.1

byproduct of the commercial collection of minerals, in particular around the mining district of Midelt. Just a decade later, the search for fossils in the Anti-Atlas was as extensive as it is today. This includes the excavation of hundreds of kilometres of shallow trenches in the middle of the desert focused on fossiliferous formations, and constitutes a way of life for thousands of people in Erfoud, Rissani and Alnif, to mention just a few of the cities most favoured by this fossil trade.

From the late 1980s, the Anti-Atlas has been considered as the classical heartland of Moroccan Paleozoic fossils. The largest commercial interest lies in Cambrian–Devonian trilobites (way ahead of the rest), Devonian ammonoids, corals, brachiopods and bryozoans, Siluro-Devonian crinoids and orthocone nautiloids, diverse invertebrate ichnofossils, and some rare Ordovician echinoderms, soft-bodied arthropods and problematica. From the overlying Cretaceous rocks sourrounding the Hamada highs, the commercial exploitation of fossils extends to the upper Lower Cretaceous Kem-Kem beds, yielding abundant dinosaurs, aquatic reptiles and pisces, as well the upper beds with Cenomanian echinoderms and molluscs.

The intensive exploitation of the Anti-Atlas fossils has brought to light hundreds of new palaeontological taxa of great scientific interest, and also highlighted the existence of some Ordovician and Cretaceous Fossil-Lagerstätten of global importance in furthering our knowledge of the evolution of life on the planet. Most of these discoveries would not have taken place if it had not been for the widespread activity of local miners and without the international demand that supports these Moroccan diggers. This constitutes a constant ethical conflict between the uncontrolled exploitation of Morocco's rich palaeontological heritage and the mode of life for a large proportion of the local population, with very little income living in a desert region with only a few means of survival.

The development of a fossil industry in the south of Morocco, the human and legal impact, and the scientific output have been increasingly cited by the world media over the last 10 years. It has also contributed to the development of a local tourism industry, which combines four-wheel drive (4WD) adventure tours with visits to fossil localities and ethnological or astronomical itineraries. The foremost popularization of Moroccan trilobites is due to David Attenborough's *First Life* documentary series, produced in 2010 for BBC in association with Discovery Channel and ABC (Australian Broadcasting Corporation). Of the non-scientific papers presenting a general overview on the Moroccan geological trade, those by Sicree (2009) and Praszkier (2011) are worth mentioning here.

The Moroccan fossil productive sector

Digging activities

From a collector and dealer's perspective, the first Paleozoic fossils from the Anti-Atlas started to appear in the late 1970s, in the mineral collection markets originating from Midelt (Mibladen and Touissit mines) and Taouz (Tawz). Originally, they were just small cephalopods (goniatites and orthoceratids; many of them hand-polished), as well as typical Devonian corals and brachiopods, and a single type of Ordovician trilobite, which was already being exhaustively excavated. They could all be purchased one piece at a time or wholesale in the local markets of Erfoud (Arfoud) and Midelt. Most of these fossils originated from the Devonian surface outcrops in the Erfoud and Alnif regions, whereas the Ordovician calymenacean trilobite *Flexicalymene ouzregui* was extracted from a single noduliferous stratigraphic horizon, which began to be intensively quarried and mined in 1977–78 to the south and SW of Alnif (Fig. 1a). At the time, the fossils from Alnif were offered for sale in Erfoud or Midelt due to the lack of sealed roads, access instead being via a poor network of dirt tracks.

By the beginning of the 1980s a massive exploitation of black Silurian limestones had started south of Erfoud, as well as Famennian limestones with large ammonoids that were polished individually or assembled in groups with orthocone nautiloids. This material was prepared mainly for decorative purposes, and small black pieces with aligned *Arionoceras* (='*Orthoceras*') started to be prepared manually in many creative ways, from individual pendants or earrings, to paperweights, ashtrays, trivets, slabs in relief, etc.

In the mid-1980s transport between the various regions in the Anti-Atlas had not yet improved significantly, but in local markets the first large phacopids and other Devonian trilobites preserved in limestone were being displayed, as well as the arrival at Erfoud of the first shark teeth from the Khouribga Basin. The latter indicates the beginning of an active exchange of commercial fossils between dealers in the Anti-Atlas and those excavating younger beds in northern regions of Morocco.

The late 1980s and the 1990s witnessed the boom of fossil-digging throughout the Alnif-Tafilalt region, in parallel with the development of fossil-preparation 'factories' and the large-scale export and sale of fossils to Europe, North America and Japan. A number of trilobites gradually became new attractions in the international market, such as the first giant Cambrian forms (*Acadoparadoxides* and *Cambropallas*) and large Ordovician species of *Platypeltoides*, *Asaphellus*, *Dikelocephalina*, *Lichakephalus*, *Birmanites* amongst others, as well as a

Fig. 1. Old and recent digging activities in the Ordovician of the Anti-Atlas. (**a**) Abandoned 'trilobite mines', exploited in the 1970s, in the *Flexicalymene ouzregui* bed (upper Katian) near Oum-jrane, now visible as a light-coloured line of collapsed talus. (**b**) Excavation by the Ben Moula family in one of the multiple occurrences of the Fezouata Fossil-Lagerstätte (upper Tremadocian) north of Zagora. (**c**) Fossil quarry in the Tafilalt Biota (Bou Nemrou site north of Ksar Tamarna, lower Sandbian) excavating from right to left, but presently exhausted and abandoned. (**d**) A quarry in the basal sandstones of the *Declivolithus titan* beds of the Upper Tiouririne Formation (middle Katian, SE of Oukhit. (**e**) Trench for echinoderms and trilobites at the Isthlou hill site (lower–middle Katian, SW of Ksar Tamarna).

variety of delicate Devonian forms, many of them spinose, partially enrolled and often prepared to museum quality by mechanical abrasion of the rock matrix. 'Normal' trilobites and other fossils were also intensively collected, generating thousands of open fossil trenches, several metres to tens of kilometres long for each rich level, which are located in the open desert, at the top of hills or following the dip of the productive levels along whole mountain faces (Fig. 1). Examples of the latter are also in the kilometric trenches at the Jbel Issoumour –shown in the BBC documentary *First Life* – or at Oufatène (both in rich Devonian trilobitic limestones), and in the exploitations of the black Silurian orthoceratid limestone south of Erfoud (Figs 2 & 3). Larger-scale local quarries were developed for fossils restricted to certain places, either hand-made with crowbars and pry bars (as in Late Ordovician sites across the El Caïd Rami Valley) or with the limited use of explosives (Cambrian *Acadoparadoxides* quarries near Alnif). Underground excavations, normally a vertical pit combined with one or more horizontal galleries up to 10 m long, are also dug to collect complete scyphocrinoids from the lower surface of the latest Silurian *Scyphocrinites* limestone south of Erfoud (Fig. 3a), as well as to reach several richly fossiliferous Late Devonian limestones from the top (see below).

The increase in wealth and local population brought about by the fossil industry, and desert and adventure tourism, supported a widespread improvement in the region's roads in the late 1990s throughout the Anti-Atlas. The search 'brigades' in the region, which included nomad tribes with Berbers and Arabs, increased the number of finds of new fossil levels, which is still growing at a good pace. This brought about the discovery in the early 2000s of the Fezouata Biota (in Lower Ordovician mudstones) in the north of Zagora, and the Tafilalt Biota (in Upper Ordovician sandstones) in the El Caïd Rami Valley and SW of Erfoud (Van Roy 2011; Lefebvre *et al.* 2016*a*, *b* and references therein). Both are made up of a number of localities with preserved skeletal fossils (trilobites, molluscs, brachiopods, etc.), as well as soft-bodied fossils with Burgess Shale- and Ediacara-type preservation, respectively. These Fossil-Lagerstätten also produce an outstanding echinoderm fauna, which has only been exploited commercially in the form of a few 'starfish beds'. Among the Kem-Kem fossils, two new Cretaceous Lagerstätten have been discovered: one with freshwater faunas preserved in fine-grained clay and the other in marine lithographic limestone (Jalil 2015).

Fossil preparation

After the fossil-diggers, a second step in the Moroccan fossil industry is that of fossil preparation, which has increasingly turned into proper 'factories', such as those seen in Erfoud and Rissani (Fig. 4). Up until the mid-1980s, the diggers sold their raw fossils to Moroccan or international middlemen, which meant that they were not particularly attractive and did not sell for a good price. With time, a few of the diggers started to prepare the fossils with rudimentary tools such as nails and hammers made from old car piston caps (Fig. 5a), by chipping off the overlying matrix. They would also stick them back together and reconstruct the damaged specimens, as will be discussed later.

As the prices rose, preparation became more mechanical, using air compressors and a variety of pneumatic air scribes (miniature jackhammers or vibro-tools) to chip away the rock surrounding the fossil. The new machines were rented or acquired as a cooperative: a powerful compressor connected to up to 10 tips, of various sizes and shapes, each operated by a worker (Fig. 5b). These cooperatives or 'fossil factories' are often set up outdoors or in windowless, unfinished buildings, just like the artisans using disk-saws and hand-held polishers in Figure 4.

The pinnacle of fossil preparation is that attained by those specialized in preparing to museum-quality level the very delicate, spiny trilobites, which fetch very high prices and have a permanent market demand. Most of them are Devonian forms obtained by specialized diggers, as these fossils are only recognized in the field by their cross-section in limestone after being dipped in water (Fig. 6a). When brought to the workshop, the taxon of the sample is identified by its section and it is then passed on to the specialist in that genus and species. The specialist then orientates the specimen and glues it back together, starting mechanical preparation with the vibro-tool from above until the dorsum of the trilobite and its main spines are reached. After this, the worker can either chose to detach the latter and continue the preparation, gluing them back at the end (Fig. 6b, c), or use the micro-sandblaster to abrade the softer matrix surrounding the specimen, until they leave all the spines exposed as they were in life (Fig. 7a, b, e, f). The worker is specialized in a specific trilobite taxon, knowing down to the smallest detail about the number, shape and size of the spines that will be encountering as the fossil is prepared from the top, so always producing amazing results (Fig. 7). According to Lebrun (2016), the quality obtained by many of the Berber prepping workers is now equivalent or even superior to their best European or American counterparts in these types of fossils.

The use of sandblasters often occurs along with other expensive equipment like that found in dental-prosthetic laboratories, such as binoculars and dust collection chambers, whose design is often imitated. The very fine abrasive powder, propelled through tiny nozzles, is usually a powdered dolomite, sodium

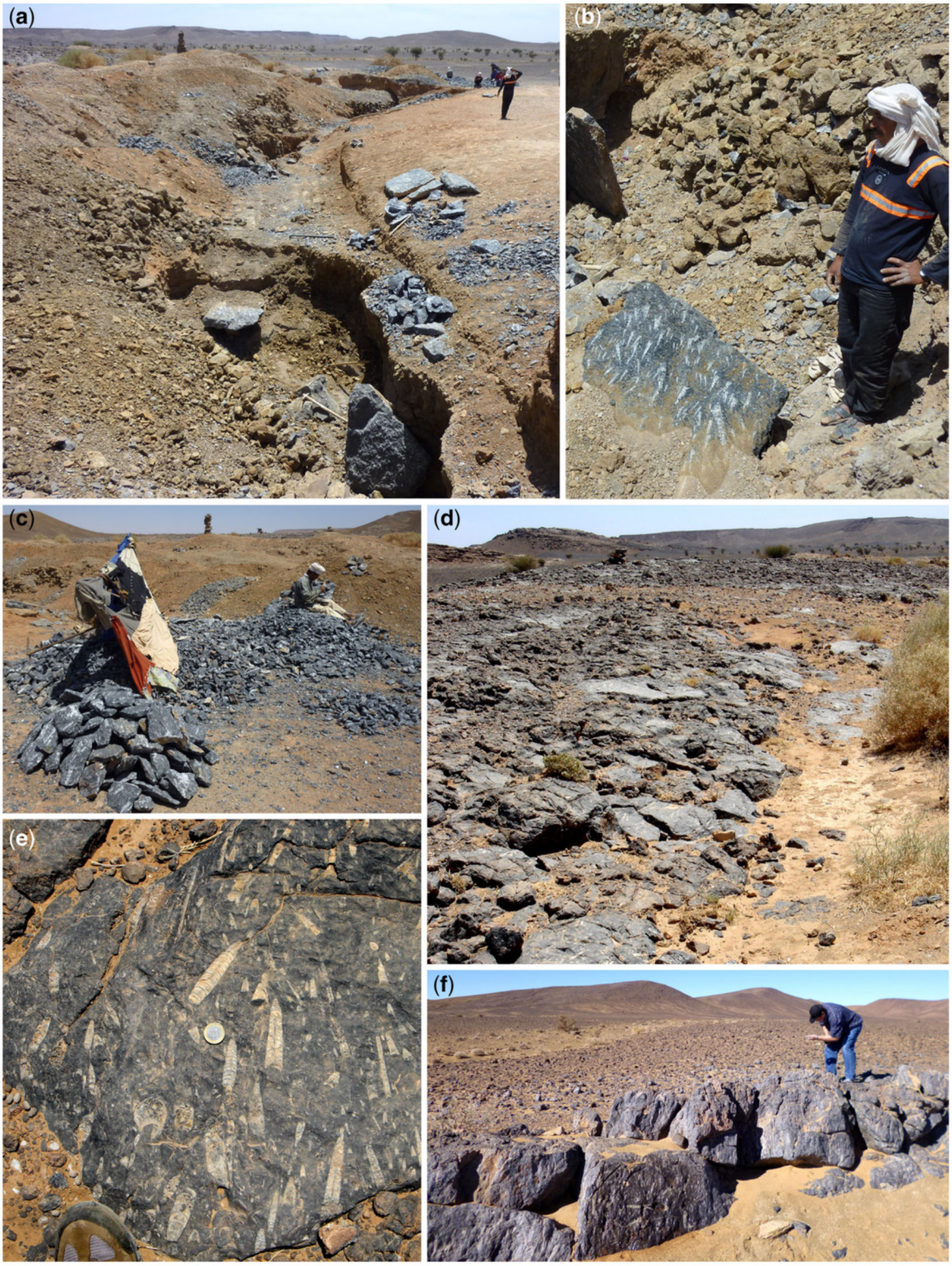

Fig. 2. Natural outcrops and extractive activities in the black orthoceratid limestone (= 'Tazarine stone marble') of the Ludfordian, SW of Erfoud. (**a**) Area where the original quick, shallow, kilometric trenches of the 1970–80s are presently being dug up to 5 m deep (foreground). (**b**) The aim is to extract larger blocks of unweathered fossiliferous rock. (**c**) Loose fragments are processed to prepare smaller objects. (**d**) Natural outcrops of the Ludlow limestone (here gently dipping to the right) are left untouched by the extraction activity and run parallel to the trenches, as the exposed limestone has become brittle and is not conducive to industrial-scale carving and polishing. (**e**) Detail of natural outcrops showing orientated shells of *Arionoceras* sp. (**f**) This ubiquitous black limestone is left unexploited in many regions of the Anti-Atlas, as seen on this vertically dipping outcrop.

Fig. 3. Digging activities in the latest Silurian *Scyphocrinites* limestone. (**a**) Aerial view (from Google Earth) of the monoclinal late Silurian sequence SW of Erfoud showing outcrops of the two distinct limestone beds (with dip and strike symbols) and the impact of the extractive industry of fossils (trenches and pits). (**b**) & (**c**) Vertical, hand-excavated pits in weathered noduliferous shales stratigraphically placed below the *Scyphocrinites* limestone, showing the regular footholds carved into the pit wall. (**d**) From each vertical pit start one or more horizontal gallerie are extended to reach the basal limestone layer, with a single level preserving the articulated stalks and calices of scyphocrinoids. (**e**) The fossiliferous horizon is extracted one fragment at a time and reassembled outside, where the clay is etched-off with a combined mechanical and chemical treatment. (**f**) Detail of two articulated calices of *Scyphocrinites elegans*, during this first *in situ* cleaning process. This will be followed by gluing the slabs together back in Erfoud.

Fig. 4. Artisan 'prep-lab' in a street of Erfoud, with workers preparing pieces of black Silurian orthoceratid limestone by cutting and polishing with the help of radial saws (**a**) & (**b**) or hand-polished with some peripheral retouch with hammer (**c**).

bicarbonate or aluminium oxide, which with enough air pressure is capable of slowly removing the surrounding micritic limestone matrix without damaging the slightly harder fossil.

The best-known workshop for commercial trilobite preparation is the one located in the Tahiri Museum in Erfoud, under the direction of specialist Mr Mohamed Ahechach. This private centre, owned by Brahim Tahiri, sustains several dozen workers among prepping specialists, fossil-diggers and employees of the museum itself. Other highly experienced trilobite preparators in the region are Mr Hammi Oubaha (Rissani), Mr Hmad Ouakki (Erfoud) and Mr Brahim Tamos (Alnif).

Fig. 5. Basic preparation of fossils preserved in a matrix: (**a**) a young man chipping off the rock matrix around a trilobite using a hammer made from a Mobylette piston cap; and (**b**)–(**d**) workers with compressed-air vibration tools, using handkerchiefs to minimize the breathing in of dust. The man in (d) is using a binocular Optivisor eye loupe.

The only case we are aware of where chemical preparation is used is on the articulated scyphocrinoid surfaces from the upper Pridoli limestone. South of Erfoud, articulated peduncles and calices of *Scyphocrinites elegans* accumulated in the contact of the limestone with the underlaying graptolitic mudstones. The surface is partially covered by clays, which are mechanically freed first, and later through dissolution with lye in the field, by the excavation wells. The only – and risky – way to extract these stunning fossil slabs is by excavating the bed from the roof of the galleries in fragments, which are later assembled, glued and consolidated outside (Fig. 3). Figure 3a is an aerial view of the wells dug as entrances to the underground tunnels where the fossils are collected, in parallel with a barely outcropping layer.

Fossil fakes

Trilobites and other invertebrate Paleozoic fossils from Morocco come from a variety of siliciclastic to carbonate rocks, and their discovery involves from broken small pieces to large slabs of fossiliferous rock, so that many specimens show some degree of breakage at the time of collection. For this reason, a lot of material is very quickly glued together, and then a careful preparation process allows the sealing and restoration of cracks where there has been loss of material with a mixture of glue (or resin) and

Fig. 6. Preparation of Devonian trilobites. (**a**) Wet, split limestone showing a tiny cross-section of an enrolled trilobite, hard to distinguish before preparation. Diggers 'mine' fossiliferous beds in long trenches and systematically split rock in search of trilobite sections, which they dip in water to enhance the contrast. Trilobites are taken to the laboratory to continue their preparation. (**b**) Once the two halves of the rock encasing the trilobite are glued back together, the fossil is slowly released from the surrounding matrix by skillfully chipping away with air scribes. (**c**) In the case of trilobites with large spines, like *Dicranurus*, these are carefully separated and arranged so that they can be glued back on the carapace at the end of the cleaning process. (**d**) The preparation ends with the use of micro-sandblasters to eliminate the remaining stuck particles. (**e**) The base of the specimen is screwed to Tupperware lids, and these containers are used for protection from dust while in storage and for transport. (**f**) Occasionally, the preparation of some trilobites with minute and specially delicate spines is performed exclusively with the sandblaster.

Fig. 7. Outstanding preparation of some Lower and Middle Devonian trilobites by: (**a**)–(**d**) & (**f**) Mr Mohamed Ahechach; and (**e**) Hmad Ouakki. (**a**) & (**b**) *Dicranurus monstruosus*, a long-spined odontopleurid featuring ram-like 'horns' on the cephalon. (**c**) & (**d**) *Paralejurus* sp., a styginid prepared ventrally as well so that it is completely free from the rock matrix. (**e**) *Walliserops trifurcatus* (left) and *W. hammi* (right), two Acastidae with a cephalic trident. (**f**) *Koneprusia* sp., a delicate, spiny odontopleurid here seen in right-lateral wiew.

dust from the same rock. Smothering the fossil with car-battery dark powder or staining to mimic the reddish to orangish colour of iron oxides hides the restoration.

As few fossils are found complete and in perfect condition, the continuous improvement of the process described above has caused an increase in the proportion of restored fossils compared to original fossils in many specimens. For example, in relatively complete specimens of large trilobites, only 60–70% of each fossil tends to be authentic. In other cases, as in the large Cambrian *Acadoparadoxides*, a single individual is often made up of parts of several specimens, and free cheeks and their genal spines, plus some thoracic segments or the entire pygidium, may be partially carved into the rock matrix. The filling-in of cracks and missing parts in the original fragments is done, as in the

previous case, using a mixture of glue or epoxy resin with powder from the surrounding matrix, or in combination with car cement as a primary core for larger volumes. Some artisans are so skilled and their techniques so sophisticated that, occasionally, the distinction between the reconstructed and original parts is difficult to recognize even for trilobite specialists (Fortey 2009; suppl. fig. 2 in Gutiérrez-Marco *et al.* 2017*a*).

Besides the activities of restoration/reconstruction indicated above, in order to make the pieces more accessible for sale, an increasing number of fossils coming out of Morocco in the last decade are partially to entirely fabricated. These started to feed a portion of the international demand, and enterprising Moroccans dedicated almost exclusively to fakery are now a reality in cities like Rissani, where a whole neighbourhood is exclusively devoted to this artistic technique for wholesale trade. The consequence is that thousands of Moroccan fakes are ubiquitously found on the market, flooding fossil shows and mineral shops around the world, alongside real fossils. From a Moroccan perspective, however, making fakes is a non-illegal activity, and the local sellers rarely try to pass them off as real fossils but rather sell them as cheap replicas of otherwise rare and expensive fossils, as decorative objects or even as artistic creations. Over the years, this alternative industry evolved as a viable income source in areas of severe poverty, becoming the main livelihood for many Moroccans who not only do not hide their activities but rather have created true 'artisan schools'.

Figures 8–10 illustrate some of the more common type of palaeontological fakes originated in the Anti-Atlas. Some of the fossil shops in the area (Fig. 11) do not hide that they do 'fossil fabrication', although a part of that fabrication relates to the treatment of ornamental fossil rocks.

The most frequent restoration of trilobites is observed in the calymenacean *Colpocoryphe grandis*, which occurs by the millions in outcrops of the Lower Katoua Formation SW of Alnif. As the fossils usually correspond to more or less complete exuvia with detached cranidium, the most common cosmetic improvement – often rather crudely done– consists of gluing the cranidium to the articulated thorax + pygidium with the aim of making the specimens look complete (Fig. 10b–e).

After the discovery of virtually monospecific assemblages in the Ordovician Fezouata and Tafilalt biotas, related to true gregarious behaviour in trilobites, Moroccan craftsmen started to produce large plates – up to 3 m^2 – with a number of specimens embedded in them, normally sticking together large asaphids or nileids (*Asaphellus*, *Megistaspis*, *Platypeltoides*, *Symphysurus*). But, occasionally, some slabs mix trilobites from different levels and localities, as occurs with the Cambrian genera *Acadoparadoxides* and *Cambropallas*, sometimes seen in 'death assemblages' that have never been documented in the field. However, the commercial value of these fakes is not only increased by its aesthetic power and the apparent rare occurrence of a large number of specimens, but also through the inclusion of some casts placed on real matrix alongside the true specimens.

The fossil fakery is widespread in localities such Rissani, Erfoud, Alnif or Tabourit. From there come the vast majority of the individual trilobite replicas seen in the market, which include the fabrication of oddities (Fig. 9f). Some imitate fossil scorpions (mass produced), others are chimeras and supposed new trilobites, created by adding original pygidia or carved cephala to falsified parts in order to produce 'fantasy taxa'.

Finally, a successful product of the last few years is the fabrication of so-called 'trilobite *paellas*' or 'composites' with several formats but generally of small size. These consist of a collection of resin casts of different species of Devonian trilobites from different ages and localities, placed on a slab as if they were a death assemblage, and showing aesthetic orientations (e.g. radial, spiral, ring-like, random). The trilobites lumped on each single plate were always different and were placed over the real rock by means of a coating surface formed by a mixture of resin or plaster, with powder of the ground matrix.

Fakery proliferation among Moroccan fossils has been repeatedly discussed in non-specialized print (e.g. Burkhard & Bode 2003; Albin 2009; Sicree 2009), as well as in multiple web pages from museums and amateurs. Beautiful examples of fakes are common in public Facebook groups such as 'Trilobite fakes and restorations'.

Fossiliferous ornamental rocks

The Paleozoic succession of the eastern Anti-Atlas has yielded several fossiliferous beds susceptible for use as ornamental rocks. A vigorous industry is being developed mainly in Erfoud to cut, carve and polish these rocks, belonging essentially to two types of fossiliferous limestones (Figs 12–14; names after Benharref *et al.* 2014):

- 'Tazarine stone' (or 'Tazarine marble'), consists of a decametric to metric black-bluish orthoceratid limestone, which shows aligned *Arionoceras* (finger-sized orthoceratids) and *Temperoceras* (larger conchs), with gorgeous fragmocones preserved in white calcite. This bed is of Ludfordian (Silurian, 'late Ludlow') age according to associated conodonts (see Corriga *et al.* 2014; Voldman *et al.* 2017).

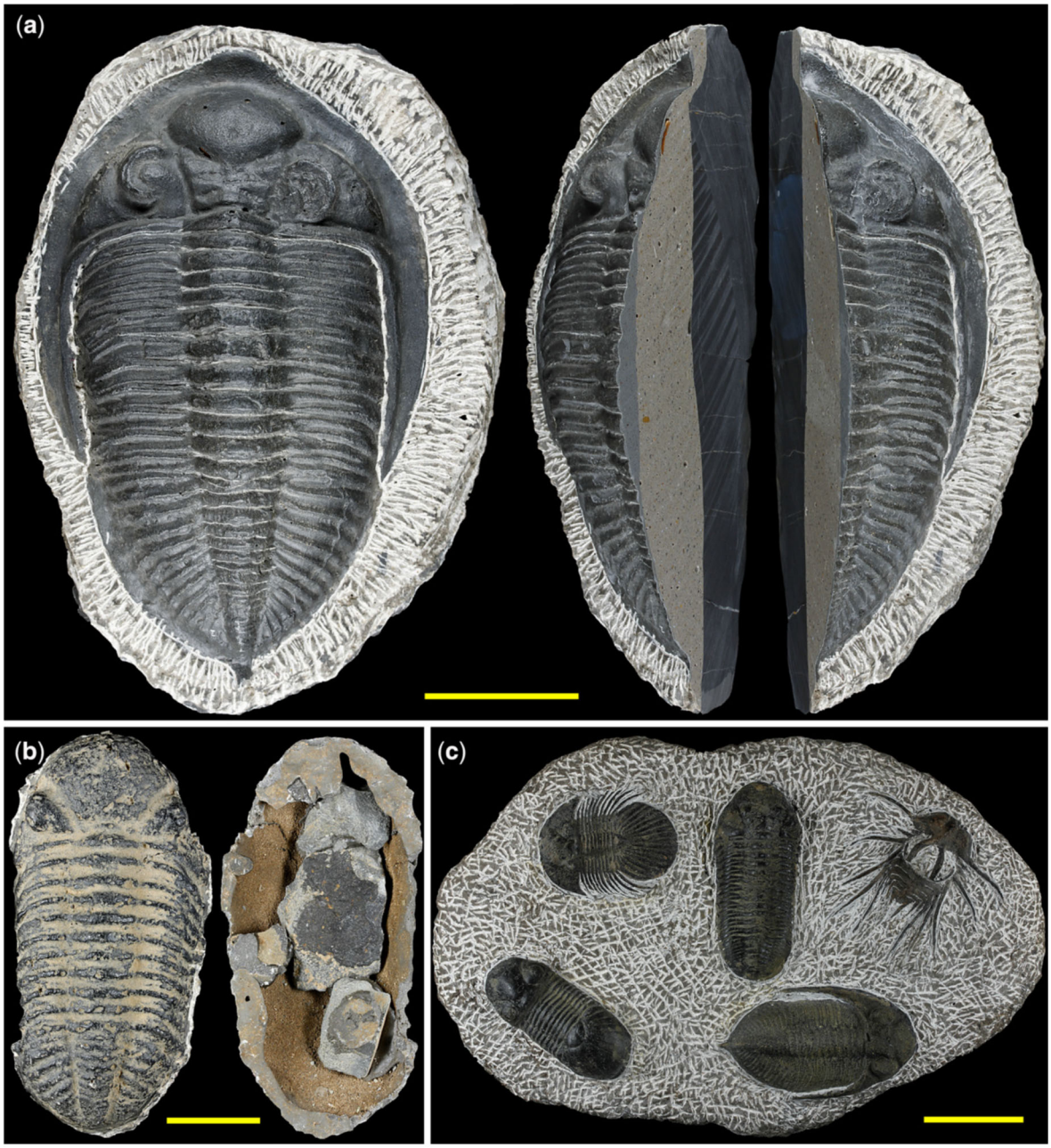

Fig. 8. Some examples of completely fake Devonian trilobites from the Anti-Atlas. (**a**) An epoxy replica of a large? *Odontochile* mounted on real rock. The longitudinal section (right) reveals that it consists of a thin layer of dark resin applied from above in a concave negative mould (it is thickened in the centre), then filled by car cement of light colour and then mounted on a grey limestone. Finally, the surrounding matrix was gauged to mimic normal preparation marks by vibro-tools or points. (**b**) Poor fake *Phacops* trilobite, entirely cast from resin, after being detached from the rock matrix. The lower view of the same specimen (right) shows the large void under the trilobite, which was internally glued to some rock chips in order to strengthen the mould and improve the mounting on the rock. (**c**) A typical 'trilobite *paella*', showing five fakes of different species, with signs of air bubbles in the matrix and exoskeletons. Scale bars: (a) & (c) 40 mm; and (b) 30 mm.

- 'Erfoud stone' (or 'Erfoud marble'), a name encompassing different brownish to reddish limestone beds with orthoceratids and ammonoids, ranging from upper Givetian to middle Famennian (Middle–Upper Devonian). The most famous of these units is the *Gonioclymenia* Limestone (Hartenfels & Becker 2018).

Both Silurian and Devonian limestones were trenched along strike for tens of kilometres in a

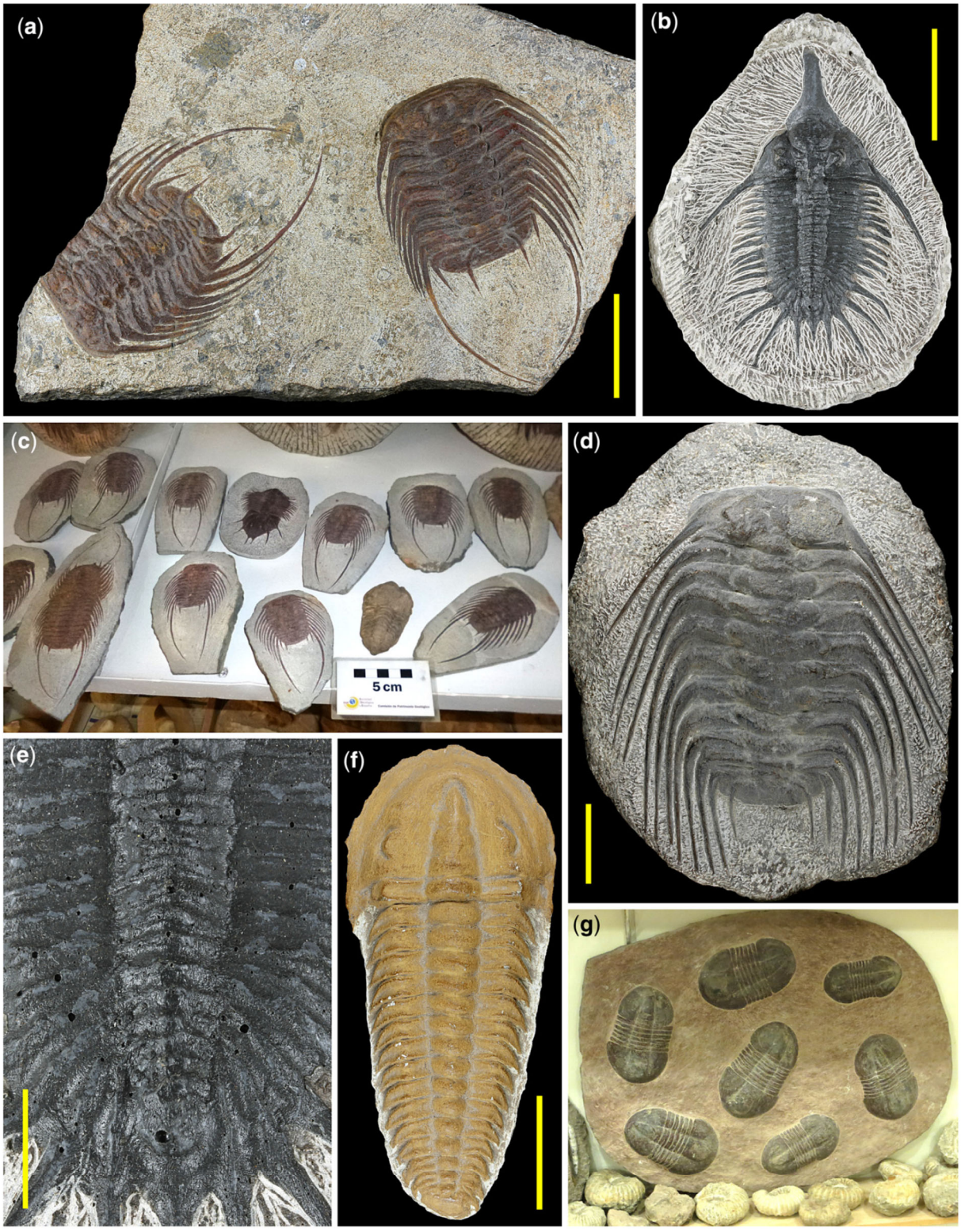

Fig. 9. More examples of trilobite fakes among (**a**), (**c**), (**d**) & (**g**) Ordovician, (**b**) & (**e**) Devonian and (**f**) supposedly Cambrian forms: (**a**) beautifully carved *Selenopeltis* in fine sandstone; (**b**) & (**e**) an entirely fake *Psychopyge elegans* mounted on limestone, surrounded by preparation marks – the detail in (c) shows small surficial bubbles (black spots); (**c**) different fakes of *Selenopeltis longispina* ready for sale; (**d**) *Selenopeltis buchi* with carved spines on a microconglomeratic sandstone slab; (**f**) invented trilobite recalling an unexisting giant lower Cambrian form, made in plaster; and (**g**) composite slab (about 80 cm across) with seven fake Tremadocian *Platypeltoides*. Scale bars: (a), (b), (d) & (f) 40 mm; and (e) 10 mm.

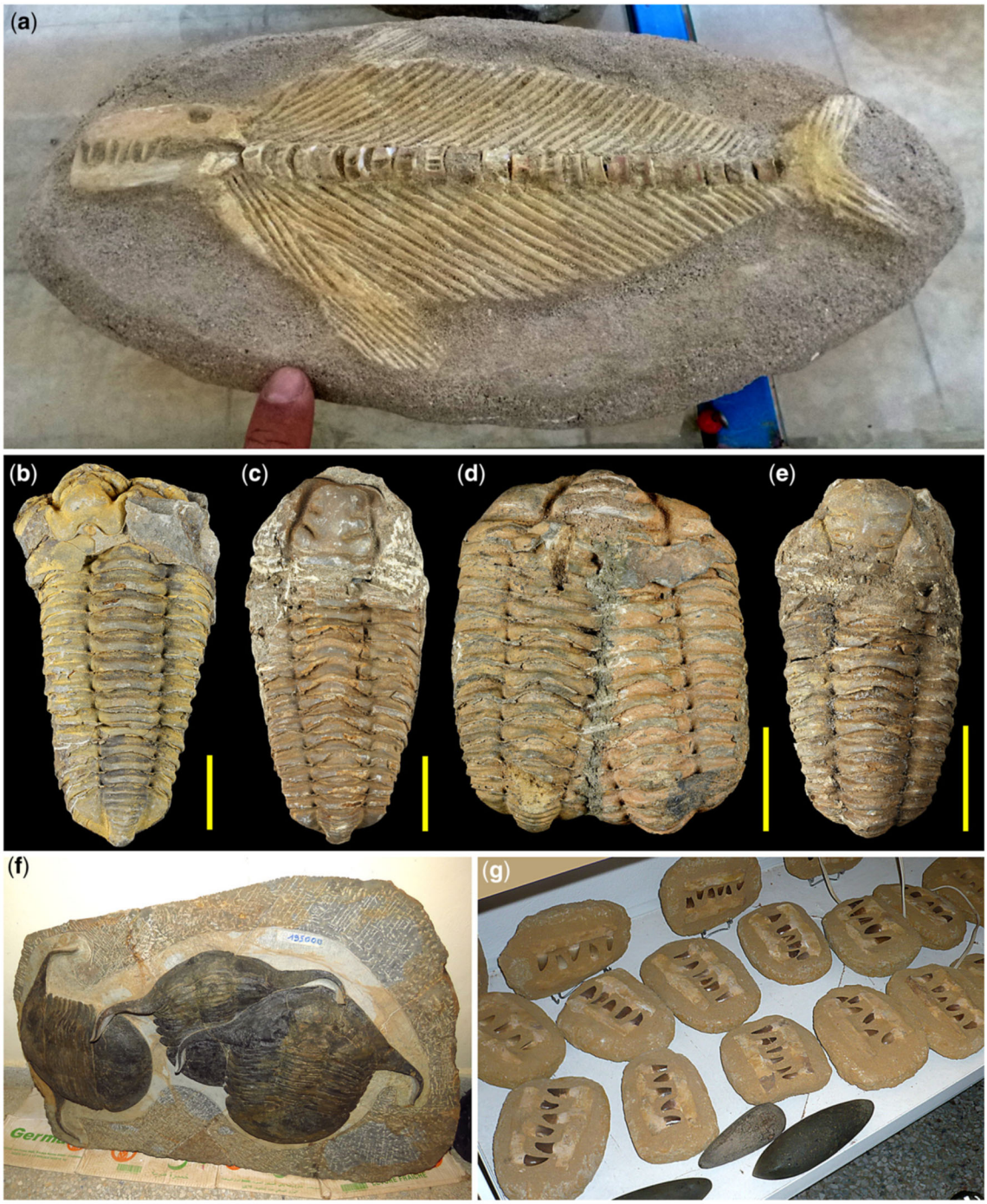

Fig. 10. Additional examples of fossil fakes seen in Erfoud shops. (**a**) A chimera that resembles a fossil fish with a reptile head, carved in plaster mixed with soil, painted and with true vertebrae of different fossil fishes mounted in its centre. (**b**)–(**e**) A series of specimens of *Colpocoryphe grandis*: (**b**) natural moult stage with inversed cranidium, (**c**) thorax + pigydium mounted with the cranidium of a larger specimen; (**d**) two thorax + pigydia combined with a single head, partly reconstructed; and (**e**) thorax + pigydium of the species mounted with a cranidium of the phacopid genus *Dalmanitina*. (**f**) A slab with three heavily reconstructed specimens of *Asaphellus stubbsi*, with unusually long and robust genal spines that are mostly fake. (**g**) A group of fake mosasaur 'mandibles' assembled with real teeth from different specimens. Scale bars: 20 mm.

first exploitation period. This was followed, in the last 15 years, by a second period where part of the trenches have been re-opened and deepened in search of larger blocks. This is what happened with the black Silurian limestone (Fig. 2) but the Famennian *Gonioclymenia* Limestone, extensively exploited

Fig. 11. Examples of facades of a (**a**) big and (**b**) small fossil shops in Erfoud, announcing the 'fabrication' of fossils, like the big ammonites sculpted in sandstone shown in (a). (**c**) Detail of a rocky slab photographed in a shop at the Tichka mountain pass (High Atlas) showing, from top to bottom, carvings of a Cretaceous ammonite, sea urchin, sea cucumber, starfish and, to the right and 'coexisting' with the others, a 'fossilized' Berber dagger.

in the western and southern Tafilalt Platform, was locally affected by subsurface mining down to 20 m depth (Fig. 12).

A more accurate extractive industry was developed on other thicker Devonian limestones. This involves a set of conventional quarries made with heavy machinery, allowing the extraction of metric-sized blocks to carry to the factories. Not being as spectacularly fossiliferous as the Famennian limestones, these only produced moderate results which has resulted in the closure or intermittent exploitation of most quarries.

To compensate for the demand of large slabs of 'Erfoud stone', rich in orthocone nautiloids and beautiful goniatitids, some of the less attractive portions have incorporated 'added' fossils before its final polishing. This process is quite evident in the fabrication of artistic 'composites' carved in this Devonian limestone, as in the creative sculptures or large slabs of artificially distributed fossils (Fig. 12d). But sometimes this work is only distinguishable by specialists, as is the case of the joined occurrences of the goniatitid genera *Gonioclymenia* and *Kalloclymenia* in slabs offered for sale, which denoted artificial assemblages (Hartenfels & Becker 2018).

The ornamental stone industry has so far focused on the cephalopod limestones from Tafilalt but the Devonian crinoid limestones may be the next ones

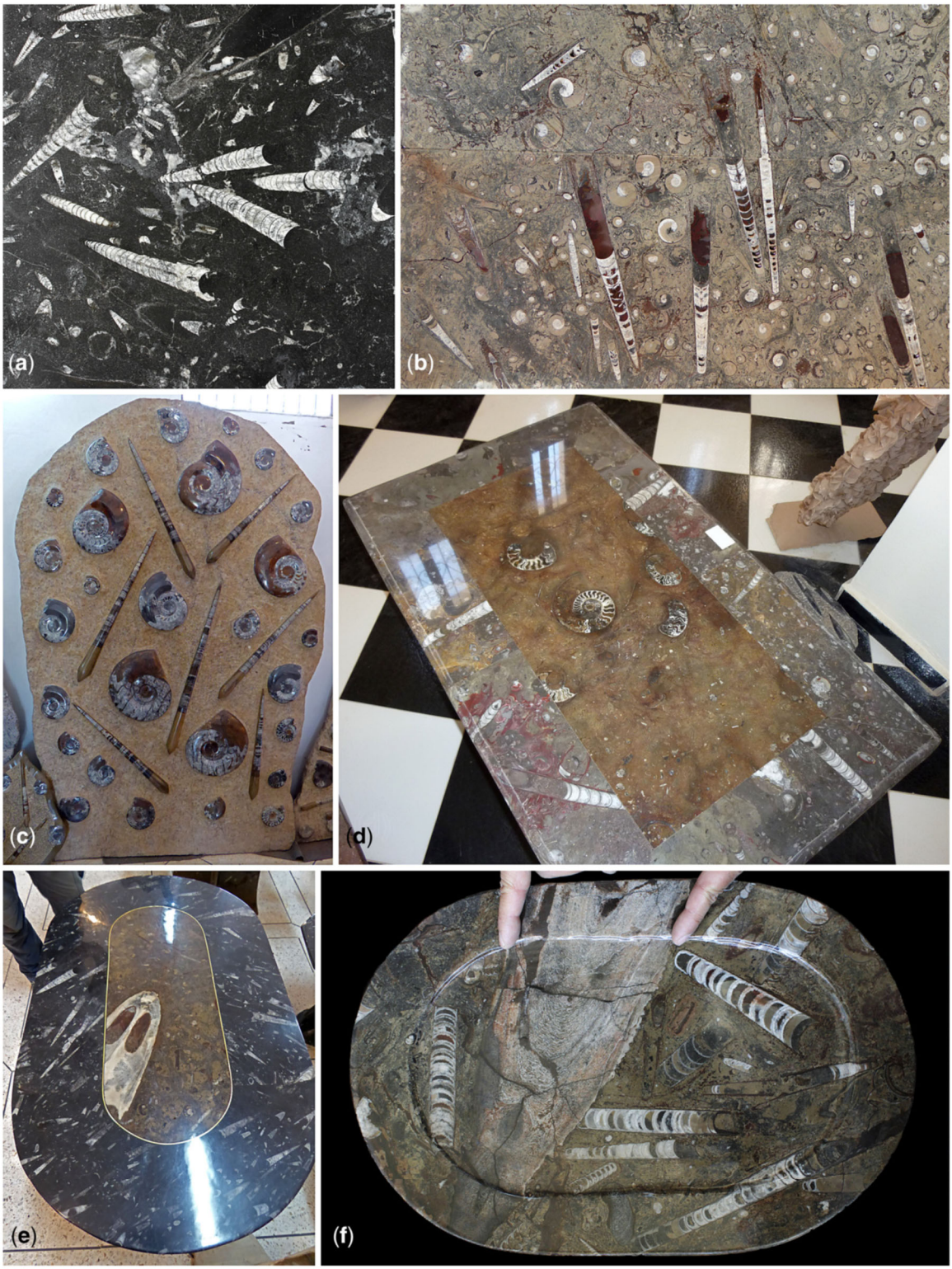

Fig. 12. Examples of ornamental rocks rich in fossils from the Tafilalt region. (**a**) Black Silurian limestone ('Tazarine stone') showing several phragmocones of Arionoceras sp. (**b**) Brown to reddish Devonian limestone ('Erfoud stone', not polished) with orientated nautiloids in a background of small goniatitid shells. (**c**) A 'composite' of polished specimens of *Gonioclymenia* (large ammonoids) and nautiloid orthocones, artificially assembled in a single slab. (**d**) Upper view of a stone tabletop combining two types of 'Erfoud marbles' from different horizons and with different fossils. (**e**) Stone tabletop combining an external piece of black Silurian limestone with a central piece of brown Devonian limestone, the latter showing a section of a fish skull. (**f**) A tray made of Devonian limestone showing nautiloid remains and a section of a even larger fish skull (see the person's fingers for scale).

Fig. 13. Diverse objects carved in fossiliferous stones from the Tafilalt. (**a**) Typical exhibition in a shop in Erfoud, where craftsmen offer fountains, shower plates, sinks, bottle racks, sculptures, dishes, etc. (**b**) Two 'composite' slabs with polished nautiloids and small ammonoids. (**c**) A selection of objects made in black Silurian limestone (tray, vase, Coca-Cola bottle). (**d**) A complete toilet bowl (real size) carved in Devonian cephalopod limestone.

to be subject to exploitation (a Famennian lenticular bed may reach up to 9 m in thickess).

'Fossil economy' and international dealers

Just as Morocco has been considered as a 'paradise for geologists' (see the monograph 'Paradis des géologues' published in 2017 by *Géologues*, the official journal of the Geological Society of France (Blaizot & Jébrak 2017)), the Anti-Atlas, and particularly Erfoud, is currently labelled the 'trilobite capital' of the world. According to an article by Lawrence Osborne published in *The New York Times* (Osborne 2000), the Moroccan fossil industry generates an annual trade of about US$ 40 million per year, although a great part of this amount would come from fossil export and later retail sales in other countries.

Despite middlemen and retailers making higher profits than Moroccan diggers and local shops in the

Fig. 14. Extractive and preparation work on the ornamental rocks in the Tafilalt. (**a**) Lower Devonian outcrop south of Erfoud with large signs made of handpainted stones indicating the access road to a quarry (=carrière) selling fossils. (**b**) Disc saw cutting a black Silurian limestone block. (**c**) Slabs cut from Devonian limestone with large ammonoids before polishing. (**d**) Abrasive polishing process and small circular polisher on a moving arm. (**e**) Aerial view (from Google Earth) showing digging activities in the Famennian *Gonioclymenia* Limestone west of Lahkraouia – notice how the bed is interrupted by a fault and presents a secondary fold, both of which are perfectly followed by the aligned trench and pits. Photographs (b) (c) & (d) are taken at the 'Macro Fossiles Kasbah', Erfoud.

area, the 'fossil capitalism' or 'trilobite' economy – as it has branded – has a considerable impact on a large part of the Anti-Atlas (Figs 15–17). Conservative estimates from 2005 by the Moroccan government calculated that not less than 50 000 of local people were involved, direct or indirectly, in the fossil

Fig. 15. Aspects of some local fossil shops specializing in Paleozoic fossils: (**a**), (**b**) & (**d**)–(**f**) near Alnif; and (**c**) in Erfoud. A number of these shops specialize in trilobite sales, as indicated on road signs and wall inscriptions. Incorrect phonetic transcription of scientific names and even the fossil group itself – for example, 'trolebette' in (d) – is quite common among the most humble fossil traders.

trade, although estimates from some professionals in Rissani (December 2017) increased this number by 8000–10 000. Most of them are poor Arab or Berber inhabitants of the rural Tafilalt and Alnif regions where only a limited number of jobs around the tourism and service sectors are available. These people, plus the nomad tribes with deep roots in the even more deserted areas of the central and eastern

Fig. 16. The interiors of various fossil shops showing the merchandise: (**a**) storage in the basement of a private house in Erfoud, with a mix of Paleozoic and Mesozoic fossils from different regions; (**b**)–(**c**) batches of fossils classified by species for sale to collectors and middlemen in the shop of the Tahiri Museum in Erfoud; and (**f**) a selection of fossils from the Fezouata Formation (brown pieces) for sale in Taychout, near Alnif.

Anti-Atlas, represent the majority of diggers and miners in the entire area. For many of these, fossils are their main business, supporting their lives and their extended families, or help to supplement what they can earn from occasional construction, pastoral or farming jobs. However, since 2016, part of this

Fig. 17. (**a**) Exterior of the Tahiri Museum of Fossils and Minerals near Erfoud. (**b**) A well-known trilobite shop in Alnif, with its owner Mr Mohamed Bouyiri holding a trilobite slab. (**c**) & (**d**) A hut with a porch selling fossils and a hand-drawn illustrated road sign near Tiguerna.

well-trained 'digging force' has moved temporarily to better-paying mining activity in the area: the open trenches extracting barite from veins hosted mainly in Cambrian rocks.

A second and better-paid step for the Moroccan workers involves people devoted to fossil preparation and fakery, even if only for not having to spend long days in the desert digging trenches or dangerous wells and underground galleries in search of fossils. They also act as small local middlemen, paying the diggers for the fossils they find, and often work for organizations that are dedicated to the larger-scale fossil trade.

The third step is that of major Moroccan middlemen, who store significant stacks of fossil material in their shops or local warehouses – thousands to tens of thousands of specimens of each type – and they sell directly to certain American, Asian and European traders. All of this material is destined for exportation, normally in containers using maritime routes, although some of them are also transported by road into Europe, normally coinciding with the main fossil shows in France and Germany.

In the past, most Moroccan fossils were offered for sale by international dealers, as most had Moroccan partners, but over the last decade a number of Moroccan wholesalers and entrepreneurs have been present at most mineral and fossil shows around the world, selling products that have purchased directly from the diggers or the local middlemen.

The improvement in communications in the region has allowed some local sellers to offer their material for sale through the Internet, including renowned online auction sites. This is also the case for the distribution and sale of large slabs with lumped fossils, some attractive *naïf* fakes, and diverse products of large weight and size elaborated in the ornamental rocks typical from the area (Figs 11–13). They are all offered to be delivered 'to your doorstep' in Europe in a truck that leaves Erfoud weekly or, in the case of air freight (e.g. to the USA), delivered to an airport customs office of your choice, with no other condition than paying the agreed transport price per kilo of rock.

The bulk of the Moroccan fossil trade is centred on the world's major fossil and mineral shows, where specimens are sold in lots to specialized boutiques, as well as gift shops in museums and shopping centres. These major shows are held annually in Tucson (Arizona, USA: January–February), Sainte-Marie-aux-Mines (France: June), Denver (Colorado, USA: September), Munich (Germany: October) and Tokyo (Japan: November–December). In some of the above-mentioned shows, the attendance of Moroccan dealers is well known: with about 100 Moroccan vendors in France in 2017 and 40 Moroccan fossil exhibitors in Munich. In addition to this, Moroccan vendors often participate in smaller but well-established annual mineral and fossil shows in more than 50 cities in Belgium, France, Germany, Italy, Spain, Switzerland and the UK. Moroccan wholesalers who participate in the trans-oceanic world's major fossil shows export large quantities of fossil annually, and the unsold material is left in storage units (as in the USA) from one year to the next.

It is the number and diversity of Moroccan Paleozoic fossils that makes it capable of sustaining this market. Each year, millions of specimens of commercial quality are collected from natural outcrops, directly sustaining about 18 000 families in the Anti-Atlas. Fossil wholesalers (mostly Moroccans, who have displaced those of other nationalities) actively participate in most European fossil fairs and a number of shows around the world. Due to the large amount of business, one such wholesaler stated that 'mineral and fossil sales are great for Morocco's economy' (Brahim Tahiri in Sicree 2009), having traded tens of thousands of specimens in just one of the major international shows.

However, this market has limits, and these are economical. For many years, the intensive exploitation of trilobite sites from the Cambrian, Ordovician and Devonian has brought new species to the markets every year, so the sales never stagnate. Also, the discovery of very large slabs with giant forms and the production of exquisitely prepared spinose trilobites has caused an huge increase in price to astronomical figures; which, however, will always be affordable to millionaires and trilobite collectors like Bill Gates and Nicolas Cage (according to Osborne 2000). But the pace of new trilobite discoveries may be reaching the top of the rarefaction curve. As a regular reporter at the Sainte-Marie-aux-Mines show indicated (Lebrun 2016), no new trilobite species were offered there for sale in 2016 and, perhaps, the fossil localities from Morocco are showing signs of exhaustion. A decline that seemed to recover slightly the following year, with trilobites coming from new Cambrian and Devonian localities (Lebrun 2017). This decline will eventually happen, even if the future of this trade is limited by new Moroccan laws strictly regulating fossil export.

Legal and geoethical problems

From the beginning, the Moroccan fossil trade has brought about various ethical problems. The most important one is the destruction of fossil sites and loss of valuable specimens, which are exported in large quantities not always with a corresponding excavation or export permit. Such permits should be attained by the application of standard trading regulations in general and mining regulations in particular.

The Association for the Protection of the Geological Heritage of Morocco (APPGM) has pointed out the lack of specific legislation regulating the country's management of its geological heritage (including palaeontological). So far, most of the fossil trade has been centred around trilobites and other invertebrate fossils, the search for which has enabled the survival of many of the poorest families settled in the desert areas of the Anti-Atlas. But the auction of a plesiosaur skeleton in Paris (7 March 2017: cancelled) and a large sauropod tail in Mexico (16 January 2018: sold), both apparently illegally exported

from Morocco, has focused the debate on vertebrate fossils. These are generally rarer and of greater concern than Paleozoic invertebrates, both for scientists and for administrations.

Even the APPGM does not support the prohibition of trade or export of some invertebrate fossil groups, especially because many families depend on the sector, but as a scientific association they push for the establishment of specific regulatory texts to prevent the export of fossils of greater value and to stop once and for all the systematic and ongoing deterioration suffered by the rich Moroccan geological heritage.

The massive exploitation of fossils in large areas of the Anti-Atlas has brought more than just economic benefit to parts of the local population and, in particular, Moroccan wholesalers selling in the markets all over the world. Also, science has benefitted from the trade as there are thousands of new marine invertebrate taxa (especially trilobites and cephalopods) discovered thanks to the number and volume of excavations, in addition to the extraordinary Cretaceous reptiles and fishes. These new fossils enable a better understanding of Paleozoic marine environments, and the palaeogeographical relationships of northern Africa with European and American basins for each epoch, which were hardly known before the boom of the fossil trade. The thorough hard work of systematically exploring the area carried out by the illiterate Berber people living there brought to the light several Fossil-Lagerstätten such as Fezouata (Lower Ordovician shales), Tafilalt (Upper Ordovician sandstones) and Kem-Kem (Upper Cretaceous), among others. These biota have opened windows into the past due to the extraordinary preservation of organisms very rarely encountered in the fossil record.

However, there are some cases where the Moroccan fossils have been in the centre of famous controversies, and not exactly caused by fakery. The oldest, and better known, triggered the uncovering of the so-called 'Gupta affaire', when a reputed Indian palaeontologist published, as derived from the Indo-Tibetan border of the Himalaya, some Devonian goniatitids identical in preservation and weathering to hematite moulds recovered from the vicinity of Erfoud, and available worldwide from fossil dealers (Talent 1989; Shah 2013 for references). A more recent case of a different nature is the 'Corbacho affaire', in which a Spanish collector and fossil dealer, acting as a pseudopalaeontologist, published more than 20 new trilobite species over the years without the appropriate scientific control of a peer-reviewed journal (Gutiérrez-Marco *et al.* 2017*b*).

With regard to the negative impact of massive commercial digs on science, we can comment on the case of the ammonoid *Gonioclymenia*, a real icon of Moroccan Devonian fossils due to its beauty and unusual large size – up to 50 cm in diameter. However, more than 30 years of intensive exploitation in search of this taxon has caused the disappearance of almost all the outcrops of Famennian *Gonioclymenia* Limestone (Hartenfels & Becker 2018), and 'nowadays hardly any new material of the genus with good preservation can be found' *in situ* (Korn & Bockwinkel 2017, p. 97).

The reverse is true for the black Silurian orthoceratid limestone, exploited along kilometric trenches dug parallel to the untouched natural outcrops, since the 'Tazarine marble' industry can only use the strong, unweathered rock under the surface. For this reason, future macro- and micropalaeontological studies of the spectacular fossils in this Ludfordian limestone (Krögger 2008; Corriga *et al.* 2014; Voldman *et al.* 2017; Pohle & Klug 2018) are guaranteed despite the regional looting and huge visual impact of its exploitation.

Notwithstanding the casuisty regarding the exploitation of single fossiliferous beds or the rich ornamental fossiliferous rocks, there is certainly an ethic movement among scientists and national authorities towards stopping the legal sale overseas of fossils illegally exported from Morocco. A part of these could be classified as Moroccan heritage at risk and are recognized as a global scientific resource but, in general, palaeontological material is sold off and circulates in huge quantities in countries that have quite restrictive laws for the effective protection of their own fossils and fossil sites, which seems rather hypocritical. Besides this, well-known research groups and museums from many countries in Europe and North America travel regularly to Morocco to buy fossils; indeed, most scientific discoveries on early Paleozoic African palaeontology in recent times have an origin in collections purchased directly from Moroccan diggers. An example of this is everything surrounding the Fezouata Lagestätte, whose most significant fossils were found (and sold) by a single family established in the Alnif region. This family is headed by Mr Mohamed Ben Moula (Oussaid Trilobites, Taichout), who is regularly acknowledged in many papers, including those in the world's leading scientific journals, and who received the 2017 Mary Anning Award from the Palaeontological Association of the UK. This distinction recognizes those non-professional people who have made an outstanding contribution to the science of palaeontology, in this case for his discovery of the Fezouata Biota and his collaboration in providing access to such special material to professional palaeontologists.

In a recent national meeting held in Rabat (November 2017) on Moroccan geological heritage, the Ministry of Energy, Mines and Sustainable Development expressed its interest in establishing mechanisms to protect, preserve, manage and

disseminate the geological and palaeontological heritage from Morocco, at both a national and international level. While waiting for a specific legal framework the ministry alludes to Article 116 of the new mining legislation, which establishes that the extraction, collection and trade of mineralogical and fossil specimens, and meteorites will be subordinated to authorization issued by the administration. On the other hand, the APPGM, co-organizer of this meeting, considers that the main objective is to remind the public authorities and the civil society of the importance of preserving the great geological heritage of Morocco, a country that deserves to have a suitable legal protection framework. A second scientific national society, the Moroccan Association of Geosciences (AMG) also has a commission on geosites and heritage, which arranges specific activities along with its regular meetings.

In any case, the search and extraction of fossils in the Anti-Atlas has also generated some very positive aspects, such as the promotion of palaeontology as an economic resource derived from the fossil trade between tourism companies (visits to fossil sites, workshops and local museums) and the important contribution of educating children and the rest of the local community about Earth's history. After all, many professional palaeontologists discovered their love of fossils from specimens bought in shops and, nowadays, Moroccan fossils can be found in shops in many of the largest natural history museums around the world.

Future developments

In spite of the existence of important fossiliferous localities in the Paleozoic of the entire region, and the impact of the fossil trade on the economy of large areas, fossils were frequently ignored or undervalued in most of modern geological guides, and selected geosites of the Anti-Atlas barely include references to fossils (Ouanaimi & Soulaimani 2011; Rjimati *et al.* 2011; Saddiqi *et al.* 2011, 2015; Soulaimani & Ouanaimi 2011). Hopefully, circumstances seem to be changing and some Cambrian, Ordovician and Devonian outcrops, among them those in Fezouata, north of Zagora, and those of Hamar Lahdag, north of Merzane, have begun to be included in strategies of scientific delimitation, conservation and geotourism (El Hariri & Lefebvre 2015; Errami *et al.* 2015; Lagnaoui *et al.* 2015; El Hassani *et al.* 2017; Beraaouz *et al.* 2018). The first steps have been taken for the dissemination and protection of the rich Moroccan geological heritage with the approval in 2014 of the M'Goun UNESCO Gobal Geopark in the central High-Atlas, the creation of the Azilal, Tazouda and Marrakech regional geological museums, and with the establishment of the Fezouata Geosite. The latter is one of the five vulnerable geological sites cited by the Alarm Call of Marrakech (signed in 2015), which promoted its consideration to be included in the UNESCO world list of global geosites.

According to the APPGM, the next step is collaborating with the government to develop a law that regulates the extraction and sale of Moroccan fossils, gives rights to workers and prevents the export of fossils, while favouring the academic training of young people and the creation of public museums that in turn can generate tourism and sustainable development. But the enactment of such a law is receiving pressure from large wholesalers and can count on the opposition of extensive sections of the local population who have fossils as their main way of life. Thus, the law will have to be very careful and find a balance to keep allowing the sale of material from particularly extensive outcrops, or those which bring the most added value to the local industry. An example of the former are the two horizons with the trilobite *Colpocoryphe grandis* located in the Lower Ktaoua Formation (Upper Ordovician), which extend for tens of kilometres and could be exploited indefinitely. This trilobite has been present in shops around the world for more than 20 years and we estimate that about 15 million specimens have been sold to date. In some shops in the Anti-Atlas they are sold in closed boxes of 100 and 200 specimens, and we recently witnessed the sale of 15 000 specimens from a single dealer to a British client. However, the present extraction of fossil beds with this almost monospecific assemblage of *C. grandis* is only minimally affecting the known extent in the Alnif region, with the possibility of extending it to other regions in the Anti-Atlas. The second example of sustainable exploitation is that of the delicately prepared Devonian trilobites, which sustain an important population of fossil diggers who specialize in the finding of these fossils by searching for their sections in the rock.

An alternative suggestion made by many protectionists is to promote the production and sale of replicas for all types of Moroccan fossils, both nationally and internationally. This may progressively substitute the massive search and exportation of original fossils, which have resulted in the exhaustion of many outcrops (Fig. 18). An alternative proposal to total protectionism regarding digging activities could be to prohibit extraction through the use of explosives or heavy machinery including portable pneumatic jackhammers, which are becoming common in many sites. The reduction to exclusively manual 'production' would be expected to limit the impact on the environment, and produce an increase in fossil prices that would compensate by increasing the benefits to the fossil workers.

Fig. 18. (**a**) One of the 46 'Kess-Kess' or deep-sea hydrothermal mud mounds of the Lower Devonian of Hamar Laghdad, with the Merzouga dunes on the horizon: the richly fossiliferous shales around them were so intensively collected that fossils have now become rare. (**b**)–(**e**) Examples of intensive collection in Devonian strata, leading to accumulations by middlemen of piles of (**b**) corals, (**c**) bryozoans and (**e**) nautiloid calcitic fragmocones, shown in more detail in (**d**), for wholesale.

Regarding museums, the Tahiri Museum of Fossils and Minerals near Erfoud and the Taddart Geological Museum of Midelt are probably the only private fossil museums in Morocco. Both preserve and display scientifically important specimens to promote geological education. The former (Fig. 17a) includes a number of dinosaur skeletons handcrafted in plaster and casts of emblematic pieces from the USA. The museum is operated by a fossil dealer and wholesaler who sells large quantities of fossils in the most important fairs around the globe. But his museum also disseminates the rich heritage of the area, while keeping some outstanding pieces in Morocco and inviting visitors to see the workshop where Devonian trilobites are prepared. Access to the museum is free, and it is sustained by the profits from his mineral and fossil shop, which is often included in international tourist routes. These examples suggest that a network of strategically placed public palaeontological museums in the Anti-Atlas could contribute to education and a sustainable development in the region. This coincidences with one of the main priorities established by the AAPGM, which argues that the preservation and promotion of the geological and palaeontological heritage of Morocco requires the creation of national and on-site museums – the first of which are planned to be built in Marrakech and Zagora, respectively – on which to base a museological culture as an useful tool for local community development and unique learning opportunities. A first catalogue of Moroccan geological heritage, including geosites, geoparks, fossils, meteorites and rock engravings, is being currently edited as a special issue of the Geological Society NMSG (Rabat), and an inventory of vulnerable geological sites is underway in a close collaboration between the ministry and Moroccan universities.

While a legal framework is developed, fossil trade in Morocco is being regulated by Article 116 of the afore-mentioned new mining legislation. But staying ahead of the new law, and following the steps taken by some countries like Madagascar, some wholesalers see part of the commercial future of Moroccan fossils by treating them as plain handcrafted objects. This interpretation enables fossils to be exportable if they have gone through any kind of handcraft processing: polished areas, sections, reconstructions, preparation of spiny trilobites, etc., or have been turned into pendants, necklaces, bracelets or charms.

Conclusions

The business of searching, preparing, 'fabricating' and selling fossils and ornamental fossiliferous rocks in Morocco has been a reality that has provided a way of life for tens of thousands of people in the region for over 25 years. Any regulation or law that curtails this activity should consider the creation of alternative income sources that ensure the survival of the affected local population. This would need to be done following the parameters for sustainable development expressed by El Hassani *et al.* (2017) or the Association for the Protection of the Geological Heritage of Morocco (APPGM).

The main characters directing the trade and export of fossils in Morocco and the numerous middlemen and wholesalers of that nationality, who have gradually replaced the international dealers, now offer an unlimited amount of fossil material in fossil fairs and shows globally, and in particular in Europe and North America.

The immense extent of the excavations in search of commercially exploitable fossil sites, particularly in the regions of Tafilalt, Zagora and Alnif, has also produced numerous fascinating scientific discoveries. It is worth mentioning the various localities with exceptional preservation in the Ordovician, Devonian and Cretaceous, as well as hundreds of new Paleozoic invertebrate species (more than 200 just among trilobites). The huge Paleozoic palaeobiodiversity of Morocco has become unique in the African continent and, according to diverse specialists with whom we agree, the fossil trade has made knowledge advance in 20 years what would otherwise have taken almost a century of conventional studies, especially in such a remote region where rocks are uniformly veiled by desert patina.

The flip side of so many discoveries is the complete destruction of numerous fossiliferous beds after years of commercial exploitation. The persistence of these beds will need to come from finding them in other areas of the Anti-Atlas which still remain practically unexplored, due to their distance from villages and roads.

The massive search for surface fossils has irreversibly damaged many sections of high geological relevance, diminishing their potential as geosites of national or international value.

Hopefully, the increasing institutional interest shown by Moroccan universities and scientific associations, as well as the Ministry of Energy, Mines and Sustainable Development, will lead to a movement of knowledge and protection of the geological heritage of Morocco that may reach all the corners of the country. In addition to the above-mentioned activities organized by the APPGM and its AGM – since 2006 there has been a biennial international meeting on the evaluation and preservation of the palaeontological heritage – which will have its eighth edition organized by Moulay Ismaïl University of Errachidia in 2018. Also in this year Rabat will host the Moroccan Geological Forum, with a section devoted to geological heritage and geotourism.

From a commercial point of view, the Moroccan fossil trade is threatened by the proliferation of fakes and by a future stagnation of sales of the most valuable fossils. Extractive activity has been so intensive and extended in time that a progressive decline in the pace of new palaeontological discoveries is already noticeable, as is apparent from a decrease in the arrival of new species to the markets over the last few years.

Finally, it is worth pointing out that besides a higher or lower proportion of authentic compared to fake material in certain Moroccan fossil specimens, the large majority of material in the market is far from being correctly identified either in its taxonomic assignment, its geological provenance or its age. This makes their high scientific value as fossils or movable geological heritage somewhat more equivocal.

Acknowledgements We are greatful to Julio Martín Sánchez (Madrid) for his unfailing help in all our scientific fieldtrips to Morocco and for his first-hand recollections of the early steps in the development of the fossil industry during the 1970s; to Björn Kröger (Helsinki) and Thomas R. Becker (Munich) for the information on Silurian and Devonian cephalopods, respectively; and to Carlos Alonso (Universidad Complutense de Madrid) for the design of the plates and improvement to the photographs. We would also like to thank Dr Aaron W. Hunter (University of Cambridge, UK) as Editor of this volume, and Prof. Khadija El Hariri (Cadi Ayyad University, Marrakech, Morocco) and Dr Andrei V. Dronov (Geological Institute of Russian Academy of Sciences, Moscow, Russia) for their constructive reviews.

Funding DCGB acknowledges the financial support of Australian Research Council Future Fellowship FT130101329. Part of the activities in this paper fall within project CGL2017-87631-P of the Spanish Ministry of Science, Innovation and Universities.

References

Albin, D. 2009. Los timos jurásicos. *Interviú*, **1725**, 48–50.

Benharref, M., Álvaro, J.-J., Hibti, M., Pouclet, A., El Hadi, H. & Boudad, L. 2014. Carte Géologique du Maroc au 1/50 000. Feuille Marzouga. Mémoire explicative. *Notes et Mémoires du Service Géologique du Maroc*, **553**.

Beraaouz, M., Macadam, J., Bouchaou, L., Ikenne, M., Ernst, R., Tagma, T. & Masrour, M. 2018. An inventory of geoheritage sites in the Draa Valley (Morocco): a contribution to promotion of geotourism and sustainable development. *Geoheritage*, published online 12 August 2017, https://doi.org/10.1007/s12371-017-0256-x

Blaizot, M. & Jébrak, M. (eds) 2017. Le Maroc, paradis des géologues. *Géologues*, **194**, 126.

Burkhard, H. & Bode, R. 2003. *Trilobitenland Marokko. Keine Angst vor Fälschungen. Offizieller Katalog der 40. Mineralientage München, Turmalin und Trilobit*. Münchener Mineralienfreunde, München, 136–144.

Corriga, M.G., Corradini, C., Haude, R. & Walliser, O.H. 2014. Conodont and crinoid stratigraphy of the upper Silurian and Lower Devonian scyphocrinoid beds of Tafilalt, southeastern Morocco. *GFF*, **136**, 65–69.

Destombes, J. 2006. Carte géologique au 200 000° de l'Anti-Atlas marocain. Paléozoïque inférieur: Cambrien moyen et supérieur-Ordovicien–base du Silurien. Sommaire général sur les mémoires explicatifs des cartes géologiques au 1/200 000 de l'Anti-Atlas marocain. *Notes et Mémoires du Service Géologique du Maroc*, **515**, 1–150.

El Hariri, K. & Lefebvre, B. 2015. The Fezouata Shale: a model for promoting Moroccan geological heritage. *In*: El Hariri, K. (coord) *The International Conference the Rise of Animal Life RALI2015 – Promoting Geological Heritage: Challenges and Issues*. Cadi Ayyad University, Marrakesh, 49–50.

El Hassani, A., Aboussalam, S., Becker, T., El Wartiti, M. & El Hassani, F. 2017. Patrimoine géologique marocain et développement durable: l'exemple du Dévonien du Tafilalt, Anti-Atlas oriental. *Géologues*, **194**, 112–117.

Errami, E., Brocx, M., Semeniuk, V. & Ennih, H. 2015. Geosites, Sites of Special Scientific Interest, and potential Geoparks in the Anti-Atlas (Morocco). *In*: Errami, E., Brocx, M. & Semeniuk, V. (eds) *From Geoheritage to Geoparks. Case Studies from Africa and Beyond*. Geoheritage, Geoparks and Geotourism. Springer, Cham, Switzerland, 57–79.

Fortey, R.A. 2009. A new giant asaphid trilobite from the Lower Ordovician of Morocco. *Memoirs of the Association of Australasian Palaeontologists*, **37**, 9–16.

Gutiérrez-Marco, J.C., García-Bellido, D.C., Rábano, I. & Sá, A.A. 2017*a*. Digestive and appendicular softparts, with behavioural implications, in a large Ordovician trilobite from the Fezouata Lagerstätte, Morocco. *Scientific Reports*, **7**, 39728, https://doi.org/10.1038/srep39728

Gutiérrez-Marco, J.C., Sá, A.A., García-Bellido, D.C. & Chacaltana, C.A. 2017*b*. Recent geoethic issues in Moroccan and Peruvian paleontology. *Annals of Geophysics*, **60**, Fast Track 7, https://doi.org/10.4401/ag-7475

Hartenfels, S. & Becker, T.R. 2018. Age and correlation of the transgressive Gonioclymenia Limestone (Famennian, Tafilalt, eastern Anti-Atlas, Morocco). *Geological Magazine*, **155**, 586–629, https://doi.org/10.1017/S0016756816000893

Jalil, N. 2015. Fossils, patrimony and knowledge: the need to protect Moroccan geoheritage. The case of the 'Kem Kem beds' fossils. *In*: El Hariri, K. (coord) *The International Conference the Rise of Animal Life RALI2015 – Promoting Geological Heritage: Challenges and Issues*. Cadi Ayyad University, Marrakesh, 59.

Korn, D. & Bockwinkel, J. 2017. The genus *Gonioclymenia* (Ammonoidea; Late Devonian) in the Anti-Atlas of Morocco. *Neues Jarhbuch für Geologie und Paläontologie Abhandlungen*, **285**, 97–115.

Krögger, B. 2008. *Nautiloids Before and During the Origin of Ammonoids in a Siluro-Devonian Section in the Tafilalt, Anti-Atlas, Morocco*. Special Papers in Palaeontology, **79**.

Lagnaoui, A., Bougariane, B., Abioui, M. & Enniouar, A. 2015. Paleontological heritage of Zagora region (southeastern Morocco): a tool for local sustainable development. *In*: El Hariri, K. (coord) *The International Conference the Rise of Animal Life RALI2015 – Promoting Geological Heritage: Challenges and Issues*. Cadi Ayyad University, Marrakesh, 65.

Lebrun, P. 2016. Sainte-Marie-aux-Mines. Les fossiles de l'édition 2016. *Fossiles*, **27**, 54–61.

Lebrun, P. 2017. Sainte-Marie-aux-Mines. Les fossiles de l'édition 2017. *Fossiles*, **31**, 49–55.

Lefebvre, B., El Hariri, K., Lerosey-Aubril, R., Servais, T. & Van Roy, P. 2016*a*. The Fezouata Shale (Lower Ordovician, Anti-Atlas, Morocco): a historical review. *Palaeogeography, Palaeoclimatology, Palaeoecology*, **460**, 7–23.

Lefebvre, B., Lerosey-Aubril, R., Servais, T. & Van Roy, P. 2016*b*. The Fezouata Biota: an exceptional window on the Cambro-Ordovician faunal transition. *Palaeogeography, Palaeoclimatology, Palaeoecology*, **460**, 1–6.

Michard, A., Hoepffner, C., Soulaimani, A. & Baidder, L. 2008. The Variscan Belt. *In*: Michard, A., Saddiqi, O., Chalouan, A. & Frizon de Lamotte, D. (eds) *Continental Evolution: The Geology of Morocco*. Lecture Notes in Earth Sciences, **116**. Springer, Berlin, 65–132.

Michard, A., Soulaimani, A., Hoepffner, C., Ouanaimi, H., Baidder, L., Rjimati, E.C. & Saddiqi, O. 2010. The south-western branch of the Variscan Belt. Evidence from Morocco. *Tectonophysics*, **492**, 1–24.

Osborne, L. 2000. The fossil frenzy. *The New York Times*, 29 October.

Ouanaimi, H. & Soulaimani, A. 2011. Circuit C5. Anti-Atlas Central. *In*: Michard, A., Saddiqi, A., Chalouan, A., Rjimati, E. & Mouttaqi, A. (eds) *Nouveaux guides géologiques et miniers du Maroc, Volume 3. Notes et Mémoires du Service Géologique du Maroc*, **558**, 73–122.

Piqué, A., Cornée, J.-J., Muller, J. & Roussel, J. 1991. The Moroccan Hercynides. *In*: Dallmeyer, R.D. & Lécorché, J.P. (eds) *The West African Orogens and Circum-Atlantic Correlations*. Springer, Berlin, 229–263.

Pohle, A. & Klug, C. 2018. Body size of orthoconic cephalopods from the late Silurian and Devonian of the Anti-Atlas (Morocco). *Lethaia*, **51**, 126–148.

Praszkier, T. 2011. Morocco: tea and minerals. *Rock & Minerals*, **86**, 492–517.

Rjimati, E.-C., Michard, A. & Saddiqi, O. 2011. Circuit C10. Anti-Atlas occidental et Provinces sahariennes. *In*: Michard, A., Saddiqi, A., Chalouan, A., Rjimati, E. & Mouttaqi, A. (eds) *Nouveaux guides géologiques et miniers du Maroc, Volume 6. Notes et Mémoires du Service Géologique du Maroc*, **561**, 1–89.

Saddiqi, O., Baidder, L. & Michard, A. 2011. Circuit C1. Haut Atlas et Anti-Atlas, Circuit Oriental. *In*: Michard, A., Saddiqi, A., Chalouan, A., Rjimati, E. & Mouttaqi, A. (eds) *Nouveaux guides géologiques et miniers du Maroc, Volume 2. Notes et Mémoires du Service Géologique du Maroc*, **557**, 9–75.

Saddiqi, O., Rjimati, E., Michard, A., Soulaimani, A. & Ouanaimi, H. 2015. Recommended geoheritage trails in Southern Morocco: a 3 Ga record between the Sahara Desert and the Atlantic Ocean. *In*: Errami, E., Brocx, M. & Semeniuk, V. (eds) *From Geoheritage to Geoparks. Case Studies from Africa and Beyond*. Geoheritage, Geoparks and Geotourism. Springer, Cham, Switzerland, 91–108.

Shah, S.K. 2013. *Himalayan Fossil Fraud – A View from the Galleries*. Palaeontological Society of India, Special Publications, **4**.

Sicree, A.A. 2009. Morocco's trilobite economy. *Saudi Aramco World*, **60**, 34–39.

Soulaimani, A. & Burkhard, M. 2008. The Anti-Atlas chain (Morocco): the southern margin of the Variscan belt along the edge of the West African craton. *In*: Ennih, N. & Liégeois, J.-P. (eds) *The Boundaries of the West African Craton*. Geological Society, London, Special Publications, **297**, 433–452, https://doi.org/10.1144/SP297.20

Soulaimani, A. & Ouanaimi, H. 2011. Circuit C4. Anti-Atlas et Haut Atlas, Circuit Occidental. *In*: Michard, A., Saddiqi, A., Chalouan, A., Rjimati, E. & Mouttaqi, A. (eds) *Nouveaux guides géologiques et miniers du Maroc, Volume 3. Notes et Mémoires du Service Géologique du Maroc*, **558**, 9–72.

Talent, J.A. 1989. The case of the peripatetic fossils. *Nature*, **338**, 613–615.

Termier, G. & Termier, H. 1950*a*. Paléontologie Marocaine. Tome II, Invertébrés de l'Ere Primaire. Fascicule II, Bryozoaires et Brachiopodes. *Notes et Mémoires du Service Géologique du Maroc*, **77**, 1–253.

Termier, G. & Termier, H. 1950*b*. Paléontologie Marocaine. Tome II, Invertébrés de l'Ere Primaire. Fascicule III, Mollusques. *Notes et Mémoires du Service Géologique du Maroc*, **78**, 1–246.

Termier, G. & Termier, H. 1950*c*. Paléontologie Marocaine. Tome II, Invertébrés de l'Ere Primaire. Fascicule IV, Annélides, Arthropodes, Échinodermes, Conularides et Graptolithes. *Notes et Mémoires du Service Géologique du Maroc*, **79**, 1–279.

Van Roy, P. 2011. New insights from exceptionally preserved Ordovician biotas from Morocco. *In*: Gutiérrez-Marco, J.C., Rábano, I. & García-Bellido, D.C. (eds) *Ordovician of the World*. IGME Cuadernos del Museo Geominero, **14**, 21–26.

Voldman, G.G., García-López, S. & Martín, M.R. 2017. Silurian conodonts from the 'Orthoceras Limestones' (Tafilalt and Tondouf basins, NW Africa). *In*: Liao, J.-C. & Valenzuela-Ríos, J.I. (eds) *Fourth International Conodont Symposium. ICOS IV. Progress on Conodont Investigation*. IGME Cuadernos del Museo Geominero, **22**, 92–104.

STOP 5.4 – Desert Oasis in Mharch

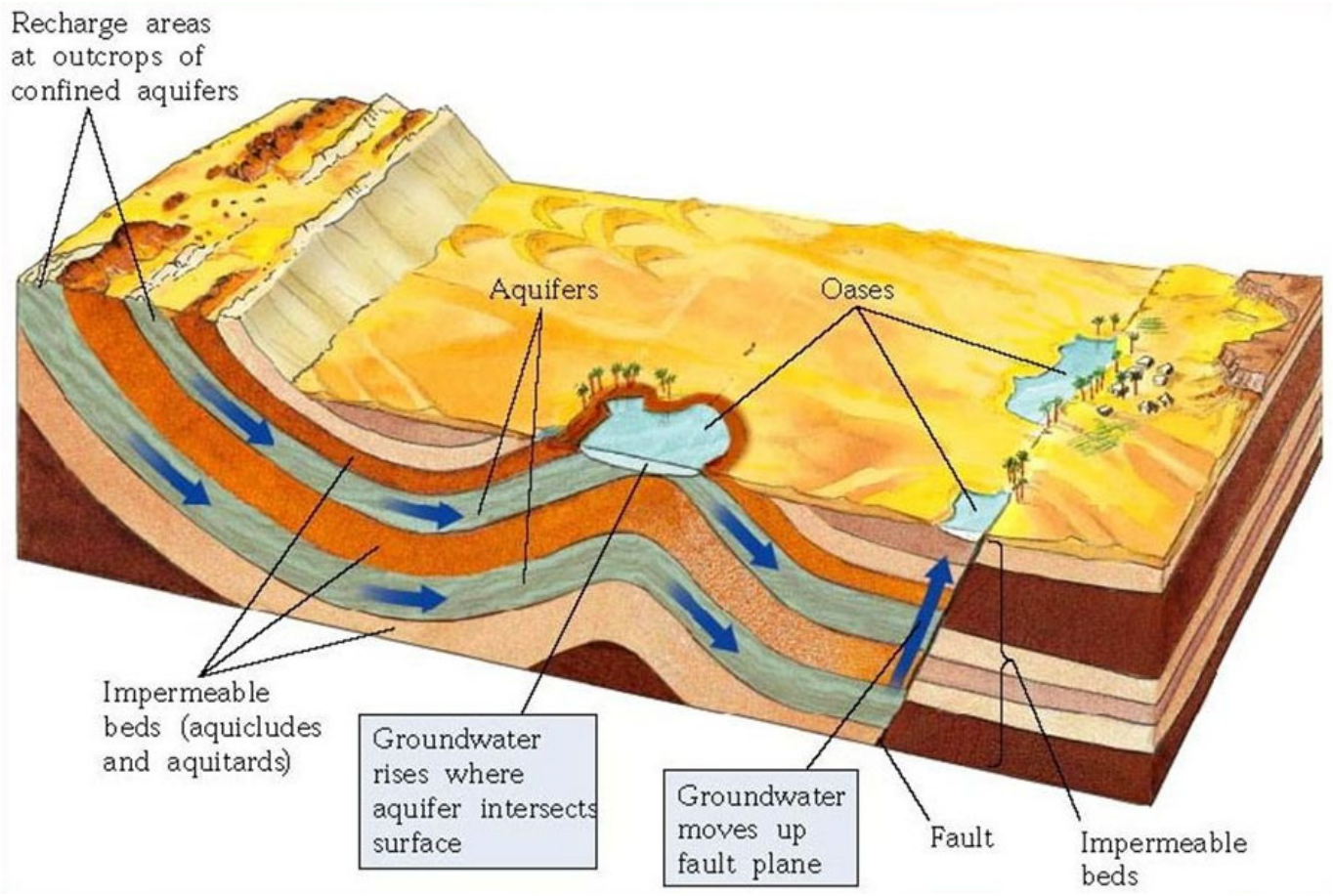

https://earthscience.stackexchange.com/questions/18634/how-do-oases-form-in-the-middle-of-the-desert

From Wikipedia:

In ecology, an oasis (/oʊˈeɪsɪs/; pl.: oases /oʊˈeɪsiːz/) is a fertile area of a desert or semi-desert environment that sustains plant life and provides habitat for animals. Surface water may be present, or water may only be accessible from wells or underground channels created by humans. In geography, an oasis may be a current or past rest stop on a transportation route, or less-than-verdant location that nonetheless provides access to underground water through deep wells created and maintained by humans. Although they depend on a natural condition, such as the presence of water that may be stored in reservoirs and used for irrigation, most oases, as we know them, are artificial.

The word oasis came into English from Latin: oasis, from Ancient Greek: ὄασις, óasis, which in turn is a direct borrowing from Demotic Egyptian. The word for oasis in the latter-attested Coptic language (the descendant of Demotic Egyptian) is wahe or ouahe which means a "dwelling place". Oasis in Arabic is wāḥa (Arabic: واحة).

Map of the Night Sky for March 10th, 2026 in Morocco
from https://in-the-sky.org/

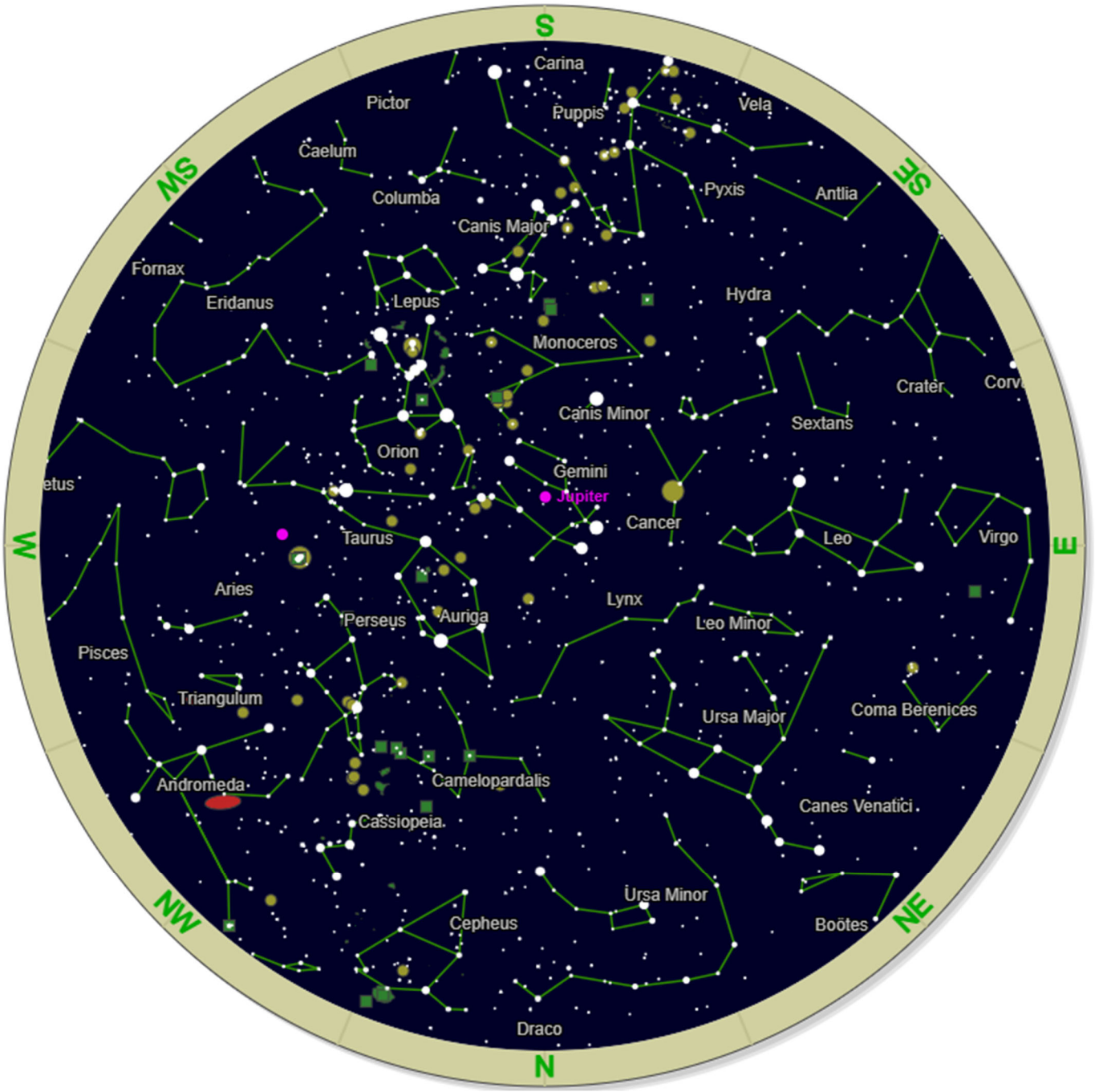

Day 6: Wednesday, March 11th, 2026 – Maider Basin to Erg Chebbi Dunes (So many fossils, you are going to throw up…)

STOP 6.1 – Guelb el Mharch
STOP 6.2 – Aferdou el Mrakib
STOP 6.3 – Jebel el Krabis
STOP 6.4 – Fezzou for lunch
STOP 6.5 – Butte 760
STOP 6.6 – Jebel Amelane
STOP 6.7 – Eifelian-Givetian GSSP Golden Spike
STOP 6.8 – Merzouga

Hotel Infromation:
Mohayut Camp
4XMP+4MG, village hassi labiad,
Merzouga 52202, Morocco

From our Guide:

Our first stop is the mud-mound of Guelb el Mharch. This is a 45m rocky peak made of crinoidal limestone that was once a submarine mud volcano formed by hydrothermal vents. In the past very rare placoderm fish fossils have been found here. The next stop Aferdou el Mrakib is a mountain which, at first sight, resembles a larger version of Guelb el Mharch, but it is in fact one of the largest known Devonian coral-stromatoporoid reefs in north-western Gondwana. It is also one of the most southerly discovered shallow-water Givetian (mid Devonian) reefs. The base of the reef contains the famous Drotops megalomanicus trilobite horizon. The next stop is at the base of Jebel el Krabis and is a place where Devonian (Famennian) ammonoids (goniatites) can be seen loose on the desert floor. They have eroded out from hypoxic pelagic shales but have, sadly, been over-collected to supply fossil shops around the world. Apart from goniatites, the Famennian of the area is an important source for brachiopods (especially Rhynchonellids), crinoids, fossil wood, deep-water solitary Rugosa corals, loxopteriid bivalves, trilobites, conodonts, and shark teeth. We then head to the village of Fezzou where we stop lunch in a café and have an opportunity to meet local people. Next, we move on to a nearby site known as Butte 760 by palaeontologists. This site also has many loose eroded fossils lying on the dessert floor; 21 different species of ammonoid have been recorded from here, although they are now rare, but brachiopods remain abundant. We then leave the Maider basin and stop at Jebel Amelane near the city of Rissani. Here Upper Devonian (Famennian) aged orthoceras and ammonoids can be seen in huge slabs of red limestone. Also, from a distance, it is also possible to view the Eifelian-Givetian global stratotype GSSP (golden spike). We then head to Merzouga and the famous sand dunes of Erg Chebbi. Here we really feel that we are in the Sahara Desert - because we are! The next two nights are spent in a 4-Star hotel in Merzouga.

STOP 6.1 – Guelb el Mharch

The following is taken from: Kaufmann, B., 1998, Facies, stratigraphy and diagenesis of Middle Devonian reef- and mud-mounds in the Mader (eastern Anti-Atlas, Morocco). Acta Geologica Polonica, vol. 48, no. 1, pp. 43-106.

Guelb el Maharch

Geological and stratigraphical setting, off-mound succession

The cone of Guelb el Maharch (Pl. 4, Fig. 1) rises above the plain of Oued Chouiref in the southeastern quarter of the Mader syncline (Text fig. 9). The mound basement with the off-mound and intermound transitions is covered by Quaternary deposits. The nearest off-mound strata are exposed 800 m southeast of the mound at the 7 km wide Jebel Maharch, which constitutes the continuation of the Jebel el Mrakib range towards NNE (Text-fig. 9). Stratigraphy, thickness of individual units and facies evolution of the Emsian to Eifelian succession at Jebel Maharch correspond to that of Jebel el Mrakib. Only the youngest bed at Jebel Maharch, a conspicuous, 50 cm thick cephalopod limestone of late Eifelian age (kockelianus Zone) could not be recognized at Jebel el Mrakib. If one projects the 6°-dipping cephalopod bed below the Guelb el Maharch mud-mound, about 80-90 m of thickness are concealed below the plain between the bed and the mound. The nearest overlying strata are bituminous styliolinid limestones (Kellwasser facies) of early Frasnian age (Lower asymmetricus Zone), exposed 2 km NNW of the mound (WENDT & BELKA 1991).

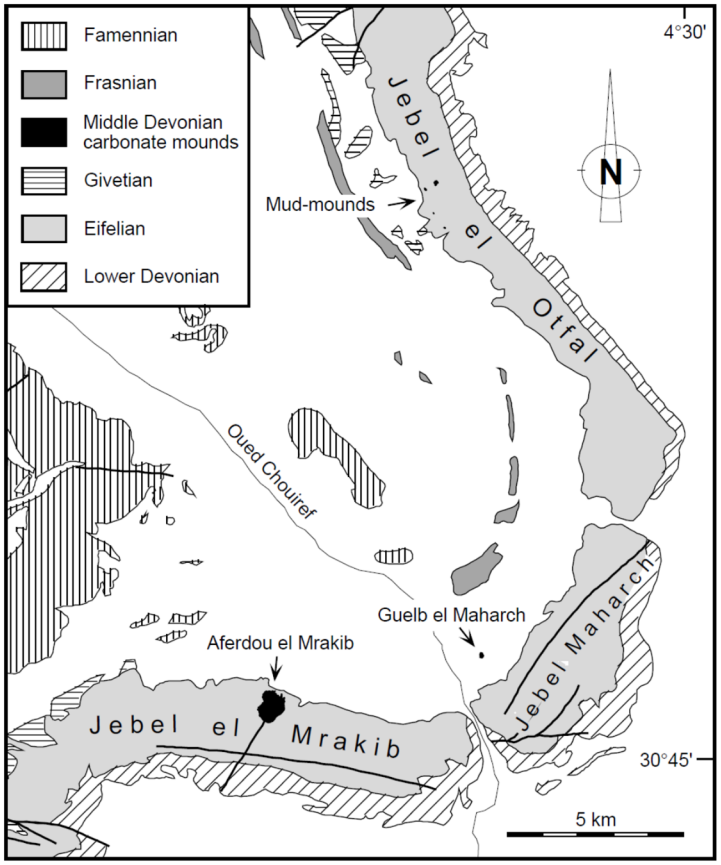

Fig. 9. Geological map of the southern central Mader area (*see* Text-fig. 2) with locations of the three most conspicuous mound occurrences (Aferdou el Mrakib, Guelb el Maharch, Jebel el Otfal); modified from the geological map 1:200.000, sheets 'Todrha-Ma'der' and 'Tafilalt-Taouz'

Size and geometry

Guelb el Maharch is the second largest mound of the Mader area. It has an exposed base-diameter of 120-180 m and a height of about 45 m (Text-fig. 15). Though the contact to the directly underlying beds is covered, the original height is probably only a few metres more, because the inclination of the mound flanks becomes more gentle at the mound periphery. Additionally, the covered thickness of 80-90 m corresponds approximately to the same interval (kockelianus to Lower varcus Zone) at Jebel el Mrakib. The mound shape is conical with a slight elongation in N-S-direction (170°). After correction for rotation of the nearest underlying strata to the horizontal (Text-fig. 16), the mound displays a slight asymmetry with steeper eastern (mean angle of inclination: 43°) than western flanks (mean angle of inclination: 35°). Steep mound flanks represent primary accretionary surfaces as is evidenced by the horizontal alignments of brachiopod infillings and laminations of internal sediments.

Lithology and sedimentary structures

In contrast to the Aferdou mound, Guelb el Maharch consists exclusively of massive limestones with no bedding features. Microfacies analyses of polished hand specimens and thin sections from a great variety of mound positions show a very uniform lithology of stromatactis-bearing boundstones (Pl. 5, Figs 3-4). Pervasive dolomitization occurs along an up to 20 m wide band, which runs in NE-SW-direction through the centre of the mound (Text-fig. 15).

Neptunian dykes are common in this mound. Generally, they are 2-5 cm wide, filled with dark mudstones and can be followed for 6-20 m (Pl. 4, Fig. 2). On the southern flank, a 1 m wide dyke, filled with a dark, crinoidal-brachiopod rudstone (Pl. 5, Fig. 2), cuts the mound from base to top (Pl. 4, Fig. 1). The two prefered directions of the dykes are NNE-SSW and WNW-ESE. Because the infillings have yielded no conodonts, the age of the dykes is unknown. Their formation was probably caused by tensional movements prior to Variscan folding though the main directions could not be related to any pre-orogenic tectonics so far.

In addition to stromatactis fabrics, irregular cavities, 5-20 cm in size and filled with dark, laminated internal sediments have been found (Pl. 4, Fig. 3; Pl. 5, Fig. 1). Cavity margins are lined with 5 mm thick, laminated cement rims (Pl. 5, Figs 1, 4) and infillings are often dolomitized (Pl. 4, Fig. 3; Pl. 5, Figs 3, 4). Because those cavities occur in the immediate neighbourhood of neptunian dykes and contain the same, dark internal sediments, their formation is probably related to the dyke formation.

Fauna

Though only 6 km apart from Aferdou el Mrakib, the Guelb el Maharch mud-mound contains an impoverished fauna (Text-fig. 14). Stromatoporoids and colonial rugose corals are absent, and solitary Rugosa are represented only by isolated metriophyllids and cf. Fletcheria. Though the diversity of the tabulate corals is also strongly reduced, they are the prevailing faunal elements, represented by auloporids (Bainbridgia sp., Pl. 5, Figs 3, 8; Cladochonus sp., Remesia sp. and Aulocystis sp.) and striatoporids (cf. Crenulipora, Pl. 5, Fig. 7; cf. Zemmourella, Pachystriatopora sp.). Crinoids are also very common, preserved mostly as isolated ossicles, but also as in situ disintegrations of longer stems. Brachiopods are mainly represented by small forms (5-10 mm in size), which could not be determined generically. Atrypids (Atrypa?, Carinatina sp.) occur rarely. Cephalopods are represented only by a few orthoconic nautiloids, oriented in their most stable position with their apices towards the mound top. As at Aferdou el Mrakib, hexactinellid sponges are found commonly as isolated spicules (smooth hexacts) in insoluble residues and thin sections, but also rarely as whole sponge bodies, about 5 cm in diameter. Insoluble residues contain occasionally agglutinated foraminifers (Sorosphaera sp., compare Pl. 13, Figs 5-8). In thin sections, dacryoconarids (common styliolinids, rare Nowakia sp.), fragments of fenestellid (Pl. 5, Fig. 6) and fistuliporid bryozoans (the latter mostly incrusting tabulate corals), small gastropods (1-2 mmsized) and rare trilobite carapaces were observed.

PLATE 4 Guelb el Maharch mud-mound

1 – Mud-mound, seen from SSW; weight of the mound is about 45 m; the base is covered by Quaternary deposits; a – Neptunian dyke (arrow a) cuts the mound vertically; infilling of dyke is shown on Pl. 5, Fig. 2; person (arrow b) for scale

2 – Neptunian dyke in mud-mound facies; dyke is filled by dark mound sediments; coin diameter is 24 mm

3 – Irregular cavity in mud-mound facies; cavity is filled with dolomitized internal sediment (see also Pl. 16, Fig. 4); isopachous calcite cement layer (arrowed), lining the cavity wall; coin diameter is 24 mm


1
a
b


2

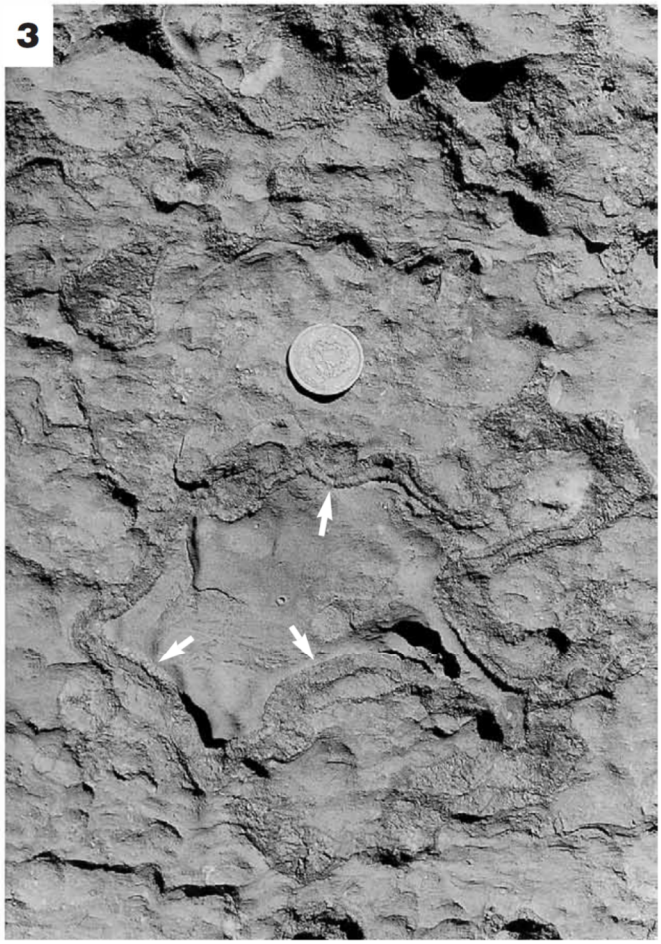
3

Occurrence and relative abundance of fossils in Middle Devonian carbonate mounds of the Mader.

	Aferdou el Mrakib	Guelb el Maharch	Jebel el Otfal Mound 1	Jebel el Otfal Mound 2	Jebel el Otfal Mound 3	Jebel el Otfal Mound 4	Jebel Ou Driss
PORIFERA							
Domical stromatoporoids	●						
Hexactinnelids	□	□	●	□	△		
Chaetetids	△						
COLONIAL RUGOSE CORALS							
"*Hexagonaria*"	□						
"*Phillipsastrea*"	□						
SOLITARY RUGOSE CORALS			×	×	×		
Heliophyllum halli moghrabiense	□						
Cystiphylloides sp.	●						
Acanthophyllum sp.	△						
Macgeea cf. *minima*	△						
Siphonophrentis sp.	□						
Stringophyllum normale	□						
Calceola sandalina	△						
Thamnophyllum ossalense	□						
Amplexocarinia sp.				△			
cf. *Fletcheria*	□	□	□		□		
cf. *Neomphyma*							□
Metriophyllids	□	△		△			
TABULATE CORALS							
Striatoporids							
cf. *Pachystriatopora*	□	□	□		□	□	
cf. *Taouzia*			□				□
cf. *Crenulipora*		□					
cf. *Zemmourella*		□					□
Dualipora preciosa						●	
Thamnoporids							
Thamnopora germanica	□						
Thamnopora proba	□						
Auloporids			×				
Bainbridgia sp.	□	●		●	□	□	
Cladochonus sp.	□	□				□	
Remesia sp.	△	□			□	□	
Aulocystis sp.		△			□		
Favositids							
Favosites cf. *goldfussi*	□						
Platyaxum (*P.*) *escharoides*	●						
Heliolitids							
Heliolites cf. *porosus*	△						
BRACHIOPODS		×	×	×	×	×	×
Pentamerids							
Ivdelinia sp.	●						
Devonogypa sp.	●						
Spiriferids				×	×		
Atrypa ?	●	□		□			
Planatrypa sp.	□						
Spinatrypa sp.	□						
Carinatina sp.	□	□					
Desquamatia sp.				□			
Spinatrypinae	□						
Orthids		×					
Schizophoria sp.	□						
Strophomenids							
Leptaena sp.	□						
Athyrids	□						
BRYOZOANS							
Fenestellids	□	□	△	□			
Fistuliporids		□		□			
MOLLUSCS							
Cephalopods	△	△			△		
Gastropods			△	□	□	△	△
Pelecypods				□			
CRINOIDS	●	□	□	●	□	□	□
TRILOBITES	□	△	□	□	□	●	□
DACRYOCONARIDS	□	□	□	□	□	△	□
OSTRACODES	□	□	△	□			△
AGGLUTINATED FORAMINIFERA		△	△	△	□	□	
MICROPROBLEMATICA							
Rothpletzella devonica	□			△			
CONODONTS							
Polygnathids	□	△	△	△	△	□	
Icriodids	□	△		△		△	△
Belodella sp.	□	□	△	□	△	△	
SHARK TEETH	△						

● = frequent □ = present △ = rare × = undetermined genera

STOP 6.2 - 6.3 – Aferdou el Mrakib & Jebel el Krabis

The following is taken from: Kaufmann, B., 1998, Facies, stratigraphy and diagenesis of Middle Devonian reef- and mud-mounds in the Mader (eastern Anti-Atlas, Morocco). Acta Geologica Polonica, vol. 48, no. 1, pp. 43-106.

Aferdou el Mrakib

Geological and stratigraphical setting, offmound succession

The Aferdou el Mrakib reef-mound is located at the northern flank of the 15 km wide, E-W- trending Jebel el Mrakib (Text-fig. 9), a range forming the southeastern limb of a 40-50 km wide Variscan syncline, which is the largest tectonic structure of the eastern Anti-Atlas (Textfig. 2). Here, a Lower to Middle Devonian (Emsian to lower Givetian) sequence is exposed (Text-fig. 31), dipping with 6° to the north. The uppermost 25 m (upper Eifelian to lower Givetian) of the succession are preserved only in the immediate surrounding of the Aferdou mound, where they form the mound basement; they were protected from erosion by the overlying mound (Pl. 1, Fig. 1; Pl. 2, Fig. 1).

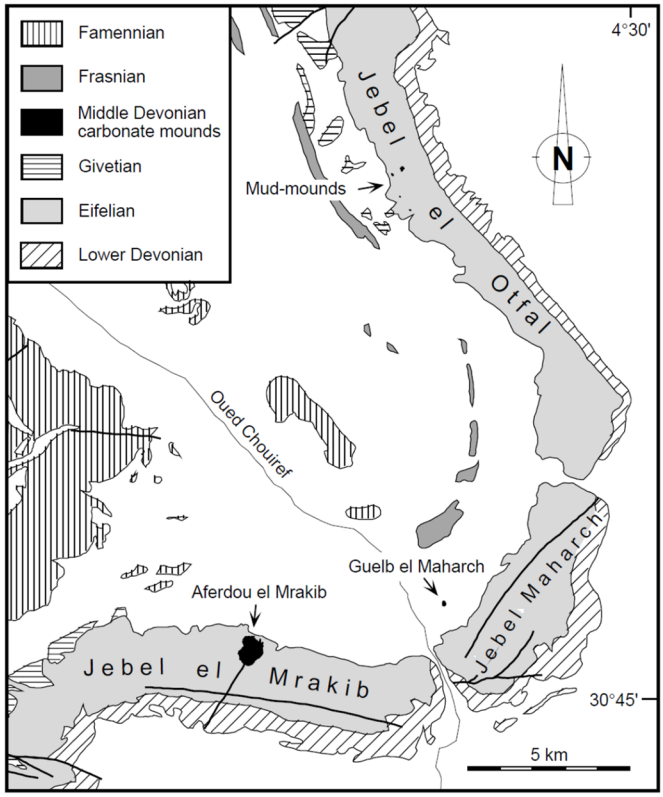

Fig. 9. Geological map of the southern central Mader area (*see* Text-fig. 2) with locations of the three most conspicuous mound occurrences (Aferdou el Mrakib, Guelb el Maharch, Jebel el Otfal); modified from the geological map 1:200.000, sheets 'Todrha-Ma'der' and 'Tafilalt-Taouz'

The Eifelian interval at Jebel el Mrakib ('El Otfal Formation' of HOLLARD 1974, 1981) is about 75 m thick (Text-fig. 31) and exhibits a shallowing-upward sequence from deep-water unfossiliferous, chert-bearing mudstones with high siliciclastic influx over burrowed, bioclastic wackestones of moderate depth to relatively shallow-water crinoidal grainstones. The latter are 22 m thick and restricted to the site of the Aferdou mound.

The base of the Givetian is marked by a 2 m thick coral-stromatoporoid boundstone (Text fig. 10; Pl. 3, Fig. 4), which directly underlies the Aferdou mound and probably served as a pioneer stage in mound development. It is overlain by crinoidal grainstones and, three metres above, these by a conspicuous, 30 cm thick trilobite wackestone (commercially exploited level with abundant Drotops megalomanicus STRUVE 1990) (Text-fig. 10). The section continues with 13 m of poorly fossiliferous mudstones which, in the middle part, contain a 3 m thick brachiopod lense (exclusively Ivdelinia sp., Pl. 13, Fig. 11). These mudstones are followed by 20 m of mound debris facies. The Aferdou mound interfingers with the off-mound strata (17 m in thickness), which overlie the initial coral-stromatoporoid bed and with the lower 5 m of the mound debris facies (Text-fig. 10). Unfortunately, the lateral transition of the mound debris facies to the coeval off-mound strata has been removed by erosion. The same applies to strata, which directly overlie the Aferdou mound. They are preserved only at two small areas on the northern flank of the Aferdou mound (Text-fig. 11), where they cap the mound debris facies. They consist of 2-3 m thick, slumped, blue-grey, poorly-fossiliferous mudstones (Pl. 1, Fig. 2; Text-fig. 10) which occasionally contain coarse mound debris.

PLATE 1 - Aferdou el Mrakib reef-mound

1 – Reef-mound, seen from W; height above underlying strata is 100-130 m; underlying upper Eifelian limestones (arrowed) are preserved only at the base of the mound, where the resistant mound structure has protected them from erosion

2 a-2b – Close-up view of the left third of Fig. 1, seen from SW; interfingering of massive reef-mound facies with bedded mound debris facies (indicated by thick line)

1

2a

2b

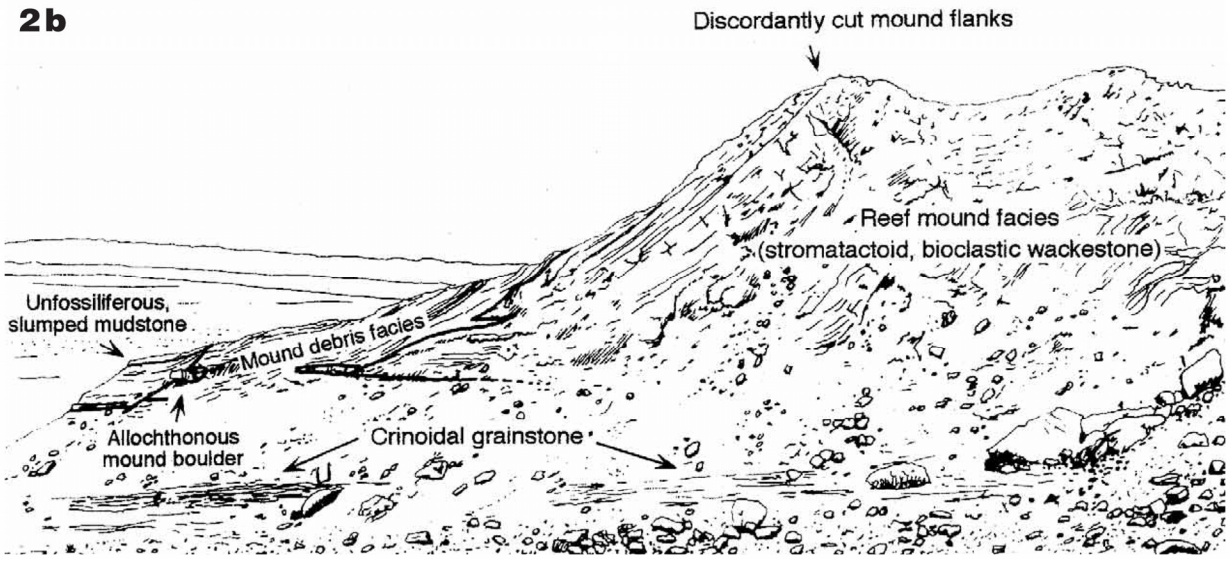

PLATE 2 Aferdou el Mrakib reef-mound

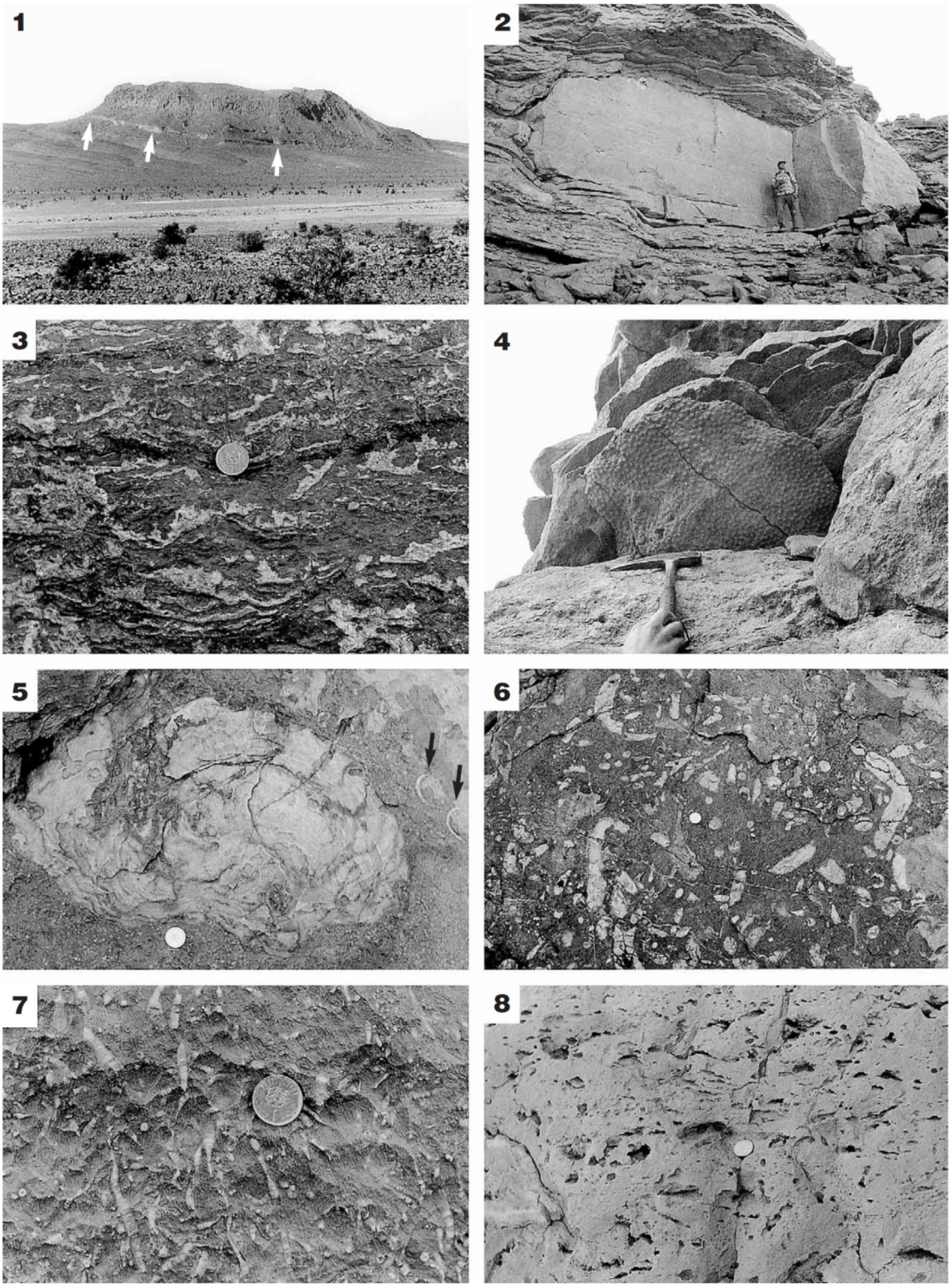

1 – Reef-mound, seen from ENE; width of the buildup is 900 m; the underlying upper Eifelian limestones (arrowed) are preserved only in the immediate surrounding of the mound, where the resistant mound structure has protected them from erosion

2 – Huge, mound-derived boulder in mound debris facies; author (1.85 m) for scale

3 – Stromatactis in reef-mound facies, aligned parallel to the accretionary surface of the mound; coin diameter is 24 mm

4 – Overturned "Phillipsastrea" in mound debris facies

5 – Domical stromatoporoid in reef-mound facies; thick-shelled pentamerids (Devonogypa sp., arrowed); coin diameter is 24 mm

6 – Solitary, rugose corals (mainly Cystiphylloides sp.) in reef-mound facies; coin diameter is 24 mm

7 – Reef-mound facies with phaceloid rugose corals, belonging to the bizarre group of Fletcheria MILNE-EDWARDS & HAIME; coin diameter is 24 mm

8 – Pervasively dolomitized reef-mound facies with mouldic porosity; coin diameter is 24 mm

Size and geometry

Aferdou el Mrakib is the largest reefal structure of the eastern Anti-Atlas. It has an almost circular outline with a diameter of about 900 m (Text-fig. 11), a truncated cone-shape (Pl. 1, Fig. 1; Pl. 2, Fig. 1) and a height of 100-130 m (Pl. 1, Fig. 1). The mound has a rather symmetrical shape (after correction of the flank inclinations for rotation of underlying northward-dipping strata, Text-fig. 12) with a mean angle of flank inclination of 35°. By adding the eroded mound flank beds on the other mound sides, an original diameter of 1700-1800 m (including mound debris facies) can be reconstructed for the Aferdou mound (Text-fig. 13). Caused by northward Variscan tilting, the north side of the mound has been prevented longer from erosion and thus displays primary mound surfaces. On the top of the mound slopes, flank beds are cut discordantly (Pl. 1, Figs 2a, b), showing postsedimentary erosion. According to WENDT (1993), the original height can be reconstructed by extrapolation of the flank beds as about 250 m (Text-fig. 13). SCHWARZACHER (1961) found similar discordant cuts of mound tops in Lower Carboniferous mud-mounds of Ireland and suggested that mound growth was controlled by wave action. Because the upper mound surface of Aferdou el Mrakib is inclined in the same direction as the underlying strata (Pl. 2, Fig. 1), it cannot be excluded that a wave-related erosion took place prior to Variscan tilting.

Lithology and sedimentary structures

The reef-mound facies is rather uniform and consists of indistinctly thick-bedded, stromatactoid boundstones (purely descriptive: wackestones and floatstones). A detailed description of stromatactis fabrics (of all Mader carbonate mounds) is given further in this paper. No distinction between flank- and core-facies can be made. A massive bedding with bed thicknesses of 0.5-1 m is ubiquitous, even in dolomitized areas. The beds dip away from the centre (Text-fig. 11), suggesting that the mound grew concentrically, both expanding laterally and vertically. Unfortunately, no informations about eventual ecological succession within the mound can be obtained, because the Aferdou mound is not cut by erosion and therefore does not exhibit its internal structure. Locally, coral boundstones occur, formed by few m2-sized in situ colonies of distinct coral species [especially Platyaxum (Platyaxum) escharoides (STEININGER 1849) (Pl. 3, Fig. 3), cf. Fletcheria (Pl. 2, Fig. 7) and Thamnophyllum ossalense (JOSEPH & TSIEN 1975)].

The mound debris facies is only preserved on the northern flanks of the mound and in an isolated occurrence on the east side (Text-fig. 11). It consists of up to 20 m thick, mound-derived coral-stromatoporoid floatstones (Text-fig. 10) which contain large mound-derived boulders (Pl. 2, Fig. 2). Interfingering with the massive mound facies can be seen on the northwestern side of the mound (Pl. 1, Figs 2a, b). Originally, the mound debris facies probably formed an aureole surrounding the mound and was later largely removed by erosion.

The central part of the mound is pervasively dolomitized (Text-fig. 11) whereby both fossils and sedimentary structures have been obliterated. A dolomitized NE-SW-trending Variscan(?) joint runs into the south side of the mound and has obviously acted as a conduit for dolomitizing fluids.

Small scale fissures and neptunian dykes, only few centimetres wide and to be followed for 2-3 metres, have been found in the Aferdou mound. Generally, they are filled with dark mudstones or, in one case, with fine-grained sandstone which is similar to the Lower Carboniferous deltaic sandstones that overlie the Devonian sucession of the eastern Anti-Atlas (WENDT 1993).

Fauna

Aferdou el Mrakib is the mound with the most abundant and most varied fauna (Text-fig. 14). It is described as ‘reef-mound’ because the potential Devonian reef-builders (stromatoporoids, colonial rugose corals) are present but do not form a rigid framework.

Stromatoporoids occur mostly as undestroyed but slightly displaced or overturned individuals, but they occur also frequently in situ (Pl. 2, Fig. 5). Domical morphotypes (Actinostroma ?, Stromatoporella ?,

Clathrodictyon ?), 20-80 cm in diameter, dominate; laminar forms are rare and dendroid forms are totally absent. According to JAMES & BOURQUE (1992), the relationship between external shape and internal growth banding geometry of stromatoporoids can be used to infer relative sedimentation rates and water roughness. In the Aferdou mound, the predominant growth forms with enveloping latilaminae without ragged margins indicate a relatively low sedimentation rate (compared with a 'true' reef) and low water roughness.

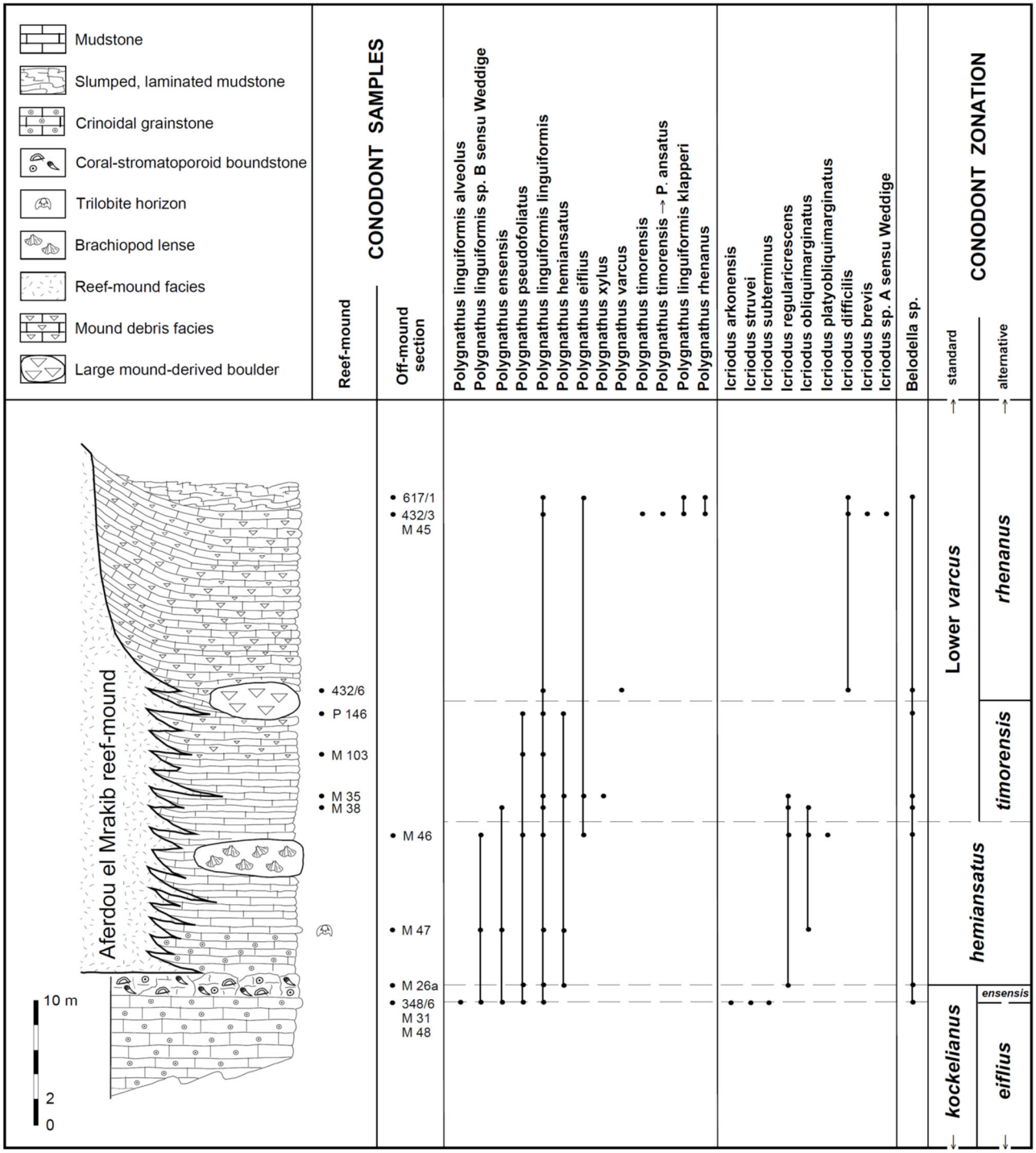

Fig. 10. Lithology of Aferdou el Mrakib off-mound section with conodont distribution; alternative conodont zonation *after* BELKA & *al*. (in press)

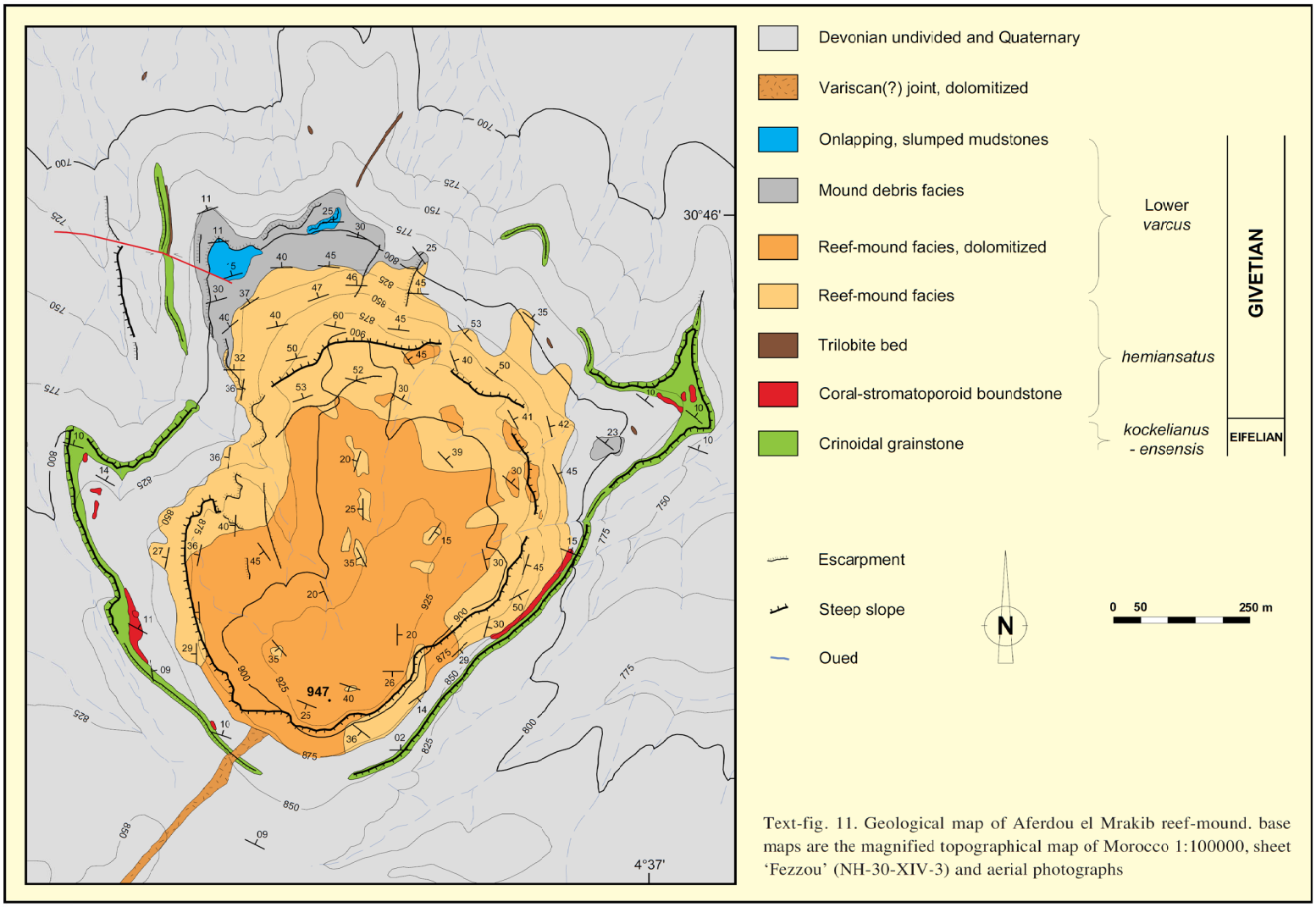

Text-fig. 11. Geological map of Aferdou el Mrakib reef-mound. base maps are the magnified topographical map of Morocco 1:100000, sheet 'Fezzou' (NH-30-XIV-3) and aerial photographs

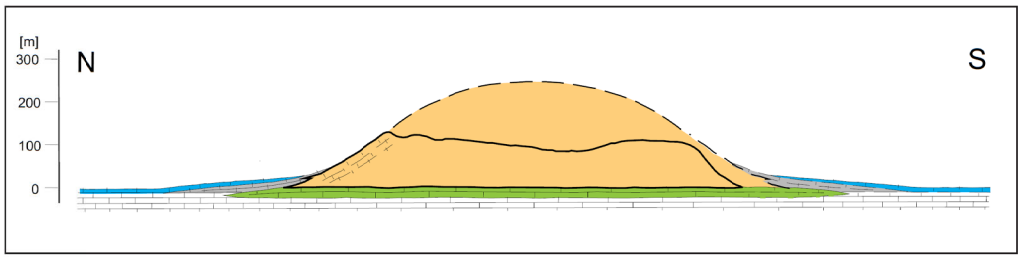

Text-fig. 13. Reconstruction of Aferdou el Mrakib reef--mound by extrapolation of discordantly cut mound flanks; thick black line is actual mound profile; legend as in Text-fig. 11

Siliceous sponge spicules (smooth hexacts; Pl. 13, Figs 9-10) of hexactinellids were found frequently in insoluble residues and in thin sections. Coralline sponges are represented by rare chaetetids.

Solitary rugose corals are represented by Heliophyllum halli moghrabiense LE MAÎTRE 1947, Cystiphylloides sp. (Pl. 2, Fig. 6), Acanthophyllum sp., Macgeea cf. minima BRICE 1970, Siphonophrentis sp., Stringophyllum normale WEDEKIND, 1922, Calceola sandalina LAMARCK, 1799 (rare) and metriophyllids. Thamnophyllum ossalense (JOSEPH & TSIEN 1975) forms some m2-sized, dendroid colonies. In addition, flat, disc-shaped colonies of "Phillipsastrea" (Pl. 2, Fig. 4) and, less common "Hexagonaria", occur. Further colonial rugose corals belong to the bizarre group of Fletcheria MILNE-EDWARDS & HAIME (Pl. 2, Fig. 7).

The tabulate coral fauna displays a high taxonomic diversity. Fragments of branching striatoporids (cf. Pachystriatopora, Pl. 3, Fig. 7), "thamnoporids" (Thamnopora germanica BIRENHEIDE, 1985, Thamnopora proba DUBATOLOV 1955) and auloporids (Bainbridgia sp., Cladochonus sp., Remesia sp.) are ubiquitous in the mound facies. Favositids are represented by massive, fascicular colonies (mainly Favosites cf. goldfussi ORBIGNY, 1850) and by 3-10 mm thick and up to 20 cm wide, in situ crusts of alveolitids [mainly Platyaxum (Platyaxum) escharoides (STEININGER, 1849), Pl. 3, Fig. 3). Heliolitids (Heliolites cf. porosus (GOLDFUSS 1826)] occur rarely as spherical colonies.

Brachiopods are abundant in the Aferdou mound. The two big-sized, thick-shelled pentamerid genera Ivdelinia sp. (Pl. 13, Fig. 11) and Devonogypa sp. form conspicuous, monotypical, several m2-sized in situ communities. GODEFROID & RACKI (1990) described similar reef-dwelling faunas from 'nests, lenses and bands' in Frasnian fore-reef limestones and attributed these brachiopods to semi-protected, intermittendly agitated habitats which would reflect the assumed moderate bathymetric position of the Aferdou mound. Other brachiopods belong to spiriferids (Atrypa?, Planatrypa sp., Spinatrypa sp., Carinatina sp., Spinatrypinae), orthids (e.g. Schizophoria sp.), athyrids and rare strophomenids (Leptaena sp.).

Crinoids are ubiquitous in the reef-mound. They are mainly disarticulated into single ossicles and rarely preserved as up to 20 cm long stems. Crowns and holdfasts have not been found.

Cephalopods (orthoconic nautiloids and goniatites) are extremely rare in the reef-mound facies.

Additionally, dacryoconarids (common styliolinids, rare Nowakia sp.), fragments of fenestellid bryozoans, trilobite carapaces, small gastropods, rare ostracods and microproblematica [Rothpletzella devonica (MASLOV 1956), Pl. 3, Fig. 8] were found in thin sections. Rare findings of shark teeth (Phoebodus fastigatus GINTER & IVANOV, 1992; Pl. 13, Figs 1-4) in insoluble residues suggest that sharks belonged to the mound's ecosystem.

STOP 6.5 – Butte 760

The following is from: Bockwinkel, J. Becker, R.T., and Ebbighausen, V., 2015, Late Givetian ammonoids from Ait Ou Amar (northern Maider, Anti- Atlas, southeastern Morocco). N. Jb. Geol. Paläont. Abh. vol. 278, no. 2, pp. 123–158.

Introduction

The late Givetian was a very peculiar interval in the early evolutionary history of the Ammonoidea. Subsequent to the faunal overturns of the global Taghanic Crises (e.g., House 1985; AboussAlAm & becker 2011), the rapid evolution of the Pharciceratacеae led to the dominance of highly multilobed forms, with a higher average suture complexity than in both earlier and subsequent times (e.g., becker 2009). On a global scale, the eastern Anti-Atlas (southern Morocco) is the region with the richest and most detailed representation of these highly distinctive faunas. Following the work by Termier & Termier (1950), PeTTer (1959), and bensAïd (1974), we began in recent years the systematic description of the late Givetian ammonoid faunas of the Anti-Atlas. We commenced our investigations with a well-preserved fauna from

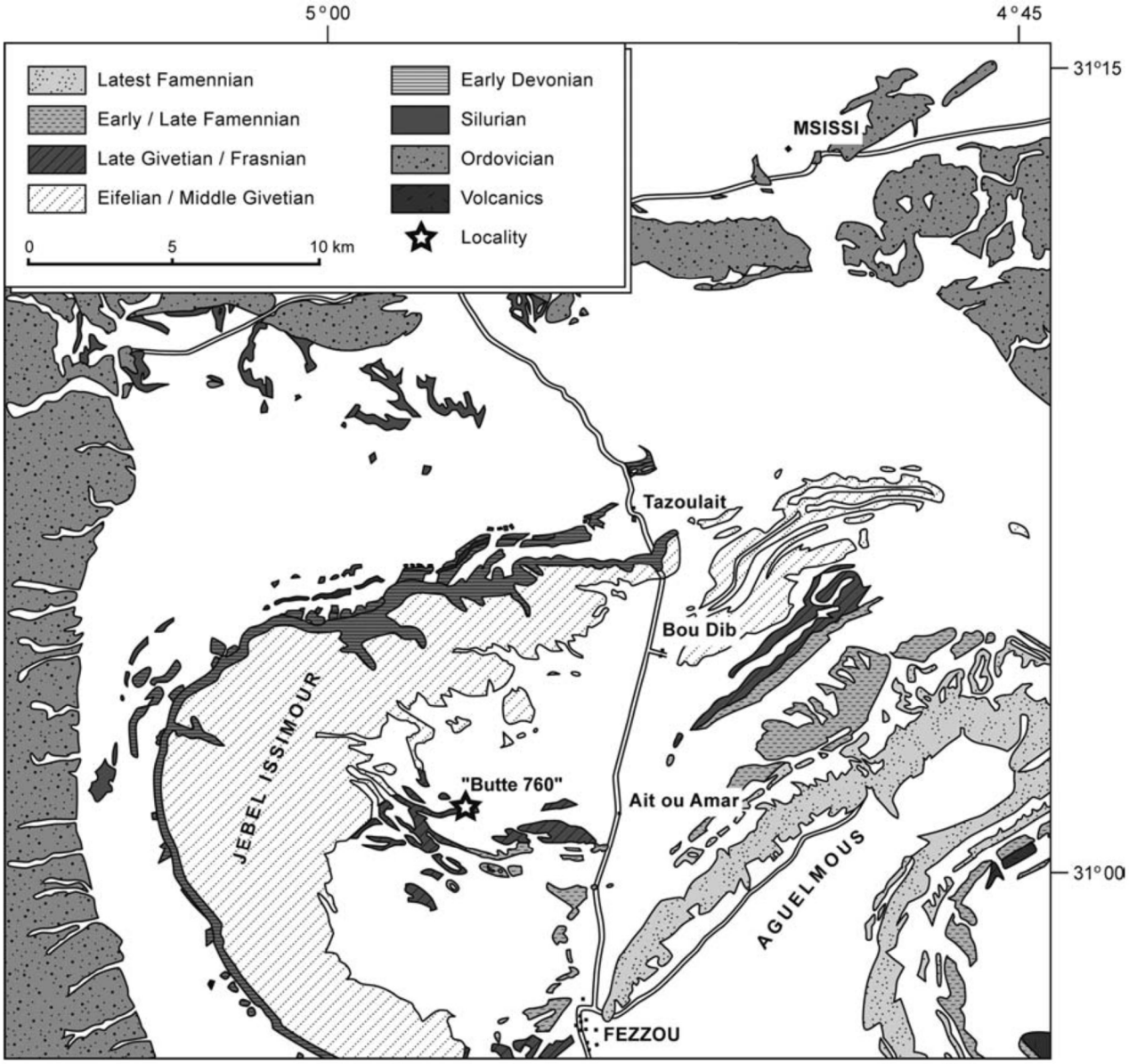

Fig. 1. The "Butte 760" locality west of Ait Ou Amar in the Maider, eastern Anti-Atlas, Morocco.

Dar Kaoua, which represents the pelagic central Tafilalt Platform (Bockwinkel et al. 2009), and continued with the extremely abundant fauna from Hassi Nebech, which represents the deeper, pelagic Tafilalt Basin (bockwinkel et al. 2013a). As a next step we document here the goniatite fauna from "Butte 760" near Ait Ou Amar in the northern Maider. The association of goethitic/haematitic ammonoids with a rich, similarly preserved brachiopod-gastropodcoral assemblage indicates a mixed neritic-pelagic setting that is very different from the contemporaneous Tafilalt localities. The comparison between the roughly contemporaneous Ait Ou Amar and Hassi Nebech faunas, both from hypoxic, argillaceous deposits, suggests differences of habitat range for individual taxa. With the support of morphometric data and suture ontogenies we address the question of whether there are potential ecomorphological differences between populations of the same species collected from goniatite shales deposited either in deeper or more shallow settings.

2. The fossil locality "Butte 760" near Ait Ou Amar

Ammonoids and associated benthic fauna were collected loose at the foot of a solitary small hill ("Butte 760") representing a late Givetian biostrome, 5 km west of the small village of Ait Ou Amar, in the plain a few km E of the centre of the Jebel Issimour, 8 km WSW of Bou Dib, in the northern Maider, Anti Atlas, southeastern Morocco (Fig. 1). The GPS coordinates on the topographic sheet, 1:100.000 Msissi, are: N 31°01'00'', W 04° 56' 24''.

The entire assemblage was collected loose from hypoxic shales. It is probably a mixture of several levels and consists of goniatites, orthoconic cephalopods (orthocerids, rare spyrocerids, and brevicones), rare cyrtobreviconic nautiloids, abundant brachiopods (atrypids, terebratulids, pentamerids, rhynchonellids, cyrtinids, and others), crinoid stem pieces, gastropods (bellerophontids, platyceratids, and others), bivalves (nuculoids and the veneroid Paracyclas), phacopid trilobites, and a few receptaculitids (Ischadites). In close association but from just above the hypoxic shales, there is a different, loose, calcitic assemblage, consisting mostly of solitary and colonial rugose corals (Phillipsastrea), branching tabulate corals (Thamnopora and others), few stromatoporoids, and brachiopods (especially atrypids, Leptaena, and orthids). The corals from the NW Maider were included in systematic studies by coen-AuberT (2002, 2005).

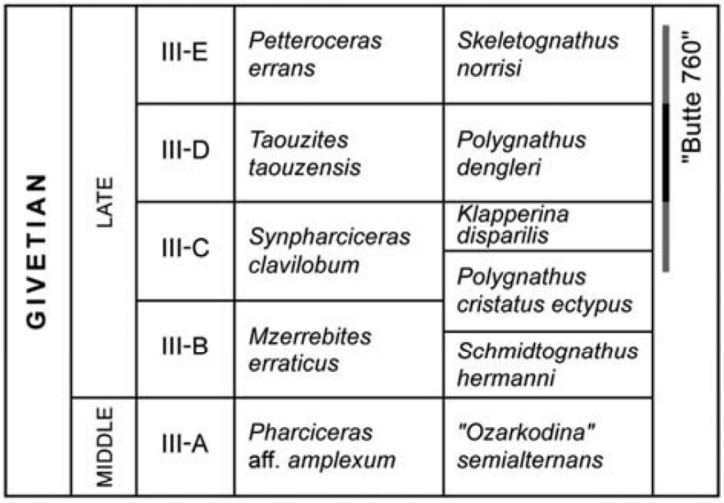

Fig. 2. Overview of the late Givetian ammonoid and conodont biostratigraphy of the eastern Anti-Atlas with the stratigraphic range of the "Butte 760" ammonoid fauna (black bar = probable level of the majority of the fauna, grey bar = minor source of faunal components).

The brachiopod-rich Pharciceras fauna, found in the northern Maider in close association with numerous phillipsastreids, was discovered by HollArd (1974), who briefly noted it in "unit ds 1.1" of his generalized Taboumakloûf succession. His basal Late Devonian age assignment was correct at the time, well before the Middle/Late Devonian boundary was re-defined as near the top of the "Pharciceras Stufe". More stratigraphic details were provided by bulTynck & Jacobs (1981), who separated adjacent, lateral "Ait Ou Amar" and "Butte 760" sections (hills). At the second locality, "Pharciceras arenicus" and "Ph. cf. P. kseirense" were recorded from an interval with Schmidtognathus? gracilis and Klapperina disparilis

(Bed 11), which suggests at least the late Givetian disparilis conodont Zone. However, it is strange that nArkiewicz & bulTynck (2010) subsequently recorded the base of the disparilis Zone somewhat higher, in Bed 12. Even higher (Bed 15), records of Polygnathus alatus and Po. paradecorosus (but identified by the authors as Po. pollocki) indicate that the alternating shales and limestones range into the norrisi Zone (see regional conodont ranges in AboussAlAm & becker 2007). Consequently, our loose faunas can be assigned to the disparilis/norrisi Zone interval, which correlates in the Tafilalt with the Synpharciceras clavilobum to Petteroceras errans Zones (Middle Devonian = MD III-C to III-E sensu becker & House 2000; see also ogg et al. 2008).

Taouzites and Pseudoprobeloceras are well represented in our new collections and both marker forms are most characteristic of the T. taouzensis Zone (MD III-D). Some Petteroceras specimens confirm that the shale unit also includes the Pett. errans Zone (MD IIIE) at the top of the Givetian (Fig. 2). The same age range applies to the main Hassi Nebech faunas of the Tafilalt Basin (bockwinkel et al. 2013a). The presence of Pharciceras pargai and Mzerrebites at "Butte 760" indicates that part of the collection derives from slightly older strata. In the Tafilalt, Mzerrebites is most characteristic of the Mz. erraticus Zone (MD III-B, e.g., AboussAlAm & becker 2011; becker et al. 2013b; becker & AboussAlAm 2013) but different species characterize that zone and there is a specimen of the genus from the Synpharciceras clavilobum Zone of the central Tafilalt. Ph. pargai is typical for the Syn. clavilobum Zone of Dar Kaoua (bockwinkel et al. 2009) but it is absent at Hassi Nebech. In summary, the majority of specimens probably came from the T. taouzensis Zone (MD III-D) but with an admixture of some specimens from the Syn. clavilobum and Petteroceras errans Zones (MD III-C and III-E).

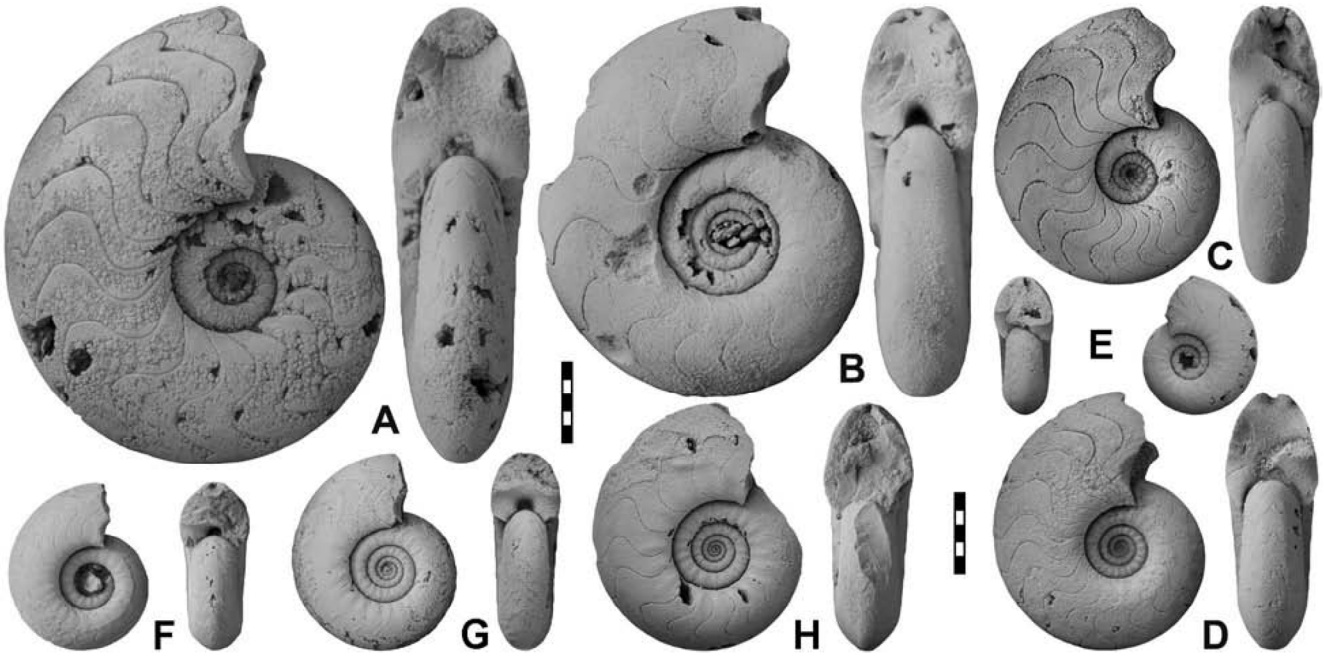

Fig. 4. Species of *Pseudoprobeloceras* from "Butte 760", all x 2. **A**, **C-E** *Pseudoprobeloceras praecox* Bockwinkel, Becker & Ebbighausen, 2013. **A** – MB.C.25090.5. **C** – MB.C.25090.8. **D** – MB.C.25090.2. **E** – MB.C.25090.1. **B**, **F-H** *Pseudoprobeloceras pernai* (Wedekind, 1918). **B** – MB.C.25091.1. **F** – MB.C.25092.2 (cf.). **G** – MB.C.25092.3 (cf.). **H** – MB.C.25092.1 (cf.).

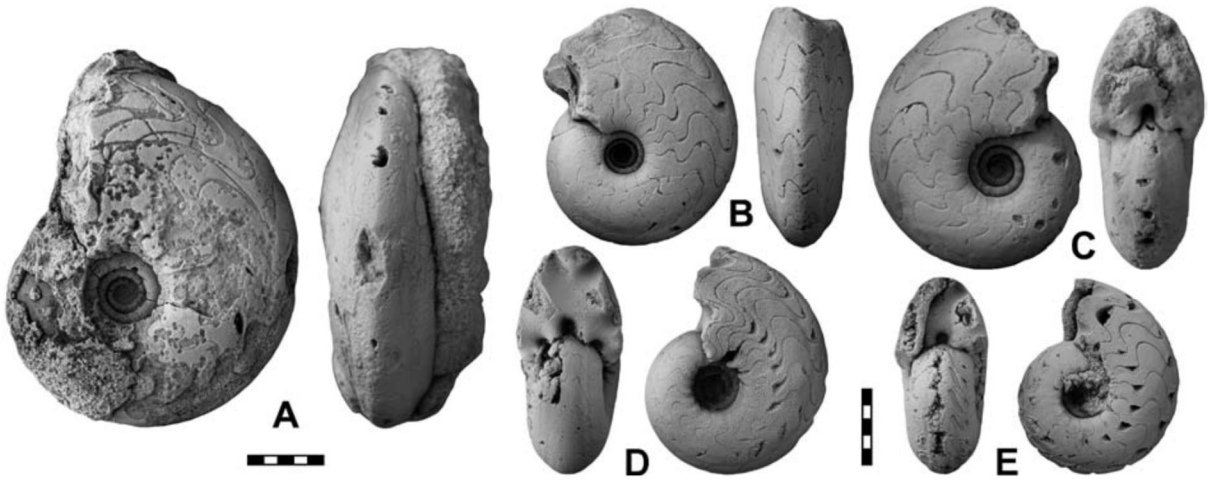

Fig. 6. Species of *Darkaoceras* and *Mzerrebites* from "Butte 760", all x 2. **A-C** *Darkaoceras velox* Bockwinkel, Becker & Ebbighausen, 2013. **A** – MB.C.25094.6. **B** – MB.C.25094.3. **C** – MB.C.25094.1. **D**, **E** *Mzerrebites amarensis* n. sp. **D** – Holotype MB.C.25093.1. **E** – Paratype MB.C.25093.2.

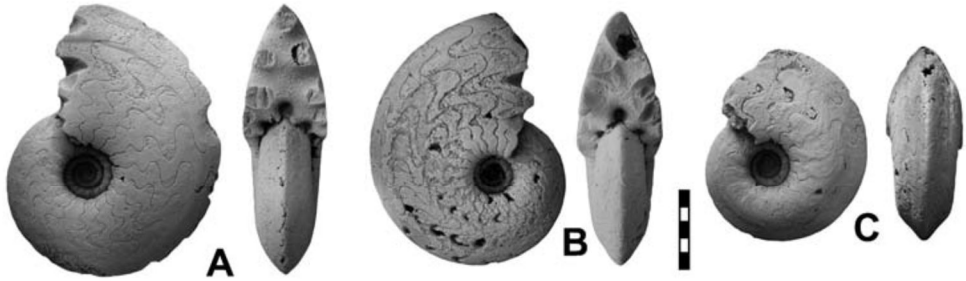

Fig. 8. *Taouzites taouzensis* (Termier & Termier, 1950) from "Butte 760", all x 2. **A** – MB.C.25095.5. **B** – MB.C.25095.4. **C** – MB.C.25095.8.

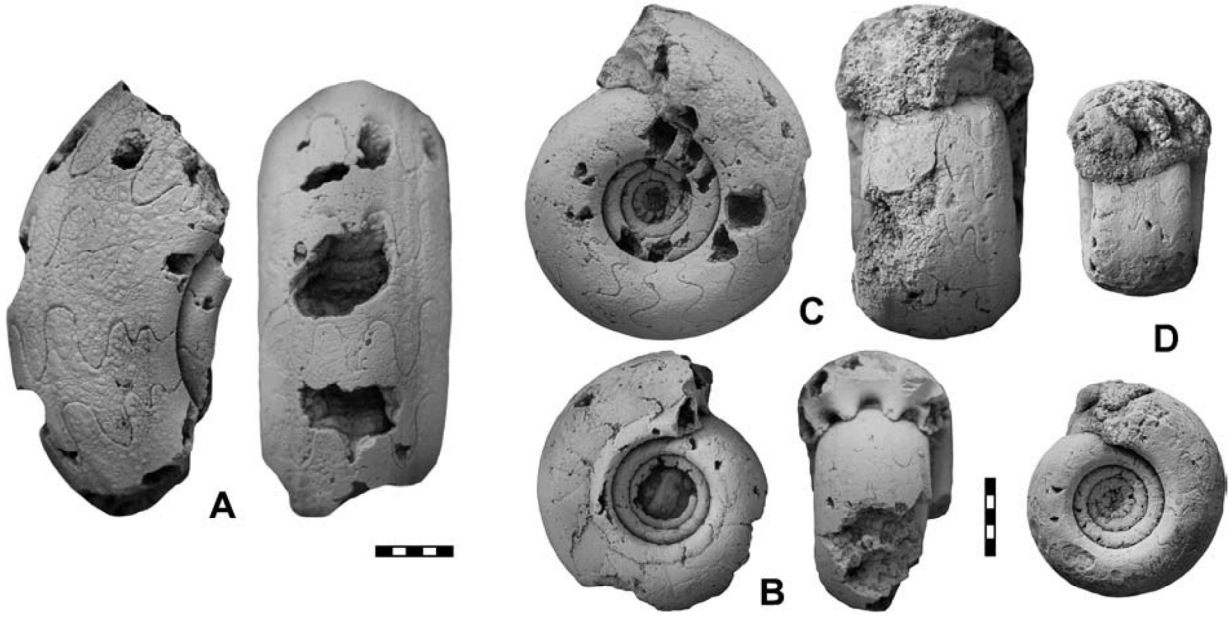

Fig. 10. Species of *Pharciceras* from "Butte 760", all x 2. **A** – *Pharciceras* sp., MB.C.25096. **B-D** *Pharciceras lateseptatum* Frech, 1902. **B** – MB.C.25098.4 (Morphotype I). **C** – MB.C.25098.3 (Morphotype II). **D** – MB.C.25098.2 (Morphotype I).

STOP 6.6 – Jebel Amelane

The following is from: Becker, R.T. and Aboussalam, Z.S., 2013, The Global Chotec Event at Jebel Ameline (Western Tafilalt Platform) – Preliminary Results. International Field Symposium "The Devonian and Lower Carboniferous of northern Gondwana" – Morocco, pp. 129-135.

1. INTRODUCTION

The term (Basal) Choteč Event was introduced byCHLUPÁČ, I. &KUKAL, Z. (1986, 1988) in Bohemia, where there is an abrupt change low in the Eifelian from the light-grey to reddish Třebotov to darker, more organic-rich ChotečLimestone. The intercalation of dark calcareous shales in some sections, ca. 1-2 m above the base, marks the peak of the transgressive event. It has recently been restudied in more detail by BERKYOVÁ (2009) and KOPTÍKOVÁ (2011), who supported the idea of a (probably eustatic) sea-level rise. The increased organic content is partly caused by sudden algal (prasinophyceen) blooms (BROCKE et al. 2009). CHLUPÁČ&KUKAL (1988) briefly summarized associated faunal changes and the possible global nature of the event. However, detailed studies in other regions are still almost lacking, with the exception of Bolivia (TROTH et al. 2011) and Nevada (ELRICK et al. 2009, PEDDER 2010). But in the latter region, the recognition of the event interval is seriously hampered by strong condensation and unconformities (VODRÁŽKOVÁ et al. 2011). For northern Spain there is a review by GARCIA-ALCALDE (1998) but more bed-by-bed data (in addition to, e.g., HENN 1985, MONTESINOS 1987, and GARCÍA-LÓPEZ&SANZ-LÓPEZ (2002) are needed. There is a detailed study in the Ossa Morena Zone of SW Iberia (MACHADO et al. 2010) but with ambiguities based on gaps in the section.

Fig. 1. Position of the Jebel AmelaneChoteč Event locality west of Rissani(red dot) on an excerpt from the geological map (sheet Tafilalt-Taouz). The red M to the south marks the Jebel MechIrdaneEifelian-Givetian Boundary Stratotype.

This preliminary report is the first detailed study on the Choteč Event in southern Morocco. The event has been first recognized in the Tafilalt by BECKER & HOUSE (1994, 2000), based on the BouTchrafine and

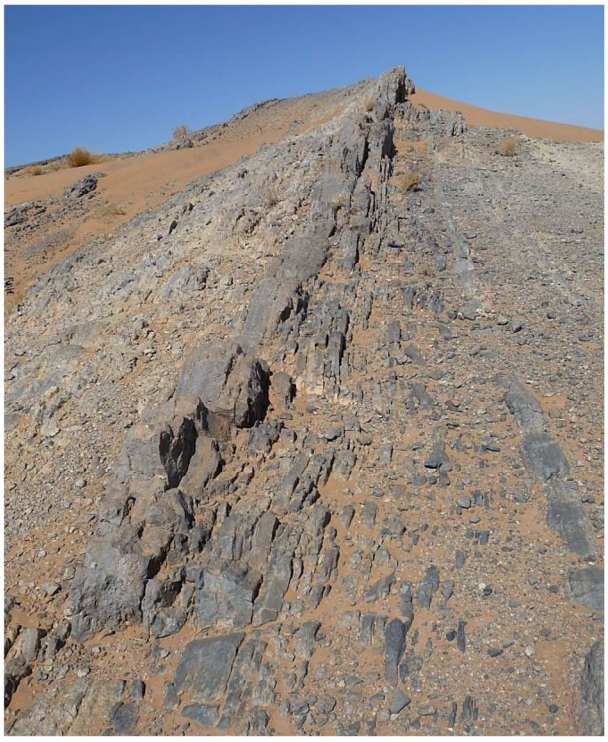

Fig. 2. Overview of the near vertical Choteč Event section near the eastern end of Jebel Amelane. Bed 3 is the solid bed to the right, Beds 11-12 form the minor cliff in the middle, Bed 13 the lower part of the lighter-grey rubbly limestone just left of it.

Jebel Amelane sections. The latter(at x = 600.4, y = 76.4) was chosen for a more detailed survey because of the very distinctive black styliolinites, marls and limestone, which interrupt an otherwise light-grey, well oxygenated hemipelagic platform setting. Emphasis was placed on the precise dating in terms of the conodont stratigraphy but modern dacryoconarid data would be desirable.KLUG (2002a, 2002b) outlined the regional significance of the Choteč Event for ammonoid diversity and morphology.

2. SEDIMENTS AND FAUNAS (Figs. 2-3)

The lower, upper Emsian part of the succession with abundant anarcestids (*Anarcestessimulans*, *Sellanarcestes* div. sp.), large bivalves (*Panenka* div. sp.), orthocones, and phacopids has been described by BECKER & HOUSE (1994). Sellanarcestids are restricted to the lower ca. 2 m, *An. lateseptatus* was found in Bed A_4. The upper part of these yellowish-weathering, nodular limestones form Beds 0-2 of the new section log. Bed 0 yielded *Panenka* and solitary

Rugosa, Bed 2 a *Fidelites* sp. Bed 3a (Fig. 4) is a solid marker limestone just below the Choteč Event Interval

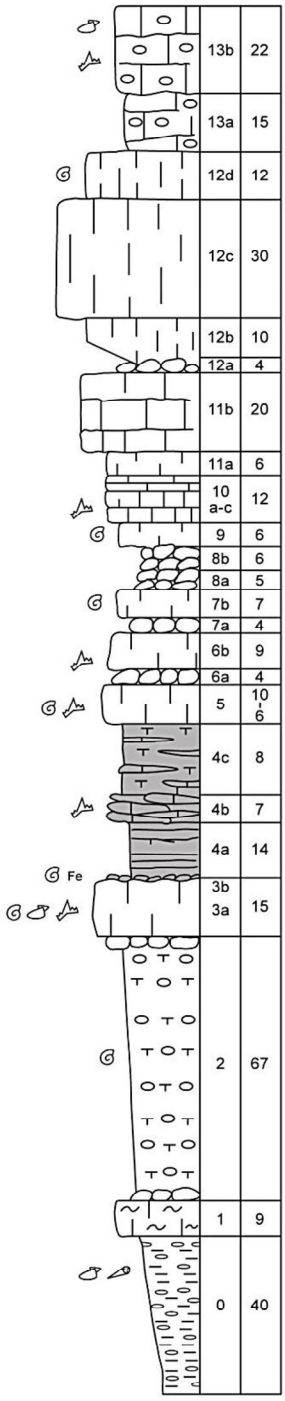

Fig. 3. Lithological log of the lower Eifelian at Jebel Amelane, showing current conodont sampling levels.

withsome more *Fidelites* and the oldest, large *Subanarcestes*cf. *marhoumensis*. A thin, nodular iron crust at the top (Bed 3b) indicates a condensation interval and shallowing upwards. The conodont assemblage from Bed 3a includes *Icriodus struvei* (Fig. 7.1), *Linguipolygnathus bultyncki* (Figs. 7.2-3), *Ling. pinguis* (Fig. 7.4), *Ling. linguiformis*, and *Ling. zieglerianus* (Fig. 7.5).

The event interval (Figs. 5-6) is marked by a sudden change to black, organic-rich, irregularly laminated, platy marls and styliolinites (*Styliolina*packstones, Beds 4a-c). This reflects a significant deepening and eutrophication pulse. So far there are no identifiable palynomorphs (R. BROCKE, oral comm.). The middle part is calcareous enough for conodont sampling. It yielded a restricted assemblage with *I. struvei, Ling. zieglerianus, Ling. coopericooperi* (Fig. 7.6), and a questionable *Po. costatuspartitus*.

Fig. 4. Thin-section of Bed 3a, a bioturbatedpackstone with abundant dacryoconarids, debris of bivalves and goniatites, gastropods, and trilobites.

Fig. 5. Details of the Choteč Event Interval at Jebel Amelane.

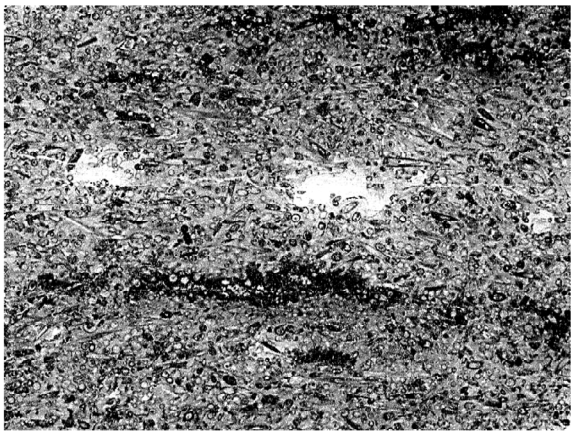

Fig. 6.Thin section of the dark, laminated styliolinites (styliolinidpackstone) of Bed 4b.

Above, there is an alternation of thin-bedded middle to light-grey nodular limestones, some with poorly preserved *Fidelites* (Beds 5, 7b, 9). Previously (BECKER & HOUSE 1994), a *Pinacites* sp. was found in Bed 5, which also contains *Ling. Pinguis* (common, Fig. 7.7), *Ling. linguiformis, Ling. Zieglerianus* (Fig. 7.8),and a single *Ling. sogdianensis* (Fig. 7.22, new record for North Africa). Slightly higher, Bed 6b, a bioturbated, crinoidal dacryoconarid packstone with trilobites and partly washed out micrite matrix, produced intermediates between *Ling. zieglerianus* and *Po. robusticostatus*, still with a short lingua (Fig. 7.9, compare WEDDIGE 1977), in association with *Ling. linguiformis* (Fig. 7.16), *Ling. pinguis, Ling. zieglerianus,* and *I. struvei*. Bed 10a has the richest conodont fauna of all samples, with first entries of *I. amabilis* (very rare, Fig. 7.11), *I.* aff. *Regularicrescens* (Fig. 7.15), *I. anterodepressus* (common, Fig. 7.13), a new "*Ozarkodina*" (very rare, Fig. 7.12), and *Po. Angusticostatus* (Fig. 7.23). *Po.costatuspartitus* is the only subspecies of the *costatus* lineage. There are also re-appearances of long-ranging icriodids, such as *Caudicriodus culicellusculicellus* (Fig. 7.10) and common*I. cornigercorniger* (Fig. 7.14), and of *Ling. coopericooperi. I. struvei* is the most common species; the icriodid dominated (> 72 %) biofacies suggests a regressive trend.

More solid limestones start with Bed 11b and Beds 12b-f form a minor cliff, which represent the peak of regression. They display cross-sections of *Subanarcestes*. The massive limestone set correlates with the massive Bed 7 at BouTchrafine (BULTYNCK 1985, BECKER & HOUSE 1994) and equivalents can be found in many other sections (KLUG 2002a, 2002b). The nodular limestones on the southern or road side of the minor cliff resemble the upper Emsian facies in the presence of nautiloids and *Panenka*. Bed 13b is characterized by a sudden flood occurrence of *Po. costatuscostatus* (Fig. 7.18) in association with a few last *Po. costatuspartitus* (Figs. 7.19-20), common *Ling. linguiformis* and *I. anterodepressus*, rare *Po. praetrigonicus* (Fig. 7.21), some *Ling. zieglerianus*, *I.*aff. *struvei*, and last *Ling. bultyncki*(Fig. 7.17),and *Ling. pinguis*.

3. CONODONT STRATIGRAPHY

The precise dating of the Choteč Event Interval in the conodont zonation faces several problems: 1. Ambiguity concerning the distinction between the three index subspecies of *Po. costatus*, which are the zonal markers around the Emsian-Eifelian boundary (see comment by MACHADO et al. 2010). Variability and intermediate morphotypes are the main problem. 2. Rarity or absence of the marker lineage in the boundary and event interval (e.g., BERKYOVÁ 2009). 3. Unclear precise ranges of possible alternative index forms, for example of *Po. praetrigonicus* (= sp. aff. *Trigonicus*sensu KLAPPER et al. 1978). Here, the Ardenne-Moroccan composite of GOUWY & BULTYNCK (2002) is most helpful. 4. Imprecise correlation between the polygnathid and icriodid successions in order to date neritic successions. Our data indicate longer regional ranges for some taxa than given in the regional composite of BELKA et al. (1997).

Ling. pinguis and *zieglerianus* date Bed 3a clearly as *partitus* Zone but the zonal marker are absent. *I. struvei* and *Ling. linguiformis* have mostly been regarded as marker species for the *costatus* Zone (e.g., BELKA et al. 1997, KONONOVA & KIM 2003) but the composite of GOUWY & BULTYNCK (2002) showed their joint earlier appearance in the upper *partitus* Zone. There is no evidence that the event interval falls already in the *costatus* Zone. *Ling. coopericooperi* is mostly thought to disappear at the end of the *partitus* Zone (BELKA et al. 1997, BERKYOVÁ 2009) but there is a short overlap with the oldest *Po. costatuscostatus* at BouTchrafine (BULTYNCK 1985). However, more material from the event interval of Jebel Amelaneis desirable, especially of the *costatus* lineage.Bed 5 falls in the upperpart of the *partitus* Zone.This is in agreement with the record of *Po. sogdianensis*, which ranges from the *partitus* into the lower *costatus* Zone (BARDASHEV 1992).*Po.*cf. *robusticostatus* (intermediate to *Ling. zieglerianus*) of Bed 6b occurs in Germany in the *partitus* Zone (WEDDIGE 1977; compare the range of the *robusticostatus* Group in KLAPPER et al. 1978).

*I. amabilis*and *Po.angusticostatus* date Bed 10a as *costatus* Zone. However, the first species has a slightly lower range in the composite of GOUWY & BULTYNCK (2002) and it is strange that the index taxon is still absent in a rich assemblage whilst *Po. costatuspartitus* does occur rarely. The presence of *Ling. coopericooperi* and *Caud.culicellusculicellus* prove a level that cannot be younger than the base of the *costatus* Zone. The stratigraphical significance of *I.*aff.*regularicrescens* is not clear; typical *I. regularicrescens* enter well above the base of the *costatus* Zone (BULTYNCK 1985, BELKA et al. 1997, GOUWY & BULTYNCK 2002).

The sudden dominance of *Po.costatus costatus* in the nodular Bed 13b provides evidence for a strong facies control on the distribution of this marker form. Associated *Ling. pinguis, Ling. bultyncki, Ling. zieglerianus,* and *Po.costatus partitus* prove that the so far investigated section top is still rather low in the *costatus* Zone (see BELKA et al. 1997).

4. GONIATITE STRATIGRAPHY

The basal, nodular part at Jebel Amelane (Bed A_1 in BECKER & HOUSE 1994) falls in the lower *An. Simulans* Zone with *Sellanarcestes* (LD IV-D1). The main, upper part of the cliff represents LD IV-D2 without that genus, which includes the *An. lateseptatus* Zone of KLUG (2002a). The first *Fidelites* is a marker of the lower Eifelian *Foorditesveniens* Zone (MD I-B). Currently, the Lower/Middle Devonian boundary has not been fixed locally The first *Subanarcestes* from Bed 3a extends the lower range of the genus in the Tafilalt (see range chart in KLUG 2002a).

The event interval is poor in goniatites but elsewhere (section El Atrous North) the first *P. jugleri*was found in equivalents of Bed 4c. This explains goethitic (originally pyritic) *Pinacites* faunas from a black shale level of the margin of the Tafilalt Basin to the east (e.g., section Tisserdimine). In agreement with data from other sections in KLUG (2002a), the lower Eifelian *Pinacites* Zone (MD I-C) ranges to the top of the sectionshown in Fig. 3.

5. CONCLUSIONS

The Jebel Amelane section provides impressive evidence for a sudden flooding and eutrophication of the otherwise oligotrophic western Tafilalt Platform during the brief Choteč Event Interval. The prevailing amorphous organic matter may indicate cyanobacteria as the main, suddenly blooming primary producers. Hypoxic to anoxic conditions arose from the biodegradation of the massive input of organic matter under conditions with low bottom circulation. The so far available conodont data suggest that this event occurred at the end of the *partitus* Zone, not in the lower *costatus* Zone. It is unlikely that the dark and shaly event phase of the Bohemian type region has a different (younger) age. Its tentative placing in the *costatus* Zone is based on the entry of *Po*. aff. *trigonicus*, a supposed alternative marker (KLAPPER et al. 1978, BERKYOVÁ 2009). However, it has been named as *Po. praetrigonicus* in BARDASHEV (19xx) and allegedly enters in Tadzhikistan in the *partitus* Zone. Additional collecting may resolve the question.

A second, smaller-scale deepening, above the regressive marker unit, enabled the bloom of the index taxon of the *costatus* Zone. This second lower Eifelian transgression has also been noted by KLUG (2002a) and correlated with the onset of Depophase 1d sensu JOHNSON et al. (1985).With respect to the pre-event shallowing upwards in Bed 3b, it seems important to recognize the Choteč Event as an equally important eustatic pulse (e.g., basal TST of Sequence Eif-1 in eastern North America, VERSTRAETEN2007).

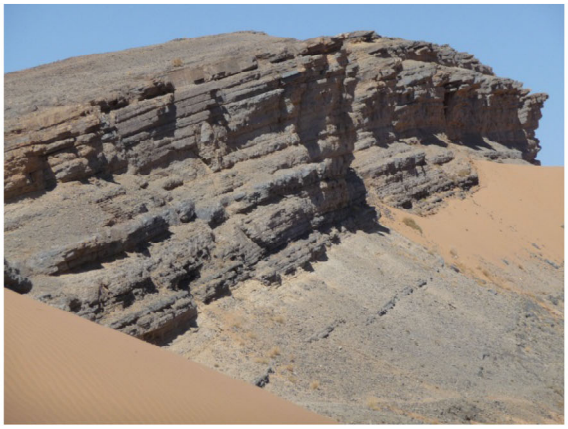

Fig. 8. LateralEifelian to Givetian cliff at Jebel Amelane, with the Kačak Event Interval as incision in the middle.

6. HIGHER STRATA

Λ complete succession through the higher Eifelian and Lower/Middle Givetian is exposed in the steep cliff just a few decameters to the west (Fig. 8, section of BECKER & HOUSE 1994, 2000; see also KLUG2002a). It includes the Kačak Event Interval but there are no associated dark shales or limestones. Similar as at the basal Givetian GSSP at Jebel MechIrdane just to the south (WALLISER et al. 1995), it is possible to collect the oldest maenioceratids (*Bensaiditeskoeneni*), with evidence that they co-occur with the youngest but very rare *Cabrieroceras*. Higher in the cliff and low in the Middle Givetian, there is a peculiar, thin goniatite coquina dominated by a new species of *Sobolewia*. The Taghanic Crisis Interval has been described by ABOUSSALAM (2003), with corrections in ABOUSSALAM & BECKER (2007). The Givetian-Frasnian boundary falls in an unconformity; the wide-spread Frasnes Event beds were mostly removed during a regression at the end of the Lower Frasnian. The Middle Frasnian is well exposed and partly rich in beloceratids (BECKER & HOUSE 2000). There is an impressive sharp base of the very fossiliferous Kellwasser Beds (Fig. 9), which top is an indistinctive but significant erosion surface. Late lower Famennian black goniatite limestones are directly encrusted; their stratigraphy was studied by BECKER (1993).

7. REFERENCES

ABOUSSALAM, Z.S. 2003. Das "Taghanic-Event" im höheren Mittel-Devon von West-Europa und Marokko. – Münstersche Forschungen zur Geologie und Paläontologie, **97**: 332 pp.

ABOUSSALAM, Z.S. & BECKER, R.T. 2007.New upper Givetian to basal Frasnianconodont faunas from the Tafilalt

(Anti-Atlas, Southern Morocco).– Geological Quarterly, **51** (4): 345-374.

BARDASHEV, I. 1992. Conodont Stratigraphy of Middle Asian Middle Devonian. – Courier Forschungsinstitut Senckenberg, 154: 31-83.

ABOUSSALAM, Z.S. 2003. Das "Taghanic-Event" im höheren Mittel-Devon von West-Europa und Marokko. – Münstersche Forschungen zur Geologie und Paläontologie, **97**: 332 pp.

ABOUSSALAM, Z.S. & BECKER, R.T. 2007.New upper Givetian to basal Frasnian conodont faunas from the Tafilalt (Anti-Atlas, Southern Morocco).– Geological Quarterly, **51** (4): 345-374.

BECKER, R.T. 1993. Stratigraphische Gliederung und Ammonoideen-Faunen im Nehdenium (Oberdevon II) von Europa und Nord-Afrika. – Courier Forschungsinstitut Senckenberg, **155**: 405 pp.

BECKER, R.T. & HOUSE, M.R. 1994.International Devonian goniatite zonation, Emsian to Givetian, with new records from Morocco. – Courier Forschungsinstitut Senckenberg, **169**: 79-135.

BECKER, R.T. & HOUSE, M.R. 2000.Devonian ammonoid successions at JbelAmelane (Western Tafilalt, Southern Morocco). – Notes et Mémoires du Service géologique du Maroc, **399**: 49-56.

BERKYOVÁ, S. 2009. Lower-Middle Devonian (upper Emsian-Eifelian, *serotinus-kockelianus* zones) conodont faunas from the Prague Basin, the Czech Republic. – Bulletin of Geosciences, **84** (4): 667-686.

BROCKE, R., BERKYOVÁ, S., BUDIL, P.,FATKA, O., FRÝDA, J. & SCHINDLER, E. 2009. Phytoplankton bloom in the early Middle Devonian (Eifelian): The Basal Choteč Event in the Barrandian area (Czech Republic). – SDGG, GeoDresden 2009, **63**: 63.

BULTYNCK, P. 1985. Lower Devonian (Emsian) – Middle Devonian (Eifelian and lowermost Givetian) conodont successions from the Ma´derand the Tafilalt, southern Morocco. – Courier Forschungsinstitut Senckenberg, **75**: 261-286.

CHLUPÁČ, I. & KUKAL, Z. 1986.Reflection of possible global Devonian events in the Barrandian area, C.S.S.R. – Lecture Notes on Earth Sciences, **8**: 171-179.

CHLUPÁČ, I. & KUKAL, Z. 1988.Possible global events and the stratigraphy of the Palaeozoicof the Barrandian (Cambrian-Middle Devonian, Czechoslowakia). – Sbornikgeologickýchvéd, Geologie, **43**: 83-146.

GARCÁ-LÓPEZ, S. & SANZ-LÓPEZ, J. 2002.Devonian to Lower Carboniferous conodont biostratigraphy of the Bernesga Valley section (Cantabrian Zone, NW Spain). – Cuadernos del Museo Geominero, **1**: 163-205.

GOUWY, S. & BULTYNCK, P. 2002. Graphic correlation of Middle Devonian sections in the Ardenne region (Belgium) and the Mader-Tafilalt region (Morocco): development of a Middle Devonian composite standard. – Aardkundige Medelingen, **12**: 105-108.

HENN, A.H. 1985. Biostratigraphie und Fazies des hohen Unter-Devon bis tiefen Ober-Devon der Provinz Palencia, Kantabrisches Gebirge, N-Spanien. – Göttinger Arbeiten zur Geologie und Paläontologie, **26**: 100 pp.

JOHNSON, J.G., KLAPPER, G. & SANDBERG, C.A. 1985.Devonian eustatic fluctuations in Euramerica. – Geological Society of America, Bulletin, **96**: 567-587.

KLAPPER, G., ZIEGLER, W. & MASHKOVA, T.V. 1978. Conodonts and correlation of Lower-Middle Devonian boundary beds in the Barrandian area of Czechoslovalia.– Geologica et Palaeontologica, **12**: 103-116.

KLUG, C. 2001. Early Emsian ammonoids from the eastern Anti-Atlas (Morocco) and their succession. – PaläontologischeZeitschrift, **74** (4): 479-515.

KLUG, C. 2002a. Quantitative stratigraphy and taxonomy of late Emsian and Eifelian ammonoids of the eastern Anti-Atlas (Morocco). – Courier Forschungsinstitut Senckenberg, **238**: 1-109.

KONONOVA, L.I. & KIM, S.-Y. 2003. Eifelian Conodonts from the Central Russian Platform. – Paleontological Journal, **39** (Suppl. 2): 134 pp.

KOPTÍKOVÁ, L. 2011. Precise position of the Basal Choteč event and evolution of sedimentary environments near the Lower-Middle Devonian boundary: The magnetic susceptibility, gamma-ray spectrometric, lithological, and geochemical record of the Prague Synform (Czech Republic). – Palaeogeography, Palaeoclimatology, Palaeoecology, **304**: 96-112.

MACHADO, G., HLADIL, J., SLAVIK, L., KOPTÍKOVÁ, L., MOREIRA, N., FONSECA, M. & FONSECA, P. 2010. An Emsian-Eifelian calciturbidite sequence and the possible correlatable pattern of the basal Choteč Event in western Ossa-Morena Zone, Portugal (Odivelas Limestone). – Geologica Belgica, **13** (4): 431-446.

MONTESINOS, J.R. 1987. Agoniatitina y Anarcestina del Dévonico Medio de la Cordillera Cantábrica (Dominios Palentino y Asturleonés, NO de España). – Cuaderno Laboratoria Xeooxico de Laxe, **12**: 99-118.

PEDDER, A.E.H. 2010. Lower-Middle Devonian rugose coral faunas of Nevada: Contribution to an understanding of the "barren" E Zone and Choteč Event in the Great Basin. – Bulletin of Geosciences, **85** (1): 1-26.

VERSTRAETEN, C.A. 2007.Basinwide stratigraphic synthesis and sequence stratigraphy, upper Pragian, Emsian and Eifelia stages (Lower to Middle Devonian), Appalachian Basin. – In: BECKER, R.T. & KIRCHGASSER, W.T. (Eds.), Devonian Events and Correlations, Geological Society of London, Special Publications, **278**: 39-81.

VODRÁŽKOVÁ, S., KLAPPER, G. & MURPHY, M.A. 2011.Early Middle Devonian conodont faunas (Eifelian, *costatus-kockelianus* zones) from the Roberts Mountains and adjacent areas in central Nevada. – Bulletin of Geosciences, **86** (4): 737-764.

WALLISER, O.H., BULTYNCK, P., WEDDIGE, K., BECKER, R.T. & HOUSE, M.R. 1995.Definition of the Eifelian-Givetian stage boundary. – Episodes, **18**: 107-115.

WEDDIGE, K. 1977. Die Conodonten der Eifel-Stufe im Typusgebiet und in benachbarten Faziesgebieten. – Senckenbergianalethaea, **58** (4/5): 271-419.

Acknowledgements

E. KUROPKA processed the conodont samples, T. FÄHRENKEMPER provided the section log. S. STICHLING, S. HARTENFELS and T. FISCHER took part in the field work and provided photos.

Fig. 9. Sharp contact between light-grey, nodular *Beloceras* Beds and the dark, bluish-grey Kellwasser Beds at Jebel Amelane.

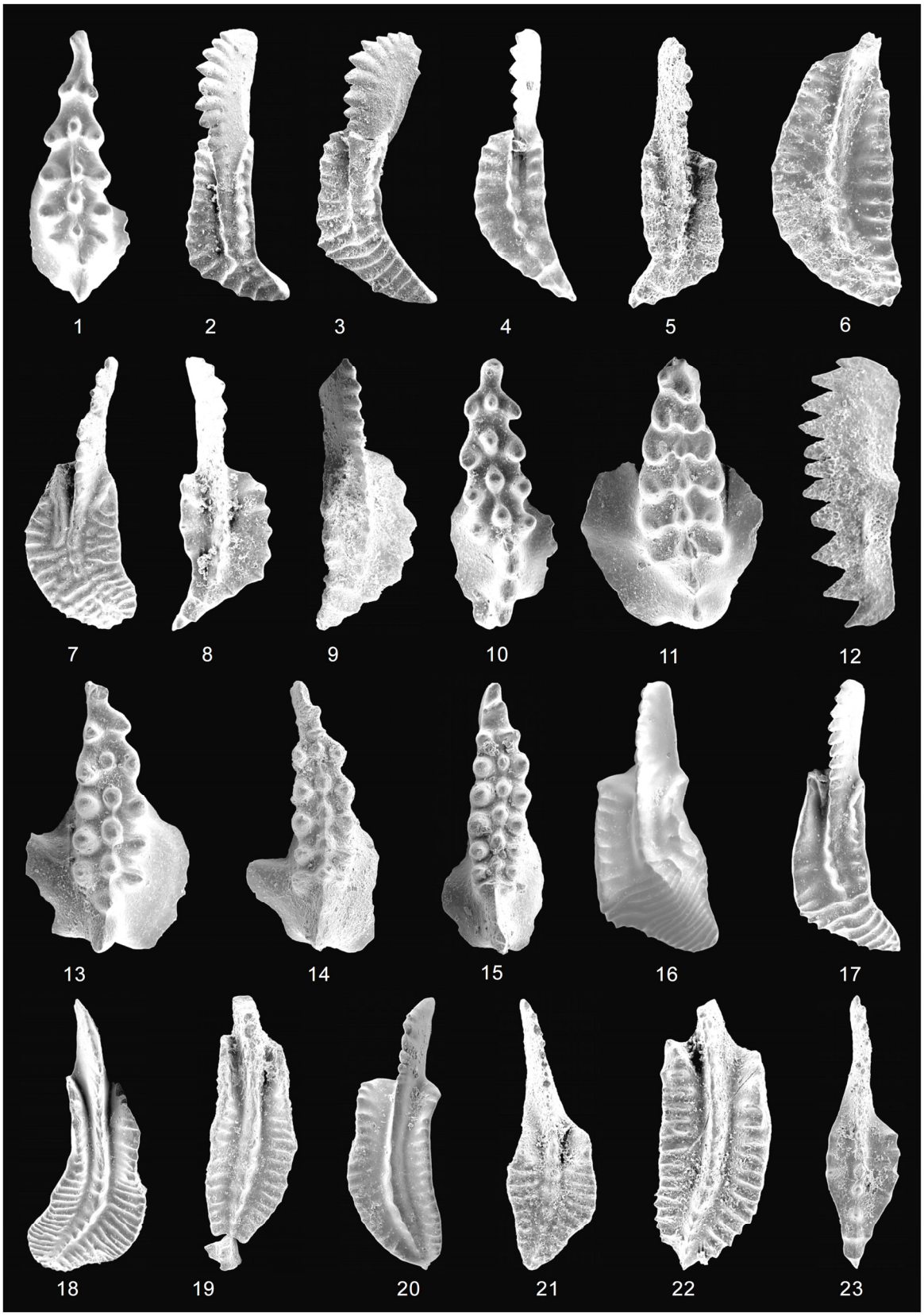

Fig. 7. Conodonts from around the Choteč Event at Jebel Amelane. 1-5 = Bed 3a, 6 = Bed 4b, 7-8 and 22 = Bed 5, 9 = Bed 6b, 10-16 and 23 = Bed 10a, 17-21 = Bed 13b. **1.***I. struvei*, **2-3, 17.***Ling. bultyncki*, **4, 7.***Ling. pinguis*, **5, 8.***Ling. zieglerianus*, **6.***Ling. coopericooperi*, **9.***Po.*cf. *robusticostatus*, **10.***Caud.culicellusculicellus*, **11.***I. amabilis*, **12.**"*Ozarkodina*" n. sp., **13.***I. anterodepressus*, **14.***I. cornigercorniger*, **15.***I.*aff.*regularicrescens*, **16.***Ling. linguiformis* γ2, **18.***Po.costatuscostatus*, **19-20.***Po.costatuspartitus*, **21.***Po.praetrigonicus*, **22.***Po.sogdianensis*, **23.***Po.angusticostatus*.

STOP 6.7 – Eifelian-Givetian GSSP Golden Spike

A Global Boundary Stratotype Section and Point (GSSP), sometimes referred to as a golden spike, is an internationally agreed upon reference point on a stratigraphic section which defines the lower boundary of a stage on the geologic time scale. The effort to define GSSPs is conducted by the International Commission on Stratigraphy, a part of the International Union of Geological Sciences. Most, but not all, GSSPs are based on paleontological changes. Hence GSSPs are usually described in terms of transitions between different faunal stages, though far more faunal stages have been described than GSSPs. The GSSP definition effort commenced in 1977. As of 2025, 81 of the 101 stages that need a GSSP have a ratified GSSP.

Rules

A geologic section has to fulfill a set of criteria to be adapted as a GSSP by the ICS. The following list summarizes the criteria:

A GSSP has to define the lower boundary of a geologic stage.
The lower boundary has to be defined using a primary marker (usually first appearance datum of a fossil species).
There should also be secondary markers (other fossils, chemical, geomagnetic reversal).
The horizon in which the marker appears should have minerals that can be radiometrically dated.
The marker has to have regional and global correlation in outcrops of the same age.
The marker should be independent of facies.
The outcrop has to have an adequate thickness.
Sedimentation has to be continuous without any changes in facies.
The outcrop should be unaffected by tectonic and sedimentary movements, and metamorphism.
The outcrop has to be accessible to research and free to access.
This includes that the outcrop has to be located where it can be visited quickly (international airport and roads), has to be kept in good condition (ideally a national reserve), in accessible terrain, extensive enough to allow repeated sampling and open to researchers of all nationalities.

GSSP for Givetian Stage

Definition:

The GSSP for the Givetian Stage is placed at the base of Bed 123 in a section at Jebel Mech Irdane in the Tafilalt of Morocco. The Eifelian-Givetian boundary coincides with the level at which conodont Polygnathus pseudofoliatus changes to Polygnathus hemiansatus. The boundary corresponds closely with the base of the goniatite Maenioceras Stufe used as a Middle Devonian division, and the entry of the dacryoconarid Nowakia otomari.

Location:

The GSSP is located at Jebel Mech Irdane, 25 km SSW of Erfoud and 12km SW of Rissani, Morocco. 1:100 000 Carte du Maroc, Feuille NH-30-XX-2, Erfoud, Lambert's coordinates: x = 599 2, y =

470 6. The locality is about 6 km from the metalled Msissi road west of Rissani and easily reached by four-wheel-drive vehicles. The GSSP is at the base of Bed 123 in the succession.

The ridge of Jebel Mech Irdane is 4 km long and exposes a full and fossiliferous succession from the Emsian to the Frasnian. The GSSP section consists mainly of pelagic calcilutites and micrites with black shales at the Kacak Event level. The Kacak Event or otomari or rouvillei Event is a widespread hypoxic sedimentary perturbation near the Eifelian - Givetian Boundary.

Primary Markers:

The Eifelian-Givetian boundary coincides with the level (Bed 123) at which conodont Polygnathus pseudofoliatus changes to Polygnathus hemiansatus.

Secondary Markers:

Goniatites: The base of the Maenioceras Stufe lies only fractionally below the GSSP.

Correlation Events:

Conodont FAD Polygnathus hemiansatus

Other Locations around the World:

Polygnathus hemiansatus can be recognized in the Cantabrian Mountains of Spain, in the Montagne Noir, France, in the Ardennes of Belgium, and the Rhenish and Eifel Mountains of Germany.

References:

Walliser, O. H., Bultynck, P., Weddige, K., Becker, R. T., and House, M. R., 1995. Definition of the Eifelian-Givetian Stage Boundary. Episodes 18/3, p. 107 - 115.

Figure 8.1. Devonian overview. Figure on next page

Most main markers for GSSPs of Devonian stages are first-appearance datums (FADs) of conodont taxa as detailed in the text and in Fig. 8.6. ("Age" is the term for the time equivalent of the rock-record "stage".) See Carboniferous chapter for discussion on potential revised definition of the Devonian/Carboniferous boundary. Magnetic polarity scale is from Becker et al. (2012) with revised Frasnian–Famennian from Hansma et al. (2015). Schematic sea-level curve was compiled by Becker et al. (2012) from various sources. An independent interpretation of Devonian sequences by Haq and Schutter (2008) is shown in Fig. 8.5. The carbon isotope (δ13C) curve is from Buggisch and Joachimski (2006) with global events (often associated with widespread anoxic events, as indicated in black) modified from Becker et al. (2012). Generalized oxygen isotope (δ18O) curve and estimates of tropical sea-surface temperatures from conodont apatite are averaged from Joachimski et al. (2009). For comparison, the adjusted tropical sea-surface temperature curve that Veizer and Prokoph (2015) derived from a synthesis of oxygen-18 values from carbonate fossils is also shown. The vertical scale of this diagram is standardized to match the vertical scales of the first stratigraphic summary figure in all other Phanerozoic chapters. PDB, PeeDee Belemnite 13C standard; SST, sea-surface temperature.

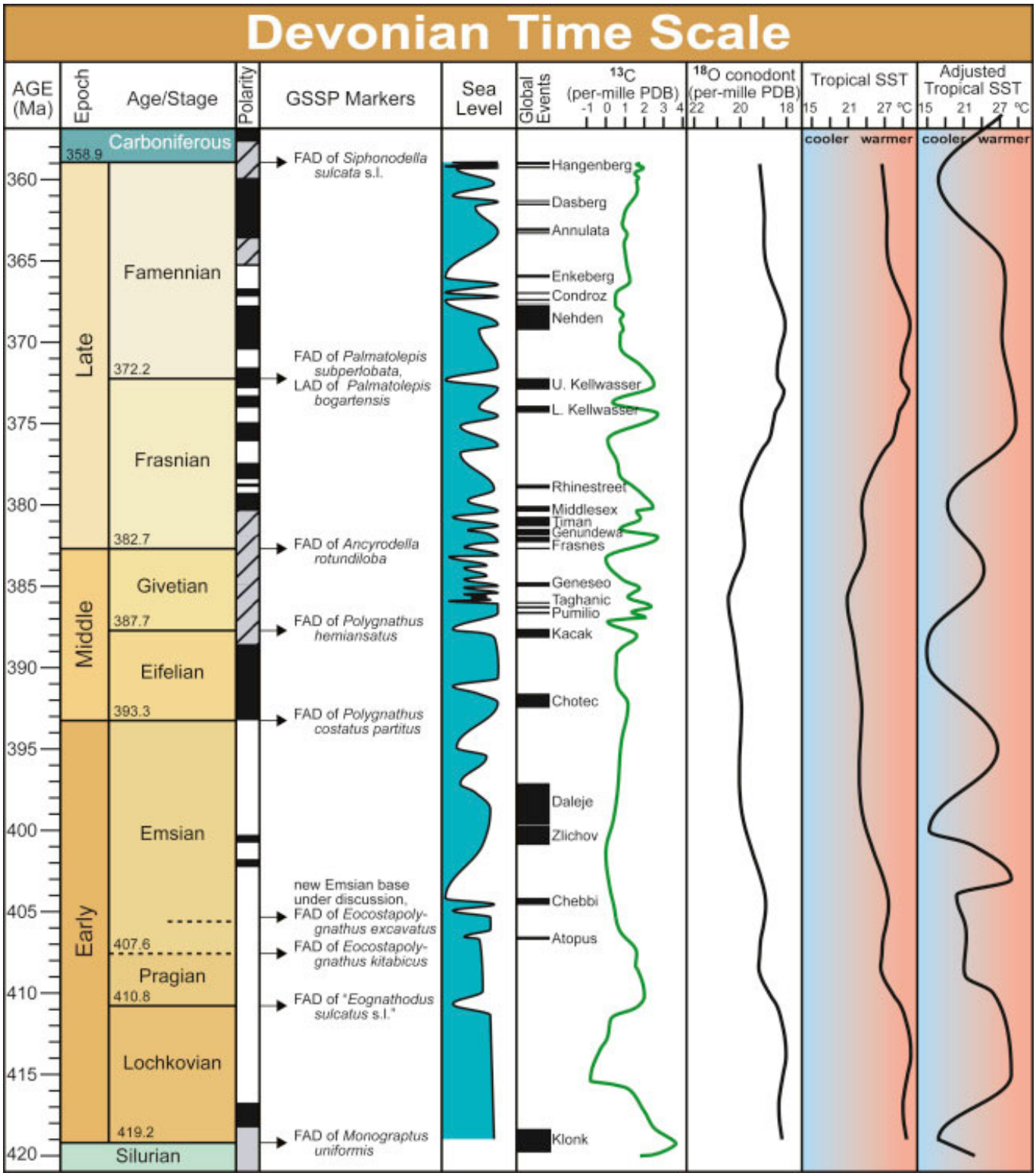
Devonian Time Scale
AGE (Ma)
Epoch
Age/Stage
Polarity
GSSP Markers
Sea Level
Global Events
13C (per-mille PDB)
-1 0 1 2 3 4
18O conodont (per-mille PDB)
22 20 18
Tropical SST
15 21 27 °C
cooler warmer
Adjusted Tropical SST
15 21 27 °C
cooler warmer
Carboniferous
358.9
Late
Middle
Early
Famennian
Frasnian
Givetian
Eifelian
Emsian
Pragian
Lochkovian
372.2
382.7
387.7
393.3
407.6
410.8
419.2
Silurian
360
365
370
375
380
385
390
395
400
405
410
415
420
FAD of Siphonodella sulcata s.l.
FAD of Palmatolepis subperlobata, LAD of Palmatolepis bogartensis
FAD of Ancyrodella rotundiloba
FAD of Polygnathus hemiansatus
FAD of Polygnathus costatus partitus
new Emsian base under discussion, FAD of Eocostapolygnathus excavatus
FAD of Eocostapolygnathus kitabicus
FAD of "Eognathodus sulcatus s.l."
FAD of Monograptus uniformis
Hangenberg
Dasberg
Annulata
Enkeberg
Condroz
Nehden
U. Kellwasser
L. Kellwasser
Rhinestreet
Middlesex
Timan
Genundewa
Frasnes
Geneseo
Taghanic
Pumilio
Kacak
Chotec
Daleje
Zlichov
Chebbi
Atopus
Klonk

STOP 6.8 – Merzouga and Erg Chebbi Dunes

The following is from: Bristow, C.S. and Duller, G.A.T., 2024, Structure and chronology of a star dune at Erg Chebbi, Morocco, reveals why star dunes are rarely recognized in the rock record. Nature: Scientific Reports, vol. 4464, no. 14, 8 pgs.

Erg Chebbi is a small sand sea (18 km by 9 km) that includes reversing barchanoid dunes and star dunes, classified as complex star dunes. The dune described here is known locally as Lala Lallia, which translates (from Berber) as the highest sacred point. On Google Earth™ it is shown as Hassilabied Gran Dune. It is a 100 m high, 700 m wide star dune with radiating arms (Fig. 1) that is located in the south of eastern Morocco close to the border with Algeria (31 08′49.46″N 04 00′34.04″W, Fig. 1). The wind regime is largely bimodal with a SW to NE 210°–240° "Sahel" wind known locally as the Sirocco, and an opposing NE-SW 45°–100° Chergui wind with a frequent, but weaker, easterly wind and supplementary text. Repeat surveys 16 months apart showed displacements perpendicular to the dune crestlines between 0 and 17 m but mostly less than 3 m. The direction of displacement was extremely variable, changing direction between adjacent dune arms and along the arms, depending on the orientation to the wind. Analysis of spatial change during the same period shows that erosion and accumulation increase with elevation, meaning that the crest area is more dynamic than the lower arms. This behavior is likely due to wind acceleration up the dune, as observed with star dunes elsewhere.

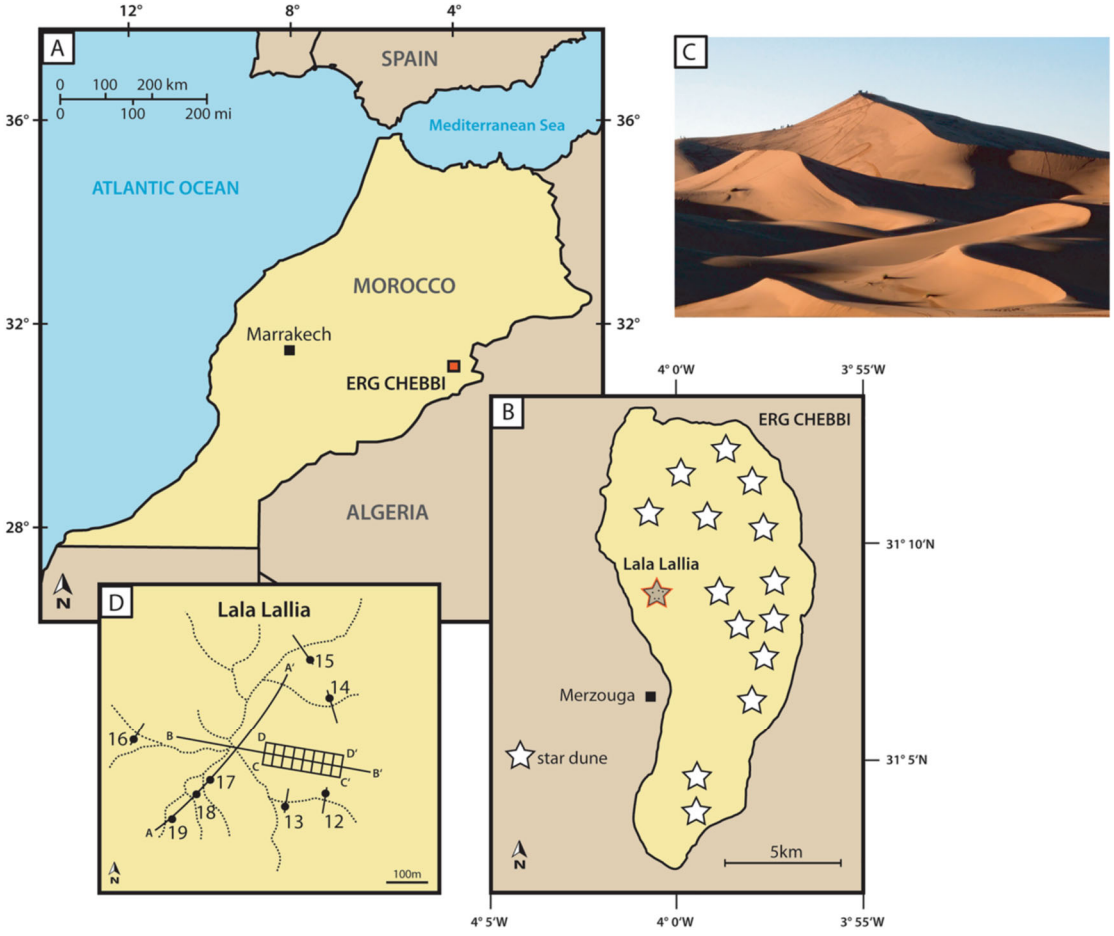

Figure 1. (**A**) Map of Morocco showing the location of Erg Chebbi. (**B**) Map of Erg Chebbi including the studied star dune Lala Lallia. (**C**) Photograph of the dune Lala Lallia from the South, looking north towards the dune crest. (**D**) Map of dune arms and crest lines (dashed lines) and GPR profiles (solid lines). Dots with numbers indicate OSL sample locations on the dune arms. Adobe Illustrator cs3 https://help.adobe.com/archive/en_US/illustrator/cs3/illustrator_cs3_help.pdf.

Day 7: Thursday, March 12th, 2026 – Kem Kem Dinosaur Beds & Filon 12 Mine

STOP 7.1 – Fulgerites!
STOP 7.2 – Kem Kem Dinosaur Mine
STOP 7.3 – Tadaout-Tizi n'Rsas anticline
STOP 7.4 – Silurian Orthoceras and Permian dikes
STOP 7.5 – Filon 12 Hematite Mine
STOP 7.6 – Late Devonian Anticline
Possible Stop – Camel Ride into the Erg Chebbi Dunes

Hotel Information:
Mohayut Camp
4XMP+4MG, village hassi labiad,
Merzouga 52202, Morocco

From our Guide:

Today we drive south through the sand dunes, stopping to see fulgerites which form when lightening hits the sand, to the frontier town of Taouz. We then head to the famous Kem Kem site which is rich in fish, crocodiles and dinosaurs. The rocks are Cretaceous (Cenomanian) in age and were by a Nile sized river. This site has also yielded many teeth and bones dinosaurs of the Spinosaurus and Carcharodontosaurus. This site is actively mined by fossil miners who dig tunnels into the sandstone. After a couple of hours at this site we move on to the Tadaout-Tizi n'Rsas anticline on the other side of Taouz. The beds in the anticline dip almost vertically so that Carboniferous, Devonian, Silurian and Ordovician rocks can be seen in a sequence. One of the most exciting sites lies on the Silurian/Devonian boundary, and here we can see the remains of pelagic crinoids and their floats which are called loboliths. Very close to this site we also see Silurian Orthoceras and Permian aged dykes. We also visit a mineral rich vein that cuts through Ordovician aged rocks. This vein is exploited by the Filon 12 mine. Filon 12 started its life as a haematite mine, but it is now a mine solely for mineralogical specimens. Minerals found here include vanadinite, goethite and haematite. At the mine we can take an underground tour, find our own specimens or buy prized specimens from the miners. Our final stop in the anticline is on the Devonian/Carboniferous boundary and here it is possible to see trace fossils from trilobites and fish tails. The night is spent at the same hotel in Merzouga, and it is possible to take an optional sunset camel ride into the Erg Chebbi dunes.

STOP 7.1 – Fulgerites!

Fulgurites (from Latin *fulgur* 'lightning' and *-ite*), commonly called "**fossilized lightning**", are natural tubes, clumps, or masses of sintered, vitrified, or fused soil, sand, rock, organic debris and other sediments that sometimes form when lightning discharges into ground. When composed of silica, fulgurites are classified as a variety of the mineraloid lechatelierite.

When ordinary negative polarity cloud-ground lightning discharges into a grounding substrate, greater than 100 million volts (100 MV) of potential difference may be bridged.[2] Such current may propagate into silica-rich quartzose sand, mixed soil, clay, or other sediments, rapidly vaporizing and melting resistant materials within such a common dissipation regime.[3] This results in the formation of generally hollow and/or vesicular, branching assemblages of glassy tubes, crusts, and clumped masses.[4] Fulgurites have no fixed composition because their chemical composition is determined by the physical and chemical properties of whatever material is being struck by lightning.

Fulgurites are structurally similar to Lichtenberg figures, which are the branching patterns produced on surfaces of insulators during dielectric breakdown by high-voltage discharges, such as lightning.[5][6]

Fulgurite

Description [edit]

Fulgurite

Fulgurites are formed when lightning strikes the ground, fusing and vitrifying mineral grains.[7] The primary SiO_2 phase in common tube fulgurites is lechatelierite, an amorphous silica glass. Many fulgurites show some evidence of crystallization: in addition to glasses, many are partially protocrystalline or microcrystalline. Because fulgurites are generally amorphous in structure, fulgurites are classified as mineraloids. Peak temperatures within a lightning channel exceed 30,000 K, with sufficient pressure to produce planar deformation features in SiO_2, a kind of polymorphism. This is also known colloquially as shocked quartz.[8]

Material properties (size, color, texture) of fulgurites vary widely, depending on the size of the lightning bolt and the composition and moisture content of the surface struck by lightning. Most natural fulgurites fall on a spectrum from white to black. Iron is a common impurity that can result in a deep brownish-green coloration. Lechatelierite similar to fulgurites can also be produced via controlled (or uncontrolled) arcing of artificial electricity into a medium. Downed high voltage power lines have produced brightly colored lechatelierites, due to the incorporation of copper or other materials from the power lines.[9] Brightly colored lechatelierites resembling fulgurites are usually synthetic and reflect the incorporation of synthetic materials. However, lightning can strike man-made objects, resulting in colored fulgurites.

The interior of Type I (sand) fulgurites normally is smooth or lined with fine bubbles, while their exteriors are coated with rough sedimentary particles or small rocks. Other types of fulgurites are usually vesicular, and may lack an open central tube; their exteriors can be porous or smooth. Branching fulgurites display fractal-like self-similarity and structural scale invariance as a macroscopic or microscopic network of root-like branches, and can display this texture without central channels or obvious divergence from morphology of context or target (e.g. sheet-like melt, rock fulgurites). Fulgurites are usually fragile, making the field collection of large specimens difficult.

Stereo image

Left frame [show]

Right frame [hide]

Parallel view (⊔) [show]

Cross-eye view (⨯) [show]

Two Type I (arenaceous) fulgurites: a section of a common tube fulgurite and one exhibiting a branch

Stereo image

Left frame [show]

Right frame [hide]

Parallel view (⊔) [show]

Cross-eye view (⨯) [show]

Two small Type I Saharan Desert fulgurites.[1] In a planar view the specimen on the right has a blade-like morphology, but its tubular nature is dramatically shown in a stereo view.

Fulgurites can exceed 20 centimeters in diameter and can penetrate deep into the subsoil, sometimes occurring as far as 15 m (49 ft) below the surface that was struck,[10] although they may also form directly on a sedimentary surface.[11] One of the longest fulgurites to have been found in modern times was a little over 4.9 m (16 ft) in length, found in northern Florida.[12] The Yale University Peabody Museum of Natural History displays one of the longest known preserved fulgurites, approximately 4 m (13 ft) in length.[13] Charles Darwin in *The Voyage of the Beagle* recorded that tubes such as these found in Drigg, Cumberland, UK reached a length of 9.1 m (30 ft).[14][15] Fulgurites at Winans Lake, Livingston County, Michigan, extended discontinuously throughout a 30 m range and arguably include the largest reported fulgurite mass ever recovered and described: its largest section extending approximately 16 ft (4.88 m) in length by 1 ft in diameter (30 cm).[4][16]

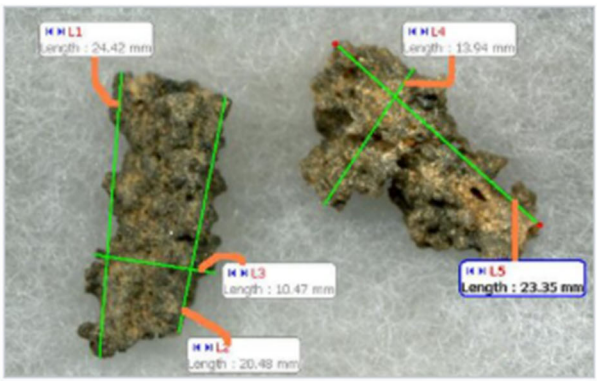

Typical broken fulgurite sections

Classification

Fulgurites have been classified[17] into five types related to the type of sediment in which the fulgurite formed, as follows:

Type I – sand fulgurites with tubaceous structure; their central axial void may be collapsed

Type II – soil fulgurites; these are glass-rich, and form in a wide range of sediment compositions, including clay-rich soils, silt-rich soils, gravel-rich soils, and loessoid; these may be tubaceous, branching, vesicular, irregular/slaggy, or may display a combination of these structures, and can produce exogenic fulgurites (droplet fulgurites)

Type III – caliche or calcic sediment fulgurites, having thick, often surficially glazed granular walls with calcium-rich vitreous groundmass with little or no lechatelierite glass; their shapes are variable, with multiple narrow central channels common, and can span the entire range of morphological and structural variation for fulguritic objects

Type IV – rock fulgurites, which are either crusts on minimally altered rocks, networks of tunneling within rocks, vesicular outgassed rocks (often glazed by a silicide-rich and/or metal oxide crust), or completely vitrified and dense rock material and masses of these forms with little sedimentary groundmass

Type V – [droplet] fulgurites (exogenic fulgurites), which show evidence of ejection (e.g. spheroidal, filamentous, or aerodynamic),[17] related by composition to Type II and Type IV fulgurites

phytofulgurite – a proposed class of objects resulting from partial to total alteration of biomass (e.g. grasses, lichens, moss, wood) by lightning,[18][19] described as "natural glasses formed by cloud-to-ground lightning." These were excluded from the classification scheme because they are not glasses, so classifying them as a subset of fulgurites is debatable.[17]

STOP 7.2 – Kem Kem Dinosaur Mine

The following is taken from: Ibrahim., N., Sereno, P.C., Varricchio, D.J., Martill, D.M., Dutheil, D.B., Unwin, D.M., Baidder, L., Larsson,H.C.E., Zouhri, S., and Kaoukaya, A., 2020, Geology and paleontology of the Upper Cretaceous Kem Kem Group of eastern Morocco. ZooKeys, vol. 928, pp. 1-216.

Introduction

Richly fossiliferous strata, commonly referred to as the "Kem Kem beds" (Lavocat 1949, Sereno et al. 1996), are exposed on the face of a long, winding escarpment near the Moroccan-Algerian border on the northwestern edge of the Sahara Desert (Figs 1–3). Secondary outcrops of similar rocks extend westward toward the Atlas Mountains from this escarpment at Erfoud to Jorf and eventually to Goulmima and Asfla. At distant locales in northern Africa, early geological and paleontological surveys identified comparable fossiliferous rocks in the Western Desert of Egypt (Stromer 1915, 1934, Nothdurft et al. 2002) and in north and central regions of the Sahara (Haug 1904, Lapparent 1951, 1960, Depéret and Savornin 1927).

The Kem Kem beds, nevertheless, are more fossiliferous, better exposed and often more accessible than comparable strata in most other northern African locations. These strata have been studied by several teams and are accessible to locals in some areas; fossils have been collected by researchers affiliated with institutional collections as well as local private collectors that often utilize commercial intermediaries. Our aim in this report is to review both the geological and paleontological aspects of the Kem Kem beds, to describe and name strata as needed, to summarize the taxonomic status of the fauna based on all major collections of Kem Kem fossils, and to evaluate paleoenvironments and the paleoecological significance of the Kem Kem assemblage.

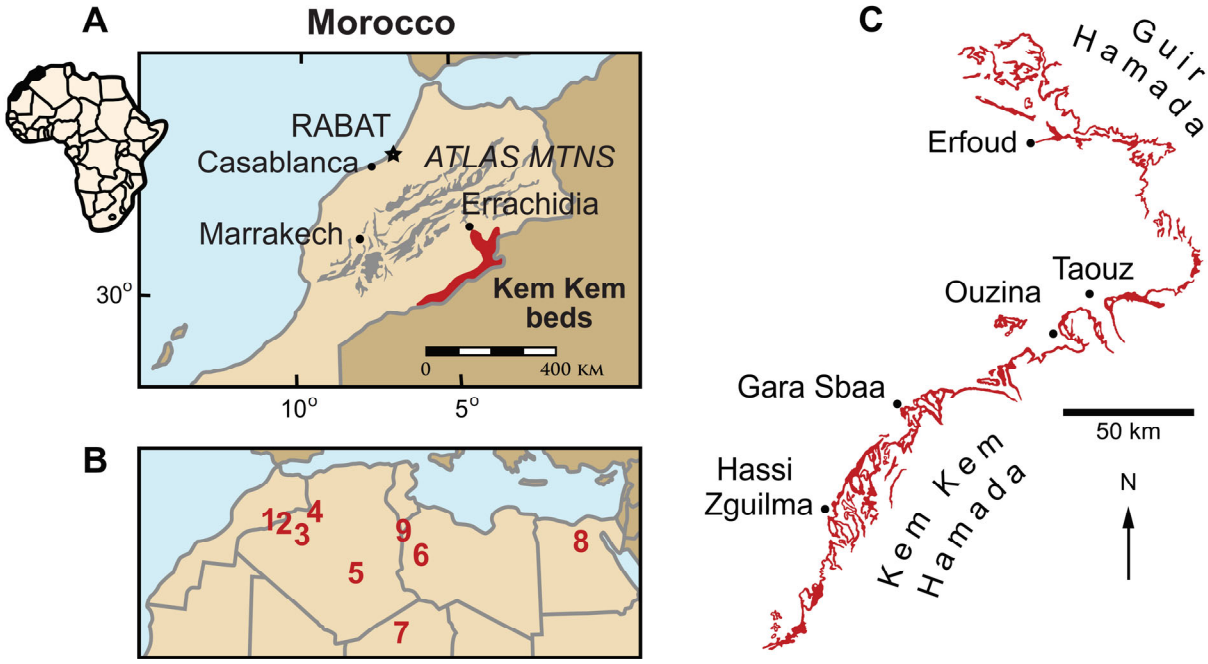

Figure 1. Geographical setting of the Kem Kem region and outcrops. **A** View of the position of Morocco in Africa and location of the Kem Kem beds (shown in red). **B** Map showing the geographical location of the Kem Kem in North Africa relative to roughly coeval sites in northern Africa. **C** Cretaceous outcrops along the Kem Kem and Guir Hamadas (modified from Sereno et al. 1996). Numbers: **1** Kem Kem, Morocco. **2** Gara Samani, Algeria. **3** Timimoun, Algeria. **4** Monts des Ksours, Algeria. **5** Djoua Valley, Algeria. **6** Al Hamra Hamada, Libya. **7** In Abangharit, Niger. **8** Bahariya, Egypt, **9** Tataouine, Tunisia.

Geological status and presumed age

Lavocat (1954a, 1954b) referred to the strata in the Kem Kem area of Morocco as a component of the “Continental intercalaire”, a term used for broadly comparable rocks in many other locales in northern Africa that are capped by a distinctive hard limestone platform of Cenomanian-Turonian age (Figs 3, 4). Lavocat (1948, 1954a) and Choubert (1952) also referred to this continental-marine package of rock as the "trilogie mésocrétacée", comprising two successive continental units underlying the marine Cenomanian-Turonian limestone. The continental beds were described by Joly (1962) as the "unité inférieure", or "grès rouges infracénomaniens", and the "unité supérieure", or "marnes versicolores à gypse." This two-part division of the continental facies beneath the Cenomanian-Turonian limestone along the escarpment in the Kem Kem region of Morocco has thus been recognized for nearly 70 years, although no formal geological nomenclature has been proposed for these fossiliferous continental facies.

Sereno et al. (1996) introduced the informal term Kem Kem beds for the two lower units of Choubert’s (1952) “trilogie mésocretacée”, which underlie the Cenomanian-Turonian limestone complex (Fig. 3). These lower beds, composed of sandstone and mudstone, reach a maximum thickness of approximately 200 m. More recently, Ettachfini and Andreu (2004) and Cavin et al. (2010) used formational names originally proposed in notes to a geological map of the High Atlas to the northwest of the Kem Kem by Dubar (1949; sometimes mis-cited as 1948). Dubar’s formational names (Ifezouane and Aoufous) are based on his observations of strata on the eastern flank of the High Atlas Mountains (Tinghir, west of Goulmima). As we discuss below, these rocks are generally un-fossiliferous, have a greater presence of evaporite facies, and lack other features of both terrestrial units of the Kem Kem beds (Sereno et al. 1996). Thus, although we do correlate the two units of the Kem Kem beds with the Ifezouane and Aoufous formations on a continuum of relatively small interconnected basins, we show that the Kem Kem units are mappable, distinctive and deserving of formal recognition, and we designate effective type sections for each. We summarize the latest geological and paleontological evidence that suggests that they accumulated on a continental ramp in the Kem Kem region through to ocean margins to the north and west (Fig. 2).

The age of the “Kem Kem beds” has been regarded variously as mid or early Late Cretaceous (Albian-Cenomanian). Lavocat (1948) described the most common faunal elements and estimated the age as Albian or Cenomanian. Choubert (1952) and Lavocat (1954b) noted similarities with the Bahariya Formation in Egypt (Stromer 1936, Dominik 1985, Soliman and Khalifa 1993), which was regarded as Cenomanian in age. Choubert (1952) and Lavocat (1954a), however, assigned the Kem Kem beds to the "infracénomanien," suggesting a probable Albian age. Although ammonites and other nonvertebrate fossils have established the Late Cenomanian-Turonian age of the overlying limestone complex (Ferrandini et al. 1985; Ettachfini and Andreu 2004; Ettachfini et al. 2005; Essafraoui et al. 2015), no fossils were known at that time from the Kem Kem beds that could be reasonably associated with stage-level temporal resolution.

Seven elasmobranchs and several dinosaur genera (Spinosaurus, Carcharodontosaurus, and Deltadromeus) reported from the Kem Kem beds are shared with the Bahariya Formation in Egypt (Sereno et al. 1996). One of these elasmobranch species (Haimirichia amonensis; Cappetta and Case 1975), in addition, has a broad circum- Mediterranean distribution seemingly restricted to Cenomanian strata. As the fauna from both lower and upper units appears similar, Sereno et al. (1996) inferred a Cenomanian age for these sediments, which has generally been accepted (Wellnhofer and Buffetaut 1999, Cavin et al. 2001, Dal Sasso et al. 2005, Cavin et al. 2010). Martin and de Lapparent de Broin (2016) recently reviewed the geology and age of the Kem Kem beds and proposed a late Albian-early Cenomanian age for the locality that yielded Lavocatchampsa.

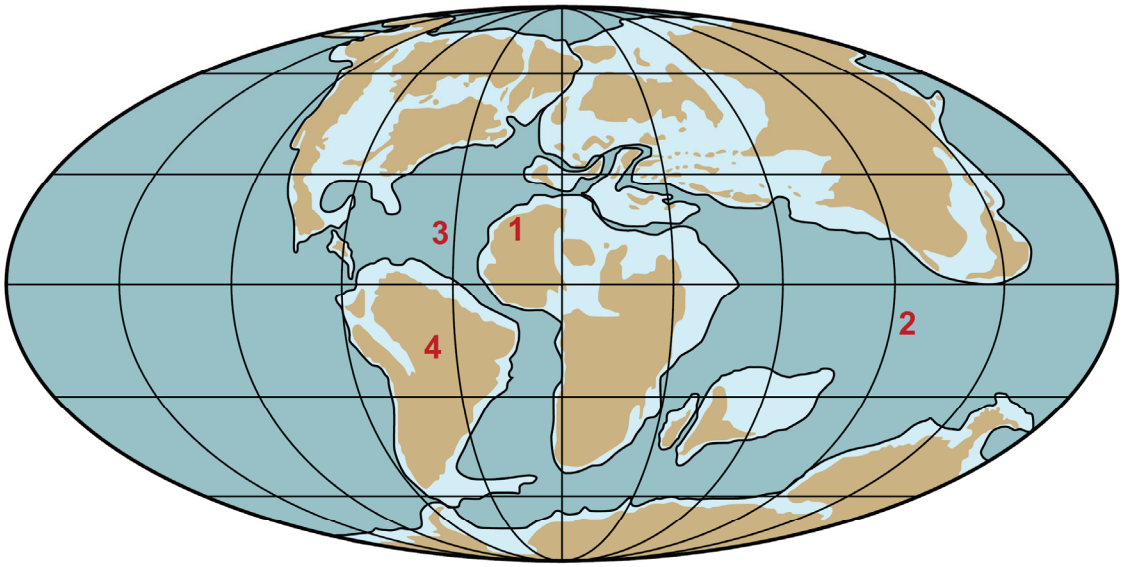

Figure 2. Geographical setting of the Kem Kem region. Cenomanian (~94 Mya) paleogeographic world map showing key localities (map after Scotese 2002, da Silva and Gallo 2007). Abbreviations: **1** Kem Kem region in Africa **2** Tethys Ocean **3** opening Atlantic Ocean **4** South America.

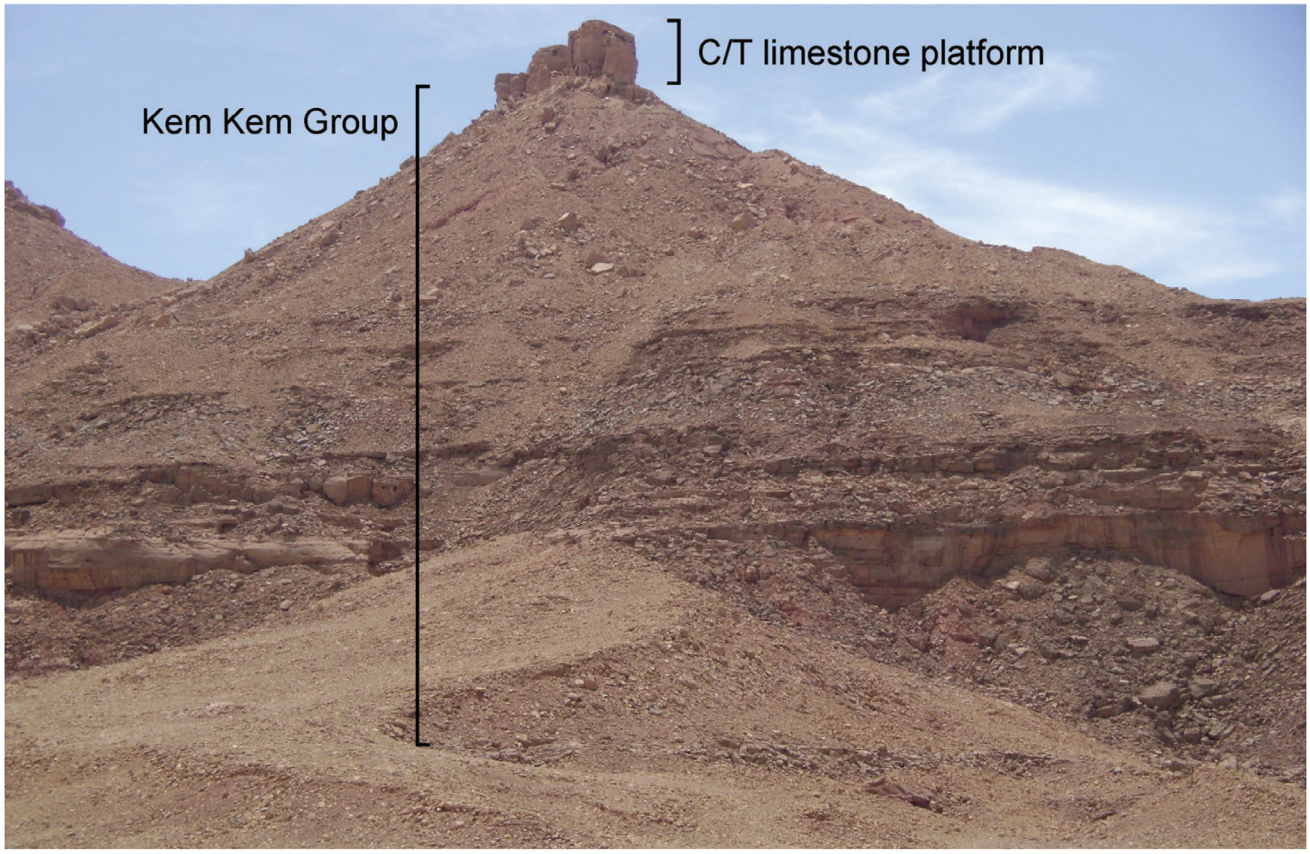

Figure 3. Outcrops of the Kem Kem sequence near Gara Sbaa. The red beds are overlain by a Cenomanian-Turonian limestone platform.

Figure 4. Example Kem Kem localities. **A** Basal outcrop at Aferdou N'Chaft **B** Iferda N'Ahouar **C** Gara Sbaa **D** Other outcrops at Gara Sbaa **E** Outcrops south of Jbel Zireg **F** Outcrop at Moher (south of Tafraoute) near the Morocco-Algeria border.

STOP 7.3 – Tadaout-Tizi n'Rsas anticline

The following is taken from: Daoud, M.A., Essalhi, M., Essalhi, A., and Toummite, A., 2021, Petrographic and Magnetic Fabric Investigation of the Tadaout-Tizi n'Rsas Dyke Swarms in the Eastern Anti-Atlas, Morocco. Economic and Environmental Geology, vol. 54, no. 6, pp. 629-647.

Geological Setting

Tafilalet region is situated at the easternmost border of the Anti-Atlas. Generally, the Moroccan Anti-Atlas consists of Precambrian basement covered by Paleozoic sedimentary sequence. Precambrian basement is exposed in several inliers oriented ENE-WSW (Choubert, 1943, 1947; Thomas et al., 2004; Gasquet et al., 2005, 2008). The most eastern Precambrian inliers are Saghro and Ougnat. However, the Precambrian basement are not limited at the two major inliers; they outcrop in the east part of Erfoud city (Gour Brikat and El Aness), and in the south-eastern border of Ougnat-Ouzina ridge in the Jbel Tazoult n'Ouzina (Destombes and Hollard, 1986). These Precambrian basements are covered by a series of folded Paleozoic sedimentary sequence (Paleozoic series, predominantly deposited in a shallow marine environment). The Ougnat-Ouzina ridge corresponds to a formation pile from Cambrian to Ordovician. Nevertheless, the Tafilalet and Maider basins, located to the east and west of the ridge, respectively, consist of a set of formations ranging from Devonian to Carboniferous (Hollard, 1974b, 1981; Raddi et al., 2007) (Fig. 1a).

Paleozoic series of the eastern Anti-Atlas are affected by the Variscan orogeny. This later appear in the development of numerous folds and the reactivation of paleofaults (Soualhine et al., 2003; Robert-Charrue, 2006; Baidder, 2007; Raddi et al., 2007; Michard et al., 2008; Baidder et al., 2008, 2016; Álvaro et al., 2014b, 2014a; Benharref et al., 2014a, 2014b, 2014c; Soulaimani et al., 2014; Ait Daoud et al., 2020). Several magmatic bodies (in the form of dykes, sills and laccoliths) intruded these series. During the Cambrian, the magmatic rocks were more developed in the south of the Ougnat inlier (Destombes and Hollard, 1986; Raddi, 2014) and between the Tafilalet and Maider basins in the Ougnat-Ouzina ridge, precisely in the Jbel Tazoult n'Ouzina anticline (Destombes and Hollard, 1986; Benharref et al., 2014a, 2014b, 2014c; Baidder et al., 2016; Pouclet et al., 2018).

According to Destombes and Hollard (1986) (geological map of Tafilalet-Taouz, scale 1 :200 000e), the Tafilalet province shows a large distribution of magmatic rocks located at the Ordovician, Silurian, Devonian and Carboniferous formations, but they don't present any indication of ages. However, recent publications about dykes and sills which crosse the folded paleozoic series of the Anti-Atlas yielded an age of 200-195 Ma. The majority of these magmatic rocks follow the NE-SW direction faults, and are attributed to the Central Atlantic Magmatic Province (CAMP) events (Hailwood and Mitchell, 1971; Hollard, 1973; Sebai et al., 1991; Derder et al., 2001; Youbi et al., 2003; Silva et al., 2004; Verati et al., 2007; Chabou et al., 2010). However, some new works present new results about the geochemical composition, petrographic and stratigraphic setting of these igneous rocks. Based on these works, the magmatic rocks of Tafilalet province have a sodic alkaline magma composition and intruded during the Famennian-Tournaisian and the early Visean (Álvaro et al., 2014b, 2014a, Benharref et al., 2014a, 2014b, 2014c, Pouclet et al., 2017, 2018). In the same way, Najih et al., (2018, 2019) confirm the geochemical affinity of these magmatic rocks, they attribute them a post-Visean and pre-Triassic age, precisely the late Permian (between 255 ± 3Ma and 264.2 ± 2.7Ma) using the biotite 40Ar/39Ar and zircon U-Pb dating. The samples were collected in the Jbel Dboa laccolith in the core of the M'Fis anticline located at 14 km NE of the TTR anticline.

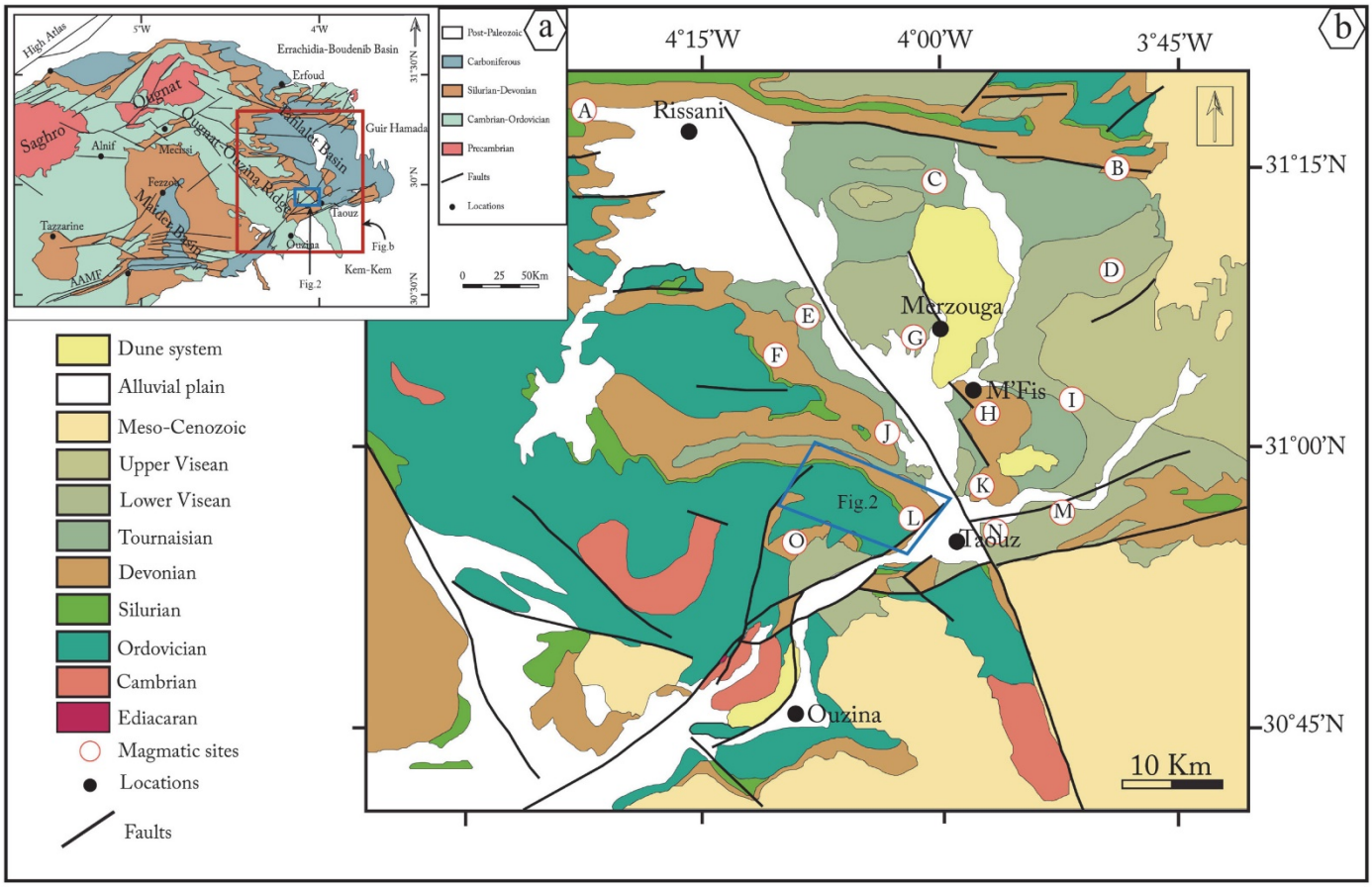

Fig. 1. (a) Simplified geological map of the eastern Anti-Atlas. (b) Simplified geological map of the Tafilalet region, based on the compilation of five maps of the Moroccan cartographic program « Plan National de Cartographie Géologique, programme Tafilalet 2009 », (Álvaro et al. 2014a-b, Benharref et al. 2014a-b-c), with the works of Destombes and Hollard (1986), Baidder et al. (2016). Location of magmatic bodies: (A) west of Rissani, (B) north Erg Chebbi, (C) Widane Chebbi, (D) NE of M'Fis, (E) upstream of Ziz valley, (F) Douar Oum El Hadj, (G) Marzouga, (H) M'Fis, (I) eastern M'Fis, (J) middel of the Ziz valley, (K) Znaigui, (L) Tadaout, (M) Begaa, (N) eastern Taouz, (O) Jbel El Mraier. Blue rectangle indicates the study area.

STOP 7.4 – Silurian Orthoceras and Permian dikes

Orthoceras, from Ancient Greek ὀρθός (*orthós*), meaning "straight", and κέρας (*kéras*), meaning "horn", is a genus of extinct nautiloid cephalopod restricted to Middle Ordovician-aged marine limestones of the Baltic States and Sweden. This genus is sometimes called *Orthoceratites* and misspelled as *Orthocera*, *Orthocerus*, or *Orthoceros*.

Orthoceras was formerly thought to have had a worldwide distribution due to the genus' use as a wastebasket taxon for numerous species of conical-shelled nautiloids throughout the Paleozoic and Triassic. Since this work was carried out and re-cataloging of the genus, *Orthoceras sensu stricto* refers to ***Orthoceras regulare***, of Ordovician-aged Baltic Sea limestones of Sweden and neighboring areas.[1]

These are slender, elongate shells with the middle of the body chamber transversely constricted, and a subcentral orthochoanitic siphuncle. The surface is ornamented by a network of fine lirae (Sweet 1964:K224). Many other very similar species are included under the genus *Michelinoceras*.

Orthoceras

Temporal range: Middle Ordovician (Dapingian to Darriwilian), 470–458 Ma [1]

Artist's reconstruction of *O. regulare*

Scientific classification

Kingdom:	Animalia
Phylum:	Mollusca
Class:	Cephalopoda
Order:	†Orthocerida
Family:	†Orthoceratidae
Genus:	†***Orthoceras*** Bruguière, 1789
Species:	†***O. regulare***

Binomial name

†***Orthoceras regulare***
(Schlotheim, 1820)

History of the name [edit]

Originally *Orthoceras* referred to all nautiloids with a straight-shell, called an "orthocone" (Fenton & Fenton 1958:40). But later research on their internal structures, such as the siphuncle, cameral deposits, and others, showed that these actually belong to a number of groups, even different orders.

According to the authoritative Treatise on Invertebrate Paleontology, the name *Orthoceras* is now only used to refer to the type species *O. regulare* (Schlotheim 1820) from the Middle Ordovician of Sweden and parts of the former Soviet Union such as Russia, Ukraine, Belarus, Estonia and Lithuania.[1] The genus might include a few related species.

Confusion with *Baculites* [edit]

Orthoceras and related orthoconic nautiloid cephalopods are often confused with the superficially similar *Baculites* and related Cretaceous orthoconic ammonoids. Both are long and tubular in form, and both are common items for sale in rock shops (often under each other's names). Both lineages evidently evolved the tubular form independently of one another, and at different times in earth history. *Orthoceras* lived much earlier (Middle Ordovician) than *Baculites* (Late Cretaceous). The two types of fossils can be distinguished by many features, most obvious among which is the suture line: simple in *Orthoceras* (see image), intricately foliated in *Baculites* and related forms.

STOP 7.5 – Filon 12 Hematite Mine

From Google AI:

The Filon 12 mine (Vein 12), located near Taouz in the Er-Rissani region of southeastern Morocco, is a well-known, active mine dedicated to producing mineral specimens, particularly vanadinite, hematite, goethite, and barite. Situated in the Sahara desert, it is a popular destination for geology tours and fossil hunters exploring the Anti-Atlas region.

Key details about the Filon 12 mine:

Location & Geology: Situated near Taouz in the Errachidia Province, the mine is part of the Paleozoic rocks in the Tafilalt (Anti-Atlas) region.

Mineral Output: It is renowned for yielding specimens of vanadinite, barite, galena, iron ores, and recent finds of goethite and hematite.

Tourism & Mining: The mine is frequently visited during geological tours, which often include tours guided by local miners and opportunities to purchase specimens.

Context: The site, sometimes referred to as a "mineral specimen mine," is distinct from the larger industrial mines in Morocco, focusing on collector-grade minerals rather than mass production. Visitors often combine a trip to Filon 12 with visits to nearby sites in the Erg Chebbi desert, which are rich in Devonian fossils.

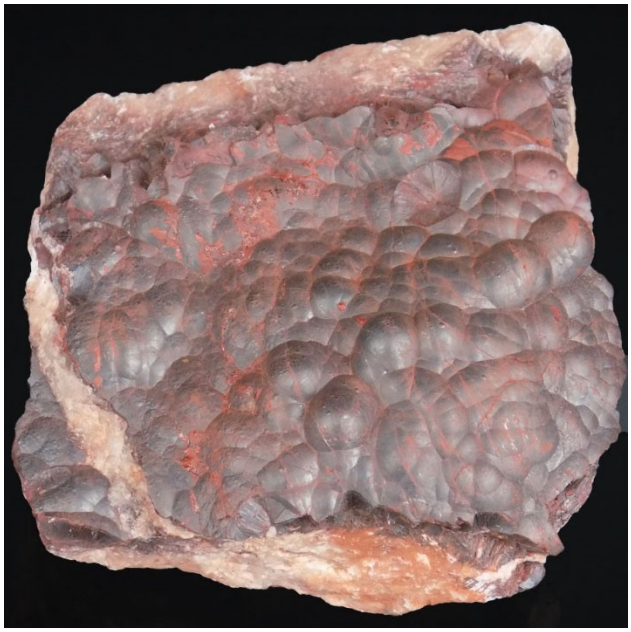

STOP 7.6 – Late Devonian Anticline

Couldn't find anything on this one

Day 8: Friday, March 13th, 2026 – Merzouga – Todra Gorge – Ouarzazate

STOP 8.1 – Hamar Laghdad (Kes Kes) Overlook
STOP 8.2 – Erfoud Orthoceras Quarry
STOP 8.3 – Erfoud Fossil Factory
STOP 8.4 – Todra Gorge Overlook
STOP 8.5 - Ouarzazate

Hotel Information:

Les Jardins de Ouarzazate
13 N9, Tarmigt 45000, Morocco
http://www.lesjardinsdeouarzazate.com/

From our Guide:

Our day begins with a panoramic stop at Hamar Laghdad, also known as Kes Kes. Like Guelb el Mharch, visited earlier in the tour, these are Devonian cold-seep mud volcano mounds upon which rich coral reefs once developed. However, this site is much larger, consisting of more than 40 carbonate mounds aligned over a 7 km-long ridge.

We then make a short stop at an Erfoud quarry, where Orthoceras slabs containing goniatites are extracted. This is followed by a visit to a nearby site where crinoids are traditionally mined from bell pits.

After a picnic lunch, we continue to the town of Erfoud to visit an Orthoceras factory and museum. During a guided tour of the factory, we observe how quarried Orthoceras slabs are transformed into a variety of decorative objects. Upstairs, the museum displays impressive fossil specimens, including large trilobites and crinoids.

Leaving Erfoud, we travel north across Cretaceous formations that are part of the Kem Kem beds. En route, we stop at a scenic viewpoint before continuing to the spectacular Todra Gorge, located roughly halfway along our route. The gorge is dramatically carved through Jurassic limestone layers at the edge of the High Atlas Mountains. We spend approximately one hour exploring the gorge.

Afterward, we continue our journey, arriving in Ouarzazate by late afternoon.

STOP 8.1 – Hamar Laghdad (Kes Kes) Overlook

From Google AI:

Hamar Laghdad (also known as Kes Kes or Kess-Kess) is a world-renowned geological site in the eastern Anti-Atlas mountains of Morocco, roughly 16-20 km southeast of Erfoud. It is famous for a series of over 40-50 conical Early Devonian mud mounds that formed as a result of submarine hydrothermal activity.

Key Geological and Geographical Features

The Mounds (Kess-Kess): These are spectacular conical carbonate mud mounds, with some rising up to 60 meters in height. They are often described as having an L-shaped or linear, clustered layout.

Formation: They are considered a "classical example" of deep-water mud mounds, interpreted as having formed in association with hydrothermal vents, where they created a "reef-like" environment for marine life.

Fossils & Biodiversity: The site is known for its high paleobiodiversity, particularly in the surrounding sediments and within the mounds themselves. It is a renowned locality for collecting fossils, including trilobites and Devonian corals.

The "Hollard Mound": Located in the eastern part of the range, this specific mound is famous for showing the internal structure of the mound core.

Reddish Facies: Due to iron compounds and dolomite, the rocks at Hamar Laghdad often have a distinctive red color.

Environmental Significance

The site is highly significant for the study of ancient hydrothermal systems (venting) and their influence on the Devonian marine environment. The mounds are well-preserved because they are covered by shales, keeping their axes vertical.

STOP 8.2-8.3 – Erfoud Orthoceras Quarry & Fossil Factory

The following is from: https://www.saharafossils.com/morocco-orthoceras/

Morocco orthoceras is the fossil you recognize even if you don't know any fossil names. It's the stone with long, straight fossil shapes running through it—often polished into black-and-cream slabs that you'll see in workshops and displays around Erfoud. Unlike trilobites (which you usually see as single "animal" fossils), orthoceras is often seen as a pattern inside fossil stone, because one slab can show many straight shells at once. In this guide, you'll learn what orthoceras is in simple words, how to recognize it quickly, and why the Erfoud region is so strongly linked to these fossils.

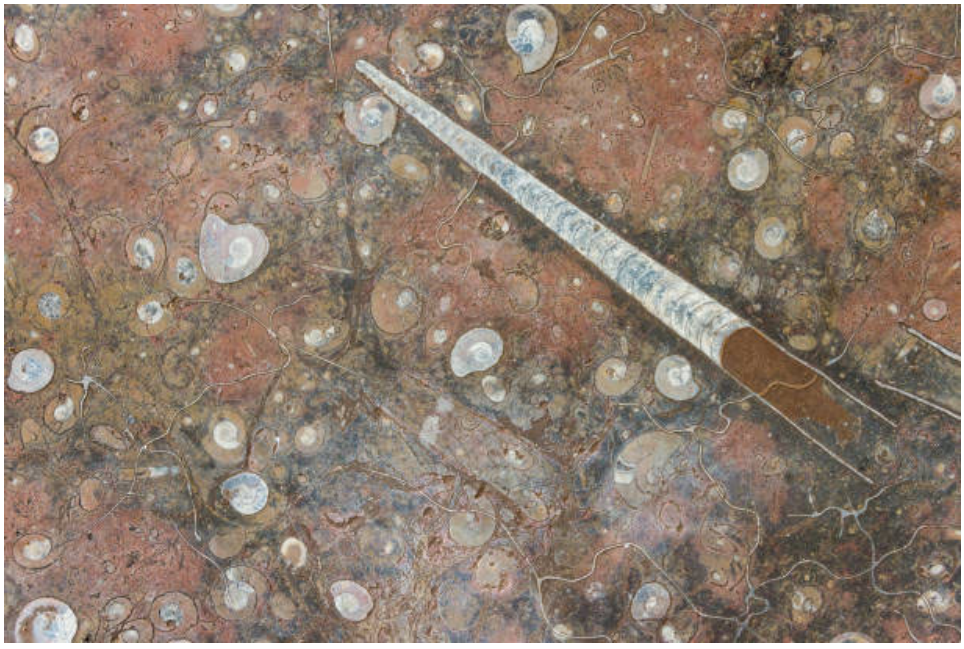

When did orthoceras live?

Orthoceras (and other straight-shelled cephalopods) lived hundreds of millions of years ago, long before dinosaurs. These animals were part of ancient seas and were relatives—very far back—of modern cephalopods like squid and nautilus. Morocco's straight-shelled fossils are usually associated with Paleozoic marine rocks, meaning they come from a time when large parts of this region were under water.

What was orthoceras, exactly?

Orthoceras was a cephalopod—a marine animal that lived in the ocean and moved using jet propulsion. It had a long shell that worked like both protection and a buoyancy tool. Inside the shell were chambers. The animal lived in the largest chamber near the opening, and the smaller chambers helped control floating—similar to how a modern nautilus uses its shell. That's why some orthoceras pieces show faint internal lines: those can be the boundaries between chambers.

Why orthoceras is so common in Morocco

Orthoceras-style fossils are common in Morocco because the right conditions happened together:

- fossil-rich marine layers formed over a very long time
- fossils became mineralized and preserved in stone
- later erosion exposed layers where fossils are visible and accessible

That's why you see orthoceras fossils not only as single specimens, but also repeated many times inside one piece of stone.

Why Erfoud is famous for orthoceras

Erfoud is known worldwide for fossils because it became a center for fossil preparation and fossil stone work. Over time, workshops in and around Erfoud developed skills to cut, shape, and finish fossil-bearing stone. This is one reason orthoceras is often linked to Erfoud:

- the region is associated with fossil-rich stone
- the town is a hub where fossils are prepared and displayed

If you're staying in Merzouga, Erfoud is close, so many travelers discover orthoceras during their Sahara trip—even if their main destination is the dunes.

How to recognize orthoceras fossils

Orthoceras pieces usually show:

- long, straight shapes (often slightly tapered)
- sometimes faint internal lines (a "chambered" look)
- repeated fossils in the same slab

On polished stone, orthoceras can look like clean straight silhouettes that stand out from the background.

Orthoceras vs ammonites (quick difference)

If ammonites are the spirals, orthoceras is the straight shell. Both are marine fossils, often discussed together in Morocco because they come from ancient sea environments and are commonly prepared in the Erfoud fossil region.

STOP 8.4 – Todra Gorge Overlook

Taken from: https://todragorge.com/todra-gorge-facts-history-geology/

Todra Gorge: 15 Surprising Facts About Morocco's Geological Masterpiece

Tucked into Morocco's High Atlas Mountains, Todra Gorge isn't just a scenic canyon—it's a portal to Earth's ancient past and a living showcase of Berber culture. With cliffs taller than the Eiffel Tower and a history spanning millions of years, this natural wonder defies expectations at every turn. Whether you're a geology geek, a culture enthusiast, or just love a good "wow" moment, these Todra Gorge facts will reshape how you see this iconic destination.

1. A 250-Million-Year-Old Time Capsule

Todra Gorge's rust-red limestone walls began forming during the Late Paleozoic Era, when Morocco was submerged under a shallow sea. Look closely, and you'll spot:

Marine fossils: Shells, coral, and trilobite imprints embedded in the rock.

Dinosaur-era layers: Upper cliffs date to the Jurassic Period (200–145 million years ago).

Fun Fact: In 2018, a French tourist found a rare 4-inch ammonite fossil near the gorge's entrance—now displayed in Tinerhir's community museum.

2. Towering Heights That Rival Skyscrapers

Cliff height: 300 meters (984 feet)—nearly as tall as the Eiffel Tower (330 meters).

Narrowest point: Just 10 meters (33 feet) wide, creating a dramatic "sky slit" effect.

Photo Tip: Visit at noon when sunlight illuminates the gorge floor, creating golden reflections on the walls.

3. A River That Carved a Canyon… Then Vanished

The Todra River sculpted the gorge over millennia, but today it's often reduced to a trickle. Why?

Modern irrigation: 90% of its water diverts to nearby palm groves.

Seasonal flow: Winter snowmelt briefly revives the river (December–March).

Local Secret: Follow the dry riverbed to find hidden pools perfect for a quick swim in summer.

4. Hollywood's Favorite Desert Backdrop

Todra's Mars-like terrain has starred in:

"Gladiator" (2000): Stood in for Roman battlefields.

"Game of Thrones": Filmed Daenerys' Essos scenes (unused footage).

"Prince of Persia" (2010): Hosted parkour-style chase sequences.

5. The Berber "Guardians of the Gorge"

For centuries, the Aït Atta Berbers has protected Todra Gorge.

Their legacy includes:

Ancient granaries: Cliffside storage rooms (agadirs) still visible today.

Sacred sites: A small shrine to Sidi Bouyaakoubi, a local Sufi saint, near the gorge's mouth.

Cultural Tip: Ask guides about the Berber "Amazigh" alphabet carved into some rocks.

6. A Climber's Paradise With 400+ Routes

Ranked among Africa's top rock-climbing spots, Todra offers:

Grades: From 5a (beginner) to 8c+ (expert-only).

Iconic routes: "La Grande Dalle" (200m vertical slab) and "Le Triangle" (overhanging challenge).

Safety Note: Local outfitters like Atlas Mountain Guides provide gear and rescue support.

7. The "Green Desert" Phenomenon

Despite its arid setting, Todra Gorge sits within a lush oasis system:

Date palms: 200,000+ trees irrigated via ancient khettara channels.

Wildlife: Barbary macaques, desert foxes, and over 80 bird species.

Eco Alert: Droughts threaten the oasis—pack reusable bottles to reduce plastic waste.

8. A Strategic Stop on Ancient Trade Routes

Todra Gorge was a key Saharan caravan checkpoint for:

Salt traders: Transporting slabs from Timbuktu to Marrakech.

Slave routes: 16th-century Portuguese texts mention captives resting here.

Historical Site: Ruins of a 17th-century kasbah (fortress) overlook the gorge's eastern entrance.

9. Record-Breaking Temperature Swings

The gorge's microclimate creates extremes:

Summer days: Up to 45°C (113°F) in nearby Tinghir.

Winter nights: Can plunge to -5°C (23°F).

Survival Story: In 2012, a German hiker survived a cold night by sheltering in a Berber sheep cave!

10. A Hollywood-Worthy Hidden Waterfall

Most tourists miss Taghia Falls, a seasonal cascade 3 hours' hike from the gorge.

Height: 60 meters (197 feet).

Best time: February–April after mountain snowmelt.

11. The Mystery of the "Disappearing Village"

In the 1950s, French archaeologists found remnants of a medieval cliff village above the gorge. Theories suggest:

Abandonment: Due to landslides or water shortages.

Purpose: A defensive outpost or spiritual retreat.

Explorer Alert: Unofficial trails lead to the site, but guides strongly recommended.

12. A Global Geology Classroom
Universities like Cadi Ayyad (Marrakech) use Todra for field studies on:
Tectonic shifts: The gorge lies on the Atlas Mountain fault line.
Erosion patterns: Wind vs. water shaping in arid climates.

13. The Full Moon Spectacle
Locals swear the gorge is most magical under a full moon:
Lunar hikes: Offered by eco-lodges like Dar Ayour.
Folklore: Berber tales say moonlit rocks reveal hidden gemstones.

14. A Test Site for Mars Rovers
In 2013, NASA tested the Juno Mars Rover prototype here due to similarities with Martian terrain.

15. The "Lucky Pebble" Tradition
Visitors often pocket small gorge stones for:
Fertility: A Berber custom for hopeful parents.
Protection: Taxi drivers in Marrakech hang them from rearview mirrors.
Please Note: Removing large rocks is illegal—stick to pebble-sized souvenirs!

STOP 8.5 – Ouarzazate

We've been here, see previous notes

Day 9: Saturday, March 14th, 2026 – Ouarzazate – High Atlas – Marrakech – Casablanca

STOP 9.1 – Mostly Driving back to Marrakech

STOP 9.2 – Marrakech

STOP 9.3 – Casablanca

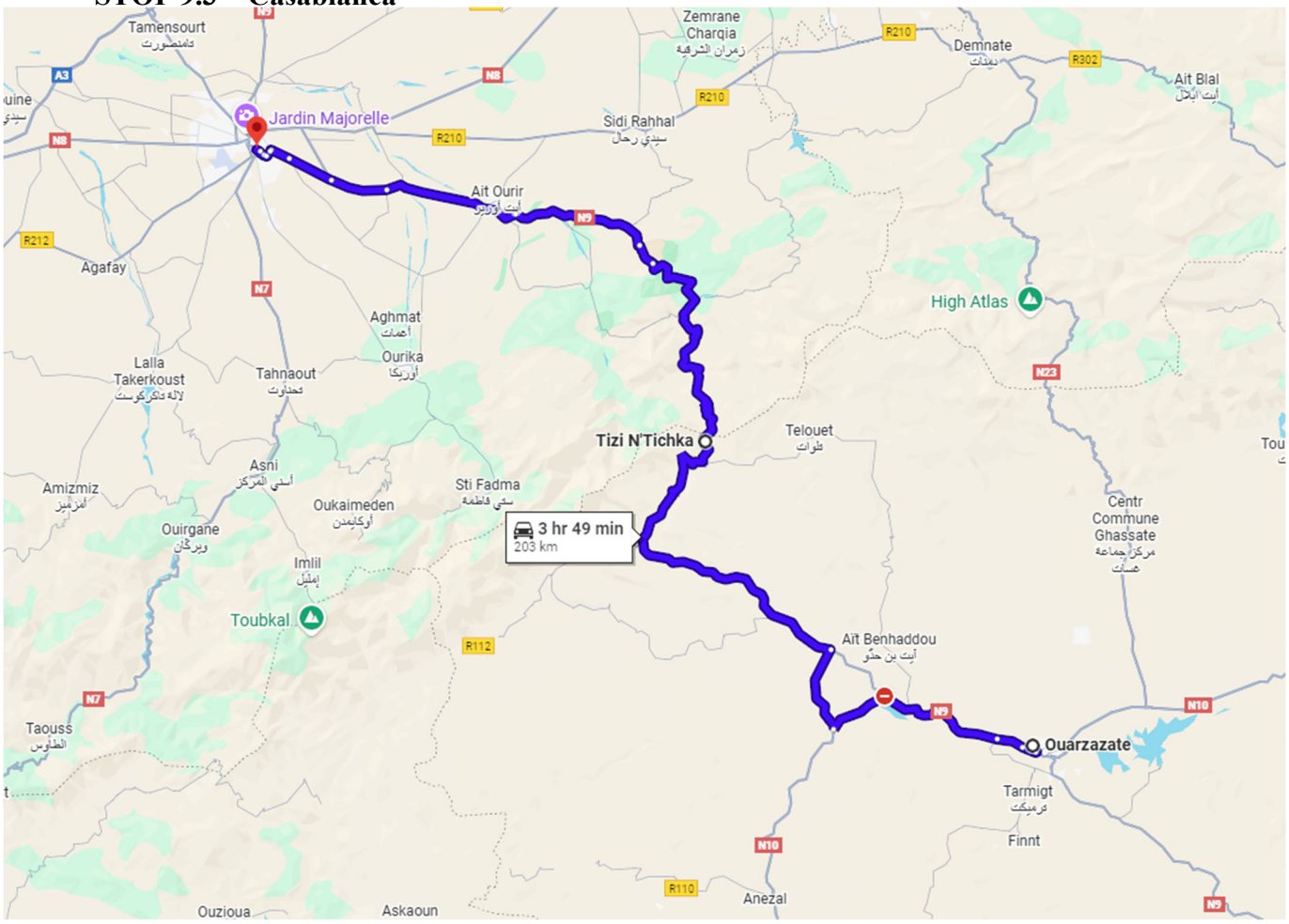

From our guide

After breakfast in Ouarzazate, we travel across the High Atlas Mountains via the Tizi n'Tichka Pass, observing folded sedimentary layers, faulted rocks, and landscapes shaped by tectonic uplift and erosion. After lunch en route, we descend into the Haouz Plain.

Upon arrival in Marrakech, enjoy free time to explore the old city, including the medina, souks, and Jemaa el-Fna Square, famous for its lively atmosphere and traditional shopping. Later, transfer to Marrakech Menara Airport, marking the end of the tour.

Flight #1: *Departure:* United Airlines, UA 1562, Saturday, March 14, 2026, 6:50PM, Marrakech (RAK) to Casablanca (CMN)
Arrival: Casablanca on Saturday, March 14, 2026 at 7:50PM

Long layover (~22hrs) for sight-seeing in Casablanca

Hotel Information:

Silver Suites Hotel & Spa Casablanca
9 Rue Kaddour El Alami, Casablanca 20250, Morocco
https://silversuiteshotel.com/

Day 10: Sunday, March 15th, 2026 – Casablanca and flight home

Flight #2: *Departure:* Royal Air Maroc, UA 5046, Sunday, March 15, 2026, 4:25PM, Casablanca (CMN) to Washington DC (Dulles – IAD)
Arrival: Washington DC on Sunday, March 15, 2026, 7:45PM

Make sure you have made arrangements for a ride home from Dulles International Airport

GEOLOGIC MAP OF MOROCCO

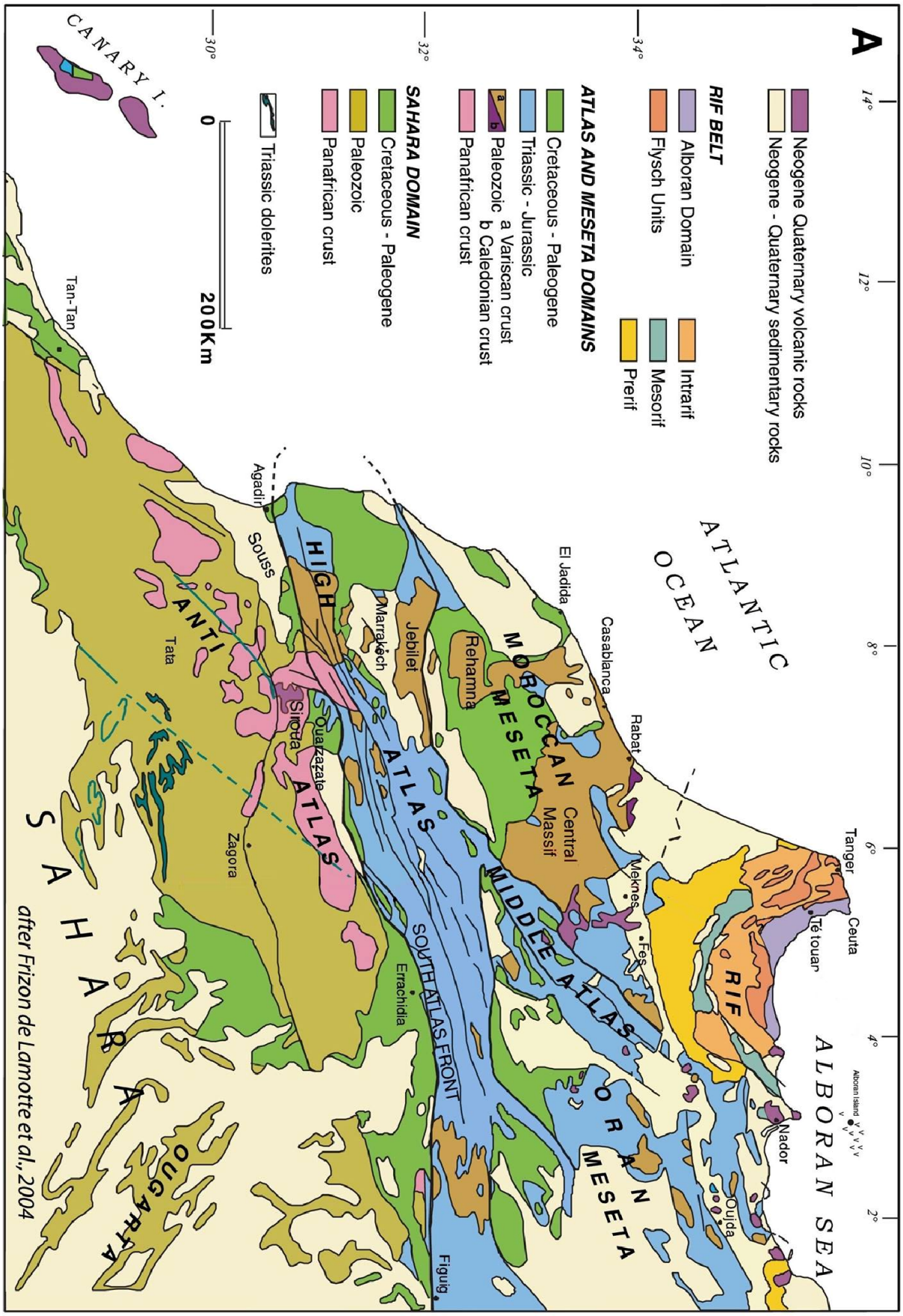

GEOLOGIC SAMPLES FOR THE PITT-JOHNSTOWN COLLECTION

Number	Sample	Description & Location
MAR26-001		
MAR26-002		
MAR26-003		
MAR26-004		
MAR26-005		
MAR26-006		
MAR26-007		
MAR26-008		
MAR26-009		
MAR26-010		

Number	Sample	Description & Location
MAR26-011		
MAR26-012		
MAR26-013		
MAR26-014		
MAR26-015		
MAR26-016		
MAR26-017		
MAR26-018		
MAR26-019		
MAR26-020		

GLOSSARY OF GEOLOGIC TERMS

Terms I should add to a glossary in this guidebook….

BUDGET INFORMATION

(as of 02/14/26)

2026 - Morocco

Total Cost of the Trip: ……**$30,228.48**

Cost per person for the trip (11 students)…….……**$1,200**
Cost per person for the trip (4 faculty)…….……....**$1,700**
Cost per person for the trip (1 non-UPJ spouse)…….……..**$2,200**
Contribution from Student Activities: ……..**$8,200**

Breakdown

1.	Airfare – Royal Air Maroc ($946.63 per round-trip ticket)	$	15,146.08
2.	Guided Geology Tour through Morocco Explorer	$	13,843.20
	The guided tour covers the following:		
	Airport pick-up and drop-off. 8 days of private, exclusive services in a comfortable, air-conditioned vehicle. Local guide and driver Hotel accommodation 6 Dinners and 7 breakfast at the hotels Picnic lunch Bottled water during day excursions Transportation in a 3 4WD Land Cruiser Airport transfer (subject to flight time)		
3.	Layover in Casablanca	$	919.20
4.	Miscellaneous		
	Guidebook (to be paid to the UPJ print shop)	$	320.00

PREVIOUS SPRING BREAK GROUPS

SPRING BREAK 2025 – GUATEMALA

Picture taken from The Mayan Face at Lake Atitlán

(L-R): Emily Mikesic, Jordan Premozic Dominic Freed, Avery Freed, Tyler Smith, Jessica Hollan, Luka Hodgson, Isabelle Boyer, Trinity McElravy – *not pictured* Ryan Kerrigan, Karan Kohler, Terry McConnell, Jessica Miller

SPRING BREAK 2024 – PORTUGAL

Picture taken from Forte de São Miguel Arcanjo, Nazare

L-R: Ryan Kerrigan, Terry McConnell, Marilyn Lindberg, Steve Lindberg, Deb Donahue, Ilia Galasso, Luka Hodgson, Jessica Hollan, Ryan Kelly, Donovan Stanley-Reeves, Trinity Chynoweth, Avery Freed, Nick Scelsi, Tyler Smith, Jordan Premozic, Pedro Barreto (Guide), Jessica Miller

SPRING BREAK 2023 – ICELAND

Picture taken from Reynisfjara Beach

Back Row (L-R): Avery Freed, Jessica Miller, Jade Smith, Olivia Weaver, Aleya Shreckengost, Holly Garrett, Nick Smith, Chris Howard, Tyler Smith; *Front Row (L-R)*: Ryan Kerrigan, Ryan Kelly, Courtney Roxby, Trish Garing (random UPJ Alum), Nick Scelsi, Ann Schaefer, Karan Kohler, Ilia Galasso – *not pictured* Terry McConnell (*she's taking the picture*)

SPRING BREAK 2022 – HAWAII

Picture taken on top Papakōlea beach (Green Sand Beach)

L-R: Steve Lindberg, Marilyn Lindberg, Elliot Finney, Terry McConnell, Alex Kijowski, Aleya Shreckengost, Cian Williamson-Rea, Olivia Weaver, Ryan Kerrigan, Jessica Miller, Delaney D'Amato, Nick Scelsi, Holly Garrett, Courtney Roxby, and Avery Freed

SPRING BREAK 2021 – COVID STRIKES AGAIN!!!
SPRING BREAK 2020 – ICELAND (CANCELLED - STUPID COVID)

SPRING BREAK 2019 – ECUADOR

Picture taken in front of ash flow from Mount Chimborazo

L-R: Jen Hlivko, Kyle Molnar, Ryan Kerrigan, Jessica Miller, Abby Wess, Alex Hockensmith, Susan Ma, Kyle Sarver, Jake Marsh, Tyler Newell, and Kim Waltermire

SPRING BREAK 2018 – SCOTLAND

Picture taken in front of Edinburgh Castle

L-R: Ryan Kerrigan, Jessica Miller, Terry McConnell, Steve Lindberg, Marilyn Lindberg, Sam Louderback, Jake Marsh, Lauren Raysich, Kim Waltermire, and Katie Roxby

Not Pictured: Bill McConnell

SPRING BREAK 2017 – HAWAII

Picture taken at the rim of Mauna Ulu in Volcanoes National Park

L-R: Jacob Williamson-Rea, Tyler Norris, Kris Miller, Allie Marra, Luke Layton, Matt Leger, Katie Roxby, and Ryan Kerrigan

SPRING BREAK 2016 – ICELAND

Picture taken on columnar joints at Reynisfjara Beach, Iceland

Top Row: Tyler Norris, Lorin Simboli, Allie Marra, Luke Layton; *Bottom Row:* Catie Bert, Matt Leger; *Not Pictured:* Ryan Kerrigan, Terry McConnell, and Steve Lindberg

SPRING BREAK 2015 – NORTH CAROLINA
Picture taken at Ray Mine Pegmatite mine, Spruce Pine, NC
Left to Right: Kris Miller, Luke Layton, Leah Marko, Andrew Barchowsky, Matt Gerber, and Ryan Kerrigan

NOTES